THE EFFECTS OF ZINC OXIDE NANOPARTICLES ON PLANTS AND ON HOST-PATHOGEN INTERACTIONS

A Dissertation
Submitted to the Graduate Faculty
of the
North Dakota State University
of Agriculture and Applied Science

By

Priyanka Deka

In Partial Fulfillment of the Requirements
for the Degree of
DOCTOR OF PHILOSOPHY

Major Program:
Environmental and Conservation Sciences

January 2019

Fargo, North Dakota

North Dakota State University
Graduate School

Title

THE EFFECTS OF ZINC OXIDE NANOPARTICLES ON PLANTS AND ON HOST-PATHOGEN INTERACTIONS

By

Priyanka Deka

The Supervisory Committee certifies that this ***disquisition*** complies with North Dakota State University's regulations and meets the accepted standards for the degree of

DOCTOR OF PHILOSOPHY

SUPERVISORY COMMITTEE:

Dr. Achintya N. Bezbaruah
Chair

Dr. Robert S. Brueggeman
Co-Chair

Dr. Kalpana Katti

Dr. Venkataramana Chapara

Dr. Chrysafis Vogiatzis

Approved:

April 12, 2019
Date

Dr. Craig Stockwell
Department Chair

ABSTRACT

Zinc oxide nanoparticles (ZnO NPs) are a type of engineered nanomaterial that is currently being explored for use in different aspects of agriculture. So far, research on this area is limited to evaluating the phenotypical responses of plants to a high concentration of the NPs which is realistically not feasible in the actual environment. This research aims to investigate the molecular-level interactions between ZnO NPs and plants, together with another significant component of the environment, a fungal plant pathogen.

Prior to studying these molecular-level interactions, the uptake of ZnO NPs *in planta* was validated using a fluorescent zinc ion sensor, Zinpyr-1 and a zinc ion chelator, TPEN in confocal laser scanning microscopy (CLSM) and Transmission Electron Microscopy (TEM). Phenotypical effects were studied in soybean plants exposed to environmentally relevant concentrations of ZnO NPs and bioaccumulation of zinc was studied in seeds of soybean and other soy products.

The next phase of this research focused on investigating the physiological responses of plants exposed to ZnO NPs. This was achieved by elucidating the complete transcriptome of the plants using a Next Generation sequencing (NGS) platform, RNA seq. A significant part of this research emphasized on exploring the effects of ZnO NPs on host-pathogen interactions. The model monocot plant, barley was used in this study, together with a necrotrophic pathogen, *Pyrenophora teres* f. *teres* (*Ptt*). The barley line which was used, CI5791 is resistant to the disease Net Form Net Blotch (NFNB), caused by *Ptt*. Rapid responses of plants to ZnO NPs were observed that subsided at the later time-points, whereas the heightened responses to the pathogen alone (P) and combined application (ZnO NP + P) persisted. Exposure to ZnO NPs also induced transcriptional reprogramming in the *Ptt* inoculated plant that resulted in compromised immunity in the otherwise resistant barley, due to the persistence of salicylic acid (SA)-related genes. In ZnO

NP-exposed *Arabidopsis thaliana*, the effects were contradictory. From the barley and Arabidopsis expression data, it could be concluded that both species react differently to ZnO NPs, giving a glimpse of the differential responses that ZnO NPs may elicit in different plant species.

ACKNOWLEDGEMENTS

I would like to thank the Divine Grace for always guiding me and providing for me.

I would like to express my sincere gratitude and deep appreciation to Dr. Achintya Bezbaruah, my advisor, and Dr. Robert Brueggeman, my co-adviser for their excellent guidance, patience, and assistance throughout. They have taught me the fundamentals of research and have continuously inspired me to perform better and to think higher.

I would like to thank the members of my dissertation committee, Dr. Marinus L. Otte, Dr. Kalpana Katti, Dr. Venkata Chapara, and Dr. Chrysafis Vogiatzis for generously offering their precious time, valuable suggestions, and guidance throughout my doctoral tenure here at NDSU. I would like to thank my research collaborator Dr. Donna Jacob for her valuable guidance. I would also like to thank Scott Payne, and Jayma Moore of Electron Microscopy Center, Dr. Pawel Borowicz of Advanced Imaging and Microscopy Lab, and Mr. Dean Sletten of Moore Engineering for their continued help. I would also like to thank all the members of Nanoenvirology Research Group, Barley Molecular Genetics and Pathology Lab, and Environmental Engineering Laboratory.

My tenure at NDSU was supported by fellowship grants from National Science Foundation (NSF), United States Department of Agriculture (USDA), and the Department of Civil and Environmental Engineering, I would also like to acknowledge my gratitude to Environmental and Conservation Sciences Program at NDSU.

Finally, I would like to acknowledge with gratitude my inspiration, my late father, and the continued support and love of my mother, sister, grandmother, uncle, aunt, and friends throughout my career, and my doctoral research program in particular.

DEDICATION

To Maa and Baba

TABLE OF CONTENTS

ABSTRACT iii

ACKNOWLEDGEMENTS v

DEDICATION vi

LIST OF TABLES xii

LIST OF FIGURES xiii

LIST OF APPENDIX TABLES xvii

LIST OF APPENDIX FIGURES xviii

CHAPTER 1 1

1.1. Background 1

1.1.1. Application of ZnO NPs in Agriculture 1

1.1.2. Zinc Oxide Nanoparticles 1

1.1.3. Routes of ZnO NP Uptake in Plants 2

1.1.4. Effects of ZnO NPs in Plants 3

1.2. Need Statement 12

1.3. Research Objectives 12

1.4. Hypotheses 13

1.5. Dissertation Organization 13

1.6. References 15

CHAPTER 2 23

2.1. Introduction 23

2.2. Materials and Methods 25

2.2.1. ZnO NP Characterization 25

2.2.2. Plant Growth 26

2.2.3. Treatment 26

2.2.4. Growth Monitoring 27
2.2.5. Preparation of Soy Concentrate and Pulp (Okara) 28
2.2.6. Inductively Coupled Plasma-Atomic Emission Spectroscopy (ICP-OES) Analysis 28
2.2.7. Statistical Analysis 29
2.3. Results and Discussion 29
2.3.1. ζ-Potential and Particle Size 29
2.3.2. Effects of ZnO NPs on the Plant Growth Metrics 30
2.4. Conclusion 38
2.5. Reference 39
CHAPTER 3 43
3.1. Introduction 43
3.2. Experimental 45
3.2.1. Materials 45
3.2.2. Plant Growth 45
3.2.3. Incubation with Zn^{2+} Sensors 46
3.2.4. Analytical Procedures 47
3.3. Results 49
3.3.1. Particle Characterization 49
3.3.2. Zinpyr-1 and TPEN Labeling 50
3.3.3. Quantification of Zinc in Samples 54
3.3.4. TEM and EDS Analyses 54
3.4. Discussion 55
3.5. Conclusion 63
3.6. Acknowledgements 63
3.7. References 64

CHAPTER 4 69
4.1. Introduction 69
4.2. Materials and Methods 70
4.2.1. ZnO NP Characterization 70
4.2.2. Plant Growth and Treatments 71
4.2.3. mRNA Extraction, RNA-Seq Library Preparation and Sequencing 71
4.2.4. Expression Analysis 72
4.2.5. Functional Annotation 73
4.2.6. Gene Enrichment Analysis 73
4.3. Results 73
4.3.1. ζ-Potential and Particle Size 73
4.3.2. RNA Seq Based Transcriptome Profiling 74
4.3.3. Gene Enrichment Analysis of DEGs Using Classification Superviewer and TopGO 75
4.4. Discussion and Conclusion 77
4.5. References 83
CHAPTER 5 88
5.1. Introduction 88
5.2. Materials and Methods 94
5.2.1. ZnO NP Characterization 94
5.2.2. Plant Growth and Treatments 94
5.2.3. Pathogen Inoculation 96
5.2.4. mRNA Extraction, RNA Seq Library Preparation and Sequencing of Barley CI5791 Leaves 97
5.2.5. mRNA Extraction, RNA Seq Library Preparation and Sequencing of Arabidopsis Leaves 98

5.2.6. Expression Analysis 98
5.2.7. Functional Annotation 99
5.2.8. Gene Enrichment Analysis 99
5.2.9. Quantitative PCR Analysis 100
5.2.10. Protein-Protein Interaction Network (PPIN) 101
5.3. Results 102
5.3.1. ζ-Potential and Particle Size 102
5.3.2. Differentially Expressed Genes (DEGs) 102
5.3.3. Gene Enrichment Analysis of DEGs 111
5.3.4. Phenotypic Analysis of CI5791 113
5.3.5. Expression of Salicylic and Jasmonic Acid-Related Genes 114
5.3.6. Identification of Putative SA-Related Genes Using Protein-Protein Interaction Network (PPIN) 121
5.3.7. Verification of PR1, PR4, and Cytochrome P450 Gene Expression Using Quantitative Real-Time PCR 125
5.4. Discussion 126
5.4.1. ZnO NPs Cause a Shift in the Magnitude of Responses in Pathogen Inoculated Plants 126
5.4.2. ZnO NPs Elicit Similar Temporal Pattern of Responses Across Time-Points in Barley CI5791 and Arabidopsis Col-0 but Their DEG Profiles Differ 128
5.4.3. Salicylic Acid (SA)-Mediated Processes Dominate Over Jasmonic Acid (JA)-Mediated Processes in ZnO NP and Combined Application Treatments in Barley Line CI5791 129
5.4.4. Application of ZnO NPs Prior to Pathogen Inoculation Promotes Susceptibility to *Pyrenophora teres f. teres* in the Resistant Barley CI5791 and is Linked to the Induction of SA-Related Genes and Oxidation-Reduction Genes 131
5.5. Conclusion 133
5.6. References 137
CHAPTER 6 147

6.1. Conclusion 147
6.2. Future Directions 149
APPENDIX A 151
APPENDIX B 153
B1. References 159
APPENDIX C 178
APPENDIX D 193

LIST OF TABLES

Table Page

2.1. Growth Stages of Soybean Plant and Treatments Applied 27

2.2. The dosages of zinc applied per pot for each treatment. The figures in parenthesis is the dosage of chemical species (ZnO NP or $ZnSO_4$) per unit weight of soil (each pot had 2.72±0.11 kg soil). The dosages of zinc species (ZnO NP or $ZnSO_4$) applied is normalized for the mass of Zn. X = 2.27 mg/kg of soil 27

3.1. Zinc concentration in spinach roots exposed to 500 mg/L of zinc and in control (no zinc). The different letters (A, B, C) denote that data are significantly different (Tukey's pairwise comparison) 54

4.1. The number of DEGs in each treatment across time-points 75

5.1. The number of DEGs in barley in each treatment across time points 104

5.2. The number of DEGs in each treatment across time points in Arabidopsis 110

LIST OF FIGURES

Figure Page

2.1. Particle characterization of ZnO NPs. (a) TEM micrograph of bare ZnO NPs, and (b) particle size distribution (based on smallest dimension) 30

2.2. (a) Plant Height (in cm) at V5-R1 Stage (b) Plant Height (in cm) at R8 Stage. Plant height is recorded on the Y-axis and treatments are on the X-axis. Means that do not share a letter are significantly different at $p<0.05$. 31

2.3. Relative chlorophyll content (SPAD) of soybean plants at: (a) R1-R2 stage (b) R6-R7 stage. 32

2.4. Number of pods per plant at maturity (R8 stage). Means that do not share a letter are significantly different at $p<0.05$. 33

2.5. Zn content in soybean seeds. Means that do not share a letter are significantly different at $p<0.05$. 34

2.6. Relationship of Zn dosage applied and Zn accumulation in the seeds. The x-axis is the concentration of soil-applied Zn in $\log_{10}$ of mg/kg, and the y-axis is the concentration of Zn accumulated in the seeds in mg/kg. 35

2.7. Zn content in soymilk (Means that do not share a letter are significantly different at $p<0.05$). 36

2.8. Zn content in pulp (Means that do not share a letter are significantly different at $p<0.05$). . 37

3.1. Chemical structures of: (a) Zinpyr-1; (b) TPEN 47

3.2. (a) TEM micrograph of bare ZnO NPs, and (b) particle size distribution of ZnO NPs based on smallest dimensions. 50

3.3. Confocal laser scanning microscopic images of the spinach roots showing Zinpyr-1 fluorescence in (a) root tip exposed to ZnO NPs, (b) root tip exposed to $ZnSO_4$, (c) control (root tip from plants not exposed to ZnO NPs or $ZnSO_4$), (d) root hairs and root hair zone exposed to ZnO NPs, (e) root hairs and root hair zone exposed to ZnSO4, and (f) control (root hairs and root hair zone from plants not exposed to ZnO NPs or $ZnSO_4$). 52

3.4. Confocal laser scanning microscope images of the spinach roots showing Zinpyr-1 fluorescence (green) being marred because of Zn^{2+} chelation by Zn^{2+} chelator TPEN, (a) root tip exposed to ZnO NPs, (b) root tip exposed to $ZnSO_4$, (c) control root tip from plants not exposed to ZnO NPs or $ZnSO_4$, (d) root hairs and root hair zone exposed to ZnO NPs, (e) root hairs and root hair zone exposed to $ZnSO_4$, and (f) control root hairs and root hair zone from plants not exposed to ZnO NPs or $ZnSO_4$ 53

3.5. Transmission Electron micrograph of Zn NPs inside the spinach root tip of ZnO NP exposed plants: (a) Root tip section with ZnO NPs (encircled) inside a root cell. Nucleus and chromatin are visible, (b) magnified view of ZnO NPs in area circled (20 nm), and (c) EDS spectrum of an electron-dense spot in the TEM scan in (a)..... 55

3.6. EDS Spectra of different Zn compounds (a) Zn NP in plant roots, (b) Zn phosphate, (c) Zn phytate (d) bare ZnO NP, and (e) overlay of Zn NP in plants, Zn phosphate, and Zn phytate spectra. 58

3.7. Comparison of EDS elemental lines of O, Zn, and P in zinc phosphate, zinc phytate and zinc NPs observed in spinach roots. 61

3.8. The model of ZnO NP internalization by plant root epidermal cells. Dissolution of ZnO NPs into ions (Zn^{2+}) occurs in the hydroponic media, which are internalized through Zn^{2+} ion transporters present in the plasma membrane of root cells. Zinc ions are transported into the vacuoles through vacuolar transporters. Inside the vacuole, the free zinc ions are chelated to organic molecules like phytic acid forming zinc-phytate nanoparticles. Endocytosis may also play a role in ZnO NP internalization, where the NPs are eventually sequestered in the vacuoles through endocytic vesicles and may also dissociate into ions in the vacuoles. The model explores the possible routes of zinc species (ZnO NP and zinc ions) transport in plant root cells from the media and does not take into account the metabolic functions of zinc or zinc NPs in plants..... 62

4.1. TEM micrograph of bare ZnO NPs, and (b) particle size distribution of ZnO NPs based on smallest dimensions..... 74

4.2. Number of up and downregulated genes at (a) 6 hpa and, (b) 48 hpa 75

4.3. The number of significant Differentially Expressed Genes (DEGs) enriched for Gene Ontology (GO) terms involved in biological processes in (a) 6 hpa ZnO NP treatment, and (b) 6 hpa $ZnSO_4$ expression data using TopGO. 77

5.1. Time-course progression of treatments when leaf samples were collected for RNA seq. 96

5.2. (a) TEM micrograph of bare ZnO NPs, and (b) particle size distribution of ZnO NPs based on smallest dimensions..... 102

5.3. Venn diagrams showing the upregulated differentially expressed genes (DEGs) that are unique to and common between the treatments. Comparisons of the DEGs of nanoparticle (NP; blue), pathogen (P; yellow), and NP+P (green) at (a) the 1st time point, (b) the 2^{nd} time point, and (c) the 3rd time point. 105

5.4. Venn diagrams showing the downregulated differentially expressed genes (DEGs) that are unique to and common between the treatments. nanoparticle (NP; blue), pathogen (P; yellow), and NP+P (green) at (a) the 1st time point, (b) the 2nd time point, and (c) the 3rd time point. 106

5.5. Volcano plot of the transcriptome of pathogen inoculated and combined application treated barley at (a) 3 hpi, (b) 21 hpi, and (c) 45 hpi. The scale on the X-axis is the $\log_2$ EDGE FC, and Y-axis is the $-\log_{10}$ test p-value. 107

5.6. Time-course comparisons of Arabidopsis DEGs and barley DEG orthologs..... 110

5.7. 7-day disease profile in (a) pathogen inoculated leaves, and (b) NP+pathogen inoculated leaves. 114

5.8. Number of DEGs in NP, and combined application (NP+P) expression data that are significantly enriched for salicylic (SA) and jasmonic acid (JA) - related processes as revealed by TopGO. 115

5.9. Number of DEGs in the nanoparticle (NP), Pathogen (P), and combined application (NP+P) treatments that were significantly enriched for salicylic (SA) and jasmonic acid (JA)-related processes as revealed by Classification Superviewer analysis..... 117

5.10. Common and unique SA- and JA-related genes in ZnO NP, pathogen, and ZnO NP+pathogen treatments in barley..... 119

5.11. Number of DEGs in NP treatment expression data in Arabidopsis that are significantly enriched for salicylic (SA) and jasmonic acid (JA) - related processes as revealed by TopGO 120

5.12. Number of DEGs in NP treatment expression data in Arabidopsis that are significantly enriched for salicylic (SA) and jasmonic acid (JA) - related processes as revealed by Classification Superviewer analysis. 121

5.13. The PPIN model showing the relationship between the cell surface receptor proteins, and the downstream genes in the signaling cascade like SA-inducible PR1 and PR4, that play probable roles in increased necrosis. Necrosis characteristics include Hypersensitive Responses (HR), oxidative bursts, and Programmed Cell Death (PCD) which are induced by ROS (Reactive Oxygen Species) production. ROS burst is thought to trigger SA signaling or vice versa (Herrera-Vásquez et al., 2015). Cytochrome P_{450} family genes participate in ROS production (Karuppanapandian et al., 2011). In combined application (NP+Ptt) treatments, PR1, PR4 and Cyt P_{450} genes were highly upregulated. 123

5.14. A model showing the hypothetical mechanism for induced susceptibility in Net Blotch-resistant barley line CI5791 upon exposure to ZnO NPs. (a) The proposed model when only necrotrophic effectors are present. Putative receptor kinases present in the cell membrane recognizes the effectors, leading to gene expression that elicits defense responses in the plant. Jasmonic acid-mediated signaling plays a key role in the defense responses that prevents the pathogen to proliferate. (b) The proposed model when ZnO NPs are present together with the necrotrophic pathogen. SA-related genes are induced in plants in response to the presence of ZnO NPs that antagonizes JA. The necrotrophic pathogens employ the SA-mediated signaling pathway to promote disease in the plants by eliciting PCD-induced necrosis in the leaves of the combined application plants (ZnO NP + Pathogen). 136

LIST OF APPENDIX TABLES

Table Page

A1. Mineral content (in mg/kg) in the seeds of soybean plant exposed to different treatments as determined by ICP-OES 152

A2. Zinc content (mg/kg) in the soil of different treatments as determined by ICP-OES 152

B1. A list of detection techniques for ENMs (other than ZnO NPs) in plant matrix 155

B2. Harmens hydroponic media composition 158

C1. GO terms enriched in biological processes in (a) 6 hpa ZnO NP treatment, and (b) 48 hpa ZnO NP, (c) 6 hpa $ZnSO_4$, and (d) 48 hpa $ZnSO_4$ expression data using TopGO 178

C2. Common and exclusive DEGs (a) 6 hpa ZnO NP Upregulated Exclusive Genes, (b) 6 hpa $ZnSO_4$ Upregulated Exclusive Genes, (c) 6 hpa ZnO NP and $ZnSO_4$ Upregulated Common Genes, (d) 6 hpa ZnO NP and $ZnSO_4$ Downregulated Common Genes, (e) 6 hpa ZnO NPs Downregulated Exclusive Genes, and (f)6 hpa $ZnSO_4$ Downregulated Exclusive Genes 181

D1. Gene enrichment for biological process in TopGO in barley exposed to ZnO NP at (a) 3 hpa, (b) 6 hpa, (c) 24 hpa, and (d) 48 hpa, pathogen at (e) 3 hpi, (f) 21 hpi, and (g) 45 hpi, and combined application (ZnO NP+ pathogen) at (h) 3 hpi, (i) 21 hpi, and (j)45 hpi 199

D2. Gene enrichment for biological process in TopGO in Arabidopsis at (a) 3 hpa, (b)6 hpa, (c) 24 hpa, and (d) 48 hpa 208

LIST OF APPENDIX FIGURES

Figure Page

B1. Dissolution of ZnO NP in DI water (40.69 mg of ZnO NPs L^{-1} added initially to water)... 153

B2. Schematic of the experimental design used for Zn^{2+} sensor Zinpyr-1 study 153

B3. ZnO NP in hydroponic media (Harmen solution) stained with Zn^{2+} sensor Zinpyr-1 in a glass slide covered by a cover-slip 154

D1. Bar charts showing gene enrichment for biological process using TopGO in (a) 3 hpa ZnO NP, (b) 6 hpa ZnO NP, (c) 3 hpi Pathogen, (d) 21 hpi Pathogen, (e) 45 hpi Pathogen, (f) 3 hpi NP+Pathogen, (g) 21 hpi NP+Pathogen, and (h) 45 hpi NP+Pathogen..... 193

D2. Bar charts showing gene enrichment for biological process using TopGO in Arabidopsis at (a) 3 hpa, (b) 6 hpa, (c) 24 hpa, and (d) 48 hpa 197

CHAPTER 1

1.1. Background

1.1.1. Application of ZnO NPs in Agriculture

Nanoparticles are increasingly being considered for addressing a myriad of problems in agriculture due to their desirable properties. One such property is the high surface area to volume ratio which increases their surface reactivity. Hence, even in low dosages, nanoparticles will be able to cause an effect which a traditional fertilizer in a much higher dosage will be able to . The most commonly used nanoparticles in agriculture are zinc oxide, silver, gold, copper oxide, titanium dioxide, silica, aluminum oxide, carbon nanotubes, iron and graphene .

1.1.2. Zinc Oxide Nanoparticles

Zinc deficiency is the most common micronutrient deficiency problem in crops . This has led to concerns as it has affected public health and infant mortality, causing growth, cognitive and immune impairment and enhanced susceptibility to diarrhea . Zinc oxide nanoparticles are considered to be effective in slow release of bioavailable zinc in soil due to their enhanced reactivity as compared to their bulk counterparts . The avenues in agriculture where the role of ZnO NPs is being currently explored are antimicrobial agents, pesticides, fungicides, herbicides, fertilizer, in soil improvement, nanobiosensors, and water purification .

ZnO NPs are chemically synthesized by a number of methods which include vapor transport synthesis, chemical reaction of zinc with alcohol, chemical reaction of zinc acetate dehydrate and sodium hydroxide, precipitation, and hydrothermal method . However, chemical synthesis has the potential disadvantage of the presence of toxic chemicals adsorbed on the surface of the particles . Alternatively, different methods of green synthesis are being explored. Green synthesis involves plant-based materials for production of ZnO NPs. Some of the methods use

flower extract of *Nyctanthes arbor-tristis* , stem bark of *Albizia lebbeck* , peels of *Aloe vera* , leaf extract of *Andrographis paniculate* , green tea , and *Passiflora caerulea* .

1.1.3. Routes of ZnO NP Uptake in Plants

With emerging reports on phytotoxicity, it becomes crucial to understand the uptake pattern of NPs in plants. With that arises the fundamental challenge of visualizing and mapping nanoscale particles in plants. Researchers have used electron microscopy, confocal microscopy, ICP, and a combination of synchrotron micro X-ray fluorescence (μXRF), X-ray absorption spectroscopy (XAS), and micro X-ray absorption near edge structure (μXANES). In velvet mesquite (*Prosopis juliflora-velutina*) seedlings exposed to ZnO NPs, zinc was traced in the vascular system of roots and leaves using μXRF, and XANES spectra revealed that zinc was present in tissues resembling $Zn(NO_3)_2$ but not as ZnO NPs . This also provided a clue that NPs can undergo biotransformation inside plants. In grains of soybean exposed to 500 mg/kg of ZnO NPs, a combination of XAS and μXANES data revealed the no ZnO NPs, but zinc citrate like species were present . XANES spectra revealed similar results in roots of soybean exposed to 4000 mg/L of ZnO NPs, where no NPs but species like zinc nitrate or zinc acetate were found . Using XANES, zinc phosphate was detected in the shoots of wheat (*Triticum aestivum*) grown in 500 mg/kg of zinc from ZnO NPs . Another study on maize exposed to ZnO NPs reported that zinc phosphate was detected in roots while hopeite or zinc phytate-like species was detected in shoots . The findings clearly indicate that ZnO NPs undergo biotransformation inside plants.

Using transmission electron microscopy (TEM), nano sized zinc clusters were also detected inside plants . However, without EDS data, it is inaccurate to assume the particles to be ZnO NPs. The presence of zinc peak in the EDS data also does not indicate that the electron-dense regions are ZnO NPs, but zinc complexed to other chelating molecules. These findings provide

evidence that there may be multiple modes of NP uptake by plants, and their subsequent interaction with plant components.

Several mechanisms are hypothesized to be involved in nanoparticle interaction with plants. NPs could dissociate into ions in the media and taken up as ions by plants, or they may be taken up as NPs and dissociate into ions inside plants, and form complexes with organic compounds. Depending on the species which is taken up by plants, the mechanism of entry into plant cells may vary. If dissolution of ZnO NP occurs in the media, and ionic Zn^{2+} is taken up by plants, the mechanism would be similar to Zn^{2+} ion transport i.e. through transporters (ZIP proteins) present in the plasma membrane . If the ZnO NPs are taken up intact, the route may be through cell wall pores of root hair cells. The NPs then enter the epidermal cell through the plasma membrane possibly via endocytosis, then into the root cortex, and ultimately enter the vascular bundle (xylem) . Both symplastic and apoplastic transport is hypothesized to facilitate movement of NPs inside plants . Overall, NP uptake in plants is considered to follow active-transport mechanism that requires cellular energy and the coordination of other processes like signaling, and endocytosis . Extensive research is needed to understand the mechanisms of NP uptake in plants from the rhizosphere, their translocation inside cells, and their transport inside tissues.

1.1.4. Effects of ZnO NPs in Plants

1.1.4.1. Phenotypical Effects and Toxicity

The recent surge of literature on the effects of ZnO NPs on plants have revealed varied and albeit contrasting results. This can be attributed to the fact that the effect of a type of NPs on plants depends on several factors like the plant species, exposure duration, mode of application, the type of plant media, concentration of the NPs in the media, particle size, shape, and other physical and chemical properties of the NPs. In addition, other chemical and physical properties also influence

NP behavior relevant to biological environment. Some of these properties are surface crystallinity, solubility, chemical reactivity, surface area, porosity, surface composition and structure of the NP, the surface energy (wettability), surface charge (zeta potential), and the presence and chemical nature of adsorbed species . The repertoire of research articles observing not one, but a spectrum of effects is therefore expected.

It is crucial to evaluate and record the effects of ZnO NPs on plants, and the parameters of exposure. Extensive work has been done on the effects of ZnO NPs on the morphology and physiology of plants. In wheat, <100 nm sized ZnO particles of dosage 500 mg/kg in sand caused a reduction in root length, proliferation of roots, increased root membrane peroxidation, and decreased chlorophyll levels in leaves when the plants were exposed for a period of 14 days . In rice, ZnO NPs of size <100 nm and concentrations 100, 500, and 1000 mg/L reduced the root, length and number of roots when the seeds were germinated in NP suspension . Similar results were observed in corn, when seeds were germinated in ZnO NP suspension of concentration 1000 mg/L, and particle size <10 nm . 1000 mg/L of ZnO NPs reduced root length of corn and cucumber but did not affect germination . Toxicity of ZnO NPs to cucumber was attributed to the Zn^{2+} ions dissolved from the NPs, while in corn, it was attributed to the nanoparticulate size of the ZnO NPs. The authors speculated that ZnO NPs entered into the root and endosperm of corn as was evident from TEM images, however, the seed coat prevented a large proportion of NPs to enter and cause acute toxicity. Zinc concentration increased with increasing concentration of ZnO NPs of size <30 nm in maize grown in sandy loam soil for 30 days . The authors also observed the translocation of zinc from the roots to the shoots. In soybean, the length ,surface area and volume of the roots and shoots decreased when the plants were grown in soil with ZnO NPs of size <50 nm and concentration 50-500 mg/kg for 8-9 weeks . Also, seeds did not develop in the plants exposed to

the highest concentration of ZnO NPs. It was evident from this study that a high concentration of ZnO NPs (500 mg/kg of soil) negatively affected soybean growth. The adverse effects were attributed to ZnO NPs because the concentration of dissolved Zn^{2+} ions in the soil was found to be very low. Similar high accumulation of zinc was found in different parts of soybean plants (root, nodule, stem, leaf and pod) grown in soil with ZnO NPs of concentrations 50, 100, and 500 mg/kg and size 10 nm for 48 days . With the highest dose of ZnO NPs, apparent toxicity symptoms were observed like low leaf and pod count, low water content in stems, pods, and roots. Soybean exposed to the same dose of ZnO NPs (50, 100, and 500 mg/kg and size 10 nm) for 48 days exhibited chlorosis on leaves, however there was no other visible signs of toxicity as they had similar growth, and yield, as compared to the controls, without increased leaf ROS or lipid peroxidation . It was also reported that ZnO NPs of concentration 100 mg/kg in soil altered the chemical composition of soybean pods with increased levels of zinc, manganese and copper . It is evident that soybean exposed to the same dose of ZnO NPs exhibited varying effects in different studies. This can be attributed to the different types of soil used in the experiments. Yoon et. al. used OECD standard soil which was composed of 69.5 percent sand, 20 percent kaolin, 10 percent peat moss, and 0.5 percent calcium carbonate, whereas Priester et. al. used organic farm soil. However, they did not provide the actual composition of the soil but the elemental composition. The bioavailability of ZnO NPs depend on soil properties like clay and organic matter content, compactness of soil particles, texture, structure, pH, and soil microbial community . Hence, the effects of the same dosage of NPs on the same species of plant would vary with the soil properties.

In tomato, plant height, leaf chlorophyll content, and lycopene content in fruits was increased with soil and foliar application of ZnO NPs of concentrations up to 250 mg/kg . An increased zinc content in fruit, shoot, and leaf was also found in ZnO NP treated plants in the same

study. NPs were found to be accumulated in roots, shoots and leaves, as found from TEM imaging. However, it cannot be deduced that the dark clusters observed were ZnO NPs as EDS data was not provided. In rapeseed, ZnO NPs of size <50 nm and concentrations 5, 10, 25, 50, 75, 100, 125, 250, and 500 mg/L caused a decrease in shoot and root length, and dry mass of plants in dose-dependent manner when the seeds were geminated with NP suspension . In a separate study, similar results were seen on rapeseed where ZnO NPs of size <50 nm and concentration 100mg/L in hydroponics decreased the plant growth and biomass, and negatively affected root and leaf anatomy and ultrastructure . The study was conducted for two months in hydroponics and fed with fresh nutrient solution and NP treatment every ten days. However, such studies do not give an accurate description of the long-term effects of ZnO NPs with regards to environmental relevance. Any chemical species in non-relevant dosages will cause adverse effects on plants grown in hydroponics. In contrast, soil composition and particles alleviate toxic effects of chemical species by making them less bioavailable. Hence, long term exposure studies in soil is environmentally relevant. Graphene oxide (GO) was found to be more toxic to oat plants in hydroponics as compared to soil, as soil particles restricted the transportation of the nanomaterial, hence reducing the contact between GO and the roots . Although most of the existing studies are conducted based on short-term exposure, long-term exposure studies are currently gaining pace. In the model species *Lemna minor*, an exposure duration of 6 weeks of ZnO NPs caused severe growth inhibition .

Indian mustard exposed to 200, 500, 1000, and 1500 mg/L of ZnO NPs (size <100 nm) in hydroponic conditions had decreased shoot and root length, and biomass . In addition, there was an increase in ROS (reactive oxygen species) generation and antioxidant enzyme activity. In black mustard, ZnO NPs of concentrations 500-1500 mg/L affected the seed germination and seedling

growth, accompanied by an increase in antioxidant enzyme activities . In cucumber, ZnO NPs of size <50 nm and a concentration of 2000 mg/L did not cause any significant changes when the plants were grown in sandy loam soil for 8 weeks . Root elongation and biomass was affected only with Zn^{2+} treatments. The authors believed that the NPs had no effect on the plants because they were immobilized in the soil, which limited their bioavailability.

Antioxidant enzyme activity was increased in cucumber grown in soil for 4 weeks with ZnO NPs (size <50 nm) of concentrations 10, 50, 100, 500, and 1000 mg/L . In another study, 400 and 800 mg/kg of ZnO NPs in soil did not alter cucumber plant growth, gas exchange, and chlorophyll content . In contrast, peanuts plants had increased seed vigor and germination with 1000 mg/L of ZnO NPs in suspension, and the treated seeds when planted had early vegetative growth and increased leaf chlorophyll content . In a halophyte from the genus *Salicornia*, ZnO NPs at concentrations 1000 mg/L in solid culture medium resulted in the decrease of shoot length in addition to generation of ROS, lipid peroxidation, and decrease in antioxidant enzyme activities . This observed toxicity was linked to the release of Zn^{2+} ions into the media. In chickpea, foliar application of 10 mg/L of ZnO NPs reduced biomass of the seedlings . In case of barley, ZnO NPs of concentrations 5, 10, 20, 40, and 80 mg/kg in soil did not significantly affect seed germination, but affected antioxidant enzyme activities . This could be because of the seed coat which hinders the movement of NPs into the seeds. Green pea plants grown in ZnO NP enriched soil in concentrations 125, 250, and 500 mg/kg had increased root elongation, and decreased chlorophyll content in leaves . In a yet recent study, the authors explored the impact of foliar and soil application of ZnO NPs on wheat, and found that plant height, spike length, chlorophyll and carotenoid content increased with increasing concentration (25, 50, 75, and 100 mg/kg ZnO NPs) . This study reveals the beneficial impact of ZnO NPs on wheat, and the possible explanation is

the environmentally relevant concentrations of Zn used in the study, which is normally 100-300 mg/kg of soil . If dissolution of ZnO NPs is taken into account, the ZnO NPs in soil would be available as ions for uptake by plants, and potentially serve as Zn fertilizer. The other important observation made in this study was that the cadmium (Cd) concentration in the plants decreased with increasing ZnO NP concentration. Cd (Cd^{2+}) and Zn (Zn^{2+}) ions being a divalent cation is known to be taken up by the same transporters in plants like heavy metal ATPases (HMA) . Hence, competitive inhibition of Cd uptake may have occurred with increasing concentration of Zn in the soil rhizosphere.

1.1.4.2. Genotoxicity

Genotoxicity of ZnO NPs on plants has not been studied as extensively as the physiological effects. Genotoxicity is defined as the destructive effects on a cell's genetic material, namely DNA and RNA . Genotoxicity takes into consideration the physical deformities or abnormalities of genetic material without the functional outcomes. *Allium cepa* (onion) is commonly used to access the genotoxicity of nanomaterials . Chromosomal aberrations were recorded in *A. cepa* roots when exposed to ZnO NPs in hydroponic media at concentrations ranging from 10-100 mg/L . Genotoxicity in the form of DNA damage was observed in *A. cepa* root and *Nicotiana tabacum* root and leaf, and chromosomal aberrations in *Vicia faba* root . Green-synthesized (using the milky latex from *Calotropis gigantea* L. R. Br) ZnO NPs was also shown to cause DNA damage in *Lathyrus sativus* L. root in a dose dependent manner, however, Zn^{2+} ions causing the most significant DNA damage .

It is worth noting that most of the studies conducted so far on plant-NP interactions involve high dosage of the NPs and assess the initial phenotypical or toxicological effects like generation of ROS, germination potential, and biomass indices. Genotoxicity measures the physical damage

of the genetic material without providing any insight on the functional outcome. However, in the context of a living system, it is very important to take into consideration the functional attributes of the genetic material, rather than considering it like a physical entity. It is crucial to evaluate plant responses to NPs in terms of gene expression, and the subsequent cascade of molecular events that shapes the phenotypical and behavioral outcomes. Here comes the need for sensitive diagnostic techniques like transcriptomics and proteomics that can provide detailed and accurate information about cellular events.

1.1.4.3. Physiological Responses and Transcriptomics

Omics-based data on plant-ZnO NP interactions is limited. A few articles have emerged recently that have reported the gene expression associated with the interaction of NPs with plants. So far, only *Arabidopsis thaliana* has been used in literature to study the molecular-level effects of NPs in plants, and microarray has been used as the standard method to determine the transcriptome of NP exposed plants. Using microarray analysis, 416 up and 961 downregulated transcripts were found in *Arabidopsis thaliana* roots exposed to 4 mg/L of ZnO NPs in hydroponic conditions for 7 days . Three species of zinc were used, viz., (1) ZnO NPs, (2) ZnO bulk particles, and (3) $ZnSO_4$ ($ZnSO_4$ dissociated quickly in hydroponics and Zn^{2+} ion was available easily). In the study, the authors found that ionic Zn^{2+} caused the highest response in terms of the number of differentially expressed genes (DEGs), followed by bulk, and ZnO NPs. However, irrespective of the zinc species, stress response genes like osmostic stress, and salt stress genes were upregulated, and genes involved in cell organization and biogenesis, DNA or RNA metabolism and structural molecular activity were downregulated . The authors have correlated this observation with the presence of Zn^{2+} ions in the media from all the three species of zinc. It is worth noting that in hydroponic media (aqueous media), the toxicity of ZnO NPs is more pronounced and comparable

to that of $ZnSO_4$ due to the dissolution of Zn^{2+} ions. However, in soil, due to the presence of probable soil adsorbents, the effect of ions in plants is negligible. In the study, it is intriguing to observe that genes like flavin monooxygenase is upregulated in the ZnO NP treated plants, which are otherwise expressed in response to pathogens. DEG overlaps were observed in all the three treatments, suggesting that zinc-specific effects were significant.

A similar 7-day study conducted on A. *thaliana* with microarray found 660 up- and 826 down-regulated genes, 232 up- and 189 downregulated genes, and 80 up- and 74 down-regulated genes for ZnO NPs, fullerene soot, and TiO_2 NPs respectively . In this study, it was observed that ZnO NPs elicited the differential regulation of most number of genes, as compared to fullerene soot, or TiO_2 NPs. The genes upregulated on ZnO NP exposure are involved in salt, oxidative, water and osmotic stresses, as well as to wounding and defense against pathogens. These observations are similar to previous reports . In the same study, similar gene expression pattern was observed with fullerene soot where the genes overexpressed were of abiotic and biotic stress, although the magnitude of gene expression was lower than that of ZnO NPs .

Microarray analysis of A. *thaliana* grown in MS media and exposed to 5mg/L silver NPs (Ag NPs) for 10 days revealed 286 upregulated and 81 downregulated genes . In the same study, stress responsive genes like cation/proton exchanger in the vacuoles, superoxide dismutase, and peroxidase were found to be upregulated and genes involved in response to pathogens and hormonal stimuli like ethylene signaling pathway genes were found to be downregulated . DEG overlaps were observed in Ag NP and Ag^+ treatments, suggesting that some of the effects stem from ionic Ag^+ released from the NPs.

Exposure of *A. thaliana* to TiO_2 NPs induced the overexpression of 1136 and 966 genes, and suppressed the expression of 653 and 798 genes in rosette leaves and roots respectively . The

authors found that some of the significantly upregulated genes with TiO_2 NP exposure are involved in triterpenoid biosynthesis, iron transport, tryptophan catabolism, and oxidation-reduction reactions, while the downregulated genes encode transcription, response to ethylene stimulus, and response to jasmonic acid. In case of nano-ceria particles, 56 and 391 genes were upregulated, and 74 and 363 genes were downregulated in *A. thaliana* rosette leaves and roots respectively . Among the upregulated genes, transcription, aging, regulation of hydrogen peroxide metabolism and cell cycle genes were the most significant, while among the downregulated genes, cell wall modifications and response to auxin stimulus genes were the most significant.

Quantitative real-time PCR (qPCR) has been used to determine the expression level of the targeted gene, however, cannot be used to elucidate the complete transcriptome of a cell. qPCR was used to evaluate the gene expression of stress response genes in *A. thaliana* exposed to cerium oxide (CeO_2) and indium oxide (In_2O_3) NPs . The authors found that one of the stress response genes, glutathione synthase was induced 3.8 to 4.6-fold in case of In_2O_3 NPs, and 2-fold in case of CeO_2 NPs. A qPCR analysis revealed that the iron regulating genes ferritin and iron-regulated transporter were upregulated in *A. thaliana* exposed to 1000 mg/L CeO_2 and 1000 mg/L In_2O_3 . Lanthanum oxide (La_2O_3) NPs of concentrations 50 and 205 mg/L was found to affect the expression of aquaporin genes like PIPs (plasma membrane intrinsic proteins), TIPs (tonoplast intrinsic proteins), NIPs (Nod26-like intrinsic proteins), and SIPs (small and basic intrinsic proteins) in the roots of maize seedling .

In all the studies mentioned so far, stress response genes have been found to be upregulated after exposure to NPs. This observation is in line with other studies which have reported ROS burst in plants after NP exposure . However, without a time-course study, it is not possible to determine the dynamics of plant behavior in response to NPs. Gene expression at a single time-point suggests

physiological responses of the plant to a stimulus, but it does not determine the true phenotypical behavior over time. Therefore, it is necessary to conduct time-course experiments that can shed light on the overall series of events.

1.2. Need Statement

It is evident from current studies that NP-induced molecular responses in plants vary with NP type, concentration and duration of exposure. Due to limited research conducted in this area, it is not feasible to determine the exact molecular mechanisms and whether these responses depend on the plant species, or the type of growth media. In the existing reports, a common phenomenon observed was the overexpression of stress response genes. However, without a detailed study, only a fragment of the complete scenario can be determined as plant and NP interactions is one of the most challenging areas of fundamental research. Extensive study is required to understand the molecular cross-talk that occurs in plants on NP exposure, and the resulting perception of plants towards NPs, or vice versa. Furthermore, NP interactions with plants in the presence of other components of the crop ecosystem is largely unknown. Pathogens that are causal agents of a host of destructive diseases in crops are undesirable yet central integral component of the ecosystem. There has been no study till date that explores the relationship between NPs and its effects on host-pathogen interactions. The gaps in the existing research need a holistic approach to understand the complex dynamics of NP interactions with plants and other components of the environment.

1.3. Research Objectives

The main objectives of this study are:

a) Investigate the effects of ZnO NPs in soybean (*Glycine max*) plants and evaluate zinc content in soy products obtained from NP-exposed plants

b) Investigate the uptake of ZnO NPs in spinach (*Spinacia oleraceae*) using a combination of microscopy techniques

c) Elucidate the complete transcriptome of barley (*Hordeum vulgare*) exposed to ZnO NPs and $ZnSO_4$

d) Investigate the physiological responses of barley to ZnO NPs in the presence of a necrotrophic fungal pathogen, *Pyrenophora teres* f. *teres*

1.4. Hypotheses

a) ZnO NPs are taken up by plants in both ionic (Zn^{2+}) and nanoparticulate forms

b) ZnO NPs in environmentally relevant concentrations in soil do not cause apparent phenotypical changes in plants

c) Gene expression is altered in plants exposed to ZnO NPs

d) ZnO NPs induce plant innate immunity genes that are characteristic of defense against biotrophs, however will compromise immunity towards necrotrophs

1.5. Dissertation Organization

There are six chapters in this dissertation. Chapter 1 is an overview of the current research, the need statement, and objectives of this research. Chapter 2 to Chapter 5 are presented in journal paper formats, which have been submitted or will be submitted for publication in peer reviewed journals. Each chapter includes an introduction, materials and methods, results, discussion and conclusion. Chapter 2 discusses the phenotypical effects of ZnO NPs on soybean plants and reports the changes in mineral content of seeds and other soy products, and Chapter 3 explores the form of zinc taken up by spinach exposed to ZnO NPs using microscopy-based techniques. Chapter 4 presents the comparative analysis in the transcriptome of barley exposed to ZnO NPs and zinc sulfate ($ZnSO_4$). Chapter 5 describes the transcriptional reprograming induced in the Net Blotch

resistant-barley line CI5791 by ZnO NPs in the presence of a necrotrophic fungal pathogen, *Pyrenophora teres* f. *teres*, the causal agent of Net Blotch disease. Chapter 6 is the conclusion and the possible future directions of this research.

1.6. References

abdal Dayem, A. et.al. The Role Of Reactive Oxygen Species (Ros) In The Biological Activities Of Metallic Nanoparticles. **Int J Mol Sci,** V. 18, N. 1, Jan 10 2017. Issn 1422-0067.

Alloway, B. J. Soil Factors Associated With Zinc Deficiency In Crops And Humans. **Environ Geochem Health,** V. 31, N. 5, P. 537-48, Oct 2009. Issn 0269-4042.

Angelé-Martínez, C. et al. Reactive Oxygen Species Generation By Copper(Ii) Oxide Nanoparticles Determined By Dna Damage Assays And Epr Spectroscopy. **Nanotoxicology,** V. 11, N. 2, P. 278-288, 2017/02/07 2017. Issn 1743-5390. Available At: < Https://Doi.Org/10.1080/17435390.2017.1293750 >.

Baker, S. et al. Nanoagroparticles Emerging Trends And Future Prospect In Modern Agriculture System. **Environmental Toxicology And Pharmacology,** V. 53, N. Supplement C, P. 10-17, 2017/07/01/ 2017. Issn 1382-6689. Available At: < Http://Www.Sciencedirect.Com/Science/Article/Pii/S1382668917301114 >.

Balážová, Ľ. et al. Zinc Oxide Nanoparticles Phytotoxicity On Halophyte From Genus Salicornia. **Plant Physiology And Biochemistry,** V. 130, P. 30-42, 2018/09/01/ 2018. Issn 0981-9428. Available At: < Http://Www.Sciencedirect.Com/Science/Article/Pii/S098194281830264x >.

Bandyopadhyay, S. et al. Comparative Phytotoxicity Of Zno Nps, Bulk Zno, And Ionic Zinc Onto The Alfalfa Plants Symbiotically Associated With Sinorhizobium Meliloti In Soil. **Science Of The Total Environment,** V. 515, P. 60-69, May 2015. Issn 0048-9697. Available At: < <Go To Isi>://Wos:000352040700007 >.

Boonyanitipong, P. et al. Toxicity Of Zno And Tio2 Nanoparticles On Germinating Rice Seed Oryza Sativa L. **International Journal Of Bioscience, Biochemistry And Bioinformatics,** V. 1, N. 4, P. 282, 2011. Issn 2010-3638.

Burman, U.; Saini, M.; Praveen, K. Effect Of Zinc Oxide Nanoparticles On Growth And Antioxidant System Of Chickpea Seedlings. **Toxicological And Environmental Chemistry,** V. 95, N. 4, P. 605-612, Apr 2013. Issn 0277-2248. Available At: < <Go To Isi>://Wos:000320913000006 >.

Chaudhary, A. et al. Antimicrobial Activity Of Zinc Oxide Nanoparticles Synthesized From Aloe Vera Peel Extract. **Sn Applied Sciences,** V. 1, N. 1, P. 136, 2018/12/31 2018. Issn 2523-3971. Available At: < Https://Doi.Org/10.1007/S42452-018-0144-2 >.

Chen, L. et al. Toxicity Of Graphene Oxide To Naked Oats (Avena Sativa L.) In Hydroponic And Soil Cultures. **Rsc Advances,** V. 8, N. 28, P. 15336-15343, 2018.

Chen, X.; O'halloran, J.; Jansen, M. A. K. Time Matters: The Toxicity Of Zinc Oxide Nanoparticles To Lemna Minor L. Increases With Exposure Time. **Water, Air, & Soil Pollution,** V. 229, N. 3, P. 99, 2018/03/05 2018. Issn 1573-2932. Available At: < Https://Doi.Org/10.1007/S11270-018-3759-4 >.

Cvjetko, P. et al. Toxicity Of Silver Ions And Differently Coated Silver Nanoparticles In Allium Cepa Roots. **Ecotoxicology And Environmental Safety,** V. 137, P. 18-28, Mar 2017. Issn 0147-6513. Available At: < <Go To Isi>://Wos:000392786400003 >.

De Andrade, L. R. et al. Absence Of Mutagenic And Recombinagenic Activity Of Multi-Walled Carbon Nanotubes In The Drosophila Wing-Spot Test And Allium Cepa Test. **Ecotoxicology And Environmental Safety,** V. 99, P. 92-97, Jan 2014. Issn 0147-6513. Available At: < <Go To Isi>://Wos:000327581800012 >.

Dhanemozhi, A. C.; Rajeswari, V.; Sathyajothi, S. Green Synthesis Of Zinc Oxide Nanoparticle Using Green Tea Leaf Extract For Supercapacitor Application. **Materials Today: Proceedings,** V. 4, N. 2, Part A, P. 660-667, 2017/01/01/ 2017. Issn 2214-7853. Available At: < Http://Www.Sciencedirect.Com/Science/Article/Pii/S2214785317300706 >.

Dimkpa, C. O. et al. Cuo And Zno Nanoparticles: Phytotoxicity, Metal Speciation, And Induction Of Oxidative Stress In Sand-Grown Wheat. **Journal Of Nanoparticle Research,** V. 14, N. 9, Sep 2012. Issn 1388-0764. Available At: < <Go To Isi>://Wos:000308225800053 >.

Dogaroglu, Z. G.; Koleli, N. Tio2 And Zno Nanoparticles Toxicity In Barley (Hordeum Vulgare L.). **Clean-Soil Air Water,** V. 45, N. 11, Nov 2017. Issn 1863-0650. Available At: < <Go To Isi>://Wos:000417176800003 >.

Duhan, J. S. et al. Nanotechnology: The New Perspective In Precision Agriculture. **Biotechnol Rep (Amst),** V. 15, P. 11-23, Sep 2017. Issn 2215-017x (Print)

2215-017x.

Ghosh, M. et al. Effects Of Zno Nanoparticles In Plants: Cytotoxicity, Genotoxicity, Deregulation Of Antioxidant Defenses, And Cell-Cycle Arrest. **Mutation Research-Genetic Toxicology And Environmental Mutagenesis,** V. 807, P. 25-32, Sep 2016. Issn 1383-5718. Available At: < <Go To Isi>://Wos:000382798100004 >.

Hernandez-Viezcas, J. A. et al. In Situ Synchrotron X-Ray Fluorescence Mapping And Speciation Of Ceo2 And Zno Nanoparticles In Soil Cultivated Soybean (Glycine Max). **Acs**

Nano, V. 7, N. 2, P. 1415-1423, Feb 2013. Issn 1936-0851. Available At: < <Go To Isi>://Wos:000315618700061 >.

Spectroscopic Verification Of Zinc Absorption And Distribution In The Desert Plant Prosopis Juliflora-Velutina (Velvet Mesquite) Treated With Zno Nanoparticles. **Chem Eng J,** V. 170, N. 1-3, P. 346-352, Jun 1 2011. Issn 1385-8947 (Print) 1385-8947.

Hussain, A. et al. Zinc Oxide Nanoparticles Alter The Wheat Physiological Response And Reduce The Cadmium Uptake By Plants. **Environmental Pollution,** V. 242, P. 1518-1526, 2018/11/01/ 2018. Issn 0269-7491. Available At: < Http://Www.Sciencedirect.Com/Science/Article/Pii/S0269749118331130 >.

Jain, A. et al. Nanomaterials In Food And Agriculture: An Overview On Their Safety Concerns And Regulatory Issues. **Critical Reviews In Food Science And Nutrition,** V. 58, N. 2, P. 297-317, 2018/01/22 2018. Issn 1040-8398. Available At: < Https://Doi.Org/10.1080/10408398.2016.1160363 >.

Jamdagni, P.; Khatri, P.; Rana, J. S. Green Synthesis Of Zinc Oxide Nanoparticles Using Flower Extract Of Nyctanthes Arbor-Tristis And Their Antifungal Activity. **Journal Of King Saud University - Science,** V. 30, N. 2, P. 168-175, 2018/04/01/ 2018. Issn 1018-3647. Available At: < Http://Www.Sciencedirect.Com/Science/Article/Pii/S1018364716303202 >.

Kaveh, R. et al. Changes In Arabidopsis Thaliana Gene Expression In Response To Silver Nanoparticles And Silver Ions. **Environmental Science & Technology,** V. 47, N. 18, P. 10637-10644, Sep 17 2013. Issn 0013-936x. Available At: < <Go To Isi>://Wos:000330096000070 >.

Kiekens, L. Zinc. In: Alloway, B. J., Ed. (Ed.). **Heavy Metals In Soils**. 2. London: Blackie Academic And Professional, 1995. P. 284-305.

Kim, S.; Kim, J.; Lee, I. Effects Of Zn And Zno Nanoparticles And Zn2+On Soil Enzyme Activity And Bioaccumulation Of Zn In Cucumis Sativus. **Chemistry And Ecology,** V. 27, N. 1, P. 49-55, 2011. Issn 0275-7540. Available At: < <Go To Isi>://Wos:000287408400005 >.

Kim, S.; Lee, S.; Lee, I. Alteration Of Phytotoxicity And Oxidant Stress Potential By Metal Oxide Nanoparticles In Cucumis Sativus. **Water, Air, & Soil Pollution,** V. 223, N. 5, P. 2799-2806, 2012. Issn 0049-6979.

Kouhi, S. M. M. et al. Long-Term Exposure Of Rapeseed (Brassica Napus L.) To Zno Nanoparticles: Anatomical And Ultrastructural Responses. **Environmental Science And Pollution Research,** V. 22, N. 14, P. 10733-10743, 2015. Issn 0944-1344.

Kumari, M. Et Al. Cytogenetic And Genotoxic Effects Of Zinc Oxide Nanoparticles On Root Cells Of Allium Cepa. **Journal Of Hazardous Materials,** V. 190, N. 1-3, P. 613-621, Jun 2011. Issn 0304-3894. Available At: < <Go To Isi>://Wos:000292427800079 >.

Landa, P. et al. The Transcriptomic Response Of Arabidopsis Thaliana To Zinc Oxide: A Comparison Of The Impact Of Nanoparticle, Bulk, And Ionic Zinc. **Environmental Science & Technology,** V. 49, N. 24, P. 14537-14545, Dec 2015. Issn 0013-936x. Available At: < <Go To Isi>://Wos:000366872300076 >.

Nanoparticle-Specific Changes In Arabidopsis Thaliana Gene Expression After Exposure To Zno, Tio2, And Fullerene Soot. **Journal Of Hazardous Materials,** V. 241, P. 55-62, Nov 30 2012. Issn 0304-3894. Available At: < <Go To Isi>://Wos:000313088300004 >.

Lopez-Moreno, M. L. et al. Evidence Of The Differential Biotransformation And Genotoxicity Of Zno And Ceo2 Nanoparticles On Soybean (Glycine Max) Plants. **Environmental Science & Technology,** V. 44, N. 19, P. 7315-7320, Oct 1 2010. Issn 0013-936x. Available At: < <Go To Isi>://Wos:000282209700025 >.

Lv, J. Et Al. Accumulation, Speciation And Uptake Pathway Of Zno Nanoparticles In Maize. **Environmental Science-Nano,** V. 2, N. 1, P. 68-77, Feb 2015. Issn 2051-8153. Available At: < <Go To Isi>://Wos:000349222200008 >.

Ma, C. X. et al. Defense Mechanisms And Nutrient Displacement In Arabidopsis Thaliana Upon Exposure To Ceo2 And In2o3 Nanoparticles. **Environmental Science-Nano,** V. 3, N. 6, P. 1369-1379, 2016. Issn 2051-8153. Available At: < <Go To Isi>://Wos:000391423400014 >.

Marslin, G.; Sheeba, C. J.; Franklin, G. Nanoparticles Alter Secondary Metabolism In Plants Via Ros Burst. **Frontiers In Plant Science,** V. 8, P. 832, 2017. Issn 1664-462x. Available At: < Https://Www.Frontiersin.Org/Article/10.3389/Fpls.2017.00832 >.

Mousavi Kouhi, S. M. et al. Comparative Phytotoxicity Of Zno Nanoparticles, Zno Microparticles, And Zn2+ On Rapeseed (Brassica Napus L.): Investigating A Wide Range Of Concentrations. **Toxicological & Environmental Chemistry,** V. 96, N. 6, P. 861-868, 2014. Issn 0277-2248.

Mukherjee, A. et al. Physiological Effects Of Nanoparticulate Zno In Green Peas (Pisum Sativum L.) Cultivated In Soil. **Metallomics,** V. 6, N. 1, P. 132-138, 2014. Issn 1756-5901. Available At: < <Go To Isi>://Wos:000328891100013 >.

Pakrashi, S. et.al. In Vivo Genotoxicity Assessment Of Titanium Dioxide Nanoparticles By Allium Cepa Root Tip Assay At High Exposure Concentrations. **Plos One,** V. 9, N. 2, Feb 2014. Issn 1932-6203.

Panda, K. K. et.al. Green Synthesized Zinc Oxide (Zno) Nanoparticles Induce Oxidative Stress And Dna Damage In Lathyrus Sativus L. Root Bioassay System. **Antioxidants (Basel),** V. 6, N. 2, May 18 2017. Issn 2076-3921 (Print) 2076-3921.

Peralta-Videa, J. R. et.al. Cerium Dioxide And Zinc Oxide Nanoparticles Alter The Nutritional Value Of Soil Cultivated Soybean Plants. **Plant Physiology And Biochemistry,** V. 80, P. 128-135, Jul 2014. Issn 0981-9428. Available At: < <Go To Isi>://Wos:000338004600016 >.

Pokhrel, L. R.; Dubey, B. Evaluation Of Developmental Responses Of Two Crop Plants Exposed To Silver And Zinc Oxide Nanoparticles. **Science Of The Total Environment,** V. 452, P. 321-332, May 2013. Issn 0048-9697. Available At: < <Go To Isi>://Wos:000318530600035 >.

Powers, K. W. et.al. Research Strategies For Safety Evaluation Of Nanomaterials. Part Vi. Characterization Of Nanoscale Particles For Toxicological Evaluation. **Toxicological Sciences,** V. 90, N. 2, P. 296-303, 2006. Issn 1096-6080. Available At: < Http://Dx.Doi.Org/10.1093/Toxsci/Kfj099 >.

Prasad, T. N. V. K. V. et.al. Effect Of Nanoscale Zinc Oxide Particles On The Germination, Growth And Yield Of Peanut. **Journal Of Plant Nutrition,** V. 35, N. 6, P. 905-927, 2012/04/01 2012. Issn 0190-4167. Available At: < Https://Doi.Org/10.1080/01904167.2012.663443 >.

Priester, J. H. et.al. Soybean Susceptibility To Manufactured Nanomaterials With Evidence For Food Quality And Soil Fertility Interruption. **Proceedings Of The National Academy Of Sciences Of The United States Of America,** V. 109, N. 37, P. E2451-E2456, Sep 11 2012. Issn 0027-8424. Available At: < <Go To Isi>://Wos:000309208000009 >.

Damage Assessment For Soybean Cultivated In Soil With Either Ceo2 Or Zno Manufactured Nanomaterials. **Science Of The Total Environment,** V. 579, P. 1756-1768, Feb 2017. Issn 0048-9697. Available At: < <Go To Isi>://Wos:000393320400076 >.

Pérez-De-Luque, A. Interaction Of Nanomaterials With Plants: What Do We Need For Real Applications In Agriculture? **Frontiers In Environmental Science,** V. 5, P. 12, 2017. Issn 2296-665x.

Rajakumar, G. et.al. Green Approach For Synthesis Of Zinc Oxide Nanoparticles From Andrographis Paniculata Leaf Extract And Evaluation Of Their Antioxidant, Anti-Diabetic, And Anti-Inflammatory Activities. **Bioprocess And Biosystems Engineering,** V. 41, N. 1, P. 21-30,

2018/01/01 2018. Issn 1615-7605. Available At: < Https://Doi.Org/10.1007/S00449-017-1840-9 >.

Rajeshwari, A. et.al. Cytotoxicity Of Aluminum Oxide Nanoparticles On Allium Cepa Root Tip—Effects Of Oxidative Stress Generation And Biouptake. **Environmental Science And Pollution Research,** V. 22, N. 14, P. 11057-11066, 2015/07/01 2015. Issn 1614-7499. Available At: < Https://Doi.Org/10.1007/S11356-015-4355-4 >.

Rajput, V. D. et.al. Effects Of Zinc-Oxide Nanoparticles On Soil, Plants, Animals And Soil Organisms: A Review. **Environmental Nanotechnology, Monitoring & Management,** V. 9, P. 76-84, 2018/05/01/ 2018. Issn 2215-1532. Available At: < Http://Www.Sciencedirect.Com/Science/Article/Pii/S2215153217302404 >.

Raliya, R. et.al. Mechanistic Evaluation Of Translocation And Physiological Impact Of Titanium Dioxide And Zinc Oxide Nanoparticles On The Tomato (Solanum Lycopersicum L.) Plant. **Metallomics,** V. 7, N. 12, P. 1584-1594, 2015. Issn 1756-5901. Available At: < <Go To Isi>://Wos:000365906300005 >.

Rao, S.; Shekhawat, G. S. Toxicity Of Zno Engineered Nanoparticles And Evaluation Of Their Effect On Growth, Metabolism And Tissue Specific Accumulation In Brassica Juncea. **Journal Of Environmental Chemical Engineering,** V. 2, N. 1, P. 105-114, 2014/03/01/ 2014. Issn 2213-3437. Available At: < Http://Www.Sciencedirect.Com/Science/Article/Pii/S2213343713002455 >.

Raskar, S. V.; Laware, S. L. Effect Of Zinc Oxide Nanoparticles On Cytology And Seed Germination In Onion. **Int J Curr Microbiol App Sci,** V. 3, N. 2, P. 467-73, 2014.

Sabir, S.; Arshad, M.; Chaudhari, S. K. Zinc Oxide Nanoparticles For Revolutionizing Agriculture: Synthesis And Applications. **The Scientific World Journal,** V. 2014, 2014. Issn 2356-6140.

Santhoshkumar, J.; Kumar, S. V.; Rajeshkumar, S. Synthesis Of Zinc Oxide Nanoparticles Using Plant Leaf Extract Against Urinary Tract Infection Pathogen. **Resource-Efficient Technologies,** V. 3, N. 4, P. 459-465, 2017/12/01/ 2017. Issn 2405-6537. Available At: < Http://Www.Sciencedirect.Com/Science/Article/Pii/S2405653717300647 >.

Shah, S. U. Importance Of Genotoxicity & S2a Guidelines For Genotoxicity Testing For Pharmaceuticals. **Iosr Journal Of Pharmacy And Biological Sciences,** V. 1, N. 2, P. 43-54, 2012.

Sinclair, S. A.; Kramer, U. The Zinc Homeostasis Network Of Land Plants. **Biochimica Et Biophysica Acta-Molecular Cell Research,** V. 1823, N. 9, P. 1553-1567, Sep 2012. Issn 0167-4889. Available At: < <Go To Isi>://Wos:000307918100015 >.

Takahashi, R. et.al. The Role Of Heavy-Metal Atpases, Hmas, In Zinc And Cadmium Transport In Rice. **Plant Signaling & Behavior,** V. 7, N. 12, P. 1605-1607, 2012. Issn 1559-2324

1559-2316. Available At: < Https://Www.Ncbi.Nlm.Nih.Gov/Pubmed/23072989 >.Available At: < Https://Www.Ncbi.Nlm.Nih.Gov/Pmc/Pmc3578901/ >.

Tumburu, L. Et.al. Molecular And Physiological Responses To Titanium Dioxide And Cerium Oxide Nanoparticles In Arabidopsis. **Environmental Toxicology And Chemistry,** V. 36, N. 1, P. 71-82, Jan 2017. Issn 0730-7268. Available At: < <Go To Isi>://Wos:000391029800011 >.

Umar, H.; Kavaz, D.; Rizaner, N. Biosynthesis Of Zinc Oxide Nanoparticles Using Albizia Lebbeck Stem Bark, And Evaluation Of Its Antimicrobial, Antioxidant, And Cytotoxic Activities On Human Breast Cancer Cell Lines. **International Journal Of Nanomedicine,** V. 14, P. 87-100, 2018. Issn 1178-2013

1176-9114. Available At: < Https://Www.Ncbi.Nlm.Nih.Gov/Pubmed/30587987 >.Available At: < Https://Www.Ncbi.Nlm.Nih.Gov/Pmc/Pmc6304255/ >.

Yoon, S.-J. et.al. Zinc Oxide Nanoparticles Delay Soybean Development: A Standard Soil Microcosm Study. **Ecotoxicology And Environmental Safety,** V. 100, P. 131-137, Feb 2014. Issn 0147-6513. Available At: < <Go To Isi>://Wos:000330161000018 >.

Yue, L. et.al. Molecular Mechanisms Of Maize Seedling Response To La 2 O 3 Np Exposure: Water Uptake, Aquaporin Gene Expression And Signal Transduction. **Environmental Science: Nano,** V. 4, N. 4, P. 843-855, 2017.

Zafar, H. et al. Effect Of Zno Nanoparticles On Brassica Nigra Seedlings And Stem Explants: Growth Dynamics And Antioxidative Response. **Frontiers In Plant Science,** V. 7, P. 535, 2016. Issn 1664-462x.

Zhang, R. et.al. Phytotoxicity Of Zno Nanoparticles And The Released Zn(Ii) Ion To Corn (Zea Mays L.) And Cucumber (Cucumis Sativus L.) During Germination. **Environ Sci Pollut Res Int,** V. 22, N. 14, P. 11109-17, Jul 2015. Issn 0944-1344.

Zhao, L. et.al. Transport Of Zn In A Sandy Loam Soil Treated With Zno Nps And Uptake By Corn Plants: Electron Microprobe And Confocal Microscopy Studies. **Chemical Engineering Journal,** V. 184, P. 1-8, 2012/03/01/ 2012. Issn 1385-8947. Available At: < Http://Www.Sciencedirect.Com/Science/Article/Pii/S1385894712000447 >.

Zhao, L. J. et.al. Influence Of Ceo2 And Zno Nanoparticles On Cucumber Physiological Markers And Bioaccumulation Of Ce And Zn: A Life Cycle Study. **Journal Of Agricultural And Food Chemistry,** V. 61, N. 49, P. 11945-11951, Dec 2013. Issn 0021-8561. Available At: < <Go To Isi>://Wos:000328439700010 >.

CHAPTER 2

2.1. Introduction

Zinc is one of the essential micronutrients for both plant and human nutrition. However, almost half (49%) of agricultural soil does not have adequate amount of zinc and one-third of global population suffers from zinc micronutrient deficiencies . Zinc deficiency is a major concern as it has affected public health, and led to infant mortality, growth, cognitive and immune impairments and enhanced susceptibility to diarrhea . Zinc is a *type 2* nutrient required for general human metabolism . Recommended daily intakes range between 3 and 16 mg Zn day^{-1} depending on age, gender, type of diet and other factors . National Institutes of Health (NIH) recommends a dose of 11 mg per day for men and 8 mg per day for women . In humans and higher animals, zinc plays roles in neurotransmitters, cells in the salivary glands, prostate, immune system and intestine . World Health Organization (WHO) estimates that zinc deficiency contributes to more than one-third of all child deaths . In socio-economically challenged countries, the zinc deficiency problem is very acute, and ~2 billion people are vulnerable to growth retardation due to zinc deficiency .

Dietary zinc is found in meat, poultry, sea food, milk and milk products, whole grains, legumes, and pumpkin among others . Animal-derived foods contain up to 189% more zinc than plant-based (unfortified) foods . It is important to ensure high zinc availability in plant-based food products. A range of strategies are proposed to alleviate zinc in human diet. A number of approaches have been studied to increase zinc availability in human foods . These approaches are: (1) supplementation, (2) food fortification, (3) food diversification, and (5) crop biofortification. Developments in genomics and transgenics have opened up new avenues to improve zinc content in wheat . Traditional agronomic methods involve application of soil fertilizers .

Soil is the main depository of zinc for plant uptake. Most agricultural soil contains 10-300 mg of zinc per kg of soil which translates to 10^{-8}-10^{-6} M in soil solution . However, uptake of zinc by plants from soil is controlled by the rhizosphere biogeochemistry. Agronomic biofortification of zinc in edible crops typically involve broadcasting zinc fertilizers .

The development in nanotechnology has opened possible avenues for nanomaterials to be used as fertilizers and fortifying agents. The greater surface to mass ratio of NPs as compared to their bulk counterparts renders them biologically active . However, the surge of literature on the effects of nanoparticles on plants have revealed contrasting results. In green pea exposed to ZnO NPs (25, 250, and 500 mg/kg soil) root elongation, reduced chlorophyll and catalase content in leaves, reduced ascorbate peroxidase activity in roots and leaves, and increased lipid peroxidation were observed . At 2000 mg/kg of ZnO NP in the soil, cucumber was found to have decreased shoot, root length, and biomass . Again, at 500 and 750 mg/kg, ZnO NPs caused 80% reduction in alfalfa (*Sinorhizobium meliloti*) root and shoot biomass . ZnO NPs did not cause a significant impact in plant biomass of wheat grown in sand matrix, although there were changes in root length (decrease) and root number (increase) as compared to the control, and bioaccumulation of Zn was also observed in the shoots . Soybean grown with ZnO NPs in soil (50, 100, 500 mg/kg) exhibited no change in growth parameters . High accumulation of Zn in different parts of soybean (root, nodule, stem, leaf and pod) was recorded when exposed to high concentration of ZnO NPs (500 mg/kg) in soil . In another study, it was found that ZnO NPs at 100 mg/kg of soil caused significant changes in soybean micronutrient and macronutrient concentrations as compared to the control, notably Zn in leaves, pods, stems and roots, Cu, Mg, K in roots, Fe in leaves, and Mo in nodules . However, most of these studies did not demonstrate effects of ZnO NPs at environmentally relevant concentrations (100-300 mg/kg). Low-dose exposure studies rather than high-dose

exposure studies are warranted . It has been observed that NPs are taken up by roots via endocytosis . Further, NPs undergo rapid dissolution in aqueous media and ions are easily taken up by plants . Our preliminary work has confirmed that ZnO NPs undergo dissolution in Harmens nutrient media and are taken up as Zn^{2+} ions by spinach plants. Nanoparticles having a core element as micronutrient have possible applications in fortification of crops. The main objective of this work is to determine the bioaccumulation of zinc in seeds and soy-products (soymilk and soy-pulp) when exposed to ZnO NPs. In the current research, we have studied the bioaccumulation of Zn in edible parts of soybean and soy-based products from the soybean grown in environmentally relevant concentrations of ZnO NPs (2.27, 22.75, 227.50 mg Zn/kg of soil). Environmentally relevant concentration of Zn in soil ranges from 100-300 mg per kg of soil . The sufficient requirement of Zn for soybean is 21-80 mg/kg of soil . Three applications of treatments were given to the soil, once after planting (at day 0), the second at the onset of V1 (first trifoliate) stage, and the third at R1 (beginning of flowering).

2.2. Materials and Methods

2.2.1. ZnO NP Characterization

For zeta (ζ)-potential and hydrodynamic diameter measurements, the nano-particles (500 mg Zn L^{-1}) were dispersed in de-ionized water using a sonicator (30 sec). The zeta (ζ)-potential and particle diameter distribution were recorded with a ZetaSizer (Nano-ZS 90, Malvern) without any pH adjustment. For particle size distribution, Transmission Electron Microscope (TEM, JEOL JEM-2100 LaB6 TEM, JEOL USA, Peabody MA); the TEM was operated at 200 kV. Bright-field images of each sample were acquired with a Gatan Orius SC1000 CCD camera; dark-field imaging utilized a Gatan 805 High Angle Annular Dark Field detector with a Gatan Digiscan II controller unit and the TEM running in scanning transmission electron microscopy (STEM) mode.

2.2.2. Plant Growth

Soybean (*Glycine max*) seeds (500 mg) were weighed and inoculated with legume-root nodule bacteria, *Bradyrhizobium japonicum* strain (88 g per 25 kg seed). Five seeds were planted per pot (30.48 cm height X 29.2 cm diameter) in soil (Sunshine Professional Gardening Mix LG 3) and placed in the greenhouse. The average weight of soil in each pot was 2.72±0.11 kg. Growth conditions were 14/10 h of light/dark, relative humidity of 27% and temperature of 21-24 ^{o}C. The experiment was designed as a completely randomized with triplicates for each treatment; the randomization was done using ARM software (Gylling Data Management, Inc).

2.2.3. Treatment

Soybean growth can be broadly classified into two stages: Vegetative stage and Reproductive stage. Vegetative stage comprises of VE (emergence), VC (unrolled unifoliate leaves), V1 (first trifoliate), V2 (second trifoliate), V4 (fourth trifoliate), and V(n) (nth trifoliate). The reproductive stage comprises of R1 (beginning of flowering), R2 (full flowering), R3 (beginning of pod formation), R4 (full pod), R5 (beginning of seed), R6 (full seed), R7 (beginning of pod maturity), and R8 (full maturity of pod). Treatment applications were given three times in the life cycle of the plant: at planting (Day 0), at the onset of V1 and at R1 stages (Table 2.1). The treatment at planting (day 0) was started after the seeds were planted in the soil. There were three treatments namely ZnO NP, $ZnSO_4$, and No Zn with three dosages for ZnO NP and $ZnSO_4$ (X, 10X, and 100X) (Table 2.2). On Day 0, the treatments i.e. ZnO NP/$ZnSO_4$ (1L) were applied on the soil after the seeds were planted whereas control seeds were watered with regular tap water (1L). The same zinc treatments were also applied at V1 and R1 stage. On other days, the plants were watered daily with tap water (0.5 L).

Table 2.1 Growth Stages of Soybean Plant and Treatments Applied

Stages of Growth in Soybean			**Treatments Applied**
Vegetative Stage	**Day 0**	Planting	**Treatment 1**
	VE	Emergence	No treatment
	VC	Unrolled unifoliate leaves	No treatment
	V1	First trifoliate	**Treatment 2**
	V2	Second trifoliate	No treatment
	V4	Fourth trifoliate	No treatment
	V5	Fifth trifoliate	Plant height measured
	V(n)	nth trifoliate	No treatment
Reproductive Stage	**R1**	Beginning of flowering	**Treatment 3** Chlorophyll content measured
	R2	Full flowering	No treatment
	R3	Beginning of pod formation	No treatment
	R4	Full pod	No treatment
	R5	Beginning of seed	No treatment
	R6	Full seed	No treatment
	R7	Beginning of pod maturity	No treatment Chlorophyll content measured
	R8	Full maturity of pod	No treatment Plant height measured

Table 2.2. The dosages of zinc applied per pot for each treatment. The figures in parenthesis is the dosage of chemical species (ZnO NP or $ZnSO_4$) per unit weight of soil (each pot had 2.72±0.11 kg soil). The dosages of zinc species (ZnO NP or $ZnSO_4$) applied is normalized for the mass of Zn. X = 2.27 mg/kg of soil

Treatment	X	10X	100X
ZnO NP	6.2 mg/pot (2.27 mg/kg soil)	62 mg/pot (22.75 mg/kg soil)	620 mg/pot (227.50 mg/kg soil)
$ZnSO_4.7H_2O$	X	10X	100X
	22.1 mg/pot (8.12 mg/kg soil)	221.5 mg/pot (81.28 mg/soil)	2215 mg/pot (812.80 mg/kg soil)
Control	No Zn Applied		

2.2.4. Growth Monitoring

Plant height (length of the plant from tip to soil surface) was measured at V5 and R8 stages using a ruler (Pickett P232E). Relative chlorophyll content was measured using a handheld SPAD meter (atLEAF Digital Chlorophyll Meter) at R1 and R7 stages.

2.2.5. Preparation of Soy Concentrate and Pulp (Okara)

Soy concentrate is the emulsion of water, oil, and protein obtained from soybean seeds. Soy concentrate was produced from dry soybeans using a method after Poliseli-Scopel . The method was modified as the amount of sample (seeds) for each treatment was less, hence we used a mortar and pestle to grind the seeds. Soybean seeds were soaked for 15 h (3:1, water:soybean) at 15 ^{o}C and then were ground. The pulp was separated by filtration (dry soybean:water ratio=1:6.27) using quantitative grade filter paper (Whatman 541). pH of the concentrate was measured using a pH meter (VWR Symphony B10P) during the storage period (The mean pH was 6.65 ± 0.5). The soymilk and the pulp (the fibrous tissue remaining on the filter paper after filtering the soy concentrate) was stored at 4 ^{o}C in a refrigerator and analyzed within 24 h.

2.2.6. Inductively Coupled Plasma-Atomic Emission Spectroscopy (ICP-OES) Analysis

Digested samples of pods, seeds, pulp, soymilk and soil samples were analyzed for elemental content with ICP-OES (Spectro Genesis). Before analysis, the samples (pods, seeds, pulp and soil) were dried in the oven (65 ^{o}C for 48 h) and were powdered and homogenized using liquid nitrogen in mortar and pestle. The samples were digested in nitric acid (HNO_3) of molarity 15.8 and deionized Milipore water (1:1) in CEM Mars Xpress microwave digester with Xpress vessels (55 mL PFA venting) with the following method: approximately 250 mg dry sample material, 5 mL concentrated acid, 5 mL distilled water, overnight pre-digestion, microwaving at 125 ^{o}C for 10 min after 20 min ramp.

The rinse solutions, digests, and blanks were analyzed via Genesis SOP ICP-OES with SmartAnalyzer Vision software (v. 3.013.0752) for Zn (wavelength 213.8 nm). Quality control included ICALization (Intelligent Calibration Logic to normalizes the wavelength scale), standard

calibration, control calibration verification, and digestion of a certified reference plant material (CRM) (NCS DC 73350 poplar leaves, China National Analysis Center of Iron and Steel). The acid extractions were analyzed for 25 elements: Ag, Al, As, B, Ba, Be, Ca, Cd, Ce, Co, Cr, Cu, Fe, K, Li, Mg, Mn, Mo, Ni, P, Pb, S, Sb, Se, Si, Sn, Sr, Ti, Tl, V, and Zn. Only elements consistently measured above the instrument detection limits are further discussed. The percent recovery was 80% for the CRM and 81% for total Zn recovered from NPs. Method detection limits (MDL) were determined by using typical sample weight, extraction volume, and the instrument detection limit, and these values were used to substitute those values below the MDL.

2.2.7. Statistical Analysis

All experiments were done in replicates (n = 3) unless otherwise specified, and the mean values are reported along with the standard deviations. One-way ANOVA followed by Tukey's Pairwise Comparison was performed on the normally distributed data using Minitab software at $\alpha = 0.05$.

2.3. Results and Discussion

2.3.1. ζ-Potential and Particle Size

The ζ-potential of the ZnO NPs was found to be 25.9±4.7 mV and hydrodynamic diameter was found to be 512.5 nm in DI water. The particle size ranged from 8-173 nm, and 92.96% of the ZnO NPs had the smallest dimension within 100 nm (Figure 2.1).

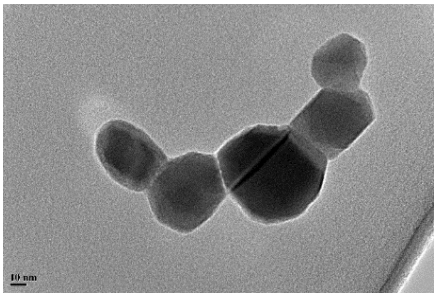

(a)

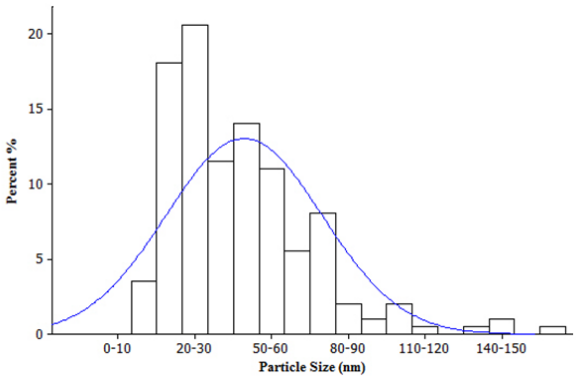

(b)

Figure 2.1. Particle characterization of ZnO NPs. (a) TEM micrograph of bare ZnO NPs, and (b) particle size distribution (based on smallest dimension)

2.3.2. Effects of ZnO NPs on the Plant Growth Metrics

2.3.2.1. Plant Height

The treatments were applied to the soil at three stages of soybean growth, at planting, at the onset of V1 stage, and at R1 stage (Table 2.2). Plant height was recorded at the end of the vegetative stage and at the maturity stage (end of reproductive stage). There is no significant difference in height between the treatments (ZnO NP, $ZnSO_4$, and No Zn) at V5 growth stage at p-value<0.05 (Figure 2.2). At R8 growth stage, there was significant difference between plant height in ZnO NP X and $ZnSO_4$ 100X treatment plants. However, since their Zn concentrations are not same, they are not comparable.

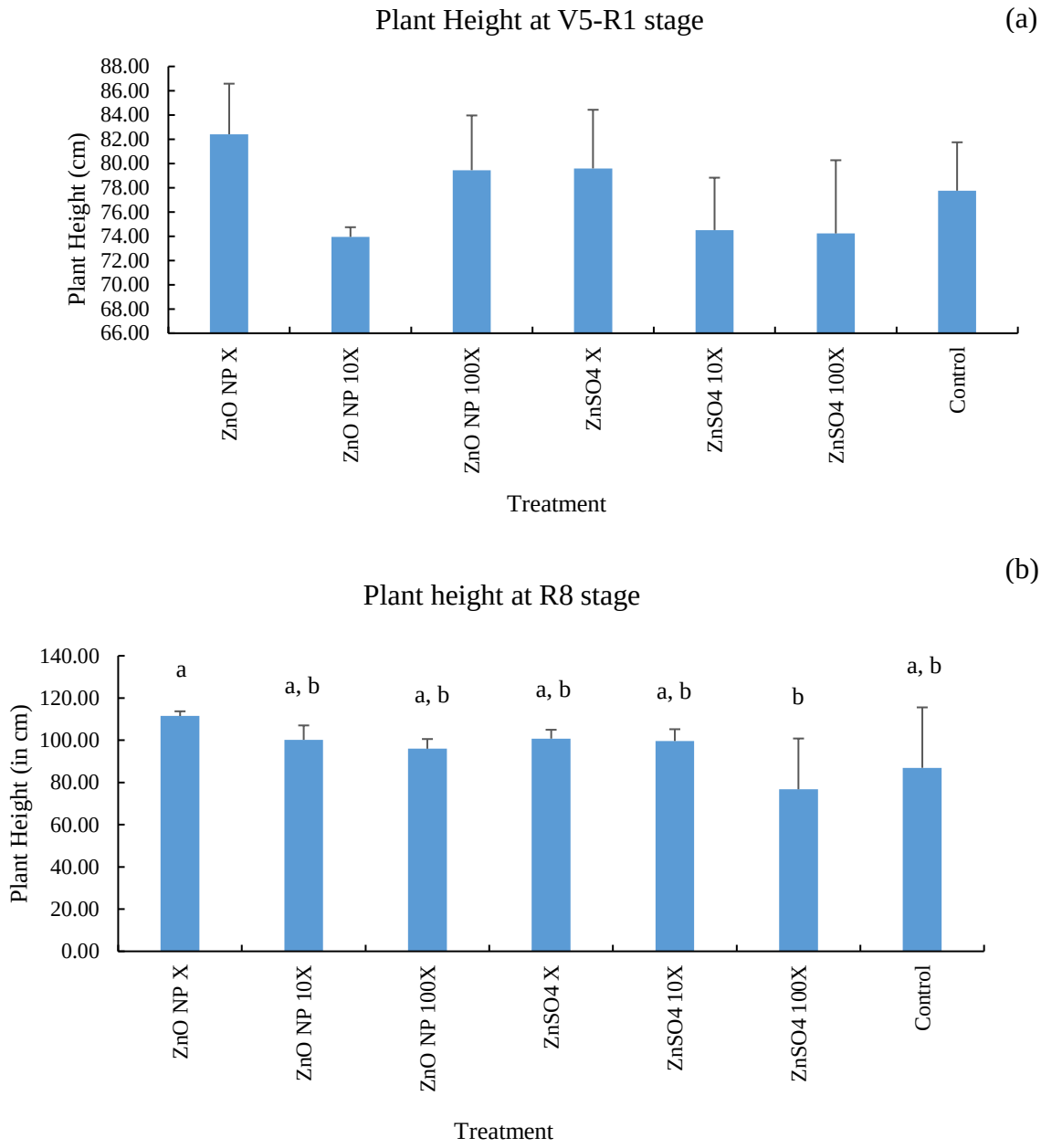

Figure 2.2. (a) Plant Height (in cm) at V5-R1 Stage (b) Plant Height (in cm) at R8 Stage. Plant height is recorded on the Y-axis and treatments are on the X-axis. Means that do not share a letter are significantly different at $p<0.05$.

2.3.2.2. Chlorophyll Content

Relative chlorophyll content was measured with the SPAD meter at two stages of plant growth, R1 stage and R7 stage. In both the stages, no significant difference was observed between

the chlorophyll content of ZnO NP and $ZnSO_4$ of all dosages and No Zn treatment at p-value<0.05. Even with the highest ZnO NP treatment (100X), the plants did not show any signs of diminished chlorophyll content. The relative chlorophyll content decreased from R1 to R7 stage which is expected as the plants were nearing maturity at R7 stage (Figure 2.3).

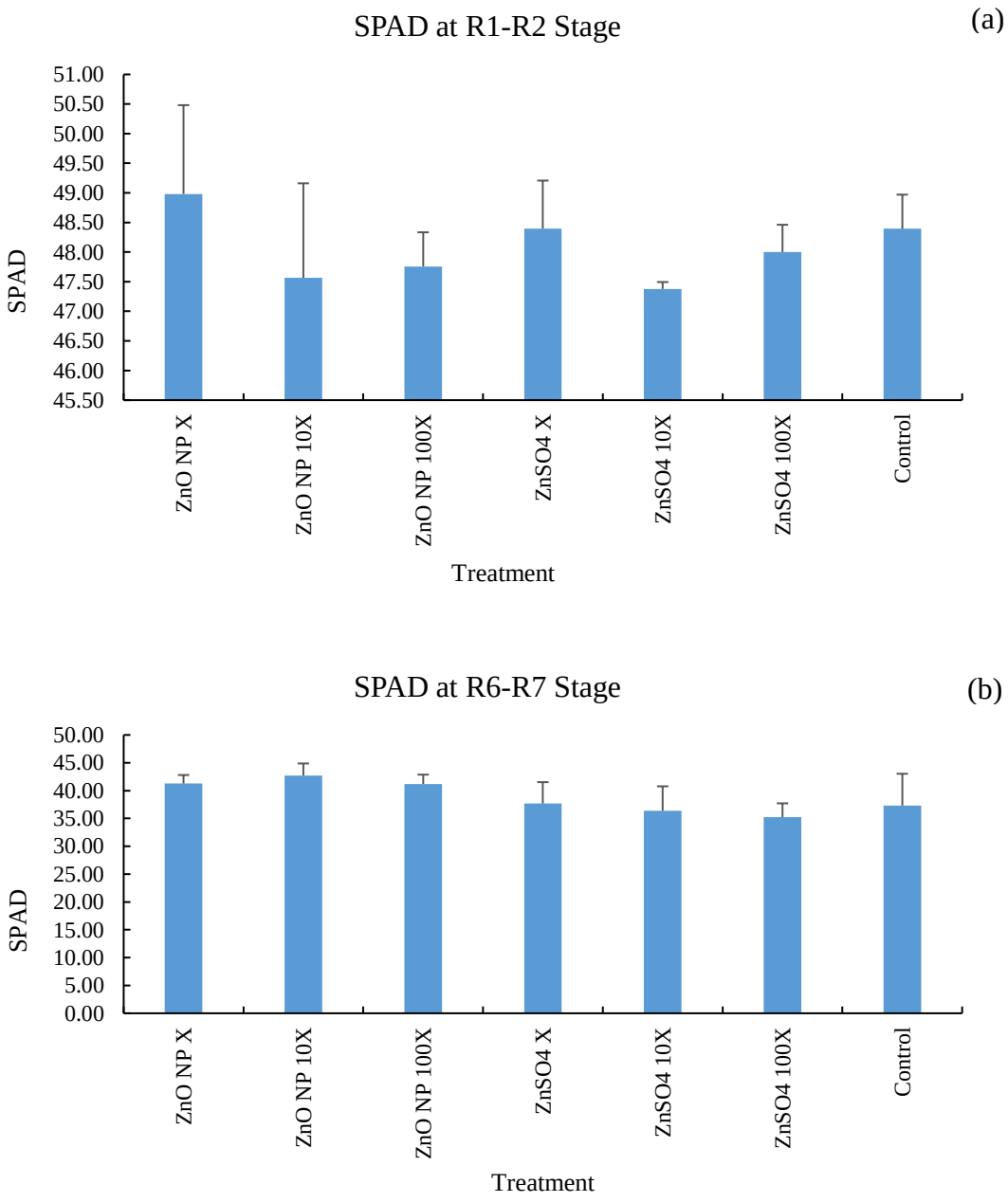

Figure 2.3. Relative chlorophyll content (SPAD) of soybean plants at: (a) R1-R2 stage (b) R6-R7 stage.

2.3.2.3. Number of Pods

The number of pods in each plant was measured at R8 stage. There was significant difference in the number of pods of plants of ZnO NP X and $ZnSO_4$ X treatments. No significant difference was observed between the number of pods of ZnO NP and $ZnSO_4$ with No Zn treatment at p-value<0.05. (Figure 2.4).

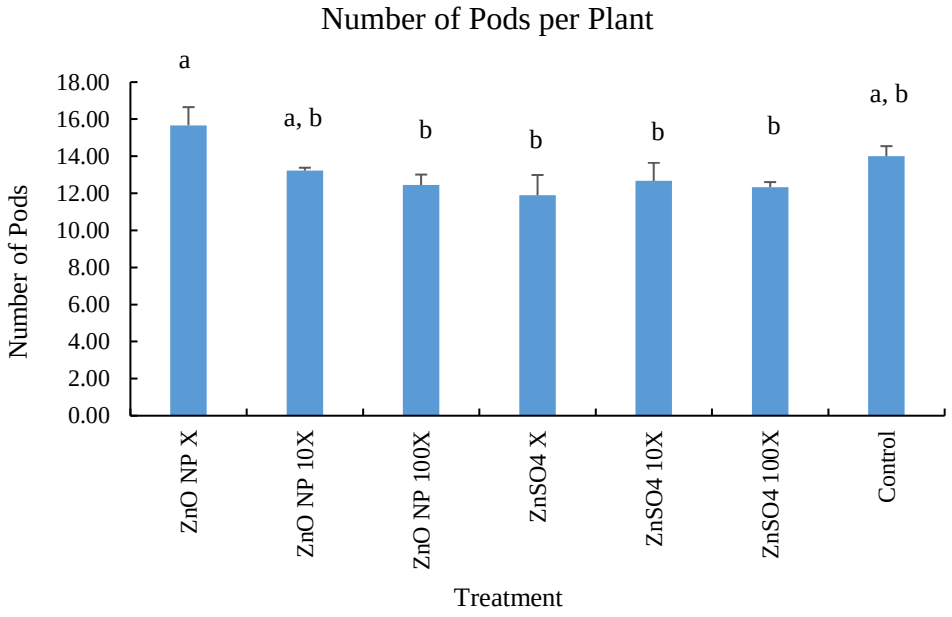

Figure 2.4. Number of pods per plant at maturity (R8 stage). Means that do not share a letter are significantly different at p<0.05.

2.3.2.4. Bioaccumulation of Zinc

ICP-OES was used to determine the mineral content present in the soybean seeds, soy concentrate (soymilk) and pulp (okara).

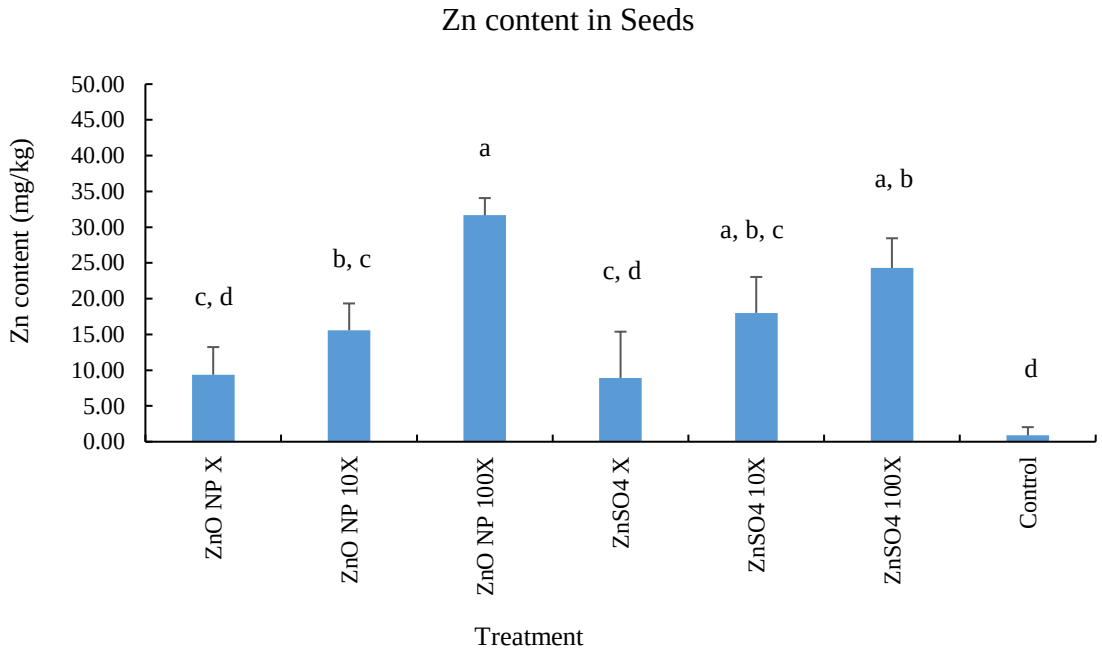

Figure 2.5. Zn content in soybean seeds. Means that do not share a letter are significantly different at $p<0.05$.

In the seeds, Zn accumulation increased in a dose-dependent manner, with 100X treatment being significantly different from X treatment in both ZnO NP and $ZnSO_4$ (Figure 2.5). Zn accumulation in ZnO NP 10X and 100X is also significantly higher than control treatment. Similar trend is observed in $ZnSO_4$ 10X and 100X. However, between ZnO NP and $ZnSO_4$ there is no significant difference in the Zn accumulation between the same dosages. The zinc content in the seeds of ZnO NP 100X was found to be 31.97±2.40 mg/kg while that of the seeds of control treatment was 0.88±1.16 mg/kg. ZnO NPs can thus contribute towards the required dietary zinc levels. A logarithmic relationship was found between the dosage of ZnO NPs applied and Zn accumulation in the seeds (R^2 0.9897). A similar relationship was found in the case of dosage of $ZnSO_4$ and Zn accumulation in the seeds (R^2 0.9469) (Figure 2.6).

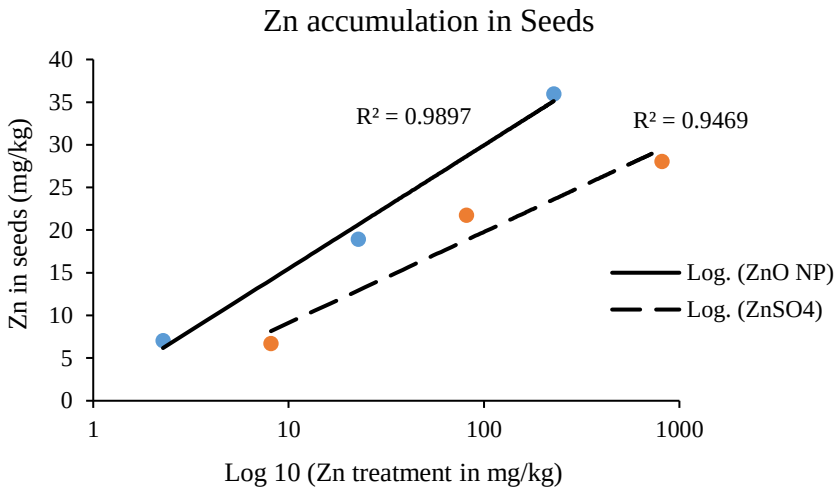

Figure 2.6. Relationship of Zn dosage applied and Zn accumulation in the seeds. The x-axis is the concentration of soil-applied Zn in $\log_{10}$ of mg/kg, and the y-axis is the concentration of Zn accumulated in the seeds in mg/kg.

The concentration of other essential elements (Ca, Fe, K, Mg, Mo, Mo, and P) in the seeds were also determined. However, there were no significant differences between the element concentration in the seeds of ZnO NP, $ZnSO_4$, and control treatments (Table 1, Appendix A). This indicates that ZnO NPs did not significantly alter the nutritional value of soybean.

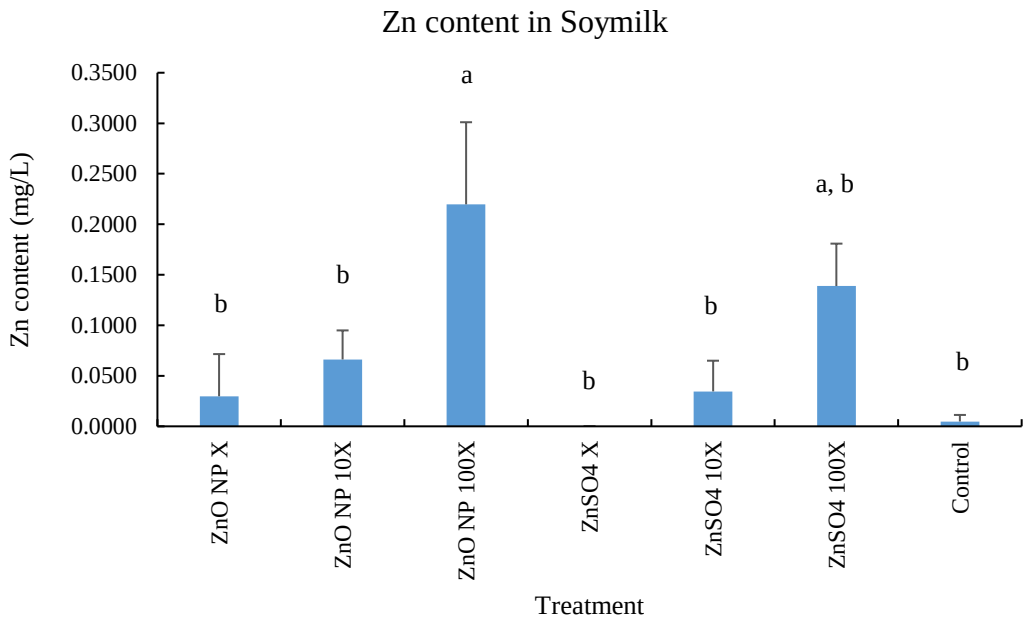

Figure 2.7. Zn content in soymilk (Means that do not share a letter are significantly different at $p<0.05$).

The Zn content in soy concentrate (soymilk) in ZnO NP 100X treatment was found to be significantly higher than control (Figure 2.7). However, the trend was not same for $ZnSO_4$ treatments, as there were no significant differences between all dosages of $ZnSO_4$ and control.

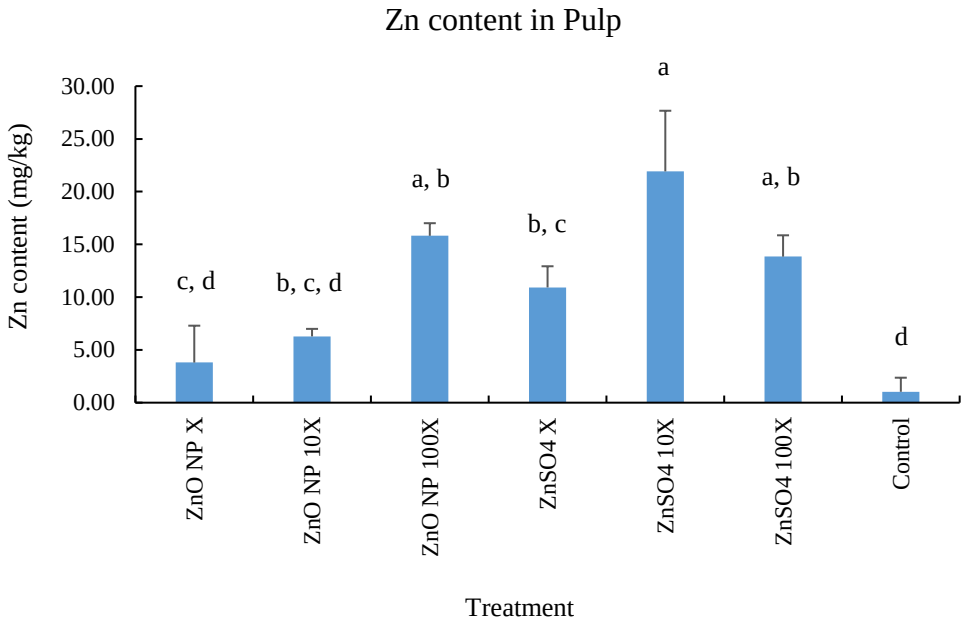

Figure 2.8. Zn content in pulp (Means that do not share a letter are significantly different at $p<0.05$).

In the case of pulp, the Zn accumulation increases in a dose-dependent manner with ZnO NP treatments (Figure 2.8). However, in the case of $ZnSO_4$ treatments, Zn accumulation increases in $ZnSO_4$ 10X treatment as compared to $ZnSO_4$ X, however, declines in $ZnSO_4$ 100X treatment. There was significant difference between Zn content of pulp of ZnO NP 100X and control, and $ZnSO_4$ 10X and control.

It is evident from the findings that there are no significant differences in plant growth parameters (height, relative chlorophyll content, and number of pods) of control plants (no Zn treatment) and ZnO NP/$ZnSO_4$ treated plants. In case of the seeds, Zn accumulation increased in a dose-dependent manner in both ZnO NP and $ZnSO_4$ treated plants. Zn accumulation in ZnO NP 10X and 100X, and $ZnSO_4$ 10X and 100X was significantly higher than control seeds. However, there was no significant difference between Zn accumulation in seeds of ZnO NP and $ZnSO_4$ treatments. Although the effects and bioaccumulation of both ZnO NPs and $ZnSO_4$ treatments are comparable at the same dosage, the amount of $ZnSO_4$ used was 3.6 times higher than ZnO NPs to

yield the same unit amount of Zn (Table 2.2). Hence, the usage of ZnO NPs can significantly lower the cost of Zn required for fortification. In addition, previous research have shown that $ZnSO_4$ has higher solubility than ZnO NPs, and the property of immediate dissolution after soil application can result in a sharp increase in soil Zn followed by a decline . However, ZnO NPs dissolve slowly and can release Zn over a longer period of time which is beneficial for crops. From an economic perspective, the market price of ZnO NPs is lower than $ZnSO_4$ ($ZnSO_4.7H_2O$). Cost comparisons of agricultural grade ZnO NPs and $ZnSO_4$ from the online database Alibaba showed that the cost of 80-99% pure ZnO NPs is $188 per unit metric ton, and that of 21% $ZnSO_4.7H_2O$ is $300 . Our findings indicate that ZnO NP is not phytotoxic at environmentally relevant concentrations, and on the contrary, can be used as an alternative to traditional Zn fertilizers like $ZnSO_4$.

2.4. Conclusion

There was accumulation of Zn in the seeds, soy concentrates and pulp from the ZnO NP treatments that was applied to the soil. However, addition of ZnO NPs did not significantly affect plant biomass and growth. Zn accumulation in ZnO NP 100X seeds is significantly different from that of control and correspond to dietary Zn levels. Furthermore, less amount of ZnO NPs is required to yield a unit of zinc as compared to $ZnSO_4$, thereby making ZnO NPs as a cost-effective alternative to traditional fertilizers like $ZnSO_4$. While Zn occurs in higher levels in meat and sea-food, there are fewer vegetarian options that contain naturally high levels of Zn. Zn fortified soymilk and soy-products like tofu and processed pulp can be a very good source of Zn for vegetarian diets. Soybean fortified using ZnO NPs in the soil is found to alleviate Zn levels in soybean seeds and pulp without affecting plant growth, biomass, and other levels of other micronutrients, thus addressing nutrient security.

2.5. Reference

alibabagroup.Com. 2018.

Bandyopadhyay, S. et al. Comparative Phytotoxicity Of Zno Nps, Bulk Zno, And Ionic Zinc Onto The Alfalfa Plants Symbiotically Associated With Sinorhizobium Meliloti In Soil. **Science Of The Total Environment,** V. 515, P. 60-69, May 2015. Issn 0048-9697. Available At: < <Go To Isi>://Wos:000352040700007 >.

Borrill, P. et al. Biofortification Of Wheat Grain With Iron And Zinc: Integrating Novel Genomic Resources And Knowledge From Model Crops. **Frontiers In Plant Science,** V. 5, Feb 21 2014. Issn 1664-462x.

Broadley, M. R. et al. Zinc In Plants. **New Phytologist,** V. 173, N. 4, P. 677-702, 2007. Issn 1469-8137.

Dimkpa, C. O. et al. Cuo And Zno Nanoparticles: Phytotoxicity, Metal Speciation, And Induction Of Oxidative Stress In Sand-Grown Wheat. **Journal Of Nanoparticle Research,** V. 14, N. 9, Sep 2012. Issn 1388-0764.

Gregory, P. J. et al. Approaches To Reduce Zinc And Iron Deficits In Food Systems. **Global Food Security,** V. 15, P. 1-10, 2017/12/01/ 2017. Issn 2211-9124. Available At: < Http://Www.Sciencedirect.Com/Science/Article/Pii/S2211912416301390 >.

Guo, D.; Xie, G.; Luo, J. Mechanical Properties Of Nanoparticles: Basics And Applications. **Journal Of Physics D: Applied Physics,** V. 47, N. 1, P. 013001, 2013. Issn 0022-3727.

Gupta, U. C.; Gupta, S. C. Sources And Deficiency Diseases Of Mineral Nutrients In Human Health And Nutrition: A Review. **Pedosphere,** V. 24, N. 1, P. 13-38, 2014/02/01/ 2014. Issn 1002-0160. Available At: < Http://Www.Sciencedirect.Com/Science/Article/Pii/S1002016013600776 >.

Helfenstein, J. et al. Zinc Deficiency Alters Soybean Susceptibility To Pathogens And Pests. **Journal Of Plant Nutrition And Soil Science,** V. 178, N. 6, P. 896-903, Dec 2015. Issn 1436-8730. Available At: < <Go To Isi>://Wos:000368436100010 >.

Hershfinkel, M.; Silverman, W. F.; Sekler, I. The Zinc Sensing Receptor, A Link Between Zinc And Cell Signaling. **Molecular Medicine,** V. 13, N. 7-8, P. 331-336, Jul-Aug 2007. Issn 1076-1551.

Joy, E. J. M. et al. Valuing Increased Zinc (Zn) Fertiliser-Use In Pakistan. **Plant And Soil,** V. 411, N. 1, P. 139-150, 2017/02/01 2017. Issn 1573-5036. Available At: < Https://Doi.Org/10.1007/S11104-016-2961-7 >.

Zinc-Enriched Fertilisers As A Potential Public Health Intervention In Africa. **Plant And Soil,** V. 389, N. 1, P. 1-24, 2015/04/01 2015. Issn 1573-5036. Available At: < Https://Doi.Org/10.1007/S11104-015-2430-8 >.

Kiekens, L. Zinc. In: Alloway, B. J., Ed. (Ed.). **Heavy Metals In Soils**. 2. London: Blackie Academic And Professional, 1995. P. 284-305.

Kim, S.; Kim, J.; Lee, I. Effects Of Zn And Zno Nanoparticles And Zn2+On Soil Enzyme Activity And Bioaccumulation Of Zn In Cucumis Sativus. **Chemistry And Ecology,** V. 27, N. 1, P. 49-55, 2011. Issn 0275-7540. Available At: < <Go To Isi>://Wos:000287408400005 >.

King, J. C. Zinc: An Essential But Elusive Nutrient. **American Journal Of Clinical Nutrition,** V. 94, N. 2, P. 679s-684s, Aug 2011. Issn 0002-9165.

Li, C. et al. Absorption Of Foliar-Applied Zn Fertilizers By Trichomes In Soybean And Tomato. **Journal Of Experimental Botany,** V. 69, N. 10, P. 2717-2729, 2018. Issn 0022-0957. Available At: < Http://Dx.Doi.Org/10.1093/Jxb/Ery085 >.

Lim, H. K. et al. Iron And Zinc Nutrition In The Economically-Developed World: A Review. **Nutrients,** V. 5, N. 8, 2013. Issn 2072-6643.

Liu, Q. et al. Carbon Nanotubes As Molecular Transporters For Walled Plant Cells. **Nano Letters,** V. 9, N. 3, P. 1007-1010, Mar 2009. Issn 1530-6984.

Lv, J. et al. Accumulation, Speciation And Uptake Pathway Of Zno Nanoparticles In Maize. **Environmental Science-Nano,** V. 2, N. 1, P. 68-77, Feb 2015. Issn 2051-8153.

Milani, N. **Zinc Oxide Nanoparticles In The Soil Environment: Dissolution, Speciation, Retention, And Bioavailability**. 2011. (Doctor Of Philosophy). Soil Science, The University Of Adelaide, Adelaide.

Miralles, P.; Church, T. L.; Harris, A. T. Toxicity, Uptake, And Translocation Of Engineered Nanomaterials In Vascular Plants. **Environmental Science &Amp; Technology,** V. 46, N. 17, P. 9224-9239, Sep 2012. Issn 0013-936x.

Mukherjee, A. Et Al. Physiological Effects Of Nanoparticulate Zno In Green Peas (Pisum Sativum L.) Cultivated In Soil. **Metallomics,** V. 6, N. 1, P. 132-138, 2014. Issn 1756-5901. Available At: < <Go To Isi>://Wos:000328891100013 >.

Peralta-Videa, J. R. et al. Cerium Dioxide And Zinc Oxide Nanoparticles Alter The Nutritional Value Of Soil Cultivated Soybean Plants. **Plant Physiology And Biochemistry,** V. 80, P. 128-135, Jul 2014. Issn 0981-9428.

Poliseli-Scopel, F. H. et al. Comparison Of Ultra High Pressure Homogenization And Conventional Thermal Treatments On The Microbiological, Physical And Chemical Quality Of Soymilk. **Lwt-Food Science And Technology,** V. 46, N. 1, P. 42-48, Apr 2012. Issn 0023-6438.

Priester, J. H. et al. Soybean Susceptibility To Manufactured Nanomaterials With Evidence For Food Quality And Soil Fertility Interruption. **Proceedings Of The National Academy Of Sciences Of The United States Of America,** V. 109, N. 37, P. E2451-E2456, Sep 11 2012. Issn 0027-8424.

Damage Assessment For Soybean Cultivated In Soil With Either Ceo2 Or Zno Manufactured Nanomaterials. **Science Of The Total Environment,** V. 579, P. 1756-1768, Feb 2017. Issn 0048-9697. Available At: < <Go To Isi>://Wos:000393320400076 >.

Rangan, A. M.; Samman, S. Zinc Intake And Its Dietary Sources: Results Of The 2007 Australian National Children's Nutrition And Physical Activity Survey. **Nutrients,** V. 4, N. 7, 2012. Issn 2072-6643.

Servin, A. D.; White, J. C. Nanotechnology In Agriculture: Next Steps For Understanding Engineered Nanoparticle Exposure And Risk. **Nanoimpact,** V. 1, P. 9-12, 2016. Issn 2452-0748. Available At: < Http://Www.Sciencedirect.Com/Science/Article/Pii/S2452074815300185 >.

Sinclair, S. A.; Kramer, U. The Zinc Homeostasis Network Of Land Plants. **Biochimica Et Biophysica Acta-Molecular Cell Research,** V. 1823, N. 9, P. 1553-1567, Sep 2012. Issn 0167-4889.

Soybean And Nutrition. Croatia, 2011.

Sutradhar, A. K. et al. Zinc For Crop Production. 2016. Avaialble At: < Https://Www.Extension.Umn.Edu/Agriculture/Nutrient-Management/Micronutrients/Zinc-For-Crop-Production/ >.

Trumbo, P. Et Al. Dietary Reference Intakes: Vitamin A, Vitamin K, Arsenic, Boron, Chromium, Copper, Iodine, Iron, Manganese, Molybdenum, Nickel, Silicon, Vanadium, And Zinc. **Journal Of The American Dietetic Association,** V. 101, N. 3, P. 294-301, Mar 2001. Issn 0002-8223.

Wang, Y.-H. Et Al. Cost Of Agronomic Biofortification Of Wheat With Zinc In China. **Agronomy For Sustainable Development,** V. 36, N. 3, P. 44, 2016/07/25 2016. Issn 1773-0155. Available At: < Https://Doi.Org/10.1007/S13593-016-0382-X >.

Wang, Z. Y. Et Al. Xylem- And Phloem-Based Transport Of Cuo Nanoparticles In Maize (Zea Mays L.). **Environmental Science &Amp; Technology,** V. 46, N. 8, P. 4434-4441, Apr 2012. Issn 0013-936x.

White, P. J.; Greenwood, D. J. Properties And Management Of Cationic Elements For Crop Growth. **Soil Conditions And Plant Growth**, P. 160-194, 2013. Issn 1118337298.

World Health Statistics. 2013

Yuan, J. et al. Internalization And Phytotoxic Effects Of Cuo Nanoparticles In Arabidopsis Thaliana As Revealed By Fatty Acid Profiles. **Environmental Science &Amp; Technology,** V. 50, N. 19, P. 10437-10447, Oct 2016. Issn 0013-936x.

Zhai, G. et al. Transport Of Gold Nanoparticles Through Plasmodesmata And Precipitation Of Gold Ions In Woody Poplar. **Environmental Science &Amp; Technology Letters,** V. 1, N. 2, P. 146-151, Feb 2014. Issn 2328-8930.

Zinc. 2016.

CHAPTER 3

3.1. Introduction

Engineered Nanomaterials (ENMs) are increasingly used in agriculture. The most commonly used nanomaterials in agriculture are iron, zinc oxide, silver, gold, copper oxide, titanium dioxide, silica, aluminum oxide, carbon nanotubes, and graphene . Zinc oxide nanoparticles (ZnO NPs) are considered to be more effective in releasing zinc to soil due to their enhanced reactivity as compared to their bulk counterparts . ZnO NPs are currently being explored for agricultural applications such as antimicrobial agent, pesticide, fungicide, herbicide, fertilizer, sensor, and general soil improvement .

Prior to commercializing ENMs for agricultural purposes, it is crucial to evaluate the possible toxicity, uptake, transport, and fate of ENMs in plants. While there are some studies on toxicity of ZnO NPs , literature on the mechanisms of ZnO NP uptake by plants is still very less. The knowledge of the form and temporal localization of ENMs and its transformation product in plants would help elucidate the mechanisms of cellular uptake of ENMs and their interactions with plants.

Detection of ZnO NPs in biological matrices is challenging due to its size and uncertainty of (bio)transformation. Inductively coupled plasma-optical emission spectrometry/mass spectroscopy (ICP-OES/MS) and Atomic Absorption Spectroscopy (AAS) have been used to measure the total metal concentration in plant tissues exposed to metallic ENMs. Although these techniques are ideal to determine total elemental concentrations in diverse types of samples, they cannot provide definitive information on whether the elements are in particulate or ionic form. Further, they cannot determine the localization of the chemical species inside tissues. Confocal microscopy-based techniques are suitable to map the location of particles inside biological tissues.

However, without fluorescence tagging of the particles and analytical validation, they are not reliable. Electron microscopy in conjunction with analytical techniques like Energy dispersive spectroscopy (EDS) and Electron energy loss spectroscopy (EELS) is a powerful and reliable tool for detection and mapping of ENMs inside plants. Transmission electron microscopy (TEM) coupled with EDS was used to detect ZnO NPs in soybean seeds, leaves, and roots, in maize, and in rice roots. The presence of ZnO NPs and their transformation products were also detected in plants using synchrotron-based techniques. Zinc citrate was found to be one of the transformation products in seeds of ZnO NP exposed-soybean plants. Zinc phytate and zinc phosphate were also detected in the shoots of maize and wheat plants respectively.

The presence of the different zinc forms like Zn-phosphate and Zn-phytate raises the question about their mechanism of translocation in the cells. The ambiguity in the form of zinc taken up by ZnO NP-exposed plants poses a challenge in understanding this complex phenomenon. A knowledge of the form of zinc taken up by the NP-exposed plants would help elucidate the mechanisms of cellular uptake.

The main objectives of this study were to determine the form of ZnO NPs (ionic or particulate) taken up by plants, and to understand the possible mechanisms of transport inside plant cells. Commercial variety of *Spinacia oleraceae* (spinach) was used as the experimental plant in this study. The form and localization of the zinc species taken up by the plants were determined using a combination of transmission electron microscopy (TEM) and confocal laser scanning microscopy (CLSM). A fluorescent zinc ion (Zn^{2+}) sensor, Zinpyr-1 and a Zn^{2+} chelator, N,N,N′,N′-Tetrakis(2-pyridylmethyl)ethylenediamine (TPEN) was used in CLSM to determine if Zn^{2+} ions are present in the samples. Based on the findings, we have proposed a model to explain

the transformation of ZnO NPs, cellular movement of zinc species, and formation and subcellular localization of zinc nanoclusters.

3.2. Experimental

3.2.1. Materials

Zinc oxide NPs (ZnO, Applied Nanotech Inc, USA), zinc sulfate ($ZnSO_4$, Alfa Aeser, USA), Zinpyr-1 (Santa Cruz Biotech, USA), N,N,N',N'-tetrakis(2-pyridylmethyl)ethane-1,2-diamine (TPEN, Santa Cruz Biotech, USA), Dimethyl sulfoxide (DMSO, Chem Cruz, Santa Cruz Biotech, USA), nitric acid (HNO_3, trace metal grade, Fisher, USA), calcium chloride dihydrate ($CaCl_2.2H_2O$, VWR, USA), zinc phytate ($C_6H_6O_{24}P_6Zn_6$, 98% pure, Bonding Chemical, USA), zinc phosphate ($Zn_3(PO_4)_2$, 99.995% pure, Alfa Aesar, USA), ethylenediaminetetraacetic acid (EDTA, Sigma Aldrich, USA), spinach seeds (Burpee), and Perlite (Schultz, USA) were used as received unless otherwise specified.

3.2.2. Plant Growth

Commercial spinach seeds were germinated in perlite in darkness at room temperature (22±2 ^oC). Young seedlings at 2-leaf stage were transferred to Harmens nutrient solution (Table 2, Appendix B) in hydroponics. ZnO NP and $ZnSO_4$ were added to Harmens solution at a concentration of 500 mg Zn L^{-1} in the ZnO NP and $ZnSO_4$ treatment respectively. The control consisted of only Harmens solution without any form of zinc. The seedlings were grown in 50 mL hydroponics solution in 50 mL plastic tubes (VWR), under 16/8 h light/dark cycle at room temperature (22±2 ^oC). For each treatment, plants were grown in triplicate (Figure 2, Appendix B) and harvested after four days. Four days of exposure was considered adequate for the detection of ZnO NPs and determination of the Zn form in which they are taken up by plant roots (based on preliminary results). Our preliminary work had shown that when applied at low concentrations,

ZnO NPs are not detected inside plants using electron microscopy, and hence a high concentration (500 mg Zn L^{-1}) was used in this study.

3.2.3. Incubation with Zn^{2+} Sensors

Young seedlings (4 days after treatment, 4 leaf stage) were harvested and roots were washed with 0.2% $CaCl_2$ to remove particles attached to the root surfaces . The roots from each seedling were carefully separated using a stainless-steel blade and transferred to a petri dish.

3.2.3.1. Zinpyr-1

A working solution of Zinpyr-1 was made in 0.9% saline from a stock solution of 1 mM in dimethyl sulfoxide (DMSO) and stored at −20 ºC. Excised roots were triple washed with deionized (DI) water and 10 mM EDTA and incubated in a 20 µM solution of Zinpyr-1 in darkness at room temperature for 3 h. The root sections were rinsed with DI water to remove excess dye. The samples were mounted on glass slides in 50% glycerol and imaged with CLSM.

Zinpyr-1 (Figure 3.1a), a fluorescein-based sensor belonging to the Zinpyr-1 or ZP family, has high quantum yield and lower excitation and emission energies . Zinpyr-1 binds to Zn^{2+} in both or either of its two di(2-picolyl)amine (DPA) arms by chelating nitrogen of DPA and a carbonyl can oxygen on the xanthone ring, and is highly specific for Zn^{2+} over other divalent cations like Ca^{2+} or Mg^{2+} . The mechanism of Zn^{2+} binding to Zinpyr-1 follows photoinduced electron transfer (PET) where in the absence of the analyte, the fluorescence is quenched and upon binding of the analyte, the fluorescence is activated . The excitation wavelength of Zinpyr-1 is 507 nm and the emission wavelength is 527 nm .

3.2.3.2. N,N,N',N'-tetrakis(2-pyridylmethyl)ethane-1,2-diamine (TPEN)

Roots were incubated in 200 µM TPEN (Santa Cruz Biotech, USA) for 15 min , and thereafter incubated with Zinpyr-1 as described earlier.

TPEN (Figure 3.1b) is a Zn^{2+} chelator, and acts via ligand-substitution reaction with its pyridyl and amine nitrogen ligands binding to Zn^{2+} .

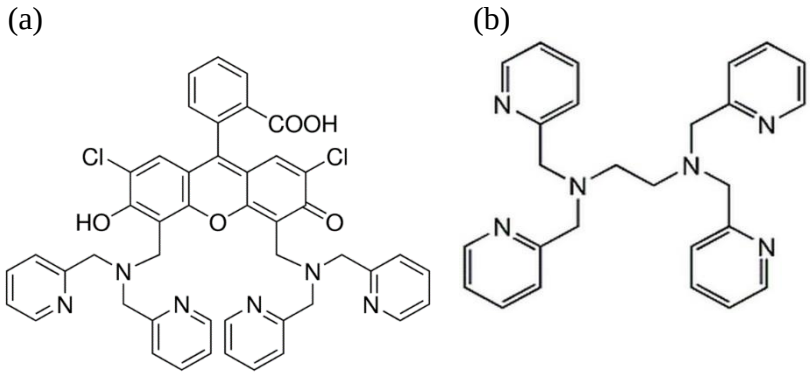

Figure 3.1. Chemical structures of: (a) Zinpyr-1; (b) TPEN

3.2.4. Analytical Procedures

3.2.4.1. Particle Characterization

For zeta (ζ)-potential and hydrodynamic diameter measurements, the ZnO NPs were dispersed in DI water and Harmens nutrient solution using a sonicator for 30 seconds at a concentration of 500 mg Zn L^{-1}. The pH of Harmens solution was adjusted to 6 (relevant to plant growth). The ζ-potential and hydrodynamic diameter were measured with a ZetaSizer (Nano-ZS 90, Malvern). For evaluating the particle size distribution, a Transmission Electron Microscope (TEM) (JEOL JEM-2100 LaB6 TEM, JEOL USA, Peabody MA) operating at 200 kV was used. Bright-field images of each sample were acquired with a Gatan Orius SC1000 CCD camera; dark-field imaging utilized a Gatan 805 High Angle Annular Dark Field detector with a Gatan Digiscan II controller unit and the TEM running in scanning transmission electron microscopy (STEM) mode.

3.2.4.2. Confocal Microscopy Imaging

Root sections of plants were imaged with a CLSM (Zeiss LSM 700, Thornwood, NY) using excitation wavelength at 488 nm for Zinpyr-1 with additional channel taken with DIC, using Plan-Apochromat 40x/1.3 oil immersion lens with emission set at 530 nm for Zinpyr-1. Leaves were not imaged because of chlorophyll interference. Unstained ZnO NPs (powder) were also checked with CLSM excited with the full spectrum and observed in 550 nm to 600 nm for any autofluorescence.

3.2.4.3. Flame Atomic Absorption Spectroscopy (Flame AA) Analysis

Dried (65 ^{o}C, 24 h) root tissues were digested in a microwave digester (CEM Mars Xpress) with 1:1 nitric acid (15.9 M) and DI water. Digested samples were analyzed with AAS (Perkin Elmer Pinnacle 900H) for Zn.

3.2.4.4. TEM and EDS Analyses

For TEM, the root samples were excised and cut into small (< 1 mm) pieces under water, then fixed in 2.5% glutaraldehyde in 0.1 M sodium phosphate buffer (pH 7.35, Tousimis Research Corporation, Rockville MD) for 1 h at 4 °C. Samples were rinsed twice in sodium phosphate buffer and then placed in 2% osmium tetroxide in the buffer for 2 h at room temperature. Samples were rinsed with DI water to remove excess osmium tetroxide and dehydrated through a graded acetone series (0-30-50-70% acetone in water) and then further dehydrated through two changes of 100% acetone. Dehydrated samples were embedded in Epon-Araldite-DDSA with DMP-30 accelerator polymerized in a 60 °C oven for 24 hours and sectioned at 60-80 nm thickness using a RMC MT XL ultramicrotome (Boeckeler Instruments, Tucson AZ). Sections were collected on copper grids. Imaging and analysis were performed on a JEOL JEM-2100 LaB6 TEM (JEOL USA, Peabody MA) operated at 200 kV. Bright-field images of each sample were acquired with

a Gatan Orius SC1000 CCD camera; dark-field imaging utilized a Gatan 805 High Angle Annular Dark Field detector with a Gatan Digiscan II controller unit and the TEM running in scanning transmission electron microscopy (STEM) mode. To obtain X-ray information, a Thermo Nanotrace Energy Dispersive X-ray detector with NSS-212e acquisition engine integrated with the dark-field STEM system was used. The en-bloc uranyl acetate staining and post staining with lead citrate steps were left out for analytical clarity. TEM (JEOL JEM 2100) was used for imaging the ZnO NPs in the roots and was followed by EDS for elemental analysis. Tissues were not stained with lead for analytical clarity. Beryllium holder was used to avoid the Cu peaks which were observed in the EDS spectrum when Cu holders were used. However faint Cu peaks were still visible from the Cu grids used. For comparative analysis, ZnO NP as well as zinc phytate ($C_6H_6O_{24}P_6Zn_6$) and zinc phosphate [$Zn_3(PO_4)_2$] powders were finely ground and collected on Cu grids. They were imaged and analyzed for elemental analysis using the same settings.

3.3. Results

3.3.1. Particle Characterization

The particle size ranged from 8-174 nm with 92.96% of the ZnO NPs having the smallest dimension within 100 nm (Figure 3.2). The ζ-potential of the ZnO nanoparticles were found to be 25.9±4.7 mV in DI water and −16.8±3.9 mV in Harmens nutrient solution. The ζ-potential of the NPs in nutrient solution is negative because in the acidic nutrient media (pH 6.2) and the anions present in the media might have anchored on the particle surfaces, rendering the particle a negative charge. The average hydrodynamic diameter of the ZnO NPs was found to be 512.5 nm in DI water and 3799 nm in nutrient solution. The particles formed agglomerates/aggregates at high ionic strength of the nutrient solution, thereby increasing the hydrodynamic diameter. With increasing ionic strength, the thickness of the electric double layer surrounding a particle decreases due to

compression of this double layer, and that decreases the zeta potential and subsequently decreases the repulsive interactions between the particles .

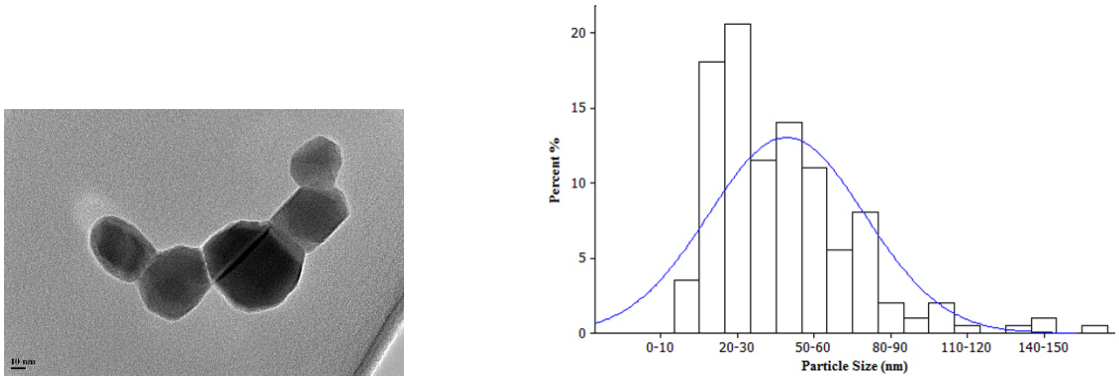

(a) (b)

Figure 3.2. (a) TEM micrograph of bare ZnO NPs, and (b) particle size distribution of ZnO NPs based on smallest dimensions.

3.3.2. Zinpyr-1 and TPEN Labeling

Zinpyr-1 was used in this study to detect Zn^{2+} speciation in spinach roots exposed to ZnO NPs. CLSM examination showed high intensity green fluorescence (Zn ions) in the primary root tips (Fig. 3.3a) and the region with root hairs (the root hair zone) (Figure 3.3d) in plants exposed to ZnO NPs. Similar high intensity fluorescence was observed in the root sections of the plants exposed to $ZnSO_4$ (Figure 3.3b and 3.3e). The control root sections (from plants grown without ZnO NPs or $ZnSO_4$) labeled with Zinpyr-1 did not show significant fluorescence (Figure 3.3c and 3.3f). Low intensity background autofluorescence of cellular organelles and vascular bundles was visible in the controls. The control experiment indicated that there was no root uptake of Zinpyr-1 as the associated fluorescence was not observed. This led us to further infer that high intensity fluorescence in the other samples is due to Zinpyr-1 tagged to zinc ions (Zn^{2+}) from ZnO NPs, and $ZnSO_4$. The Zn^{2+} ions might have come from the dissociation of the zinc compounds in the plant tissue after plant uptake or plant might have taken up dissociated Zn^{2+} ions from the hydroponic solution. The hydroponic medium mixed with ZnO NPs and Zinpyr-1 was also imaged and bright

green fluorescence was observed (Figure 3, Appendix B). We believe that the zinc, which fluoresced in the plant cell and hydroponic medium are Zn^{2+} ions as ZnO NPs are found to release Zn^{2+} ions in aqueous media (Figure 1, Appendix B). Zinpyr-1 was also successfully used by Sinclair et al. to study the localization of Zn^{2+} in the roots of mutant *Arabidopsis thaliana* upon exposure to exogenous zinc. Cellular and tissue distribution of zinc in the zinc-sensitive phenotype, *AtHMA4*-expressing *Nicotiana tabacum* was mapped by others using Zinpyr-1 .

To reconfirm that fluorescence in the samples is coming only from Zn^{2+} ions, TPEN was used to chelate the free Zn^{2+} (not complexed with any cell component) present in the roots and the samples were then labelled with Zinpyr-1. No significant fluorescence was observed in any of the samples (Figure 3.4a-3.4f). This indicates that the fluorescence is coming from Zn^{2+} ions that came from the ZnO NPs and $ZnSO_4$ taken up by plants in one form or the other.

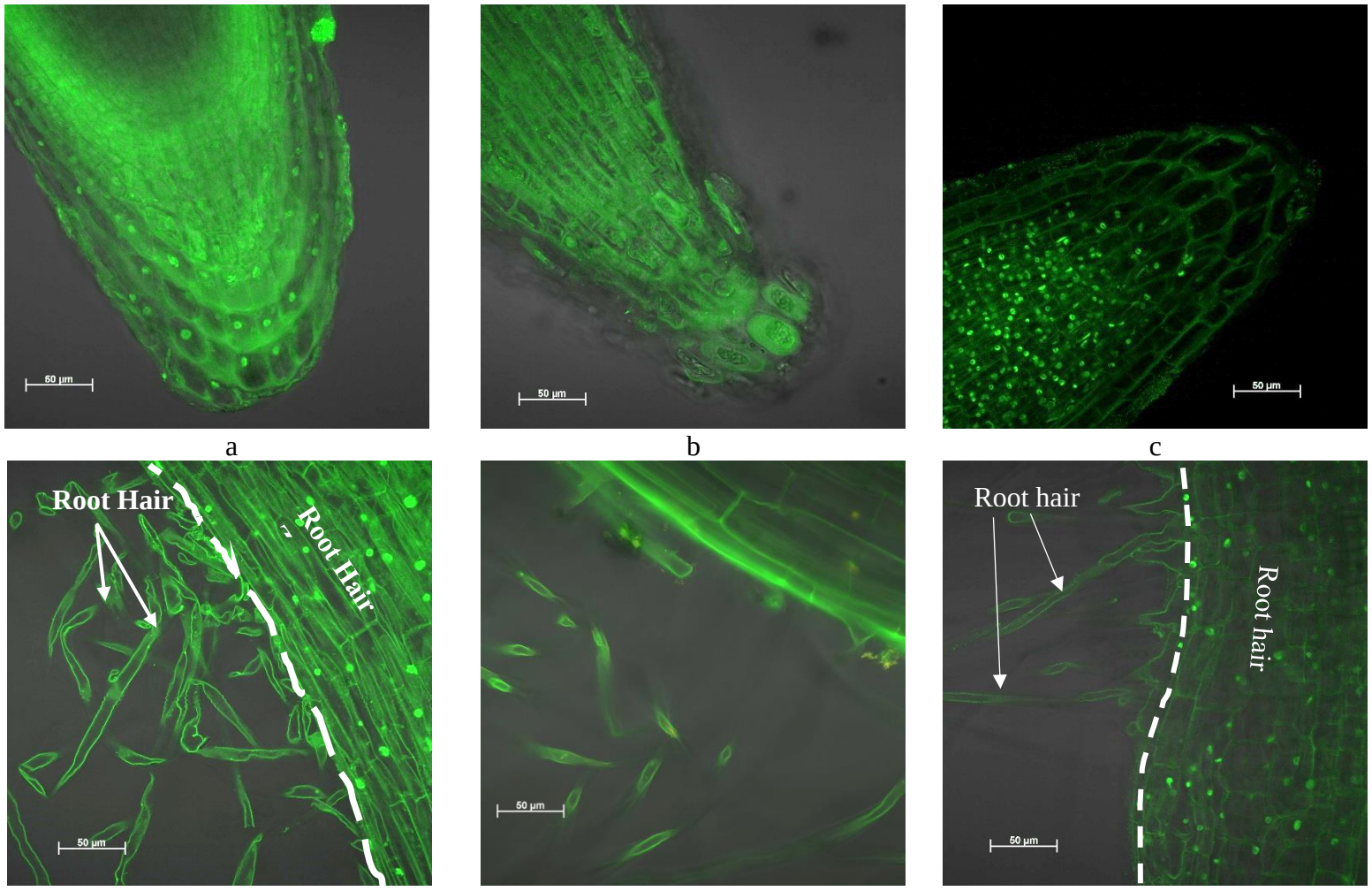

Figure 3.3. Confocal laser scanning microscopic images of the spinach roots showing Zinpyr-1 fluorescence in (a) root tip exposed to ZnO NPs, (b) root tip exposed to $ZnSO_4$, (c) control (root tip from plants not exposed to ZnO NPs or $ZnSO_4$), (d) root hairs and root hair zone exposed to ZnO NPs, (e) root hairs and root hair zone exposed to ZnSO4, and (f) control (root hairs and root hair zone from plants not exposed to ZnO NPs or $ZnSO_4$).

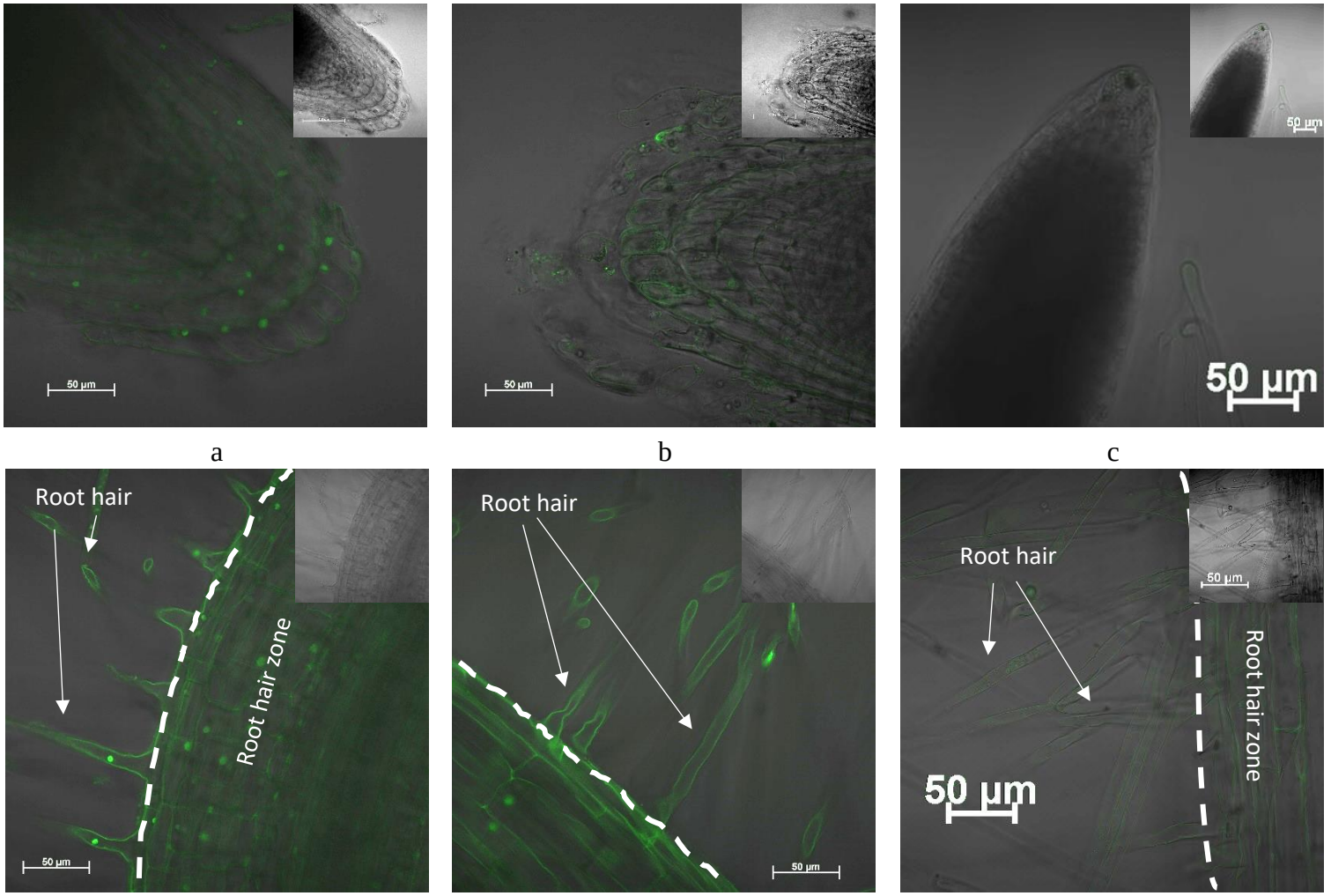

Figure 3.4. Confocal laser scanning microscope images of the spinach roots showing Zinpyr-1 fluorescence (green) being marred because of Zn^{2+} chelation by Zn^{2+} chelator TPEN, (a) root tip exposed to ZnO NPs, (b) root tip exposed to $ZnSO_4$, (c) control root tip from plants not exposed to ZnO NPs or $ZnSO_4$, (d) root hairs and root hair zone exposed to ZnO NPs, (e) root hairs and root hair zone exposed to $ZnSO_4$, and (f) control root hairs and root hair zone from plants not exposed to ZnO NPs or $ZnSO_4$

3.3.3. Quantification of Zinc in Samples

The presence of zinc in the root samples was verified with Flame AA spectrometric analysis (Table 3.1). Zinc was found in the roots of ZnO NP and $ZnSO_4$ treated plants. Trace amount of zinc was also detected in the control (no zinc treatment) plants. This is possibly due to the endogenous zinc present in the plant tissues. It was found that the zinc concentration was the highest in $ZnSO_4$ samples. One-way ANOVA and Tukey's comparison test reveals that the zinc accumulation in roots exposed to ZnO NPs, $ZnSO_4$ and no zinc are significantly different (denoted with different letters) (Table 3.1).

Table 3.1. Zinc concentration in spinach roots exposed to 500 mg/L of zinc and in control (no zinc). The different letters (A, B, C) denote that data are significantly different (Tukey's pairwise comparison)

Treatment	Zinc Concentration in the roots (mg/g)
ZnO NP	$34.214 \pm 20.9_B$
$ZnSO_4$	$72.626 \pm 10.3_A$
Control	$0.003 \pm 0.0005_C$

3.3.4. TEM and EDS Analyses

TEM images revealed clusters of Zn NPs in the vacuoles of root cells of ZnO NP exposed plants, but not in $ZnSO_4$ or the control plant root cells (Figure 3.5a, b). Individual particles had a diameter of ~40 nm and provided evidence that in addition to the Zn^{2+} ions, zinc in plant cells was present in nano-sized particle form in plants exposed to ZnO NPs. Energy Dispersive Spectroscopy (EDS) was conducted on the clusters to confirm that they were zinc (Figure 3.5c). In the EDS spectrum, zinc peaks were visible at 1.03, 8.64, and 9.57 keV corresponding to $L_{\alpha 1}$, $K_{\alpha 1}$, and $K_{\beta 1}$ lines. Phosphorus peak was visible at 2.02 keV corresponding to $K_{\alpha 1}$ line, indicating the presence of phosphorus in the identified NPs. In addition, Cu peaks were visible at 8.05 keV corresponding to $K_{\alpha 1}$. The presence of Cu can be attributed to the Cu-holders that were used to mount the sample.

O peak was visible at 0.53 keV corresponding to $K_{\alpha 1}$, and C peak was visible at 0.28 keV corresponding to $K_{\alpha 1}$.

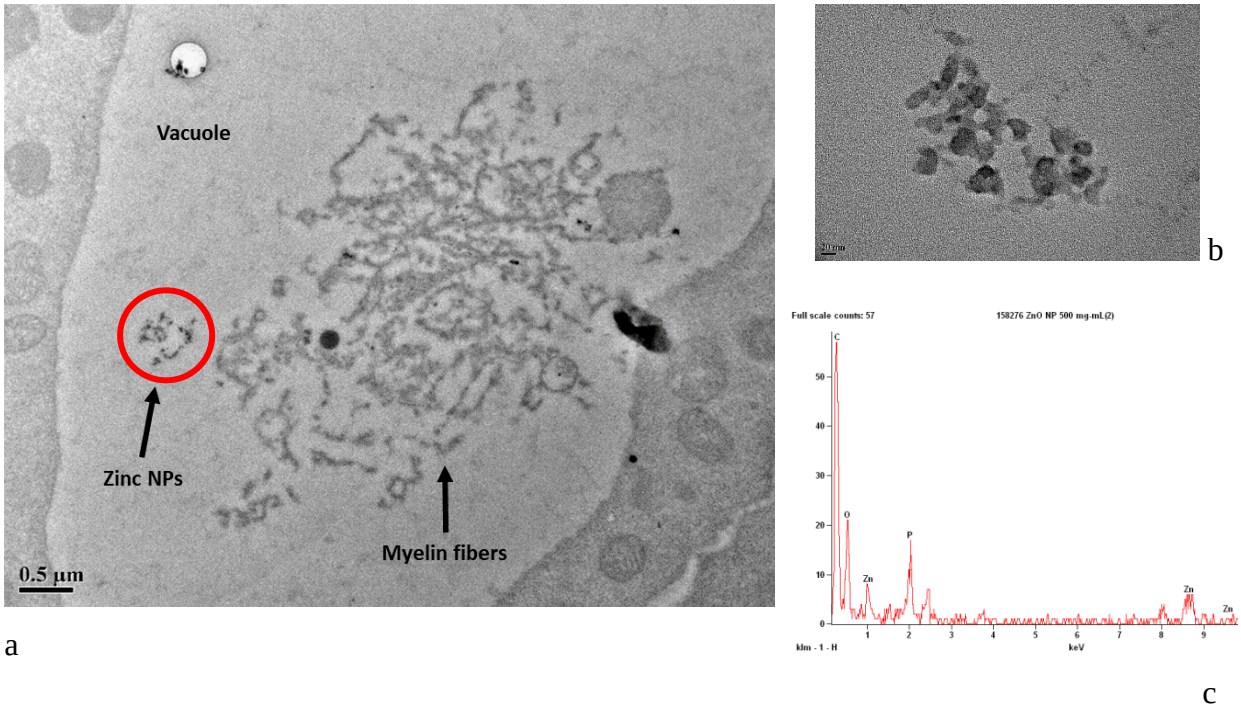

Figure 3.5. Transmission Electron micrograph of Zn NPs inside the spinach root tip of ZnO NP exposed plants: (a) Root tip section with ZnO NPs (encircled) inside a root cell. Nucleus and chromatin are visible, (b) magnified view of ZnO NPs in area circled (20 nm), and (c) EDS spectrum of an electron-dense spot in the TEM scan in (a).

3.4. Discussion

Uptake of ZnO NPs has been reported in different plants, although there is no consensus on the nature of uptake. In our study, ionic zinc (Zn^{2+}) was observed in the roots. Fluorescence corresponding to Zn^{2+} ions was observed in the cell periphery, as well as within the cytoplasm of root cells and in the hydroponic solution. This indicates dissolution of ZnO NPs to Zn^{2+} ions in the hydroponic media prior to uptake by plants. Interestingly, dissolution of ZnO NPs in aqueous environments have been documented in many instances , and we also observed a gradual dissolution of zinc in Harmen's solution (Figure 1, Appendix B). Total zinc uptake by the plants

was determined with Flame AA spectroscopic analysis of the plant root samples, and it was found that the zinc concentration was the highest in $ZnSO_4$ samples.

Our TEM studies revealed the presence of dense dots in the cytoplasm of root tip cortical/undifferentiated cells of ZnO NP exposed seedlings. EDS confirmed these dense nano-sized particles to be zinc-rich deposits. The zinc nano clusters were sequestered in a vacuole (Figure 3.5). It appeared that several NPs were coalesced together suggesting that the NPs could be compartmentalized within a subcellular vesicle and that plant possibly traffics and sequesters the NPs to these specific subcellular compartments. Vacuoles are known to play an important role in heavy metal homeostasis and detoxification by sequestration .

The presence of phosphorus peak in the EDS spectrum suggests that phosphorus was present with the zinc nanoparticles. Comparing the spectra of Zn NPs in plant roots and commercial ZnO NP (Figure 3.6 a and d), it is evident that the NPs in the plant roots are not ZnO NPs, but Zn NPs in a complex with phosphorus. Comparing its spectra with that of Zn-phosphate and Zn-phytate (Figure 3.6 d), it is evident that there is distinct overlap of Zn, Cu, P, and O peaks in all the three compounds, however, peak heights of Zn, P, and O were distinctly smaller in Zn NPs in plants, indicating a smaller lattice structure. Normalizing the intensity of the K and L lines of the elements, it is observed that the C and O counts are higher in Zn NP in plants as compared to Zn-phosphate and Zn-phytate (Figure 3.7). This is largely due to the presence of inherent C and O in the plant sample. Hence, it was not possible to place the Zn NP observed in plants in either of the categories with EDS data alone. However, comparing the normalized net intensity of the elemental peaks, it can be inferred that the observed Zn NPs inside plants resembles Zn-phytate (Figure 3.7). Thus, the nanoparticles observed in the vacuoles are more likely to be zinc phytate-like nano-sized particles, and not zinc oxide nanoparticles. We think that ZnO NPs were

dissociated into zinc ions prior to plant uptake or inside plants and subsequently sequestered in the vacuole forming nano-sized complexes with organic acid like phytic acid. In zinc tolerant plants like tufted hairgrass (*Deschampsia cespitosa*) and crop plants like wheat, maize, soybean, tomato, rapeseed, cabbage, and radish, zinc was found to be complexed with phytate (myo-inositol kis-hexaphosphate) forming globular deposits in the vacuoles of cortical cells of root tips . Moreover, zinc phytate-like species was observed in ZnO NP exposed roots of maize plants, although subcellular localization was not reported .

Although there is substantial evidence for the dissociation of ZnO NPs in the aqueous media, and subsequent zinc ion uptake by roots, endocytosis of ZnO NPs cannot be ruled out. Endocytosis of NPs have been reported in a number of studies in both plant and mammalian cells . It is known that the transport of NPs into cells also depend on the type of the nanomaterial. Single walled carbon nanotubes and CuO NPs were shown to enter plant cells via endocytosis . However, there is no evidence of endocytosis of ZnO NPs in plant cells although it has been reported in mammalian cells . ZnO NPs dissolution in aqueous media and our preliminary data (Figure 1, Appendix B) makes zinc ions available for uptake by plants. Hence, the possibility of endocytosis of ZnO NPs in plants is limited. Based on our observations, we have proposed a model for the uptake of zinc into root cells exposed to ZnO NPs. The model explains our observations on zinc internalization and sequestration of zinc NPs in vacuoles of epidermal cells. The ZnO NPs dissolves into Zn^{2+} ions in the hydroponic media and is taken up as ions via cell wall and plasma membrane transporters, and is sequestered into the vacuole through vacuolar transporters, where they complex with phosphorus forming Zn-phytate-like nanoclusters (Figure 3.8).

a

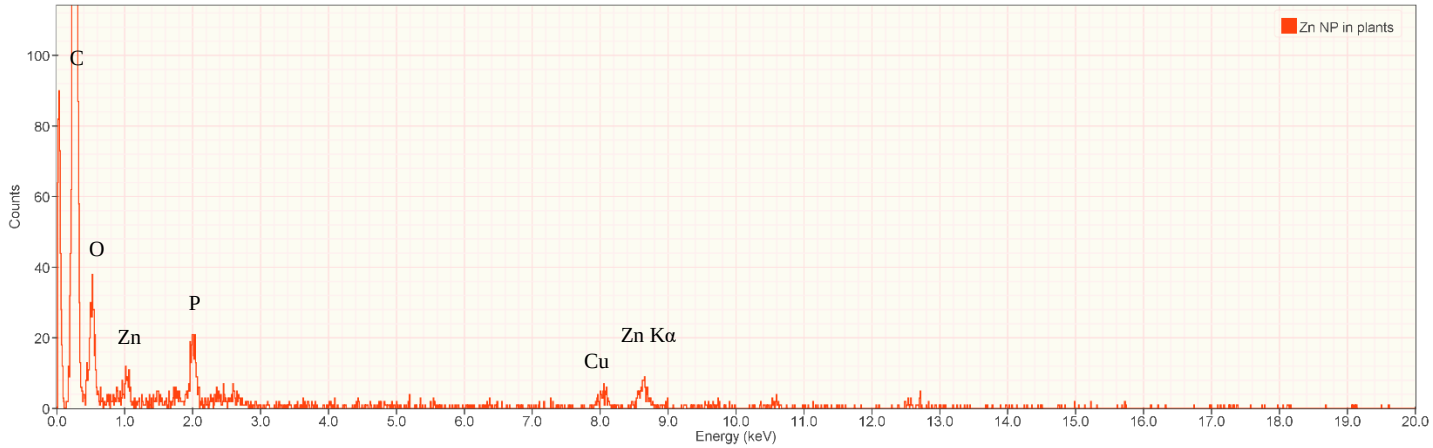

b

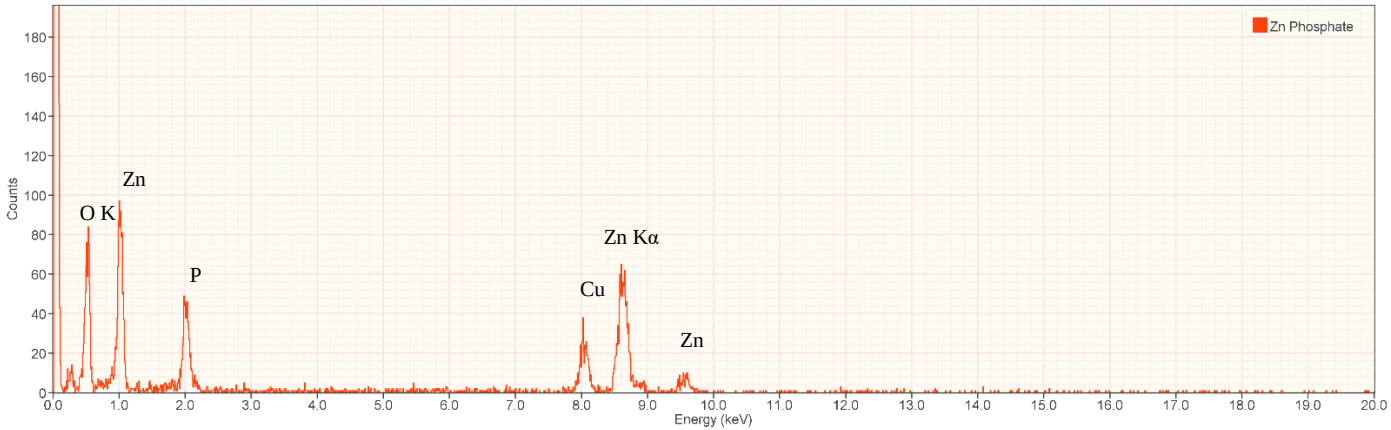

Figure 3.6. EDS Spectra of different Zn compounds (a) Zn NP in plant roots, (b) Zn phosphate, (c) Zn phytate (d) bare ZnO NP, and (e) overlay of Zn NP in plants, Zn phosphate, and Zn phytate spectra

c

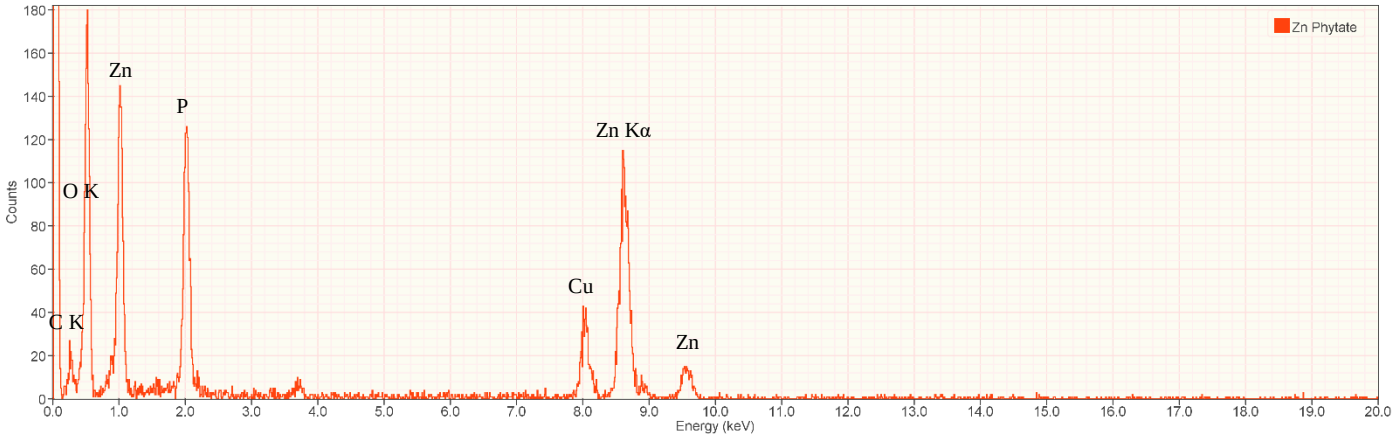

d

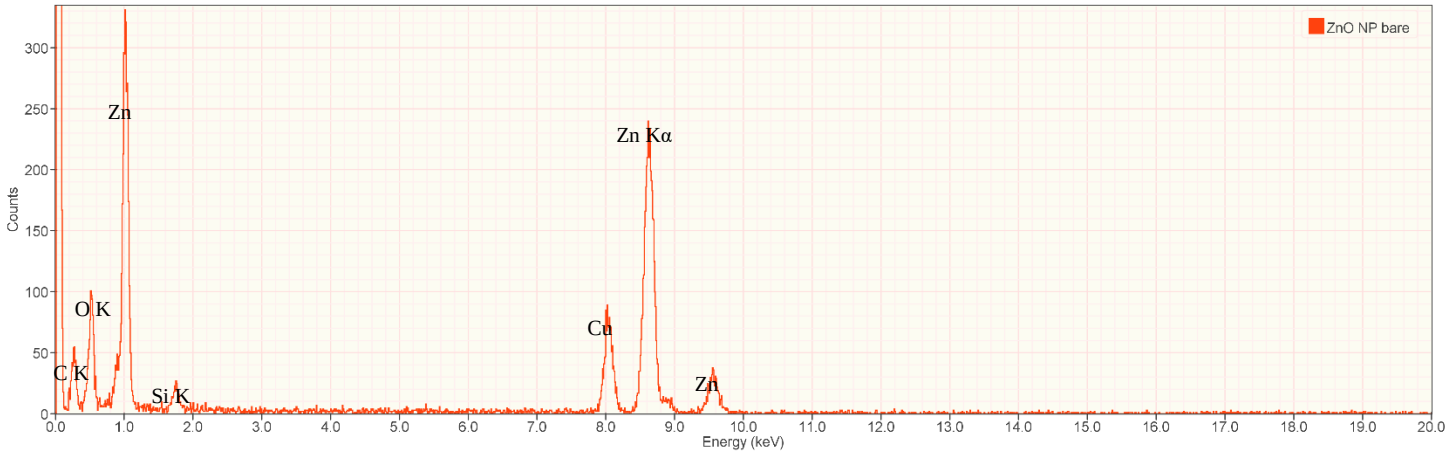

Figure 3.6. EDS Spectra of different Zn compounds (a) Zn NP in plant roots, (b) Zn phosphate, (c) Zn phytate (d) bare ZnO NP, and (e) overlay of Zn NP in plants, Zn phosphate, and Zn phytate spectra (continued)

e

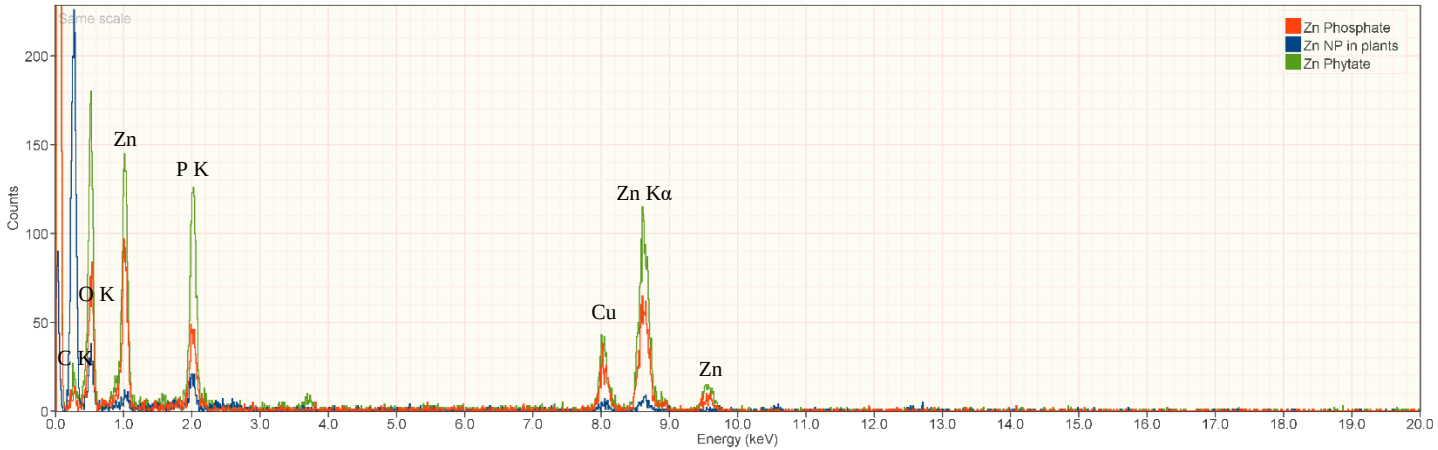

Figure 3.6. EDS Spectra of different Zn compounds (a) Zn NP in plant roots, (b) Zn phosphate, (c) Zn phytate (d) bare ZnO NP, and (e) overlay of Zn NP in plants, Zn phosphate, and Zn phytate spectra (continued)

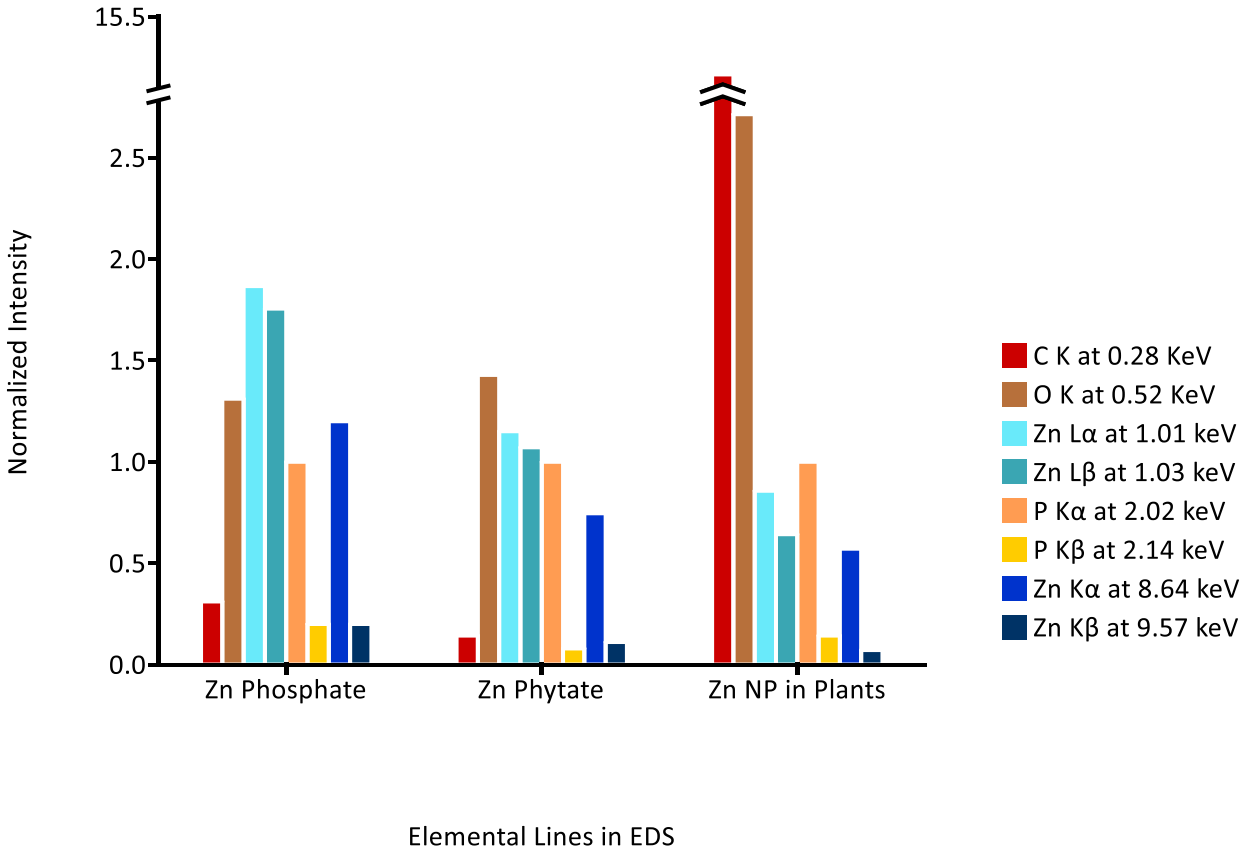

Figure 3.7. Comparison of EDS elemental lines of O, Zn, and P in zinc phosphate, zinc phytate and zinc NPs observed in spinach roots.

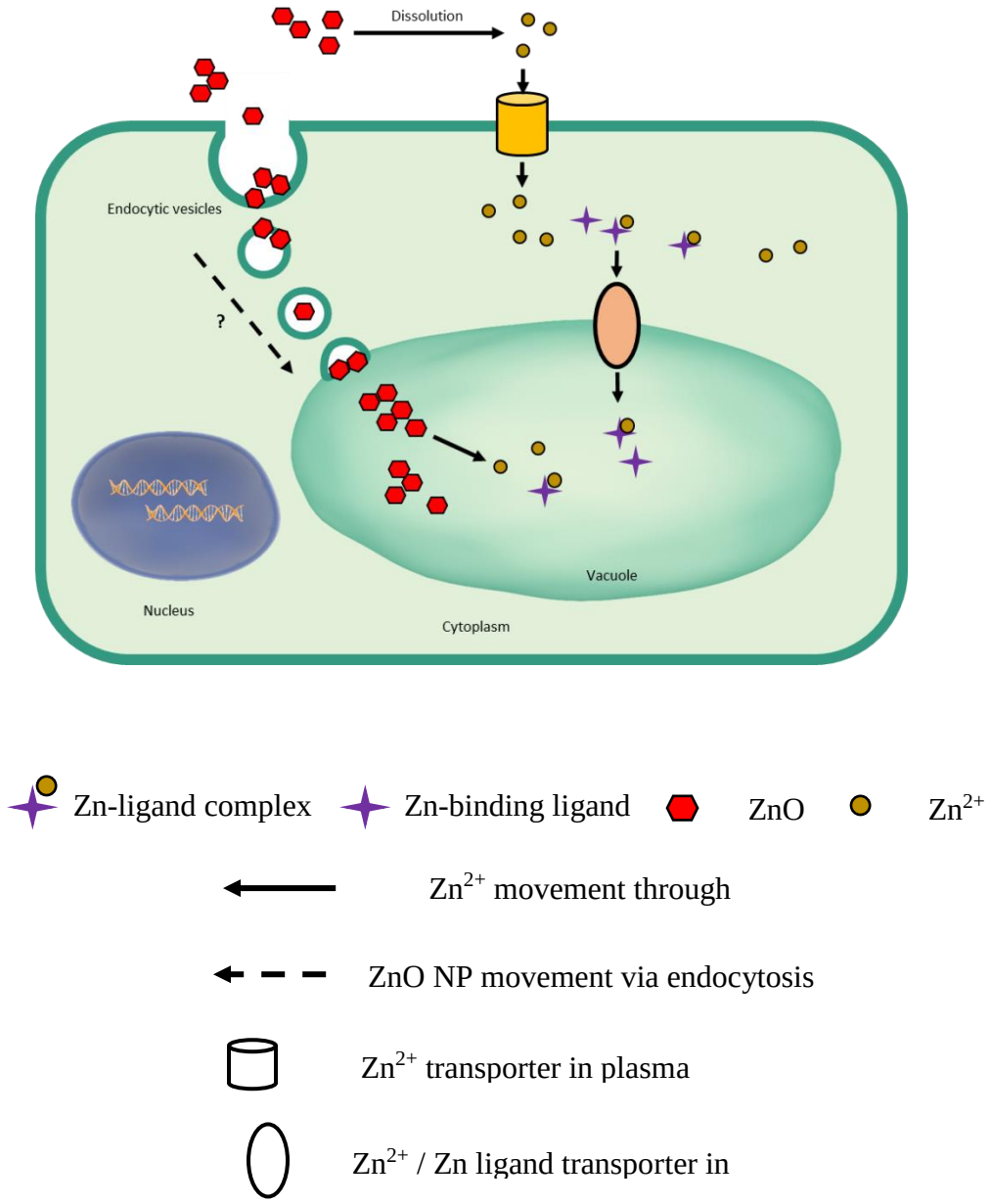

Figure 3.8. The model of ZnO NP internalization by plant root epidermal cells. Dissolution of ZnO NPs into ions (Zn^{2+}) occurs in the hydroponic media, which are internalized through Zn^{2+} ion transporters present in the plasma membrane of root cells. Zinc ions are transported into the vacuoles through vacuolar transporters. Inside the vacuole, the free zinc ions are chelated to organic molecules like phytic acid forming zinc-phytate nanoparticles. Endocytosis may also play a role in ZnO NP internalization, where the NPs are eventually sequestered in the vacuoles through endocytic vesicles and may also dissociate into ions in the vacuoles. The model explores the possible routes of zinc species (ZnO NP and zinc ions) transport in plant root cells from the media and does not take into account the metabolic functions of zinc or zinc NPs in plants.

3.5. Conclusion

The detection of ENMs and their speciation products in plants is challenging because low-resolution techniques cannot detect particles in the nanometer size range. Also, the form of ENM (ionic or nanoparticle) taken up by plants is difficult to determine using conventional techniques because they can only detect the total elemental concentration. In this study, using a combination of a fluorescent Zn^{2+} sensor, Zinpyr-1 and a Zn^{2+} chelator, TPEN in CLSM, Zn^{2+} ions were found to be the dominating species in plant roots exposed to ZnO NPs. TEM imaging coupled with EDS revealed the presence of dense zinc nanoparticles sequestered in vacuoles. We think that the zinc nanoparticles are zinc phytate, based on the presence of phosphorus peak in the EDS spectrum of the zinc clusters, and our comparison with Zn-phytate spectrum. This is in agreement with existing reports on the biotransformation of ZnO NPs to zinc phytate-like species in plants. With the derivations made from our microscopy studies, we were able to hypothesize a model for the uptake routes of ZnO NPs and their dissociation products (Zn ions) in plant cells.

3.6. Acknowledgements

This work was funded by the United States Department of Agriculture-National Institute of Food and Agriculture (USDA-NIFA, Grant# 2012-67018-30186). Zeta-sizer purchase was funded by an USDA-NIFA (Grant# 2015-67018-23107). The authors acknowledge the NDSU Advanced Imaging and Microscopy Core Laboratory, and NDSU Electron Microscopy Core Laboratory for microscopy and imaging conducted in this study (National Science Foundation Grant No. CMMI-0821655). Any opinions, findings, and conclusions or recommendations expressed in this paper are those of the author(s) and do not necessarily reflect the views of the funding agencies.

3.7. References

Adam, N. et al. The Chronic Toxicity Of Zno Nanoparticles And Zncl2 To Daphnia Magna And The Use Of Different Methods To Assess Nanoparticle Aggregation And Dissolution. **Nanotoxicology,** V. 8, N. 7, P. 709-717, 2014/11/01 2014. Issn 1743-5390. Disponível Em: < Https://Www.Tandfonline.Com/Doi/Abs/10.3109/17435390.2013.822594 >.

Albanese, A.; Chan, W. C. W. Effect Of Gold Nanoparticle Aggregation On Cell Uptake And Toxicity. **Acs Nano,** V. 5, N. 7, P. 5478-5489, Jul 2011. Issn 1936-0851. Disponível Em: < <Go To Isi>://Wos:000293035200024 >.

Baker, S. et al. Nanoagroparticles Emerging Trends And Future Prospect In Modern Agriculture System. **Environmental Toxicology And Pharmacology,** V. 53, N. Supplement C, P. 10-17, 2017/07/01/ 2017. Issn 1382-6689. Disponível Em: < Http://Www.Sciencedirect.Com/Science/Article/Pii/S1382668917301114 >.

Carter, K. P.; Young, A. M.; Palmer, A. E. Fluorescent Sensors For Measuring Metal Ions In Living Systems. **Chemical Reviews,** V. 114, N. 8, P. 4564-4601, Apr 23 2014. Issn 0009-2665. Disponível Em: < <Go To Isi>://Wos:000335086300015 >.

Chen, J. et al. Phytotoxicity And Bioaccumulation Of Zinc Oxide Nanoparticles In Rice (Oryza Sativa L.). **Plant Physiology And Biochemistry,** V. 130, P. 604-612, 2018/09/01/ 2018. Issn 0981-9428. Disponível Em: < Http://Www.Sciencedirect.Com/Science/Article/Pii/S0981942818303577 >.

Dimkpa, C. O. et al. Cuo And Zno Nanoparticles: Phytotoxicity, Metal Speciation, And Induction Of Oxidative Stress In Sand-Grown Wheat. **Journal Of Nanoparticle Research,** V. 14, N. 9, Sep 2012. Issn 1388-0764. Disponível Em: < <Go To Isi>://Wos:000308225800053 >.

Duhan, J. S. et al. Nanotechnology: The New Perspective In Precision Agriculture. **Biotechnol Rep (Amst),** V. 15, P. 11-23, Sep 2017. Issn 2215-017x (Print)

2215-017x.

Gao, C.; Zhao, Q.; Jiang, L. Vacuoles Protect Plants From High Magnesium Stress. **Proceedings Of The National Academy Of Sciences Of The United States Of America,** V. 112, N. 10, P. 2931-2932, 02/26 2015. Issn 0027-8424

1091-6490. Disponível Em: < Http://Www.Ncbi.Nlm.Nih.Gov/Pmc/Articles/Pmc4364218/ >.

Goldsmith, C. R.; Lippard, S. J. Analogues Of Zinpyr-1 Provide Insight Into The Mechanism Of Zinc Sensing. **Inorganic Chemistry,** V. 45, N. 16, P. 6474-6478, Aug 7 2006. Issn 0020-1669. Disponível Em: < <Go To Isi>://Wos:000239394300054 >.

Hackenberg, S. et al. Genotoxic Effects Of Zinc Oxide Nanoparticles In Nasal Mucosa Cells Are Antagonized By Titanium Dioxide Nanoparticles. **Mutation Research/Genetic Toxicology And Environmental Mutagenesis,** V. 816-817, P. 32-37, 2017/04/01/ 2017. Issn 1383-5718. Disponível Em: < Http://Www.Sciencedirect.Com/Science/Article/Pii/S1383571816302091 >.

Hall, J. L. Cellular Mechanisms For Heavy Metal Detoxification And Tolerance. **J Exp Bot,** V. 53, N. 366, P. 1-11, Jan 2002. Issn 0022-0957 (Print)

0022-0957.

Harris, A. T.; Bali, R. On The Formation And Extent Of Uptake Of Silver Nanoparticles By Live Plants. **Journal Of Nanoparticle Research,** V. 10, N. 4, P. 691-695, Apr 2008. Issn 1388-0764. Disponível Em: < <Go To Isi>://Wos:000253626900015 >.

Hernandez-Viezcas, J. A. et al. In Situ Synchrotron X-Ray Fluorescence Mapping And Speciation Of Ceo2 And Zno Nanoparticles In Soil Cultivated Soybean (Glycine Max). **Acs Nano,** V. 7, N. 2, P. 1415-1423, Feb 2013. Issn 1936-0851. Disponível Em: < <Go To Isi>://Wos:000315618700061 >.

Jacob, D. L. Et Al. Uptake And Translocation Of Ti From Nanoparticles In Crops And Wetland Plants. **International Journal Of Phytoremediation,** V. 15, N. 2, P. 142-153, 2013 2013. Issn 1522-6514. Disponível Em: < <Go To Isi>://Wos:000310603700004 >.

Jiang, J.; Oberdorster, G.; Biswas, P. Characterization Of Size, Surface Charge, And Agglomeration State Of Nanoparticle Dispersions For Toxicological Studies. **Journal Of Nanoparticle Research,** V. 11, N. 1, P. 77-89, Jan 2009. Issn 1388-0764. Disponível Em: < <Go To Isi>://Wos:000262125200008 >.

Jo, M.-R. Et Al. Effects Of Zinc Oxide Nanoparticle Dispersants On Cytotoxicity And Cellular Uptake. **Molecular & Cellular Toxicology,** V. 12, N. 3, P. 281-288, 2016/09/01 2016. Issn 2092-8467. Disponível Em: < Https://Doi.Org/10.1007/S13273-016-0033-Y >.

Kowalczyk, T.; Lin, Z.; Van Voorhis, T. Fluorescence Quenching By Photoinduced Electron Transfer In The Zn2+ Sensor Zinpyr-1: A Computational Investigation. **Journal Of Physical Chemistry A,** V. 114, N. 38, P. 10427-10434, Sep 30 2010. Issn 1089-5639. Disponível Em: < <Go To Isi>://Wos:000282018200011 >.

Linares, J. Et Al. Endocytic Mechanisms Of Graphene Oxide Nanosheets In Osteoblasts, Hepatocytes And Macrophages. **Acs Applied Materials & Interfaces,** V. 6, N. 16, P. 13697-13706, Aug 2014. Issn 1944-8244. Disponível Em: < <Go To Isi>://Wos:000341122000048 >.

Liu, Q. Et Al. Carbon Nanotubes As Molecular Transporters For Walled Plant Cells. **Nano Letters,** V. 9, N. 3, P. 1007-1010, Mar 2009. Issn 1530-6984. Disponível Em: < <Go To Isi>://Wos:000264142100017 >.

Lopes, S. et al. Zinc Oxide Nanoparticles Toxicity To Daphnia Magna: Size-Dependent Effects And Dissolution. **Environmental Toxicology And Chemistry,** V. 33, N. 1, P. 190-198, 2014/01/01 2013. Issn 0730-7268. Disponível Em: < Https://Doi.Org/10.1002/Etc.2413 >. Acesso Em: 2018/05/16.

Lv, J. et al. Accumulation, Speciation And Uptake Pathway Of Zno Nanoparticles In Maize. **Environmental Science-Nano,** V. 2, N. 1, P. 68-77, Feb 2015. Issn 2051-8153. Disponível Em: < <Go To Isi>://Wos:000349222200008 >.

Martinoia, E.; Maeshima, M.; Neuhaus, H. E. Vacuolar Transporters And Their Essential Role In Plant Metabolism. **Journal Of Experimental Botany,** V. 58, N. 1, P. 83-102, 2007. Issn 0022-0957. Disponível Em: < Http://Dx.Doi.Org/10.1093/Jxb/Erl183 >.

Meeusen, J. W.; Nowakowski, A.; Petering, D. H. Reaction Of Metal-Binding Ligands With The Zinc Proteome: Zinc Sensors And N,N,N ',N '-Tetrakis(2-Pyridylmethyl)Ethylenediamine. **Inorganic Chemistry,** V. 51, N. 6, P. 3625-3632, Mar 19 2012. Issn 0020-1669. Disponível Em: < <Go To Isi>://Wos:000301624500033 >.

Miralles, P.; Church, T. L.; Harris, A. T. Toxicity, Uptake, And Translocation Of Engineered Nanomaterials In Vascular Plants. **Environmental Science & Technology,** V. 46, N. 17, P. 9224-9239, Sep 2012. Issn 0013-936x. Disponível Em: < <Go To Isi>://Wos:000308260700004 >.

Odzak, N. et al. Dissolution Of Metal And Metal Oxide Nanoparticles In Aqueous Media. **Environmental Pollution,** V. 191, P. 132-138, Aug 2014. Issn 0269-7491. Disponível Em: < <Go To Isi>://Wos:000338605200017 >.

Oh, N.; Park, J. H. Endocytosis And Exocytosis Of Nanoparticles In Mammalian Cells. **International Journal Of Nanomedicine,** V. 9, P. 51-63, 2014. Issn 1178-2013. Disponível Em: < <Go To Isi>://Wos:000349961100006 >.

Priester, J. H. et al. Soybean Susceptibility To Manufactured Nanomaterials With Evidence For Food Quality And Soil Fertility Interruption. **Proceedings Of The National Academy Of Sciences Of The United States Of America,** V. 109, N. 37, P. E2451-E2456, Sep 11 2012. Issn 0027-8424. Disponível Em: < <Go To Isi>://Wos:000309208000009 >.

Rico, C. M. et al. Effect Of Cerium Oxide Nanoparticles On Rice: A Study Involving The Antioxidant Defense System And In Vivo Fluorescence Imaging. **Environmental Science &Amp; Technology,** V. 47, N. 11, P. 5635-5642, Jun 2013. Issn 0013-936x.

Sabir, S.; Arshad, M.; Chaudhari, S. K. Zinc Oxide Nanoparticles For Revolutionizing Agriculture: Synthesis And Applications. **The Scientific World Journal,** V. 2014, 2014. Issn 2356-6140.

Shin, Y.-J. et al. Dissolution Of Zinc Oxide Nanoparticles In Exposure Media Of Algae, Daphnia, And Fish Embryos For Nanotoxicological Testing. **Chemistry And Ecology,** V. 34, N. 3, P. 229-240, 2018/03/16 2018. Issn 0275-7540. Disponível Em: < Https://Doi.Org/10.1080/02757540.2017.1405943 >.

Siemianowski, O. et al. Development Of Zn-Related Necrosis In Tobacco Is Enhanced By Expressing Athma4 And Depends On The Apoplastic Zn Levels. **Plant Cell And Environment,** V. 36, N. 6, P. 1093-1104, Jun 2013. Issn 0140-7791. Disponível Em: < <Go To Isi>://Wos:000318176800003 >.

Sinclair, S. A. et al. The Use Of The Zinc-Fluorophore, Zinpyr-1, In The Study Of Zinc Homeostasis In Arabidopsis Roots. **New Phytologist,** V. 174, N. 1, P. 39-45, 2007 2007. Issn 0028-646x. Disponível Em: < <Go To Isi>://Wos:000244520700006 >.

Song, W. Y. et al. A Receptor Kinase-Like Protein Encoded By The Rice Disease Resistance Gene, Xa21. **Science,** V. 270, N. 5243, P. 1804-1806, Dec 15 1995. Issn 0036-8075. Disponível Em: < <Go To Isi>://Wos:A1995tk47600040 >.

Taccola, L. et al. Zinc Oxide Nanoparticles As Selective Killers Of Proliferating Cells. **International Journal Of Nanomedicine,** V. 6, P. 1129-1140, 05/30

05/28/Received 2011. Issn 1176-9114

1178-2013. Disponível Em: < Http://Www.Ncbi.Nlm.Nih.Gov/Pmc/Articles/Pmc3118687/ >.

Thakur, S. et al. Plant-Driven Removal Of Heavy Metals From Soil: Uptake, Translocation, Tolerance Mechanism, Challenges, And Future Perspectives. **Environmental Monitoring And Assessment,** V. 188, N. 4, P. 206, 2016/03/03 2016. Issn 1573-2959. Disponível Em: < Https://Doi.Org/10.1007/S10661-016-5211-9 >.

Van Steveninck, R. F. M. et al. The Binding Of Zinc In Root Cells Of Crop Plants By Phytic Acid. **Plant And Soil,** V. 155, N. 1, P. 525-528, 1993/10/01 1993. Issn 1573-5036. Disponível Em: < Https://Doi.Org/10.1007/Bf00025099 >.

The Binding Of Zinc, But Not Cadmium, By Phytic Acid In Roots Of Crop Plants. **Plant And Soil,** V. 167, N. 1, P. 157-164, 1994/11/01 1994. Issn 1573-5036. Disponível Em: < Https://Doi.Org/10.1007/Bf01587611 >.

Wang, Z. Y. et al. Xylem- And Phloem-Based Transport Of Cuo Nanoparticles In Maize (Zea Mays L.). **Environmental Science & Technology,** V. 46, N. 8, P. 4434-4441, Apr 2012. Issn 0013-936x. Disponível Em: < <Go To Isi>://Wos:000302850300026 >.

Yoon, S.-J. et al. Zinc Oxide Nanoparticles Delay Soybean Development: A Standard Soil Microcosm Study. **Ecotoxicology And Environmental Safety,** V. 100, P. 131-137, Feb 2014. Issn 0147-6513. Disponível Em: < <Go To Isi>://Wos:000330161000018 >.

Yuan, J. et al. Internalization And Phytotoxic Effects Of Cuo Nanoparticles In Arabidopsis Thaliana As Revealed By Fatty Acid Profiles. **Environmental Science & Technology,** V. 50, N. 19, P. 10437-10447, Oct 2016. Issn 0013-936x. Disponível Em: < <Go To Isi>://Wos:000384841900017 >.

Zhai, G. et al. Transport Of Gold Nanoparticles Through Plasmodesmata And Precipitation Of Gold Ions In Woody Poplar. **Environmental Science & Technology Letters,** V. 1, N. 2, P. 146-151, Feb 2014. Issn 2328-8930.

Zhang, L. W.; Monteiro-Riviere, N. A. Mechanisms Of Quantum Dot Nanoparticle Cellular Uptake. **Toxicological Sciences,** V. 110, N. 1, P. 138-155, Jul 2009. Issn 1096-6080. Disponível Em: < <Go To Isi>://Wos:000267227800013 >.

Zhu, Z.-J. et al. Effect Of Surface Charge On The Uptake And Distribution Of Gold Nanoparticles In Four Plant Species. **Environmental Science & Technology,** V. 46, N. 22, P. 12391-12398, Nov 20 2012. Issn 0013-936x. Disponível Em: < <Go To Isi>://Wos:000311873500019 >.

CHAPTER 4

4.1. Introduction

Engineered Nanomaterials (ENMs) are finding use in the agricultural sector as nano-based fertilizers and pesticides. The use of this technology would introduce huge amounts of ENMs into the environment that could have positive or negative effects on agro- and natural ecosystems. Thus, numerous studies have been conducted over the last decade that focus on the effects ENMs on plants . These lines of investigation are crucial to elucidate how ENMs act as effectors that alter plant physiology to answer challenging questions like how plants perceive and react to these stimuli resulting in physiological reprograming. A powerful tool to characterize and analyze these responses is through measurements of transcriptome changes post ENM exposure. The limited transcript analysis studies conducted to date have shown that significant changes occur in plant transcriptomes that are predicted to alter the physiology and biological processes of the plant as a result of NP exposure . However, more thorough analyses are required to allow for a better understanding of how plants perceive ENMs and how they deal with these stimuli. Many of these early studies utilized microarray analysis to track plant gene expression profiles post ENM exposure. In *Arabidopsis thaliana* roots the lowest numbers of differentially regulated genes occurred upon exposed to ZnO NPs, when compared to bulk ZnO and ionic Zn^{2+} treated plants. However, the genes that were upregulated post interaction with the ZnO NPs were enriched for signal transduction and stress response genes . In another study, it was found that ZnO NPs elicited a larger number of genes and the differentially expressed genes were involved in abiotic and biotic stress responses in *A. thaliana* as compared to fullerene soot and $nTiO_2$. Quantitative real time PCR, which is used in all fields of biology is a reliable tool to study gene expression, although only one gene can be studied as a time. In canola roots and shoots exposed to ENMs, genes such as auxin responsive protein and protein kinase decreased with increasing concentration of ZnO

NPs (at 1000 mg/L), as revealed by the qPCR study . In A. *thaliana* exposed to ZnO NPs, zinc homeostasis genes like AtHMA3 and AtHMA4, macro- and microelement homoeostasis genes were upregulated in the shoots, and the hormone regulation genes like AtNAC1, AtASA1 were upregulated in roots but downregulated in the shoots .

RNA sequencing (RNA Seq) is the most comprehensive tool to analyze global transcriptome profiles and also offers a precise measurements of levels of transcripts nearly as accurate as qPCR which can be used to look at a single gene and is much more accurate than microarray analysis which can look at a large set of genes but does not provide a comprehensive look at the entire transcriptome . In our study, RNA Seq was employed to survey the full transcriptome of the model monocot plant, *Hordeum vulgare* (barley) exposed to ZnO NPs. We have used ionic Zn^{2+} ($ZnSO_4$) exposed barley for comparative analysis. The objective of this study was to investigate the gene profiles of barley in response to ZnO NPs and $ZnSO_4$.

4.2. Materials and Methods

4.2.1. ZnO NP Characterization

For zeta (ζ)-potential and hydrodynamic diameter measurements, the ZnO NPs were dispersed in DI water using a sonicator for 30 seconds at a concentration of 500 mg/L of Zn. The zeta (ζ)-potential and particle size distribution was measured with a ZetaSizer (Nano-ZS 90, Malvern). For evaluating the particle size distribution, a JEOL JEM-2100 LaB6 Transmission Electron Microscope (TEM) was used (JEOL USA, Peabody MA) operating at 200 kV. Bright-field images of each sample were acquired with a Gatan Orius SC1000 CCD camera; dark-field imaging was acquired utilizing a Gatan 805 High Angle Annular Dark Field detector with a Gatan Digiscan II controller unit and the TEM running in scanning transmission electron microscopy (STEM) mode.

4.2.2. Plant Growth and Treatments

The barley cultivar CI5791 was grown in cones containing 58.2 g of saturated potting mix (Pro Mix Loose Fill). Two seeds were sowed per cone and were treated as the same sample. A total of eight cones were allocated to each treatment. Emergence was recorded at 4 days after planting. ZnO NP and $ZnSO_4$ treatment was applied at the 2-leaf stage. ZnO NPs and $ZnSO_4$ were applied in the form of de-ionized water suspension with 2.5 mg (500 mg suspended in 1L of water; pot watered with 5 ml of suspension) of zinc per treatment. Secondary leaf tissue was collected from three individual plants of each treatment, and immediately frozen in liquid nitrogen and placed in a -80°C freezer until isolation of RNA was performed for RNAseq. Leaf samples were collected at 0 h pre-application of NPs and $ZnSO_4$ (control), likewise at 6, and 48 h post-application (hpa). The plants were grown in a controlled growth chamber under photoperiod conditions of 12 h light and 12 h dark at 21ºC.

4.2.3. mRNA Extraction, RNA-Seq Library Preparation and Sequencing

Three leaf samples of equal size (~2 cm) from each replicate per treatment were combined in a single tube and used for total RNA extraction. The total RNA was extracted from these frozen leaf samples using the RNeasy mini kit (Qiagen, Chatsworth, CA) following the manufacturers standard protocol. RNA concentrations were measured using the Qubit® Broad Range RNA kit on a Qubit® 2.0 fluorometer (ThermoFisher Scientific), and RNA samples were visualized on 1% agarose gels stained with gel red (Biotium) to confirm the integrity of samples. RNA samples with four sharp ribosomal RNA (rRNA) bands; approximate molecular weights of 3.4, 1.8, 1.5, and 1.1 kb corresponding to nuclear 28S and 18S rRNAs and 23S and 16S plastid rRNAs, respectively, without a high molecular weight genomic DNA contamination band were considered quality RNA. 1µg of total RNA was used for RNA sequencing (RNA-Seq) library construction using the TruSeq

RNA Library Prep Kit v2 (Illumina, San Diego, CA) following the manufacture's standard protocol. The final library was validated and quantified on the Agilent 2100 Bioanalyzer. The cDNA library from 15 different samples were pooled into one single tube and were normalized according to the manufacturer's protocol. The library pool was diluted to a concentration of 1.8 pm and sequenced on the Illumina NextSeq 500 sequencer on a single flow cell at the USDA Cereal Genotyping Centre, Fargo, ND, USA. A total of 3 flow cells were used. The NextSeq® 500/550 High Output Kit v2 (150 cycles) was used for the generation of 150 bp single end sequencing reads. The raw sequencing reads were demultiplexed and converted into individual fastq files using bcl2fastq software v2.17.1.14 (Illumina, San Diego, CA). The fastq reads were quality trimmed in CLC Genomics Workbench v8.0.3 (CLC bio, Aarhus, Denmark) using default settings.

4.2.4. Expression Analysis

The analysis pipeline for mapping reads to reference genome, quality check, and for expression analyses was performed as previously described by Sharma Poudel 2018. In short, high quality trimmed sequencing reads were mapped to the barley RefSeq v1.0 (http://webblast.ipk-gatersleben.de/barley_ibsc/) in CLC Genomics Workbench v8.0.3 to obtain barley specific genes. Gene specific and transcript specific reads were obtained from the reference gene as well as from the gene track and mRNA tract information. This enabled reads to align to both intronic and intergenic regions. Reads less than 90% identical for 90% of the read length and that mapped to more than 10 positions were discarded. The total reads mapped for each gene model were normalized to obtain reads per kilobase of exon model per million mapped reads (RPKM) values for each sample. In all the comparisons, the false discovery rate (FDR) corrected p-values were calculated by the exact test using EdgeR bioconductor package in CLC genomics. Genes with EDGE fold change>3 and FDR corrected p-value<0.05 were considered as differentially expressed

genes (DEGs). All treatments were compared with 0 h control. Venn diagrams were prepared using VENNY to compare the DEGs between the treatments.

4.2.5. Functional Annotation

The high confidence genes were annotated in the publicly available IBSC RefSeq v1.0 (http://webblast.ipk-gatersleben.de/barley_ibsc/downloads/). The annotations were supplemented by performing a local BlastX of the whole set of predicted barley proteins to the reannotated Arabidopsis Col-0 genome (Araport11) (https://www.araport.org/ data/araport11) . The top hits of high confidence barley genes with predicted amino acid homologies greater than 30% and alignment lengths greater than 50% with Arabidopsis annotated genes were used to assign Arabidopsis gene IDs to the barley genes.

4.2.6. Gene Enrichment Analysis

The GO term mapping for the best Arabidopsis gene hits for the barley DEGs were used for gene enrichment analysis. GO term enrichment analysis was performed in bioconductor R package TopGO version 2.28.0 . In the TopGO package, Fisher's exact test was performed to calculate the significance of GO term enrichment. The cut-off for number of genes annotated for a single GO term was fixed at 5 genes with p-value less than 0.001.

4.3. Results

4.3.1. ζ-Potential and Particle Size

The ζ-potential and hydrodynamic diameter of the ZnO NPs was found to be 25.9±4.7 mV and 512.5 nm in DI water respectively. The particle size ranged from 10-170 nm (smallest value is 8 nm and largest value is 173.33 nm), 92.96% of the ZnO NPs had the smallest dimension within 100 nm (Figure 4.1).

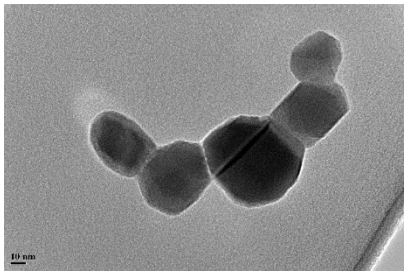

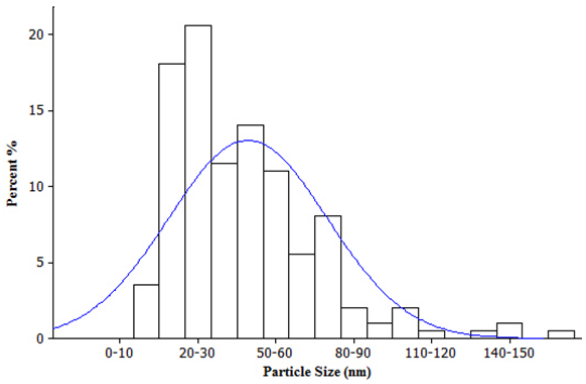

(a) (b)

Figure 4.1. TEM micrograph of bare ZnO NPs, and (b) particle size distribution of ZnO NPs based on smallest dimensions.

4.3.2. RNA Seq Based Transcriptome Profiling

Time course RNAseq analyses from leaf samples at 0, 6, and 48 hours post ZnO NP and $ZnSO_4$ application (hpa) identified differentially expressed genes (DEGs) in response to the treatments (Table 4.1). The number of DEGs in response to ZnO NP treatment was the highest at 6 hpa, showing 71 upregulated, and 134 downregulated genes. At 48 hpa of ZnO NP, the number of DEGs significantly decreased from the 6 hpa level to 2 upregulated and 14 downregulated genes. For the $ZnSO_4$ treatment the temporal changes of DEG was similar to the ZnO NP treatment, showing 79 upregulated and 122 downregulated genes at the 6 hpa timepoint. At the 48 hpa timepoint similar to the ZnO NP treatment the DEGs began to return to their basal expression levels showing 2 upregulated and 83 downregulated genes. The gene expression levels of the experimental treatments were compared with the 0 h control (no application). It was evident from the gene expression analysis that barley seedlings of the CI5791 genotype had temporally similar response after ZnO NP and $ZnSO_4$ application at the initial time-points which gradually falls back to basal levels at the later time-points.

Table 4.1. The number of DEGs in each treatment across time-points

	Upregulated Genes	Downregulated Genes
ZnO NP		
6h	71	134
48h	2	14
$ZnSO_4$		
6h	79	122
48h	2	83

For the ZnO NP and $ZnSO_4$ treatments at 6 hpa there were 55 common upregulated DEGs, and at 48 hpa, 1 common upregulated DEG. For downregulated DEGs there were 76 common genes at 6 hpa, and 13 common genes at 48 hpa, when comparing the ZnO NP and $ZnSO_4$ treatments (Figure 4.2a and b). Among the upregulated genes, 60% and, among the downregulated genes, 74% of the common genes had higher fold changes (absolute value) in $ZnSO_4$ treatments.

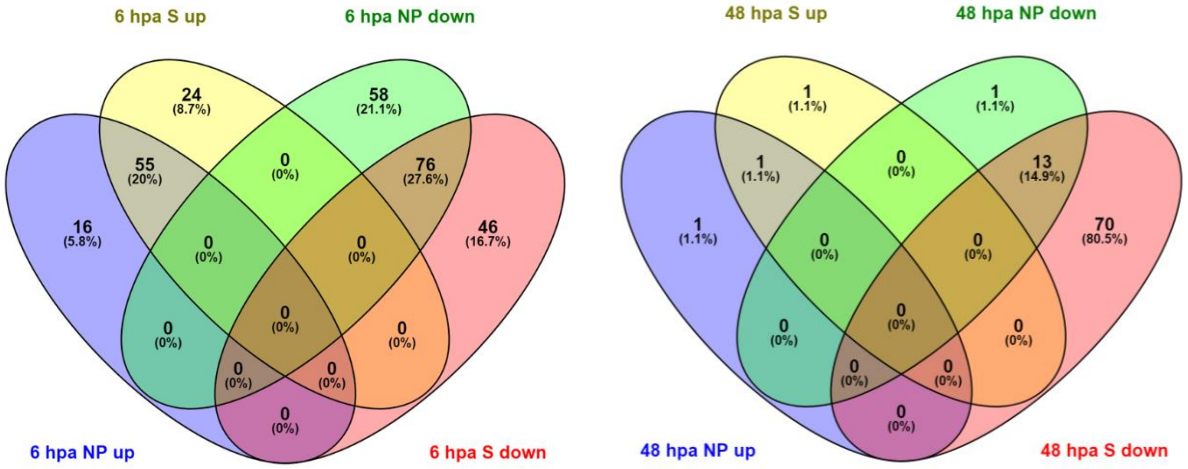

(a) 6 hpa (b) 48 hpa

Figure 4.2. Number of up and downregulated genes at (a) 6 hpa and, (b) 48 hpa

4.3.3. Gene Enrichment Analysis of DEGs Using Classification Superviewer and TopGO

TopGO analyses of the upregulated genes revealed that the most significant GO terms enriched were translation, and ribosome biogenesis at 6 hpa for both ZnO NP and $ZnSO_4$

treatments (Figure 4.3a, b and Appendix C Tables 1a, c). For downregulated genes, at 6 hpa, the most significant GO terms enriched were photosynthesis, and negative regulation of photomorphogenesis in ZnO NP, and photosynthesis and protein-chromophore linkage in the $ZnSO_4$ treatments. 48 hpa expression data for upregulated genes in ZnO NP is not discussed as the dataset did not yield any significantly enriched GO terms. However, GO term enrichment for downregulated genes at 48 hpa for ZnO NP yielded response to wounding. For $ZnSO_4$ treatments at 48 hpa, the significant GO terms enriched were maturation of LSU-rRNA from tricistronic rRNA transcript, and regulation of rRNA processing for upregulated genes, and response to wounding for downregulated genes. It is evident from the enrichment analyses that ZnO NP and $ZnSO_4$ elicit similar biological processes in plants for the earlier time point and differential responses occurred at the later time point.

(a) Biological Process enriched at 6 hpa ZnO NP treatment

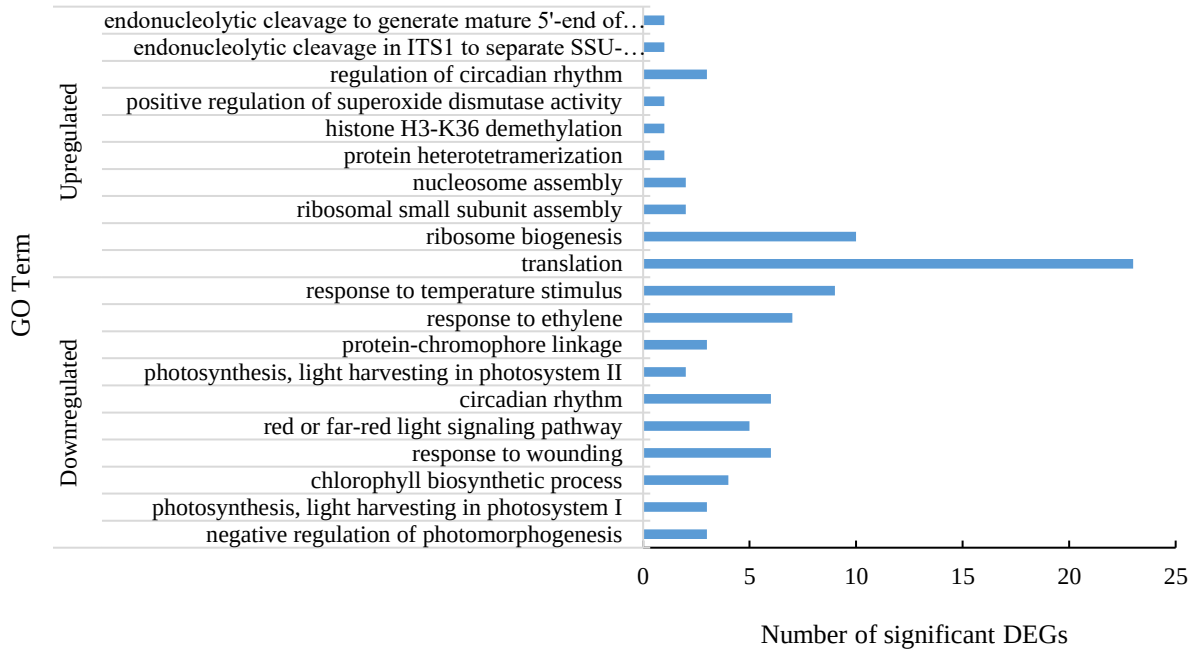

Figure 4.3. The number of significant Differentially Expressed Genes (DEGs) enriched for Gene Ontology (GO) terms involved in biological processes in (a) 6 hpa ZnO NP treatment, and (b) 6 hpa $ZnSO_4$ expression data using TopGO.

(b) Biological Process enriched at 6 hpa $ZnSO_4$ treatment

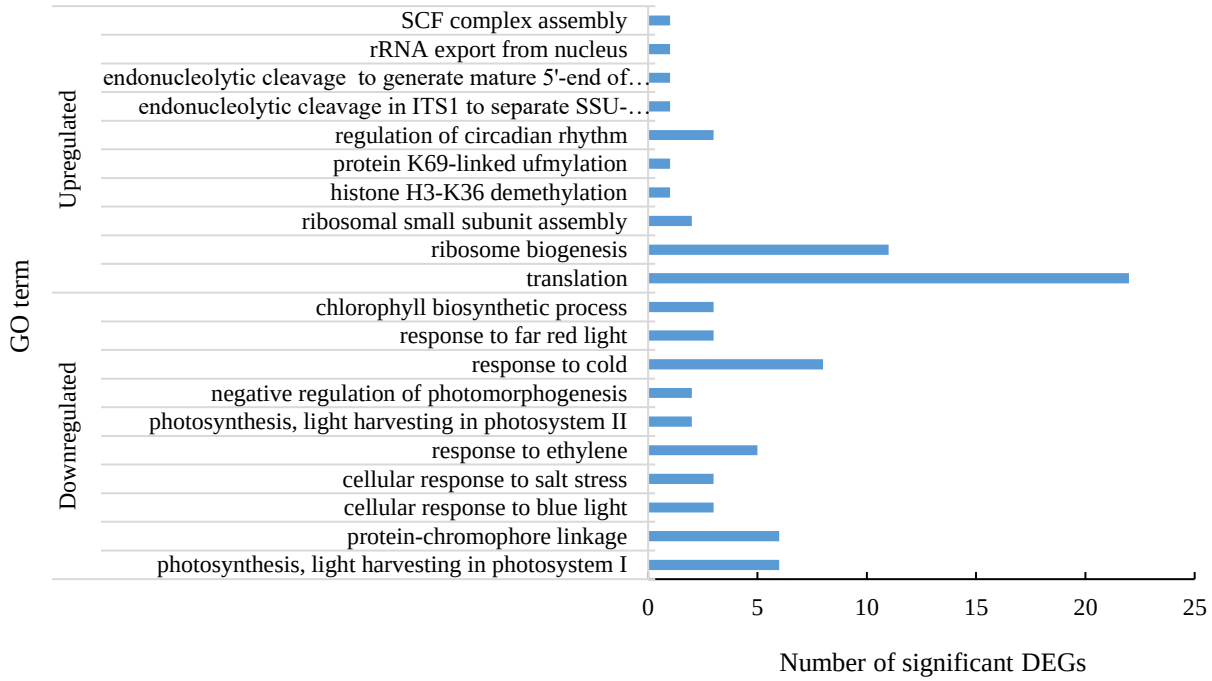

Figure 4.3. The number of significant Differentially Expressed Genes (DEGs) enriched for Gene Ontology (GO) terms involved in biological processes in (a) 6 hpa ZnO NP treatment, and (b) 6 hpa $ZnSO_4$ expression data using TopGO (continued)

4.4. Discussion and Conclusion

From the RNAseq analysis of barley line CI5791, it was evident that at the earlier time-point after NP exposure (6 hpa), there was a rapid response to ZnO NPs which returned to basal levels at 48 hpa. In $ZnSO_4$ treatments, a similar response pattern was observed at 6 hpa which persisted at 48 hpa. However, a close inspection of the DEG profile at 6 hpa revealed that 26.9% of the total DEGs were exclusive to ZnO NP, and 25.4% of the total DEGs were exclusive to $ZnSO_4$ exposed barley leaves (Figure 4.2a). At 48 hpa, 2.2% of the total DEGs were exclusive to ZnO NP, and 81.6% of the total DEGs were exclusive to $ZnSO_4$ exposed barley leaves (Figure 4.2b). The common DEGs between both the treatments can be attributed to the effect of dissolved Zn^{2+} ions in the media in case of both ZnO NP and to $ZnSO_4$. However, the presence of exclusive DEGs in each treatment indicates that plant perception of ZnO NPs is also unique to that of $ZnSO_4$.

This unique gene expression of ZnO NP exposed plants may stem from physical attributes of the NPs like the size and chemical attributes like slow dissolution rate. The common genes that are differentially expressed may be a response to the Zn^{2+} ions that dissolved from the $ZnSO_4$ and ZnO NPs.

At 6 hpa, 16 genes upregulated were exclusive to ZnO NP alone (Table 2a, Appendix C). Out of the 16 genes, 5 genes code for ribosomal proteins. The other DEGs exclusive to the ZnO NP treatment include heat stress transcription factor C-1b (HORVU3Hr1G069590), nucleosome assembly protein (HORVU6Hr1G051930), Yellow Stripe-like 7 (HORVU6Hr1G059420), Adenosyl-homocysteinase (HORVU2Hr1G109370), thionin (HORVU6Hr1G000720), and, a 4-hydroxy-tetrahydrodipicolinate reductase (HORVU1Hr1G021120) gene. Yellow Stripe-like 7 gene (HORVU6Hr1G059420) was upregulated 3.28 folds in the ZnO NP treatment. The predicted protein is annotated with 6 transmembrane domains, suggesting its membrane localization. It shares 97% identity with a probable metal-nicotianamine transporter YSL14 in *Aegilops tauschii*. The Arabidopsis ortholog is the Yellow stripe-like (YSL) 7 (AT1G65730) gene which shares 68% amino acid similarity with the barley gene model HORVU6Hr1G059420. YSL proteins are implicated in the transport of nicotianamine (NA)-metal complexes, like Fe(II)-NA , and also play a role in the transport of Zn and Cu from leaves into seeds . The Arabidopsis AtYSL7 protein has also been found to transport *Pseudomonas* virulence factor Syringolin A into plant cells . It hints at the possibility that it is not a substrate specific transporter, indicating that it may play a role in ZnO NP transport. Another gene HORVU6Hr1G000720 was upregulated 24.5 folds at 6 hpa in ZnO NP-exposed plants. The protein shares 89% identity with *Hordeum jubatum* thionin. Thionin is a family of plant antimicrobial peptide that is effective against bacteria, fungi, and yeast . In *Arabidopsis thaliana*, Thionin 2.4 was expressed in the cell wall and contributed to suppressed

toxicity against *Fusarium graminearum* . The mechanism of resistance involved blocking of the *F. graminearum* secreted-fungal fruit body lectin (FFBL) in *Arabidopsis* by thionin 2.4. It is interesting to note that *F. graminearum* is a hemibiotroph that exhibits a brief biotrophic phase prior to a necrotrophic phase . In our study, on ZnO NP exposure, the barley plants expressed a gene (thionin) which is known to play a role in defense against hemibiotrophic pathogens that exhibit an initial biotrophic lifestyle during early colonization of their plant host. On the contrary, with $ZnSO_4$ exposure, a gene (thaumatin-like) was expressed that is involved in defense against a necrotroph.

At 6 hpa, 24 upregulated genes were exclusive to the $ZnSO_4$ treatment (Table 2b, Appendix C). Out of the 24 genes, 5 genes were predicted to encode ribosomal proteins. The other genes were predicted to encode proteins that included osmotin 34 (HORVU5Hr1G051970), kiwellin (HORVU5Hr1G067760), wound-induced proteins (HORVU3Hr1G113120 and HORVU3Hr1G113620), organic cation/carnitine transporter 3 (HORVU0Hr1G003480), F-box protein PP2-B1 (HORVU4Hr1G086110), zinc finger protein (HORVU7Hr1G042080), glutathione S-transferase family protein (HORVU4Hr1G081100), and indole-3-glycerol phosphate synthase (HORVU7Hr1G114660).

Wound induced proteins or pathogenesis-related protein 4 (PR-4) are well-known to play multiple roles in plant defense signaling . Protein HORVU3Hr1G113120 shares 98% and 74% identities with wheat PR-4 and Arabidopsis PR-4 respectively. The gene was upregulated 200.84 folds in $ZnSO_4$-exposed plants at 6 hpa. PR-4c in pepper (*Capsicum annuum*) is a plasma membrane protein that is an important component of plant defense signaling and is found to confer resistance against the pathogens *Pseudomonas syringae* pv. *tomato* and *Hyaloperonospora arabidopsidis* . Another protein, osmotin 34 (HORVU5Hr1G051970) is a pathogenesis-related

thaumatin superfamily protein which was upregulated 586.7 folds at 6 hpa. The *Triticum aestivum* (wheat) ortholog is thaumatin-like protein (TLP) with 98% amino acid identity to the HORVU5Hr1G051970 protein model. TLPs are pathogenesis-related (PR) proteins that are induced by pathogen infection . In Arabidopsis, expression of a TLP, ObTLP1 enhanced tolerance to the necrotrophic fungal pathogens, *Scleretonia sclerotiorum* and *Botrytis cinerea* . The expression of PR proteins in $ZnSO_4$ and not in ZnO NP exposed plants hints at the possibility of plants perceiving $ZnSO_4$ as more toxic compared to ZnO NPs. This may be attributed to the high levels of Zn^{2+} ions from the dissolved $ZnSO_4$, as it is known to dissolve faster than ZnO NPs . The resultant surge of Zn^{2+} ions in the soil media can possibly be the source of toxicity .

Out of the 55 common genes to both ZnO NP-exposed and $ZnSO_4$-exposed plants upregulated at 6 hpa, 22 genes code for ribosomal proteins (Table 2c, Appendix C). The other significant DEGs common to both tratments included the cold regulated gene (HORVU4Hr1G077480), salt-inducible protein (HORVU4Hr1G089560), aquaporin-like superfamily protein (HORVU4Hr1G085250), pumilio 7 (HORVU5Hr1G038840), mitochondrial glycoprotein family proteins (HORVU7Hr1G046980 and HORVU3Hr1G011460), protein kinase superfamily protein (HORVU2Hr1G075470), and hypersensitive-induced response protein 4 (HORVU7Hr1G017190). Protein HORVU5Hr1G038840 was upregulated 100.28 and 76.47 folds at 6 hpa in ZnO NP and $ZnSO_4$-exposed plants respectively. It shares 96% and 91% sequence identities with pumilio-like protein 7 in *Aegilops tauschii* and *Triticum urartu*, respectively. Pumilio proteins have diverse cellular functions like translation initiation, cytoplasmic de-adenylation, translational repression through RNA localization or RNA decay, mitochondria motility and biogenesis, and rRNA processing and ribosome biogenesis in Arabidopsis. HORVU4Hr1G089560 was upregulated 124 folds at 6 hpa in both ZnO NP and $ZnSO_4$-exposed

plants. It shares 84% amino acid identity with a salt-inducible protein in *Leymus chinensis*. The homolog, LcSAIN1 was found to be induced in *Leymus chinensis* in response to high salt stress, and its overexpression in Arabidopsis and rice induced tolerance against salt stress.

The downregulated genes reflect the gene expression that declined after exposure to the treatments. 76 genes were downregulated common to both ZnO NP and $ZnSO_4$ treatments at 6 hpa (Table 2d, Appendix C). Some of the genes downregulated that were common to both ZnO NPs and $ZnSO_4$ encoded chlorophyll a/b binding proteins, although there were no visible changes in chlorophyll content. The chlorophyll a/b binding proteins are light harvesting proteins, and their downregulation indicates stress responses.

In case of 6 hpa ZnO NP treatment, out of 134 downregulated genes, 56 were exclusive (Table 2e, Appendix C). Such genes include heavy metal transport/detoxification superfamily protein (HORVU1Hr1G036920), WRKY DNA-binding protein 33 (HORVU3Hr1G088200), cysteine synthase D1 (HORVU5Hr1G005980), subtilisin-like protease (HORVU4Hr1G013170), trehalose phosphate synthase (HORVU6Hr1G084190), and protein kinases like calcium-dependent protein kinase 28 (HORVU6Hr1G014700), and receptor-like protein kinase (HORVU1Hr1G088680). In case of $ZnSO_4$ treatments, out of 122 downregulated genes, 46 were exclusive (Table 2f, Appendix C). These genes include protein NRT1/ PTR FAMILY 8.5 (HORVU2Hr1G001320), peroxisomal membrane protein 2 (HORVU1Hr1G022840), mitochondrial substrate carrier family protein (HORVU3Hr1G025820), glycogen synthase (HORVU7Hr1G025390), and NAD-dependent epimerase/dehydratase (HORVU7Hr1G083360).

The gene expression profiles of ZnO NP and $ZnSO_4$ treated barley indicate that plant responses fall back to basal levels at 48 hpa, implying that the plant responses reach equilibrium at 48 hpa. Although there is similar gene expression pattern in plants treated with ZnO NPs and

$ZnSO_4$, there are notable differences in the gene profile. The DEGs common to both the treatments potentially reflect plant responses to Zn^{2+} ions dissociated from the ZnO NPs and $ZnSO_4$ in soil. The DEGs exclusive to both the treatments can be attributed to the plants responding differently to the particle size and Zn^{2+} ion dissociation rate of ZnO NPs and $ZnSO_4$.

4.5. References

Abbasi, N.; Park, Y.-I.; Choi, S.-B. Pumilio Puf Domain Rna-Binding Proteins In Arabidopsis. **Plant Signaling & Behavior,** V. 6, N. 3, P. 364-368, 2011. Issn 1559-2324

1559-2316. Available At: < Https://Www.Ncbi.Nlm.Nih.Gov/Pubmed/21350339 >.Available At: < Https://Www.Ncbi.Nlm.Nih.Gov/Pmc/Pmc3142416/ >.

Alexa, A.; Rahnenfuhrer, J. Topgo: Enrichment Analysis For Gene Ontology. **R Package Version,** V. 2, N. 0, 2010.

Alexa, A.; Rahnenführer, J.; Lengauer, T. Improved Scoring Of Functional Groups From Gene Expression Data By Decorrelating Go Graph Structure. **Bioinformatics,** V. 22, N. 13, P. 1600-1607, 2006. Issn 1460-2059.

Asano, T. Et Al. The Secreted Antifungal Protein Thionin 2.4 In Arabidopsis Thaliana Suppresses The Toxicity Of A Fungal Fruit Body Lectin From Fusarium Graminearum. **Plos Pathogens,** V. 9, N. 8, Aug 2013. Issn 1553-7374. Available At: < <Go To Isi>://Wos:000323888200069 >.

Bilgin, D. D. Et Al. Biotic Stress Globally Downregulates Photosynthesis Genes. **Plant, Cell & Environment,** V. 33, N. 10, P. 1597-1613, 2010/10/01 2010. Issn 0140-7791. Available At: < Https://Doi.Org/10.1111/J.1365-3040.2010.02167.X >. Accessed On: 2018/12/13.

Burman, U.; Saini, M.; Praveen, K. Effect Of Zinc Oxide Nanoparticles On Growth And Antioxidant System Of Chickpea Seedlings. **Toxicological And Environmental Chemistry,** V. 95, N. 4, P. 605-612, Apr 2013. Issn 0277-2248. Available At: < <Go To Isi>://Wos:000320913000006 >.

Dai, Y. Et Al. Interaction Of Cuo Nanoparticles With Plant Cells: Internalization, Oxidative Stress, Electron Transport Chain Disruption, And Toxicogenomic Responses. **Environmental Science: Nano,** V. 5, N. 10, P. 2269-2281, 2018.

Didonato, R. J., Jr. Et Al. Arabidopsis Yellow Stripe-Like2 (Ysl2): A Metal-Regulated Gene Encoding A Plasma Membrane Transporter Of Nicotianamine-Metal Complexes. **Plant J,** V. 39, N. 3, P. 403-14, Aug 2004. Issn 0960-7412 (Print)

0960-7412.

Dimkpa, C. O. Et Al. Cuo And Zno Nanoparticles: Phytotoxicity, Metal Speciation, And Induction Of Oxidative Stress In Sand-Grown Wheat. **Journal Of Nanoparticle Research,** V. 14, N. 9, Sep 2012. Issn 1388-0764. Available At: < <Go To Isi>://Wos:000308225800053 >.

Du, W. Et Al. Differential Effects Of Copper Nanoparticles/Microparticles In Agronomic And Physiological Parameters Of Oregano (Origanum Vulgare). **Science Of The Total Environment,** V. 618, P. 306-312, 2018/03/15/ 2018. Issn 0048-9697. Available At: < Http://Www.Sciencedirect.Com/Science/Article/Pii/S0048969717331005 >.

Girilal, M. Et Al. Comparative Stress Physiology Analysis Of Biologically And Chemically Synthesized Silver Nanoparticles On Solanum Lycopersicum L. **Colloid And Interface Science Communications,** V. 24, P. 1-6, 2018/05/01/ 2018. Issn 2215-0382. Available At: < Http://Www.Sciencedirect.Com/Science/Article/Pii/S2215038217300754 >.

Hofstetter, S. S. Et Al. Arabidopsis Yellow Stripe-Like7 (Ysl7) And Ysl8 Transporters Mediate Uptake Of Pseudomonas Virulence Factor Syringolin A Into Plant Cells. **Molecular Plant-Microbe Interactions,** V. 26, N. 11, P. 1302-1311, 2013. Issn 0894-0282.

Kaveh, R. Et Al. Changes In Arabidopsis Thaliana Gene Expression In Response To Silver Nanoparticles And Silver Ions. **Environmental Science & Technology,** V. 47, N. 18, P. 10637-10644, Sep 17 2013. Issn 0013-936x. Available At: < <Go To Isi>://Wos:000330096000070 >.

Kim, N. H.; Hwang, B. K. Pepper Pathogenesis-Related Protein 4c Is A Plasma Membrane-Localized Cysteine Protease Inhibitor That Is Required For Plant Cell Death And Defense Signaling. **The Plant Journal,** V. 81, N. 1, P. 81-94, 2015/01/01 2014. Issn 0960-7412. Available At: < Https://Doi.Org/10.1111/Tpj.12709 >. Accessed On: 2018/12/09.

Kitajima, S.; Sato, F. Plant Pathogenesis-Related Proteins: Molecular Mechanisms Of Gene Expression And Protein Function. **J Biochem,** V. 125, N. 1, P. 1-8, Jan 1999. Issn 0021-924x (Print)

0021-924x.

Landa, P. Et Al. The Transcriptomic Response Of Arabidopsis Thaliana To Zinc Oxide: A Comparison Of The Impact Of Nanoparticle, Bulk, And Ionic Zinc. **Environmental Science & Technology,** V. 49, N. 24, P. 14537-14545, Dec 2015. Issn 0013-936x. Available At: < <Go To Isi>://Wos:000366872300076 >.

Nanoparticle-Specific Changes In Arabidopsis Thaliana Gene Expression After Exposure To Zno, Tio2, And Fullerene Soot. **Journal Of Hazardous Materials,** V. 241, P. 55-62, Nov 30 2012. Issn 0304-3894. Available At: < <Go To Isi>://Wos:000313088300004 >.

Li, X. Et Al. Lcsain1, A Novel Salt-Induced Gene From Sheepgrass, Confers Salt Stress Tolerance In Transgenic Arabidopsis And Rice. **Plant Cell Physiol,** V. 54, N. 7, P. 1172-85, Jul 2013. Issn 0032-0781.

Liu, J.-J.; Sturrock, R.; Ekramoddoullah, A. K. M. The Superfamily Of Thaumatin-Like Proteins: Its Origin, Evolution, And Expression Towards Biological Function. **Plant Cell Reports,** V. 29, N. 5, P. 419-436, 2010/05/01 2010. Issn 1432-203x. Available At: < Https://Doi.Org/10.1007/S00299-010-0826-8 >.

Madden, T. The Blast Sequence Analysis Tool. 2013.

Milani, N. **Zinc Oxide Nanoparticles In The Soil Environment: Dissolution, Speciation, Retention, And Bioavailability**. 2011. (Doctor Of Philosophy). Soil Science, The University Of Adelaide, Adelaide.

Misra, R. C. Et Al. A Thaumatin-Like Protein Of Ocimum Basilicum Confers Tolerance To Fungal Pathogen And Abiotic Stress In Transgenic Arabidopsis. **Scientific Reports,** V. 6, P. 25340, 05/06

10/14/Received

04/13/Accepted 2016. Issn 2045-2322. Available At: < Http://Www.Ncbi.Nlm.Nih.Gov/Pmc/Articles/Pmc4858651/ >.

Movafeghi, A. Et Al. Effects Of Tio2 Nanoparticles On The Aquatic Plant Spirodela Polyrrhiza: Evaluation Of Growth Parameters, Pigment Contents And Antioxidant Enzyme Activities. **Journal Of Environmental Sciences,** V. 64, P. 130-138, 2018/02/01/ 2018. Issn 1001-0742. Available At: < Http://Www.Sciencedirect.Com/Science/Article/Pii/S1001074217303212 >.

Nair, P. M. G.; Chung, I. M. Regulation Of Morphological, Molecular And Nutrient Status In Arabidopsis Thaliana Seedlings In Response To Zno Nanoparticles And Zn Ion Exposure. **Science Of The Total Environment,** V. 575, P. 187-198, Jan 2017. Issn 0048-9697. Available At: < <Go To Isi>://Wos:000390373400021 >.

Nawrot, R. Et Al. Plant Antimicrobial Peptides. **Folia Microbiologica,** V. 59, N. 3, P. 181-196, 10/04

04/18/Received

09/17/Accepted 2014. Issn 0015-5632

1874-9356. Available At: < Http://Www.Ncbi.Nlm.Nih.Gov/Pmc/Articles/Pmc3971460/ >.

Rahmani, F. Et Al. Impact Of Zinc Oxide And Copper Oxide Nano-Particles On Physiological And Molecular Processes In Brassica Napus. **Indian Journal Of Plant Physiology,** V. 21, N. 2, P. 122-128, 2016. Issn 0019-5502.

Raliya, R. Et Al. Mechanistic Evaluation Of Translocation And Physiological Impact Of Titanium Dioxide And Zinc Oxide Nanoparticles On The Tomato (Solanum Lycopersicum L.) Plant. **Metallomics,** V. 7, N. 12, P. 1584-1594, 2015. Issn 1756-5901. Available At: < <Go To Isi>://Wos:000365906300005 >.

Reed, R. B. Et Al. Solubility Of Nano-Zinc Oxide In Environmentally And Biologically Important Matrices. **Environmental Toxicology And Chemistry,** V. 31, N. 1, P. 93-99, 2012. Issn 1552-8618

0730-7268. Available At: < Https://Www.Ncbi.Nlm.Nih.Gov/Pubmed/21994124 >.Available At: < Https://Www.Ncbi.Nlm.Nih.Gov/Pmc/Pmc4713012/ >.

Sels, J. Et Al. Plant Pathogenesis-Related (Pr) Proteins: A Focus On Pr Peptides. **Plant Physiology And Biochemistry,** V. 46, N. 11, P. 941-950, 2008/11/01/ 2008. Issn 0981-9428. Available At: < Http://Www.Sciencedirect.Com/Science/Article/Pii/S0981942808001137 >.

Stintzi, A. Et Al. Plant 'Pathogenesis-Related' Proteins And Their Role In Defense Against Pathogens. **Biochimie,** V. 75, N. 8, P. 687-706, 1993. Issn 0300-9084 (Print)

0300-9084.

Trail, F. For Blighted Waves Of Grain: <Em>Fusarium Graminearum</Em> In The Postgenomics Era. **Plant Physiology,** V. 149, N. 1, P. 103, 2009. Available At: < Http://Www.Plantphysiol.Org/Content/149/1/103.Abstract >.

Tumburu, L. Et Al. Molecular And Physiological Responses To Titanium Dioxide And Cerium Oxide Nanoparticles In Arabidopsis. **Environmental Toxicology And Chemistry,** V. 36, N. 1, P. 71-82, Jan 2017. Issn 0730-7268. Available At: < <Go To Isi>://Wos:000391029800011 >.

Wang, Z.; Gerstein, M.; Snyder, M. Rna-Seq: A Revolutionary Tool For Transcriptomics. **Nature Reviews Genetics,** V. 10, N. 1, P. 57-63, Jan 2009. Issn 1471-0056. Available At: < <Go To Isi>://Wos:000261866500012 >.

Waters, B. M. Et Al. Mutations In Arabidopsis Yellow Stripe-Like1 And Yellow Stripe-Like3 Reveal Their Roles In Metal Ion Homeostasis And Loading Of Metal Ions In Seeds. **Plant Physiology,** V. 141, N. 4, P. 1446-1458, 2006. Issn 0032-0889.

Yoon, S.-J. Et Al. Zinc Oxide Nanoparticles Delay Soybean Development: A Standard Soil Microcosm Study. **Ecotoxicology And Environmental Safety,** V. 100, P. 131-137, Feb 2014. Issn 0147-6513. Available At: < <Go To Isi>://Wos:000330161000018 >.

Zafar, H. Et Al. Effect Of Zno Nanoparticles On Brassica Nigra Seedlings And Stem Explants: Growth Dynamics And Antioxidative Response. **Frontiers In Plant Science,** V. 7, P. 535, 2016. Issn 1664-462x.

CHAPTER 5

5.1. Introduction

Engineered nanoparticles (ENPs or NPs) are increasingly being explored for use in agriculture. Some of the applications of NPs in agriculture are plant protection products like nanopesticides and nanofertilizers, nano-clay soil improvement products, water purification, nanosensors, and nucleic acid delivery systems. Among the metal NPs, silver, copper, and zinc oxide are the most widely used as nanofertilizers and nanopesticides, and among the non-metallic NPs, carbon and graphene are commonly used in environmental sensors . The effect of NPs on plant development and physiology is still largely unknown as their effects have been reported to vary depending on different parameters like types of growth media, plant species, NP type, concentration and size. In a recent review, the authors highlighted important knowledge gaps that need to be filled before NP use could be effectively translated to agricultural uses in the field. To address these knowledge gaps, the authors suggested the utilization of "omic" approaches including transcriptomics, proteomics and metabolomics for in-depth analyses of plant-nanoparticle interactions. These sensitive techniques can provide accurate and comprehensive information on the global gene regulation changes and dynamic physiological response required of a sessile organism when exposed to external stimuli that can be perceived as beneficial or a challenge to existence. Transcriptomic assays reflect the genes that are differentially regulated in response to beneficial stimuli but equally important are the differentially regulated genes in responses to abiotic or biotic stresses.

Before the recent advancements of next generation sequencing technologies made global plant transcriptome analysis possible, microarray technology was being used to elucidate the transcriptomic responses of the model plant species *Arabidopsis thaliana* exposed to NPs like ZnO

, TiO_2 and CeO , and Ag . Quantitative real time PCR was also used to determine the expression pattern of important genes in *Arabidopsis thaliana* like MADS-box genes in response to Ag NPs , auxin signaling genes and Fe-SOD genes in response to CuO NPs. In the majority of the studies , abiotic and biotic stress-related genes were found to be upregulated in the NP exposed plants, however these methodologies, microarray and qPCR are limited to targeted genes and did not provide information on the global transcriptional reprogramming occurring in response to the nanoparticle perception and interactions.

Although NPs have been reported to induce abiotic stress responses in plants, their interaction, crosstalk and possible synergy with other stress inducers in plants is still an under explored area, which would require in-depth transcriptional and physiological analysis in order to fill important knowledge gaps. One such synergistic interaction was partially characterized in canola plants. It was shown by Rossi et al., (2016) that canola treated with NaCl induced higher salt stress responses as compared to plants treated with both CeO_2 NPs and NaCl . Although a limited study, it shows that NP induced responses can suppress responses to an abiotic stress that could be essential for the plants' survival when growing under conditions that could include both abiotic or biotic stresses.

Biotic stresses due to microbial pathogens as well as invertebrates have been one of the most critical factors contributing to global food security issues and historically have had devastating consequences for social and political stability. Plant disease and insect epidemics on crops have resulted in famine, mass migration of people and the downfall of political systems since ancient times. Biotic stress due to pathogens still accounts for about 15% loss in global food production, and poses a major challenge when breeding for new crop varieties as although genetic resistance is the most economic and environmentally sustainable form of pest resistance, the

complex nature of host-parasite genetic interactions can leave deploying resistant crop varieties beyond our reach. Fungal phytopathogens are the most destructive among the infectious disease causing agents in plants and account for significant crop yield losses . Based on fungal lifestyle, phytopathogens can be categorized as necrotrophic, biotrophic, or hemibiotrophic. Necrotrophic pathogens derive nutrition from dead tissues in contrast to biotrophic pathogens that feed on living tissues. Hemibiotrophs are somewhat intermediate to biotrophs and necrotrophs because they have an initial biotrophic phase during early colonization and after colonization during their biotrophic existence in the host they shift to a necrotrophic phase where they produce toxins of necrotrophic effectors that induce cell death and then acquire nutrient and complete their life cycle on the resulting dying or dead host cells. Plants evolved complex mechanisms to recognize and respond to pathogen infection, typically based on the ability of the host plant to recognize molecules specific to pathogens called effectors. Plant recognition of the pathogen effectors, which is mediated by cell surface or cytoplasmic immunity receptors, triggers signaling pathways that lead to an incompatible reaction, disease resistance. The lack of recognition or the plants' inability to recognize a potential pathogen, either due to evasion via effector mutation or loss or a plant genotype lacking the appropriate immunity receptor, results in an incompatible reaction or susceptibility. Thus, the ability of the host plant to recognize a pathogen depends on whether the plant harbors the functional proteinaceous immunity receptor, typically encoding a dominant resistance gene (*R* gene) that recognizes a proteinaceous effector that is encoded by a single dominant pathogen avirulence gene. This plant-pathogen interaction is said to follow the "gene-for-gene model" . Resistance and susceptibility may not be absolute but may range from complete resistance to increased susceptibility. Plant defense responses characteristic to the "gene-for-gene model" includes oxidative burst where the production of reactive oxygen species occurs, and the

hypersensitive response (HR) which is a form of programmed cell death. These immunity responses evolved in plants to protect themselves against biotrophic pathogens that require the maintenance of living host cells harboring their feeding structures to acquire nutrient from their host. On the other hand, necrotrophic pathogens counter-evolved mechanisms to trick the host into inducing immunity responses leading to PCD and HR as they benefit from these responses because they can derive nutrients from dead plant tissues similar to saprophytic fungi that live on dead or decomposing plant matter.

Necrotrophic fungal pathogens are the causal agents of a plethora of plant diseases, which causes significant damage to a wide variety of crops. *Pyrenophora teres* f. *teres* (*Ptt*) is a necrotrophic phytopathogen, which is the causal agent of the net form net blotch (NFNB) disease of barley. In barley, NFNB can cause 10-40% yield loss when sufficient inoculum is available, a susceptible host genotype is being grown, and the environment is conducive to disease formation . The disease NFNB is characterized by elongated striated necrotic lesions on the leaf that show a net like pattern often surrounded by chlorosis. The disease causes yield loss by reduced kernel size and bulk density . It has been shown that necrotrophic pathogens produce necrotrophic effectors (NE) that induce susceptibility, and recognition of the NEs by appropriate plant receptors leading to programmed cell death (PCD), enabling the necrotrophs to survive and proliferate. This specific host-necrotrophic pathogen interaction follows an inverse gene-for-gene model or NE-triggered susceptibility (NETS), which is in contrast to the gene-for-gene model where recognition of pathogen effectors by plant receptors leads to resistance responses.

Salicylic acid (SA) has been shown to mediate biotrophic pathogen resistances through the induction of controlled programmed cell death (PCD) responses or hypersensitive responses (HR), which induces a foci of dead plant cells at the site of pathogen colonization. This immunity

response in plants evolved to deprive the biotrophic pathogens of nutrients, as they need to colonize living cells to extract host derived nutrient. The HR response leads to pathogen death and disease resistance. Thus, plants evolved an innate immunity mechanism where preformed immunity receptors in each plant cell triggers a localized PCD which effectively sacrifices a few cells in order to save the whole plant from infection. It was shown that susceptibility to the biotroph, *Hyaloperonospora arabidopsidis* was enhanced in Arabidopsis following a shift from SA-signaling to JA/ET-signaling. In Arabidopsis F1 hybrids obtained by crossing Col-0 and Sei-0, SA biosynthesis was found to be enhanced, contributing to increased resistance against the biotrophic bacterial pathogen, *Pseudomonas syringae* pv. *tomato* (Pst) DC3000. Exogenous application of SA in wheat and increased SA accumulation in AtNPR1- expressing wheat enhanced basal resistance to the wheat hemibiotrophic pathogen *F. graminearum*.

Jasmonic acid (JA) mediated responses are known to play a major role in conferring resistance to necrotrophic pathogens. Although the role of JA signaling in barley resistance to *Ptt* has not been established, JA responses and their effect on necrotrophic pathogen disease suppression have been studied extensively in other pathosystems. Jasmonate deficiency increased susceptibility in tomato to the necrotrophic pathogens *F. oxysporum* and *V. dahlia* . It is also well established in other pathosystems that SA and JA interactions are mutually antagonistic . Thus, JA responses that are known to be important for necrotroph resistances in plants is in part due to the inhibition of SA responses leading to suppressed PCD. Necrotrophs have been found to hijack the SA-mediated defense signaling pathways of their hosts to induce PCD and tailor an environment conducive to colonization, nutrient acquisition, and lifecycle completion which promotes virulence and further disease development. SA-mediated signaling was also shown to enhance susceptibility to another necrotrophic fungal pathogen, *Alternaria solani*, in tomato. The necrotrophic pathogen,

Botrytis cinerea has been found to produce an exopolysaccharide, β-(1,3)(1,6)-d-glucan which suppresses JA-mediated responses eliciting SA pathway and consequent susceptibility in tomato. Other phytohormones also play a role in the cross talk leading to compatible and incompatible interactions between plant hosts and pathogens. For example, it was also recently shown that *B. cinerea* strain B05.10 suppresses the Arabidopsis transcription factor WRKY33 leading to elevated levels of the phytohormone abscisic acid (ABA). The elevated ABA levels had an antagonistic effect on JA signaling and defense responses against the necrotroph and induced susceptibility (Liu et al., 2017).

Our current understanding of how plants respond to a secondary stress inducer, either biotic or abiotic, after responding to the perception of NP, which also act to induce transcriptional reprogramming and differential hormonal signaling events is limited. However, this is a major grand challenge to utilizing NPs as subtle changes in these hormone signaling pathways which have complex cross talk could have major effects on how the plants respond to the NPs or react to stresses pre- or post-application in the field. So far, NPs have been studied in controlled environments where abiotic/biotic stresses were not applied or not taken into consideration but under field conditions these factors are an inherent part of the ecosystem. In the present study, we have explored the dynamics of plant and NP interaction, in the presence of a secondary stress inducer, a necrotrophic phytopathogen. We have shown that SA-related genes are highly expressed in barley (*Hordeum vulgare*) under combined stress i.e. zinc oxide engineered nanoparticles (ZnO NPs) and the necrotrophic pathogen, *Pyrenophora teres* f. *teres* (*Ptt*) which correlates with the reduced expression of JA-related genes, leading to compromised immunity towards the necrotroph in the most resistant cultivar of barley, CI5791. Next Generation Sequencing (NGS) was used for RNA seq analysis to access temporal changes in the transcriptome of the stress-induced plants.

Barley responses to ZnO NPs were compared to the model monocot, *Arabidopsis* responses, and it was shown that within the model dicot and model monocot systems opposite outputs were observed in response to the same NPs with regards to JA and SA signaling. This further reiterates the importance of understanding these interactions and outcomes using diverse species of NPs and plants, as well as under different environmental conditions and when interacting with diverse biotic and abiotic stresses. Thus, the objective of this research was to investigate the effects of ZnO NPs on barley and *Ptt* interactions.

5.2. Materials and Methods

5.2.1. ZnO NP Characterization

For zeta (ζ)-potential and hydrodynamic diameter measurements, the ZnO NPs were dispersed in DI water using a sonicator for 30 seconds at a concentration of 500 mg L^{-1} of Zn. The zeta (ζ)-potential and particle size distribution was measured with a ZetaSizer (Nano-ZS 90, Malvern). For evaluating the particle size distribution, a JEOL JEM-2100 LaB6 Transmission Electron Microscope (TEM) was used (JEOL USA, Peabody MA) operating at 200 kV. Bright-field images of each sample were acquired with a Gatan Orius SC1000 CCD camera; dark-field imaging was acquired utilizing a Gatan 805 High Angle Annular Dark Field detector with a Gatan Digiscan II controller unit and the TEM running in scanning transmission electron microscopy (STEM) mode.

5.2.2. Plant Growth and Treatments

Barley cultivar CI5791 was grown in cones containing 58.2 g of saturated potting mix (Pro Mix Loose Fill). Two seeds were sowed per cone and were treated as the same sample. A total of eight cones were allocated to each treatment. Emergence was recorded at 4 days after planting. ZnO NP treatment was applied at the 2-leaf stage. ZnO NPs were applied in the form of de-ionized

water suspension with 2.5 mg (500 mg suspended in 1L of water; pot watered with 5 ml of suspension) of zinc per treatment. For the double interaction (NP+P), ZnO NPs were applied as described 3h before pathogen inoculation (Figure 5.1). Secondary leaf tissue was collected from three individual plants of each treatment, and immediately frozen in liquid nitrogen and placed in a -80° C freezer until isolation of RNA was performed for RNA seq. Leaf samples were collected at 0 h pre-application of NPs, 3, 6, 24, and 48 h post NP application (hpa), and 3, 21, and 45 h post pathogen inoculation (hpi). The plants were grown in a controlled growth chamber under photoperiod conditions of 12 h light and 12 h dark at 21^0C.

Arabidopsis was grown in similar cones containing 58.2 g of saturated potting mix (Pro Mix Loose Fill), and in a controlled growth chamber under photoperiod conditions of 12 h light and 12 h dark at 20 ^{o}C. Five seeds were sowed per cone and upon germination (14 days), the numbers were scaled to two plants per cone. After rosette leaves were fully developed (~30 days from planting), treatments were applied. The treatments consisted of ZnO NPs and no zinc control. ZnO NPs were applied in the form of de-ionized water suspension with 2.5 mg (500 mg suspended in 1L of water; pot watered with 5 ml of suspension) of zinc per treatment, and the control plants were treated with de-ionized water. Rosette leaves were collected from three individual plants of each treatment and immediately frozen in liquid nitrogen and placed in a -80 ^{o}C freezer until isolation of RNA was performed for RNA seq. Leaf samples were collected at 0 h pre-application of NPs, 3, 6, 24, and 48 h post NP application (hpa).

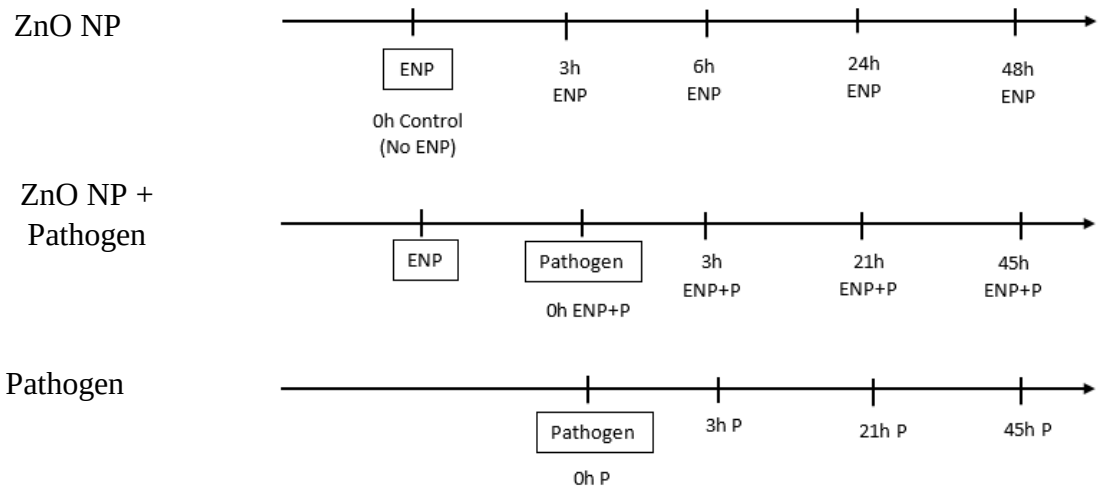

Figure 5.1. Time-course progression of treatments when leaf samples were collected for RNA seq.

5.2.3. Pathogen Inoculation

Only barley was used for pathogen inoculation. The *Pyrenophora teres* f. *teres* (*Ptt*) isolate ND89-19 was used to inoculate the resistant barley line CI5791. Inoculations were carried out after the secondary leaves of the barley seedlings were fully expanded (~14 days post planting). Inoculum preparation was performed as previously described in Friesen et al., (2006). In short *P. teres* f. *teres* isolate ND89-19 conidia spores were harvested from 10 days-old cultures by irrigation with water, and filtering through cheesecloth. The inoculum concentration was adjusted to 7500 conidia per ml^{-1} and two drops of Tween 20 (polyoxyethylene sorbitan monolaurate) were added per 100 ml of the inoculum. The plants were inoculated with a spray inoculator until leaves were saturated with droplets but before runoff. Post inoculation, the plants were placed in 100% relative humidity in the dark at 21^0 C for 24 h following the previously established protocol. Thereafter, the plants were kept in a controlled growth chamber as described previously. Disease evaluations were carried out on day 7 post inoculation, and the 1–10 scale described by Tekauz

(1985) was used to score disease reactions . An average of 7 plants were scored for each treatment for disease.

5.2.4. mRNA Extraction, RNA Seq Library Preparation and Sequencing of Barley CI5791 Leaves

Three leaf samples of equal size (~2 cm) from each replicate per treatment were combined in a single tube and used for total RNA extraction. The total RNA was extracted from these frozen leaf samples using the RNeasy mini kit (Qiagen, Chatsworth, CA) following the manufacturers standard protocol. RNA concentrations were measured using the Qubit® Broad Range RNA kit on a Qubit® 2.0 fluorometer (ThermoFisher Scientific), and RNA samples were visualized on 1% agarose gels stained with gel red (Biotium) to confirm the integrity of samples. RNA samples with four sharp ribosomal RNA (rRNA) bands; approximate molecular weights of 3.4, 1.8, 1.5, and 1.1 kb corresponding to nuclear 28S and 18S rRNAs and 23S and 16S plastid rRNAs, respectively, without a high molecular weight genomic DNA contamination band were considered quality RNA. 1µg of total RNA was used for RNA sequencing (RNAseq) library construction using the TruSeq RNA Library Prep Kit v2 (Illumina, San Diego, CA) following the manufacture's standard protocol. The final library was validated and quantified on the Agilent 2100 Bioanalyzer. The cDNA libraries from 12 different samples were pooled into one single tube and were normalized according to the manufacturer's protocol. Each of the library pools were diluted to a concentration of 1.8 pm and sequenced on the Illumina NextSeq 500 sequencer on a single flow cell at the USDA Cereal Genotyping Centre, Fargo, ND, USA. A total of 3 flow cells were used. The NextSeq® 500/550 High Output Kit v2 (150 cycles) was used for the generation of 150 bp single end sequencing reads. The raw sequencing reads were demultiplexed and converted into individual fastq files using bcl2fastq software v2.17.1.14 (Illumina, San Diego, CA). The fastq reads were

quality trimmed in CLC Genomics Workbench v8.0.3 (CLC bio, Aarhus, Denmark) using default settings.

5.2.5. mRNA Extraction, RNA Seq Library Preparation and Sequencing of Arabidopsis Leaves

Three leaf samples of equal size (~0.5 cm) from each replicate per treatment were combined in a single tube and used for total RNA extraction. The total RNA extraction and quality check was done similar to that of barley. 1µg of total RNA was used for RNA Seq library construction using the NEB #E7490 (New England Biolabs, Ipswich MA) for mRNA extraction, NEB #E7771S (New England Biolabs, Ipswich MA) for first strand synthesis, NEB #E6111S (New England Biolabs, Ipswich MA) for second strand synthesis, and NEB #E6270S (New England Biolabs, Ipswich MA) for DNA library prep, following the manufacture's standard protocol. The final library was validated and quantified on the Agilent 2100 Bioanalyzer. The cDNA libraries from 12 different samples were pooled into one single tube and were normalized according to the manufacturer's protocol. Each of the library pools were diluted to a concentration of 100 pm and loaded on the Ion Chef for chip prep. A single chip, Ion 540 Chip (Ion Torrent, Life Technologies, Carlsbad, CA) was used for sequencing on the Ion S5 System (Ion Torrent, Life Technologies, Carlsbad, CA). The fastq reads obtained were quality trimmed in CLC Genomics Workbench v8.0.3 (CLC bio, Aarhus, Denmark) using default settings.

5.2.6. Expression Analysis

The analysis pipeline for mapping reads to reference genome, quality check, and for expression analyses was performed as previously described by Sharma Poudel 2018. The high-quality trimmed sequencing reads were mapped to the barley RefSeq v1.0 (http://webblast.ipk-gatersleben.de/barley_ibsc/) in CLC Genomics Workbench v8.0.3 to obtain barley specific genes.

Gene specific and transcript specific reads were obtained from the reference gene as well as from the gene track and mRNA tract information. This enabled reads to align to both intronic and intergenic regions. Reads less than 90% identical for 90% of the read length and that mapped to more than 10 positions were discarded. The total reads mapped for each gene model were normalized to obtain reads per kilobase of exon model per million mapped reads (RPKM) values for each sample. In all the comparisons, the false discovery rate (FDR) corrected p-values were calculated by the exact test using the EdgeR bioconductor package in CLC genomics. Analyses were based on a threshold of 0.05 for FDR-corrected p-value and fold change of 3. All treatments were compared with 0 h control (no NP application or *Ptt* inoculation).

Venn diagrams were prepared using VENNY to compare the DEGs between the treatments. Heat maps were generated using Heatmapper.

5.2.7. Functional Annotation

The high confidence genes were annotated in the publicly available IBSC RefSeq v1.0 (http://webblast.ipk-gatersleben.de/barley_ibsc/downloads/). The annotations were supplemented by performing a local BlastX of the whole set of predicted barley proteins to the reannotated Arabidopsis Col-0 genome (Araport11) (https://www.araport.org/ data/araport11) (Madden et al., 2013). The top hits of high confidence barley genes with predicted amino acid homologies greater than 30% and alignment lengths greater than 50% with Arabidopsis annotated genes were used to assign Arabidopsis gene IDs to the barley genes.

5.2.8. Gene Enrichment Analysis

The GO term mapping for the best Arabidopsis gene hits for the barley DEGs were used for gene enrichment analysis. GO term enrichment analysis was performed in bioconductor R package TopGO version 2.28.0 , and in the web-based Classification Superviewer . In the TopGO

package, Fisher's exact test was performed to calculate the significance of GO term enrichment. The cut-off for number of genes annotated for a single GO term was fixed at 5 genes with p-value less than 0.001. In both the enrichment tools, the analyses were done to identify the significantly enriched GO terms specific to subontology categories like molecular function (MF), biological processes (BP) and cellular component (CC).

In both TopGO and Classification Superviewer, all DEGs across the treatments were subdivided into two groups, upregulated and downregulated genes, and enrichment analysis was conducted on each set separately.

5.2.9. Quantitative PCR Analysis

The RNA samples used for RNA Seq were further analyzed for *HvPR1*, *HvPR4*, and *HvCytP450* expression using qPCR. Complementary DNA (cDNA) was prepared from the total RNA using GoScriptTM Reverse Transcription System (Promega) following the manufacturer's protocol which is as follows: ~500 ng of total RNA was mixed with oligo(dT)15 primer (0.5 µg) and incubate at 70 ^{o}C for 5 minutes. The RNA sample was then mixed with 15 µl of reverse transcription reaction mix (GoScriptTM Reaction Buffer (5X), $MgCl_2$ (1.5 mM), PCR Nucleotide Mix (0.5 mM each dNTP), Recombinant RNasin Ribonuclease Inhibitor (20 units), and Reverse Transcriptase) and incubated at 25 ^{o}C for 5 min followed by 42 ^{o}C for 60 min and inactivated at 70 ^{o}C for 15 minutes. The 20 µl cDNA synthesis reactions were diluted with 30 µl H_2O, giving a total of 10 ng/µl. A 20 µl qPCR reaction was prepared by mixing 4 µl (~40 ng DNA) of diluted cDNA, 10 µl SsoAdvanced Universal SYBR Green Supermix (Bio-Rad), and 1 µl of each forward and reverse primer (10 µM). The qPCR was conducted in a CFX96 Real-time system thermalcycler (Bio-Rad) with cycling parameters of 95 °C for 30 sec followed by 40 cycles of 95 °C for 15 seconds and 62 °C for 30 seconds; 65 °C for 30 sec; and 60 cycles of temperature increasing from

60 °C to 95 °C with fluorescence readings acquired at 0.5 °C increments per cycle. Three technical replications were used for each biological replicate. The barley *HvSnor14* gene was used as the reference to normalize *HvPR1*, *HvPR4*, and *HvCytP450* gene expression. Efficiency of qPCR for *HvPR1*, *HvPR4*, *HvCytP450,* and *HvSnor14* primers were calculated by generating a standard curve by running qPCR on a 10-fold serial dilution starting from 200 pg of PCR amplified template of *HvPR1*, *HvPR4*, *HvCytP450*, and *HvSnor14*. Differential expression was calculated by using the ΔΔCT method, followed by one-way ANOVA and Tukey's comparison test to determine the statistical significance. For PR1, primers were designed across its only exon:

HvPR1-qpcr-F1 (5'- ATGCAGACGCCCAAGCTAGCCATCT-3') and HvPR1-qpcr-R1 (5'-CTCTGGTTGGCGTAGTTCTGGGCGA- 3') that specifically amplifies a 191 bp region in cDNA and gDNA. For PR2, primers were designed across its only exon: HvPR4-qpcr-F2 (5'-AACAACGTCCGGGCGACGTAC-3') and HvPR4-qpcr-R2 (5'-GAACGCCGTCCAGCCGTACTT-3') that specifically amplifies a 144 bp region in cDNA and gDNA. For CytP450, primers were designed across two exons: HvCytP450-qpcr-F1 (5'-GCACTCTGGAACAAGCACCCATGAG-3') and HvCytP450-qpcr-R1 (5'-CATGGCCAGGAATTCCAGAGTCGAC- 3') that amplifies a 232 bp region in cDNA, and a 366 bp region in gDNA.

5.2.10. Protein-Protein Interaction Network (PPIN)

For PPIN, the up and downregulated genes having fold change greater than 10 were used in the analysis. We set this threshold because most of the important genes that we were interested in like the ones coding for cell surface receptor proteins had a higher fold change than 10. We solved the Steiner tree problem on these proteins of interest using the Kou approximation algorithm and we present the results here. A *Steiner Tree* problem was used as the model to

identify a collection of interactions of maximum reliability such that all the proteins of interest (based on up- and down-regulated genes) are connected. Due to the large-scale nature of the obtained network, the Kou approximation algorithm was used to find a heuristic solution in reasonable time. The underlying network is generated based on the STRING-DB database for *Arabidopsis thaliana*, while visualization is done using NetworkX .

5.3. Results

5.3.1. ζ-Potential and Particle Size

The ζ-potential and hydrodynamic diameter of the ZnO NPs was found to be 25.9±4.7 mV and 512.5 nm in DI water respectively. The particle size ranged from 10-170 nm (smallest value is 8 nm and largest value is 173.33 nm), 92.96% of the ZnO NPs had the smallest dimension within 100 nm (Figure 5.2).

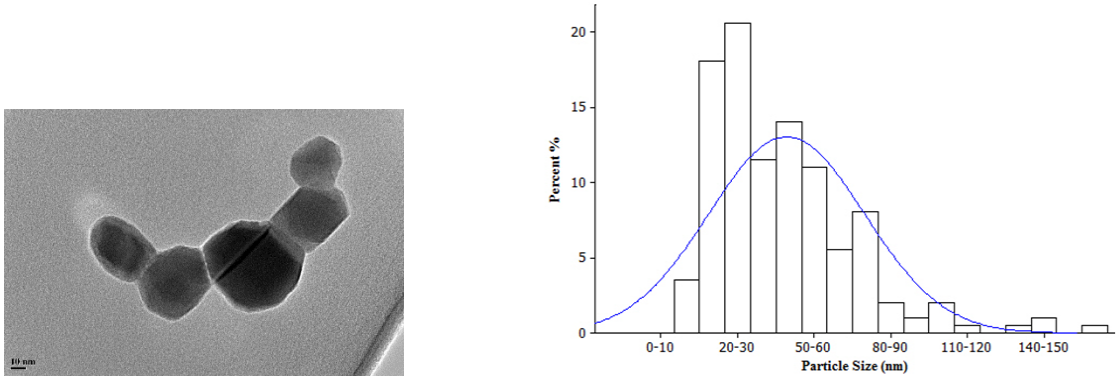

(a) (b)

Figure 5.2. (a) TEM micrograph of bare ZnO NPs, and (b) particle size distribution of ZnO NPs based on smallest dimensions.

5.3.2. Differentially Expressed Genes (DEGs)

5.3.2.1. Barley

Time course RNAseq analyses from leaf samples at 0, 6, 24 and 48 hours post ZnO NP application (hpa) or 3, 21, 45 h post pathogen inoculation (hpi) identified differentially expressed genes (DEGs) in response to the treatments showing rapid responses to ZnO NPs alone at 6 hpa

that quickly returned to basal levels at 24 hpa. However, treatments with the pathogen alone and pathogen + ZnO NP showed DEG profiles that persisted up to 48 hpi (Table 5.1), the latest time point analyzed in the experiments. The number of DEGs in the combined application/inoculation (pathogen + ZnO NP) was the highest across all time-points compared to the pathogen and ZnO NPs alone. The number of DEGs in response to ZnO NPs was the highest at 3 hpa with 225 significantly upregulated and 461 downregulated genes. At 6 hpa, the number of upregulated genes decreased to 71 and downregulated genes decreased to 134. At 24 hpa, the number of up and downregulated genes were 1 and 49 respectivelycand at 48 hpa, the number of DEGs upregulated were 2 and 14 downregulated. For the pathogen inoculated treatments, at 3 hpi, the number of DEGs were 1020 upregulated and 954 for downregulated. As the infection process progressed the number of DEGs increased then began to decrease over time. At 21 hpi, the numbers of DEGs were 1302 upregulated and 1021 for downregulated genes and at 45 hpi, 814 were upregulated and 487 were downregulated. In case of the combined application treatments,of NP and Pathogen inoculation the largest response in terms of DEGs was observed at 3 hpi (6 hpa of NP) with 1359 upregulated and 1033 downregulated genes. The number of genes upregulatd slightly increased over time and downregulated genes began to decrease. At 21 hpi (24 h hpa of NP), the number of DEGs were 1534 upregulated and 983 for downregulated. The number DEGs then began to decrease over time as at 45 hpi (48 hpa of NP) there were 1100 upregulated and 594 downregulated. Thus, overall it was observed that the amplitude of barley responses in terms of the number of DEGs was the lowest with the ZnO NPs alone followed by pathogen alone with the combined application of nanoparticles followed by pathogen inoculation showing the strongest responses across all time points examined (Figure 5.1).

Table 5.1. The number of DEGs in barley in each treatment across time points

	Upregulated			Downregulated		
Time-points	**NP**	**P**	**NP+P**	**NP**	**P**	**NP+P**
3 hpa	225			461		
6 hpa/ 3 hpi	71	1020	1359	134	954	1033
24 hpa/ 21 hpi	1	1302	1534	73	1281	1292
48 hpa/ 45 hpi	2	814	1100	14	487	594

Comparative analysis of the DEG profiles across the time courses with the NP, pathogen and NP+pathogen treatments allowed for the identification of common and unique DEGs to each treatment. The NP treatment alone at 6, 24, and 48 hpa were compared with the 3, 21, and 48 hpi time points, respectively, with the pathogen alone and NP+pathogen, to compare treatments such that the timing of the plant interaction with NP or pathogen alone aligned directly with each treatment across the dual interaction analysis with NP+pathogen.

The upregulated genes at the first time-point of the dual NP+pathogen treatment (6 hpa/3 hpi) identified 4 unique barley genes that were common to both the NP and combined application, 951 that were common to the pathogen alone and combined application, and 15 that were common for all the treatments (Figure 5.3a). There were 52 genes Upregulated genes that were exclusive for NP, 54 genes for pathogen, and 389 that were exclusively upregulated at this time point during the combined NP + pathogen treatment. For the second time-point (24 hpa/21 hpi), 1208 upregulated genes were common for the pathogen and combined NP + pathogen treatments. There was 1 DEG that was exclusive for NP alone, 94 for pathogen alone, and 326 for the combined application (Figure 5.3b). At the third time-point (48 hpa/45 hpi), 749 upregulated genes were common to the pathogen and combined application, and 2 genes were common for all the treatments. There were 63 upregulated DEGs exclusive for pathogen inoculation, and 349 for the combined application (Figure 5.3c).

For downregulated genes at the first time-point (6 hpa/3 hpi), there were 810 unique barley DEGs that were common for pathogen and combined applications, 1 common for NP and pathogen alone, 1 common for NP and combined application, and 57 that were in common for all the treatments. There were 75 genes exclusive for NP alone, 86 genes exclusive for pathogen alone, and 165 that were exclusive for the combined application (Figure 5.4a). At the second time-point (24 hpa/21 hpi), there were 879 down regulated genes common for pathogen and combined application, 1 between NP and pathogen, and 15 that were common for all treatments. There were 33 genes exclusively downregulated for NP alone, 126 for pathogen alone, and 89 for the combined application (Figure 5.4b). At the third time-point (48 hpa/45 hpi), 438 downregulated genes were common for the pathogen and combined application, 1 gene was common for all the treatments and there were 13 genes exclusive to the NP alone, 48 for pathogen alone, and 155 for the combined application (Figure 5.4c).

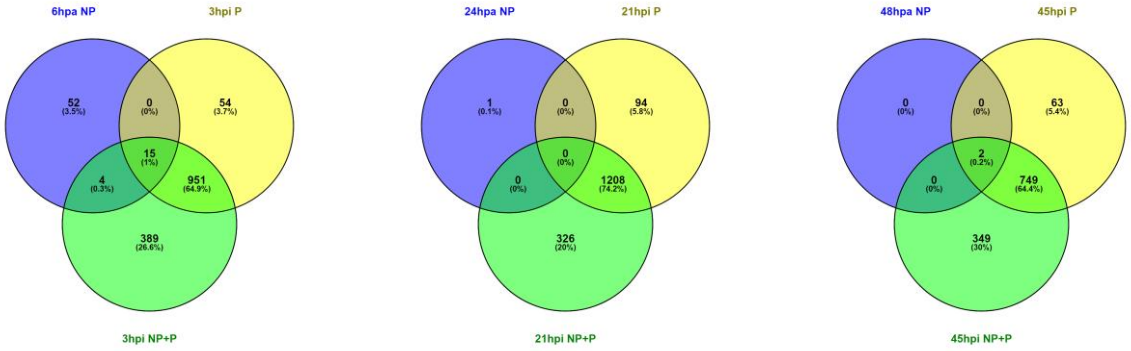

(a) (b) (c)

Figure 5.3. Venn diagrams showing the upregulated differentially expressed genes (DEGs) that are unique to and common between the treatments. Comparisons of the DEGs of nanoparticle (NP; blue), pathogen (P; yellow), and NP+P (green) at (a) the 1st time point, (b) the 2nd time point, and (c) the 3rd time point.

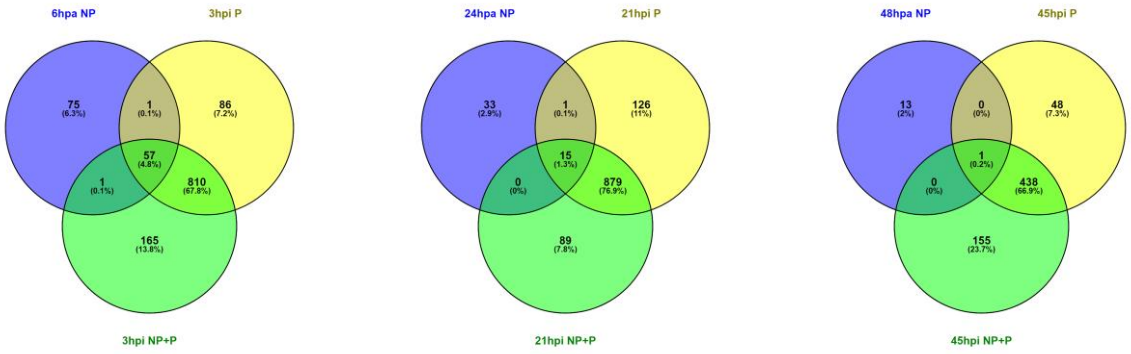

(a) (b) (c)

Figure 5.4. Venn diagrams showing the downregulated differentially expressed genes (DEGs) that are unique to and common between the treatments. nanoparticle (NP; blue), pathogen (P; yellow), and NP+P (green) at (a) the 1st time point, (b) the 2nd time point, and (c) the 3rd time point.

Across all treatments, the number of DEGs that were exclusive for the combined application of NP+pathogen were higher than those exclusive for NP or pathogen alone. This means that the responses of combined application plants were not entirely due to pathogen or NP alone but that a unique subset of genes that were affected by the combined NP and pathogen interaction gave an amplified response as compared to the individual treatments alone.

To estimate ZnO NP induced fold changes of the DEGs, comparisons were made between pathogen inoculated and combined application datasets at each time-point. It was evident from the volcano plots (Figure 5.5) that there is an increase in the number of DEGs having fold change higher in the combined application from 3 to 45 hpi. In the volcano plot, each dot represents a single transcript. The scale of the X-axis which is depictive of the fold change, is seen to be increasing from 3.5 at 3 hpi to 7.5 at 45 hpi, indicating that at the later time-point (45 hpi), there are increasing number of gene transcripts having higher fold changes.

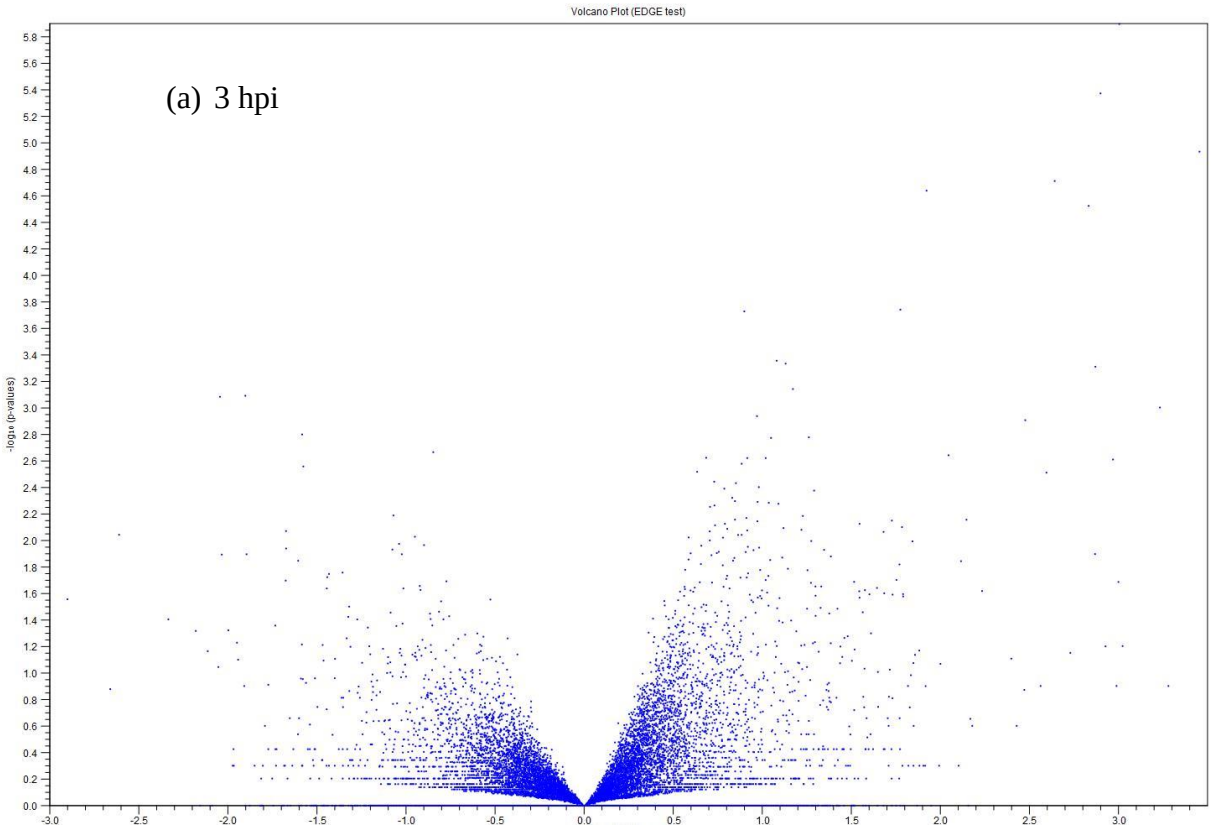

Figure 5.5. Volcano plot of the transcriptome of pathogen inoculated and combined application treated barley at (a) 3 hpi, (b) 21 hpi, and (c) 45 hpi. The scale on the X-axis is the $\log_2$ EDGE FC, and Y-axis is the $-\log_{10}$ test p-value

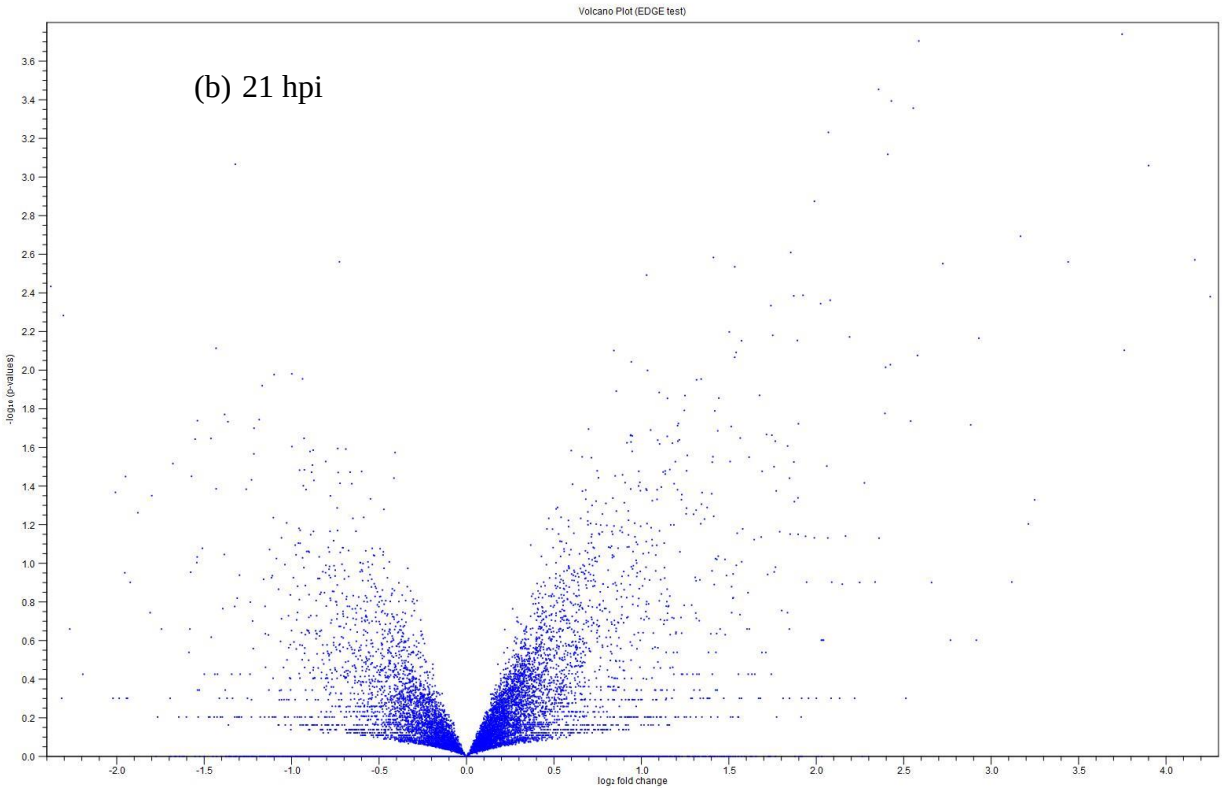

Figure 5.5. Volcano plot of the transcriptome of pathogen inoculated and combined application treated barley at (a) 3 hpi, (b) 21 hpi, and (c) 45 hpi. The scale on the X-axis is the $\log_2$ EDGE FC, and Y-axis is the $-\log_{10}$ test p-value (continued)

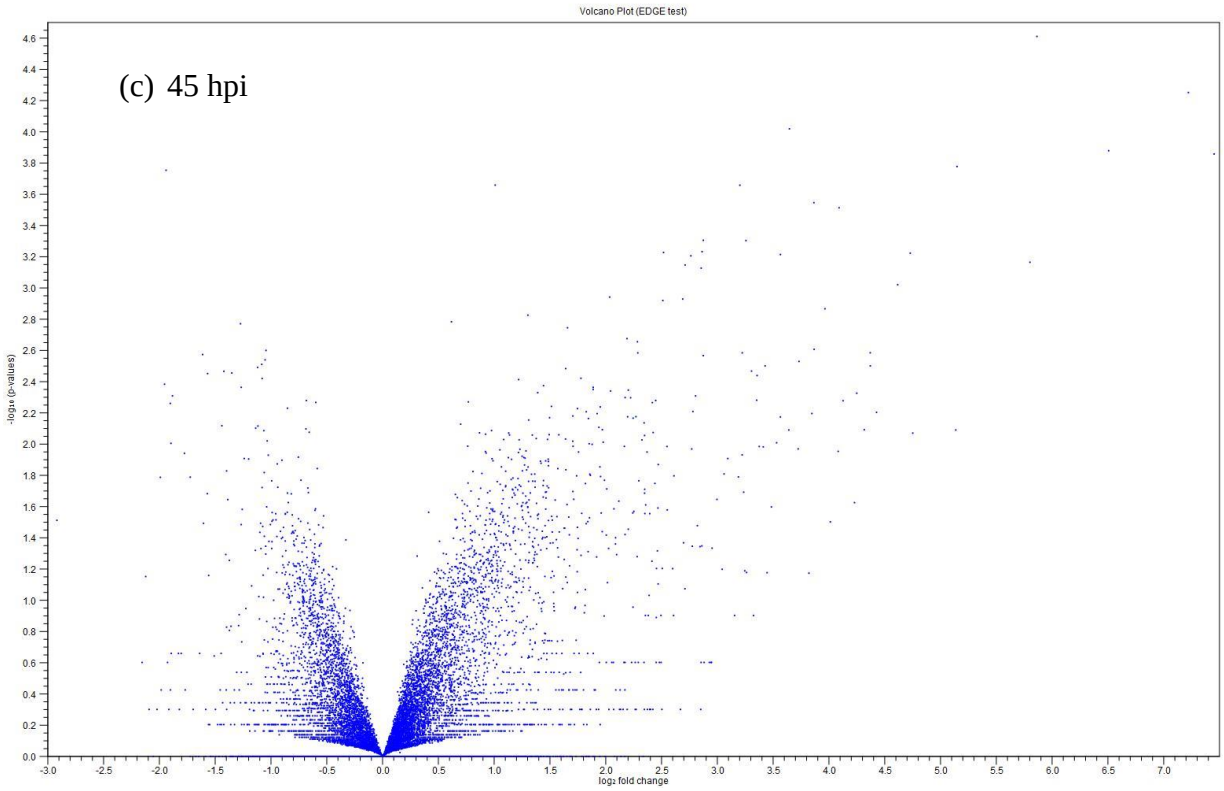

Figure 5.5. Volcano plot of the transcriptome of pathogen inoculated and combined application treated barley at (a) 3 hpi, (b) 21 hpi, and (c) 45 hpi. The scale on the X-axis is the $\log_2$ EDGE FC, and Y-axis is the $-\log_{10}$ test p-value (continued)

5.3.2.2. Arabidopsis

Time course RNA seq analyses from leaf samples of Arabidopsis at 0, 3, 6, 24 and 48 hours post ZnO NP application (hpa) identified transcriptional regulation responses similar to barley in the context of the timing of the responses. There were rapid transcriptional reprogramming responses that occurred post NP application that persisted till 6 hpa, after which the majority of genes showing differential regulation returned back toward basal levels at 24 hpa similar to what was observed in barley seedlings not exposed to the NP which was represented by the 0 hpa timepoint (Table 5.2). The number of DEGs was the highest at 6 hpa with 304 upregulated and 209 downregulated genes. At 24 hpa, the number of upregulated genes decreased to 4 and

downregulated genes decreased to 58. At 48 hpa, the number of DEGs were 22 for upregulated and 110 for downregulated genes.

Table 5.2. The number of DEGs in each treatment across time points in Arabidopsis

Time-points	Upregulated	Downregulated
3 hpa	127	198
6 hpa/ 3 hpi	304	209
24 hpa/ 21 hpi	4	58
48 hpa/ 45 hpi	22	110

Although the timing of the responses to the ZnO NP was similar in the model monocot species barley and dicot model species Arabidopsis, a comparison of orthologous DEGs revealed different gene profiles between the two model species (Figure 5.6). For upregulated genes, using barley and Arabidopsis orthologous gene annotations, only 3, and 1 gene were common at the 3, and 6 hpa time points, respectively. For downregulated genes, 16, 9, 3, and 2 genes were common at the 3, 6, 24, and 48 hpa timepoints, respectively. This implies that although barley and Arabidopsis share similar temporal responses to ZnO NP, the two model plants for the monocot and dicot lineages of plant evolution show different transcriptomic responses in terms of the genes that respond to the same class of NP.

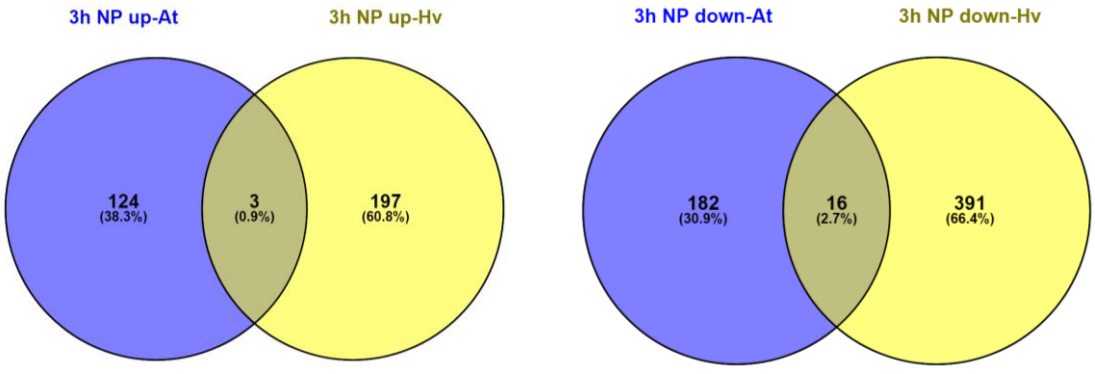

(a) (b)

Figure 5.6. Time-course comparisons of Arabidopsis DEGs and barley DEG orthologs.

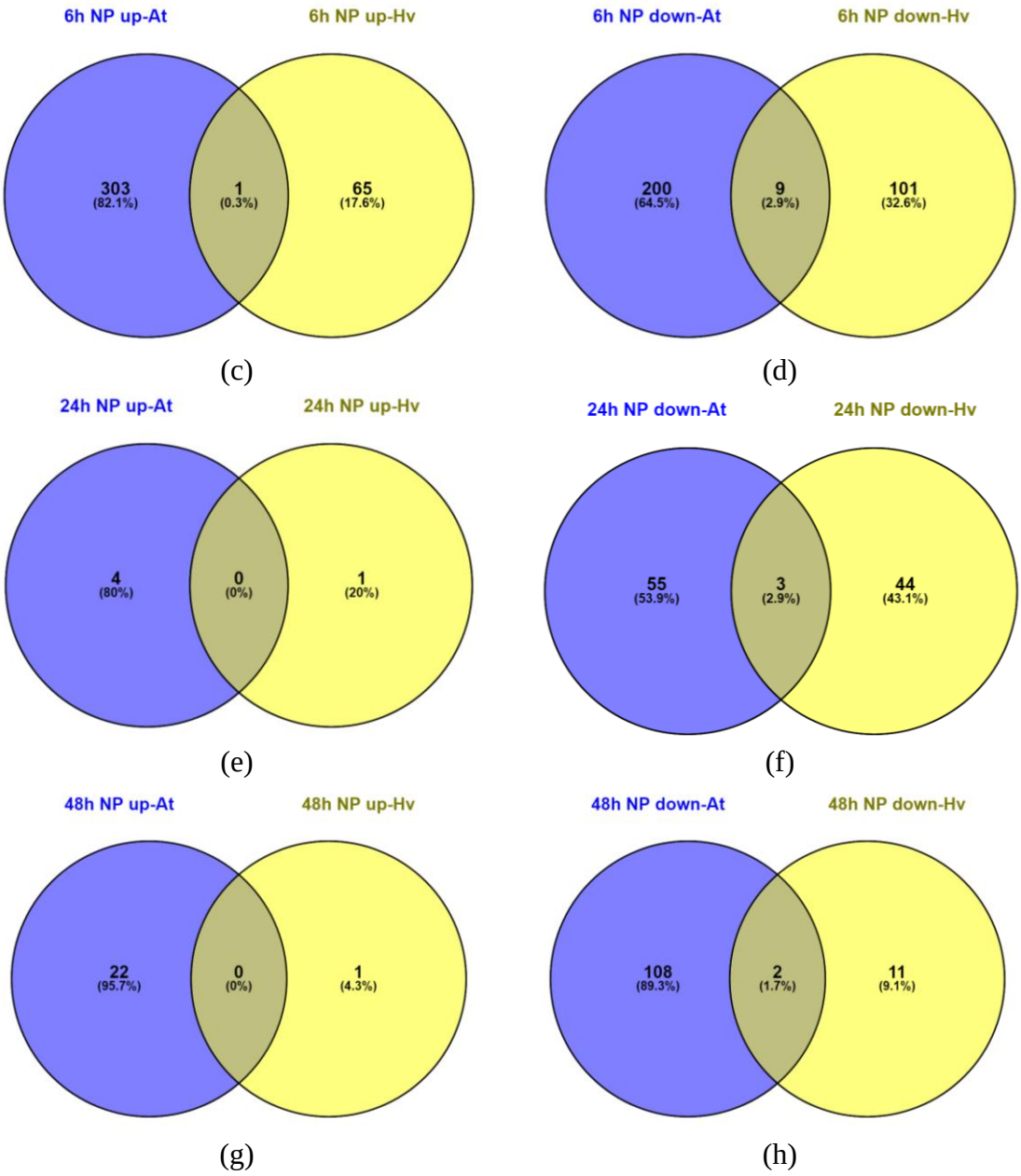

Figure 5.6. Time-course comparisons of Arabidopsis DEGs and barley DEG orthologs (continued).

5.3.3. Gene Enrichment Analysis of DEGs

5.3.3.1. Barley

Gene enrichment using gene ontology (GO) terms was conducted in TopGO. For ZnO NP, the barley 3 hpa expression data showed that the most significant GO terms (p-value < 1e-10)

enriched for upregulated genes were translation and response to cadmium ions, and photosynthesis and protein-chromophore linkage for downregulated genes (Figure 1a and Table 1a, Appendix D). At 6 hpa, translation and ribosome biogenesis were the most significant upregulated genes, and for downregulated genes, photosynthesis and negative regulation of photomorphogenesis were the most significant (Figures 1a-b and Tables 1a-d, Appendix D).

In the pathogen inoculated samples, across all time-points, protein phosphorylation and response to wounding were the most significant terms for upregulated genes, and for downregulated genes, photosynthesis, and protein-chromophore linkage were the most significant (Figures 1c-e and Tables 1e-g, Appendix D).

In the combined application treatments, across all time-points, protein phosphorylation, and response to wounding were the most significant for upregulated genes. For downregulated genes, photosynthesis, and protein-chromophore linkage were the most significant (Figures 1f-h and Tables 1h-j, Appendix D).

It is evident that the ZnO NPs do not elicit responses typical of stress, although photosynthesis genes were downregulated. However, in response to the pathogen and combined application, the upregulated genes were characteristic of stress responses.

5.3.3.2. Arabidopsis

Using TopGO, gene enrichment analysis on the Arabidopsis expression data at 3 and 6 hpa, the most significant terms enriched were for response to wounding and response to jasmonic acid for upregulated genes, and photosynthesis and protein-chromophore linkage were the most significant for downregulated genes (Figures 2a-d and Tables 2a-d, Appendix D).

5.3.4. Phenotypic Analysis of CI5791

Pathogen inoculated and combined application (NP + pathogen) plants were evaluated for disease reaction. The average disease reaction scores were calculated from six trials and 9-12 leaves per treatment per trial. The average disease reaction scores for combined application plants ranged from 1.93 to 4.08 with an overall mean of 2.71, and for untreated pathogen inoculated plants, the score ranged from 1.63 to 2.55 with an overall mean of 1.92 (Figure 5.7). A rating of 1 shows a highly resistant reaction (incompatibility), whereas a rating of 10 shows a highly susceptible reaction (compatibility). The rating for combined application plants indicated a higher proportion of plants that were moderately susceptible, whereas for plants inoculated with the pathogen alone the disease ratings ranged from resistant to moderately resistant. From the disease scores observed for the combined application plants it was clear that the highly resistant barley line CI5791 developed higher levels of susceptibility to *P. teres* f. *teres* isolate ND89-19 after exposure to the ZnO NP. The increased susceptibility of the combined application plants can be attributed to the overexpression of SA-related genes that are known to antagonize the expression of JA-related genes, which are important in necrotrophic defense responses for which CI5791 is highly resistant to almost all *P. teres* f. *teres* isolates collected from around the world. Interestingly, it was also observed for the combined application treatments, that genes related to oxidation-reduction processes had higher fold change upregulation than in the pathogen alone treatments. The oxidation-reduction processes result in reactive oxygen species (ROS) that is a precursor and signaling molecule that leads to programmed cell death. In the context of necrotrophic pathogen resistance, it is well established that resistance relies on suppressing ROS and subsequent PCD through the suppression of SA-mediated responses via upregulation of the JA-mediated responses. Thus, the downregulation of oxidation-reduction processes in the CI5791 resistance mechanism is

expected to result in the compatible interaction and the NP induced upregulation of oxidation-reduction processes would result in higher levels of susceptibility, which was observed in the dual interaction phenotyping analysis.

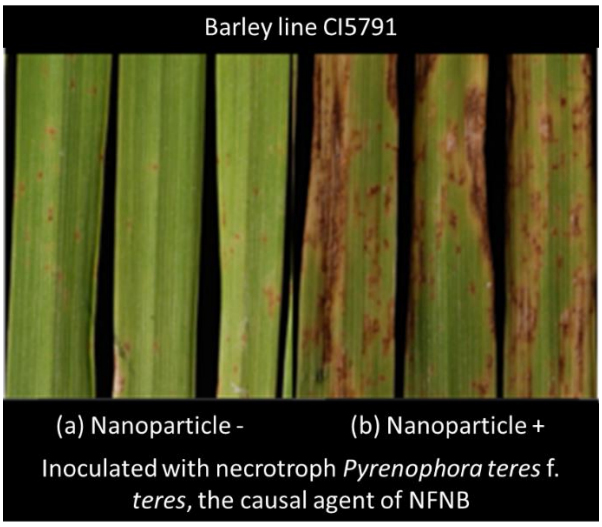

Figure 5.7. 7-day disease profile in (a) pathogen inoculated leaves, and (b) NP+pathogen inoculated leaves.

5.3.5. Expression of Salicylic and Jasmonic Acid-Related Genes

5.3.5.1. Barley

To identify differentially regulated SA and JA-response genes, enrichment analysis using GO terms was performed in TopGO and the Classification Superviewer. The expression data for the treatments across all the time point were separated into upregulated and downregulated genes, and gene enrichment analysis was conducted on each set separately. Using TopGO, with DEGs from the ZnO NP treated barley seedlings, gene enrichment analysis revealed 2 JA-related genes that were downregulated at 24 hpa, and 1 JA-related gene downregulated at 48 hpa. No SA or JA-related genes were found to be significantly upregulated in the ZnO NP treatment. In the combined NP application and pathogen-inoculated seedlings, 19 SA-related genes were upregulated at 45 hpi (Figure 5.8). It was evident from the enrichment analysis that at the latest time-point i.e. 48

hpa/45 hpi, there was persistent expression, upregulation, of SA-related processes, whereas JA-related processes did not appear to be significantly enriched. For the ZnO NP treated barley seedlings, there was a downregulation of SA-related genes (Figure 5.8).

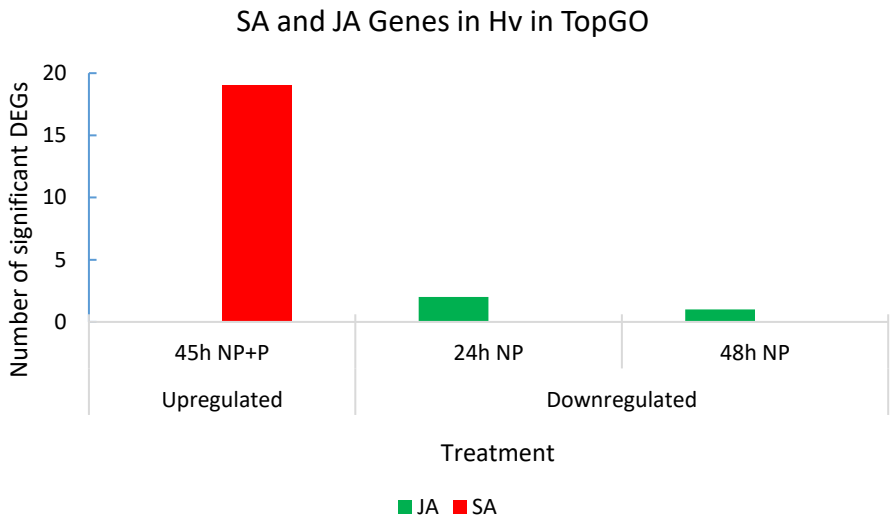

Figure 5.8. Number of DEGs in NP, and combined application (NP+P) expression data that are significantly enriched for salicylic (SA) and jasmonic acid (JA) - related processes as revealed by TopGO.

With the Classification Superviewer, the time course analysis across all treatments revealed that the numbers of upregulated SA-related genes were higher in the combined application than NP or pathogen inoculated treatments alone (Figure 5.9). For the ZnO NP treatments, 5 SA-related process genes were upregulated at 3 hpa. For the pathogen inoculated barley seedlings the numbers of upregulated SA-related process genes were 41, 43, and 38 at 3, 21, and 45 hpi, respectively. For the combined NP application followed by pathogen inoculation, the numbers of upregulated SA-related process genes were 53, 52, and 43 for 3, 21, and 45 hpi, respectively. When specifically analyzing JA-related genes upregulated in response to NP application only 4 genes were upregulated at 3 hpa. For the pathogen inoculation alone treatment across the time course analyzed, 25, 32, and 23 genes were upregulated at 3, 21, and 45 hpi that fell into the JA-related processes,

respectively. For the combined application, the numbers of JA-related process genes upregulated were 35, 35, and 28 at 3, 21, and 45 hpi, respectively. For the ZnO NP treatments the numbers of SA-related process downregulated genes were 12, 2, 5, and 3 genes at 3, 6, 24, and 48 hpa, respectively. For the pathogen inoculation alone the numbers of SA-related process downregulated genes were 18, 23, and 10 genes at 3, 21, and 45 hpi, respectively. For the combined NP application followed by pathogen inoculation, the numbers of SA-related process genes downregulated were 20, 22, and 12 genes at 3, 21, and 48 hpa/45 hpi, respectively. For the NP treatment alone 10, 1, 6, and 3 JA-related process genes were downregulated at 3, 6, 24, and 48 hpa, respectively. For the pathogen treatment alone 15, 18, and 11 SA-related process genes were downregulated at 3, 21, and 45 hpi respectively. For the combined application 14, 17 and 11 SA-related process genes were downregulated at 3, 21, and 45 hpi, respectively. All the Classification Superviewer data with regards to SA- and JA-related processes are shown in Fig 5.9.

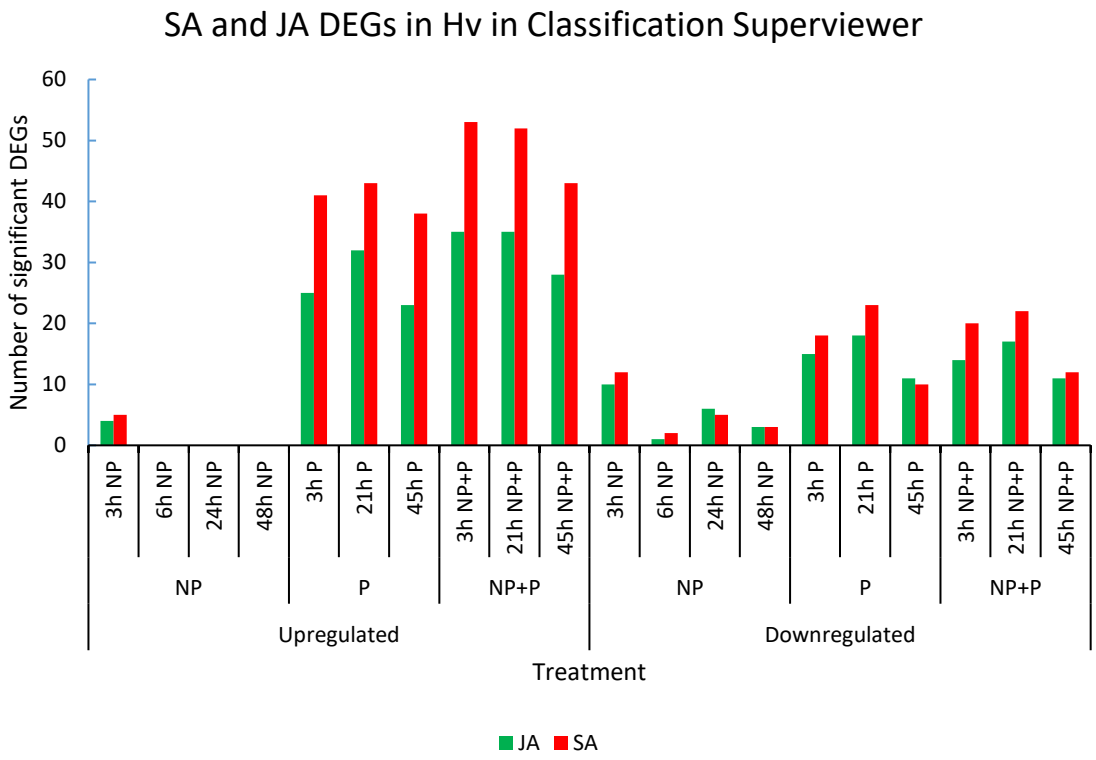

Figure 5.9. Number of DEGs in the nanoparticle (NP), Pathogen (P), and combined application (NP+P) treatments that were significantly enriched for salicylic (SA) and jasmonic acid (JA)-related processes as revealed by Classification Superviewer analysis.

It is evident from both TopGO and Classification Superviewer gene enrichment analysis that there was expression amplification of SA-related processes genes in the combined application plants as indicated by higher number of upregulated genes related to SA-processes.

Comparisons between the SA and JA-related DEGs across ZnO NP, pathogen and combined application treatments identified the common and unique DEGs. For the upregulated SA genes, 1 gene was common between NP and combined application, whereas 58 were common between pathogen and combined application (Figure 5.10a). For upregulated JA genes, 34 were common to pathogen and combined application, and 2 common to all the treatments (Figure 5.10c). It is interesting to note that 11 SA-genes, and 8 JA-genes were uniquely expressed in the combined

application plants. This provides evidence that there are unique molecular activities in combined application that did not occur in either NP or pathogen treatment alone. The outcome of these differentially expressed plant hormone related genes known to be involved in stress responses and disease resistance are hypothesized to have contributed to the observed higher levels of disease when phenotyping the barley seedling that were exposed to NPs then inoculated with the necrotrophic pathogen. Overall, it was observed that the amplified induction of SA activity in the combined application seedlings may have subsequently induced upregulation of oxidation-reduction processes and PR gene activity that resulted in higher levels of programmed cell death and susceptibility to the necrotrophic pathogen.

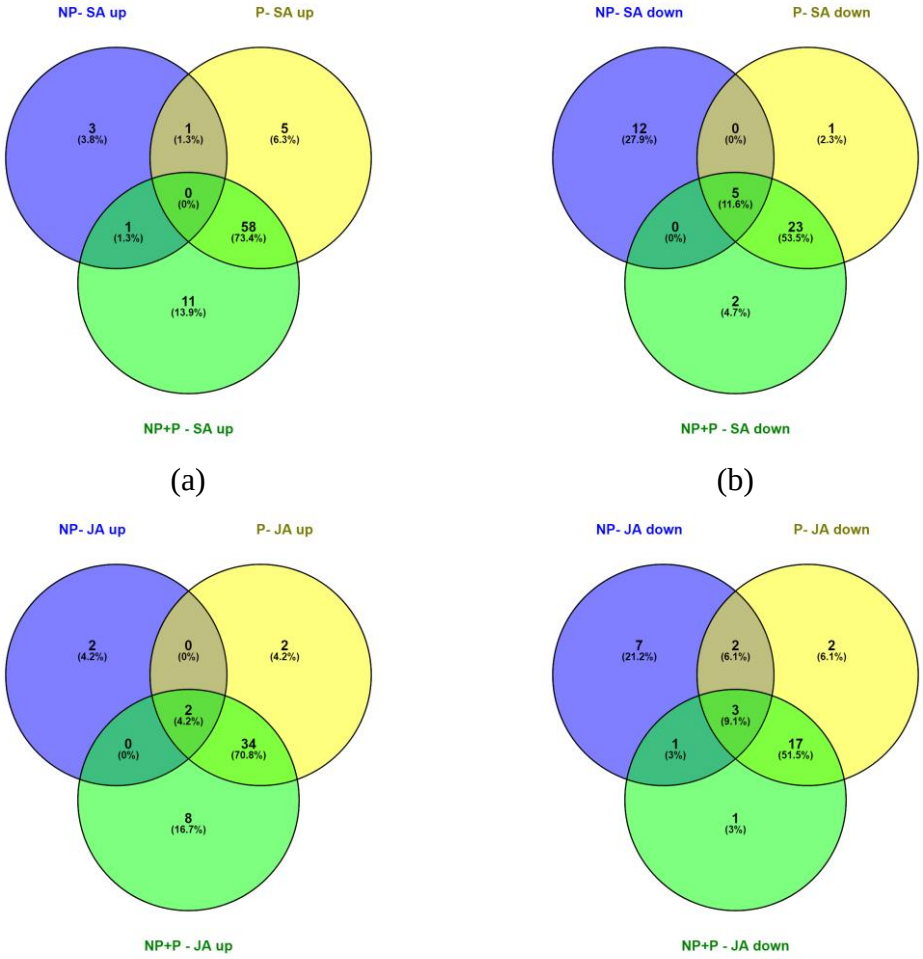

Figure 5.10. Common and unique SA- and JA-related genes in ZnO NP, pathogen, and ZnO NP+pathogen treatments in barley.

5.3.5.2. Arabidopsis

Enrichment analysis in Arabidopsis with TopGO revealed contrasting results compared to barley regarding SA and JA-related genes. In ZnO NP treatment, a higher number of upregulated genes were found to be enriched for JA-related processes at 3 and 6 hpa, whereas downregulated genes at 48 hpa were enriched for SA (Figure 5.12). This is in contrast to barley where SA-related genes were upregulated at 48 hpa, and JA-related genes were downregulated at 24, and 48 hpa.

Similar results were observed when enrichment was done with Classification Superviewer software (Figure 5.11) where upregulated genes were significantly enriched for JA-related processes at 3, and 6 hpa. Thus, it is evident that the model dicot Arabidopsis responded differently to ZnO NPs as compared to the model monocot barley.

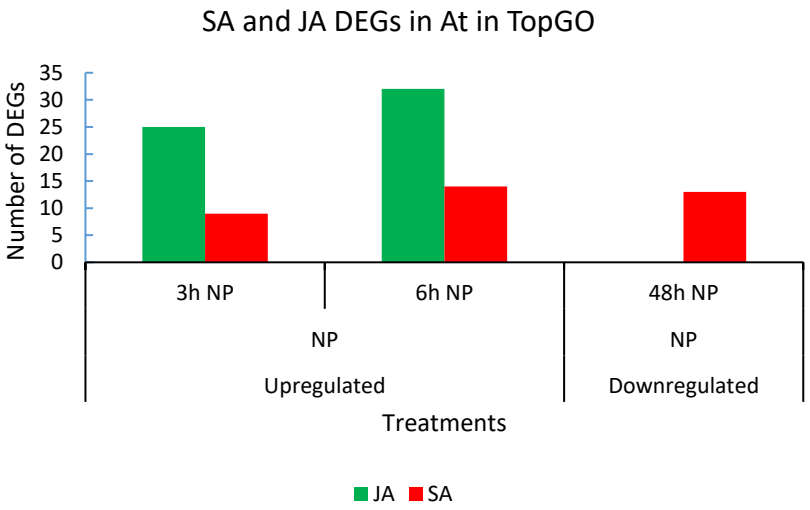

Figure 5.11. Number of DEGs in NP treatment expression data in Arabidopsis that are significantly enriched for salicylic (SA) and jasmonic acid (JA) - related processes as revealed by TopGO

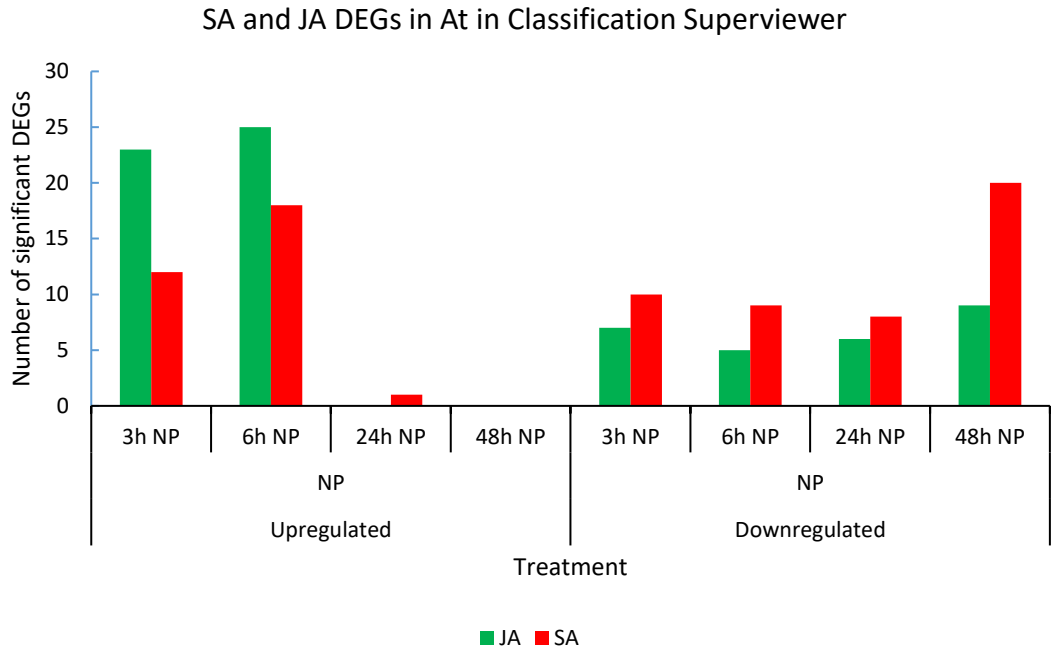

Figure 5.12. Number of DEGs in NP treatment expression data in Arabidopsis that are significantly enriched for salicylic (SA) and jasmonic acid (JA) - related processes as revealed by Classification Superviewer analysis.

5.3.6. Identification of Putative SA-Related Genes Using Protein-Protein Interaction Network (PPIN)

A protein-protein interaction network (PPIN) is a graph theoretic construct where proteins are represented by nodes, and their interactions by edges. Often, every interaction is assigned a weight that signals its reliability; the higher the weight of an edge, the more reliable the interaction that it describes. Due to the increasing availability of proteomic data in curated databases and the advances in complex network analysis, PPINs and their topological structures have been used to identify genes involved in complex biological signaling networks . PPIN analysis was conducted using the Arabidopsis ortholog of the corresponding annotated barley genes. For recent surveys trying to summarize the use and analysis of PPINs, see, among others, the works of Rasti & Vogiatzis , Bhowmick and Seah , and Li et al.

In this work, PPIN analysis was conducted using the Arabidopsis ortholog of the corresponding annotated barley genes. A Steiner Tree problem was used as the model to identify a collection of interactions of maximum reliability such that all the proteins of interest (based on up- and down-regulated genes) are connected. Due to the large-scale nature of the obtained network, the Kou approximation algorithm was used to find a heuristic solution in reasonable time. The underlying network is generated based on the STRING-DB database for Arabidopsis thaliana, while all visualizations and graph processing operations are done using NetworkX .

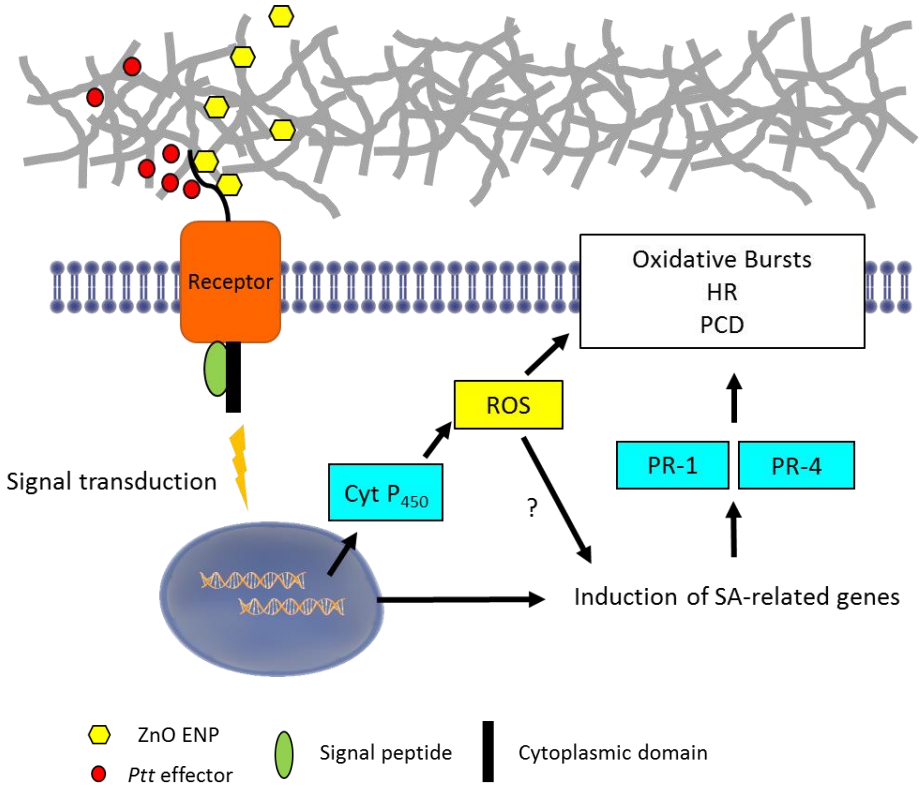

Figure 5.13. The PPIN model showing the relationship between the cell surface receptor proteins, and the downstream genes in the signaling cascade like SA-inducible PR1 and PR4, that play probable roles in increased necrosis. Necrosis characteristics include Hypersensitive Responses (HR), oxidative bursts, and Programmed Cell Death (PCD) which are induced by ROS (Reactive Oxygen Species) production. ROS burst is thought to trigger SA signaling or vice versa . Cytochrome P_{450} family genes participate in ROS production . In combined application (NP+Ptt) treatments, PR1, PR4 and Cyt P_{450} genes were highly upregulated.

The goal of the PPIN analysis was to begin characterizing the underlying mechanism of increased necrosis and disease observed in the plants treated with both ZnO NP and the necrotrophic pathogen *P. teres* f. *teres*, as compared to the resistant barley line CI5791 seedlings only inoculated with the pathogen. The increased necrosis has been hypothesized to be partly induced by SA-mediated expression of oxidation-reduction process and PR genes. These genes include pathogenesis related protein 1 (PR1) (HORVU7Hr1G033530), and pathogenesis related protein 4 (PR4) (HORVU3Hr1G113120). These genes are speculated to contribute to HR-mediated programmed cell death observed in the barley leaves infected with both ZnO NPs and

Ptt. PR1, PR5 and PR8 were induced by SA in *Malus hupehensis*. SA-marker gene, PR1 was found to be induced in Arabidopsis treated with folic acid, and locally enhanced susceptibility to the necrotroph *Alternaria brassicicola*. PR1b1 in tomato was also found to be induced by low temperature, and is linked to the accumulation of SA. A PR4 protein identified in pepper (*Capsicum annuum*), *CaPR4c* is shown to play a role in H_2O_2 accumulation and HR cell death upon pathogen infection in pepper. CaPR4b is also shown to positively regulate defense signaling mediated by SA production, and activating HR cell death. Interestingly, PR4 can be considered marker for both SA and JA, as it is shown to be induced by both SA and JA in wheat, indicating that it is involved in both SA- and JA-dependent defense response pathways. These data also point to the interaction or upregulation of the PR genes and the subsequent upregulation of oxidation-reduction processes that lead to H_2O_2 accumulation and enhanced PCD.

Using PPIN, these PR proteins are identified to be downstream genes in a network of signaling cascades that originate in probable recognition of *Ptt*-effectors and ZnO NPs by cell-surface receptors (Figure 5.13). Some of these cell-surface proteins upregulated in the ZnO NP+*Ptt* application plants that possibly lead to downstream expression of PR genes are Wall associated kinases (WAKs), Somatic embryogenesis receptor-like kinase 1 (SERK1), Concanavalin A-like lectin protein kinase family protein, Late embryogenesis abundant (LEA) hydroxyproline-rich glycoprotein family, and S-locus lectin protein kinase family protein. SERKs are known to be RLKs which function as co-receptors of diverse cell-surface receptors involved in MAMP and DAMP recognition. Recent findings suggest that SERKs also play a role in abiotic stress tolerance as HvSERK1 was upregulated in the roots of barley seedlings under salt stress. The role of SERKs in hypersensitive responses is evidenced by the accumulation of salicylic acid (SA), and

overexpression of cell-death inducing genes like BONs, BIRs, and SOBIR in BAK1/SERK3-overexpressing transgenic Arabidopsis.

5.3.7. Verification of PR1, PR4, and Cytochrome P450 Gene Expression Using Quantitative Real-Time PCR

From RNA-seq, the expression of HvPR1 (HORVU7Hr1G033530) was induced in combined application plants with fold change of 55.4 at 3 hpi, 1354.3 at 21 hpi, and 2919.5 at 45 hpi. In pathogen-inoculated plants, the fold change expression was 14.7 at 3 hpi, 1650.5 at 21 hpi, and 1417.3 at 45 hpi. The expression of HvPR4 (HORVU3Hr1G113120) was induced in combined application plants with fold change of 31.9 at 3 hpi, 631.6 at 21 hpi, and 1196.6 at 45 hpi. In pathogen-inoculated plants, the fold change expression was 13.5 at 3 hpi, 800.4 at 21 hpi, and 683.2 at 45 hpi. The expression of HvCYP450 (HORVU2Hr1G004550) was induced in combined application plants with fold change of 159.0 at 3 hpi, 345.6 at 21 hpi, and 466.3 at 45 hpi. In pathogen-inoculated plants, the fold change expression was 90.02 at 3 hpi, 286.53 at 21 hpi, and 227.02 at 45 hpi.

The qPCR experiment conducted on the same plants showed that HvPR1 is upregulated 5349.97 folds at 3 hpi, 48394.13 folds at 21 hpi and 50335.02 folds at 45 hpi in *Ptt*-inoculated plants. The expression of HvPR1 in combined application plants were 3127.30 folds at 3 hpi, 42344.95 folds at 21 hpi, and 379169.65 folds at 45 hpi. The expression of HvPR4 in *Ptt*-inoculated plants was 759.21 folds at 3 hpi, 9563.50 folds at 21 hpi, and 10792.80 folds at 45 hpi. In the combined application plants, HvPR4 was upregulated 355.66 folds at 3 hpi, 6920.03 folds at 21 hpi, and 19660.96 folds at 45 hpi. PR1 and PR4 gene expression at the final time-point i.e. 45 hpi in combined application plants was significantly higher than that of *Ptt*-inoculated plants (p-value<0.05). In the case of HvCYP450, the gene expression was 801.27 folds at 3 hpi, 2215.20

folds at 21 hpi, and 1404.00 folds at 45 hpi in *Ptt*-inoculated plants. In the combined application plants, HvCYP450 was upregulated 463.73 folds at 3 hpi, 2497.20 folds at 21 hpi, and 3065.28 folds at 45 hpi. The gene expression at the final time-point i.e. 45 hpi in combined application plants was significantly higher than that of *Ptt*-inoculated plants (p-value<0.05). Thus, the qPCR analysis confirmed that the expression of HvPR1, HvPR4 and HvCYP450 are higher in the combined application plants at 45 hpi than in pathogen-inoculated plants, suggesting that the combined application amplifies the signaling that putatively results in enhanced PCD responses that the necrotrophs hijack to colonize the resulting dying and dead tissue facilitating further disease development.

5.4. Discussion

5.4.1. ZnO NPs Cause a Shift in the Magnitude of Responses in Pathogen Inoculated Plants

The application of ZnO NPs prior to pathogen inoculation caused an apparent shift in the magnitude of the response in terms of the number of DEGs and the fold change of the DEGs. The combined treatment had an additive effect that would be hard to predict, where both the effectors, the ZnO NP and the necrotrophic pathogen *P. teres* f. *teres* caused a higher magnitude of differential gene regulation, transcriptomic responses, than either treatment alone. Similar shifts in gene expression were observed in Arabidopsis subjected to heat, drought, and virus stress where the simultaneous exposure of these abiotic and biotic stresses increased the number of DEGs significantly as compared to exposure to a single stress alone . ZnO NPs, in addition to eliciting differential regulation of genes unique to the combined ZnO NP+*Ptt* treatment also triggered higher fold expression changes of genes that were also expressed in plants exposed to the pathogen alone. At the timepoints 3, 21 and 45 hpi, 76.5%, 58.4% and 85.4% of the total genes common to

pathogen and combined application treatments had a higher magnitude of fold change (absolute value) in the combined application, respectively An example is the gene wound induced protein (HORVU3Hr1G113120), which shares 74.2% identity with Arabidopsis PR4 (AT3G04720) gene was induced in both pathogen and combined application plants, with fold changes 13.5, 800.4, and 683.2 at 3, 21, and 45 hpi respectively in pathogen exposed plants. However, its fold change expression was 31.9, 631.6, and 1196.6 at 3, 21, and 45 hpi respectively in combined application plants. This indicates that although ZnO NPs do not trigger significant upregulation of this pathogen responsive gene alone, it amplifies its expression above levels detected by pathogen induction alone. Thus, implicating ZnO NP-plant interactions as having an effect on the transcriptional reprogramming mechanisms, which could impact the downstream responses that are required of a plant for biotic defense responses. PR4 has been implicated in responses to pathogen infection, salt, wounding, and hormone stresses in ginseng . In pepper, PR4b is involved in HR responses like plant cell death . Other PR genes like cysteine venom protein (HvPR1 or HORVU7Hr1G033530), sharing 54.8% identity with AtPR1 had 55.4, 1354.3, and 2919.5 fold upregulation at 3, 21, and 45 hpi respectively in combined application and 14.7, 1650.5, and 1417.3 fold upregulation at 3, 21, and 45 hpi respectively in pathogen inoculated plants, also indicating an amplification of expression in the ZnO NP+*Ptt* plants.

The crosstalk between abiotic and biotic stress responses in plants is a complex phenomenon. Stress conditions are known to effect plant-pathogen interactions by changing plant physiology. In Arabidopsis, drought conditions prior to herbivory altered the transcriptomic responses to a lower magnitude in terms of the number of DEGs, and induced the downregulation of defense responsive genes.

5.4.2. ZnO NPs Elicit Similar Temporal Pattern of Responses Across Time-Points in Barley CI5791 and Arabidopsis Col-0 but Their DEG Profiles Differ

Time-course comparisons of the DEG profiles in barley and Arabidopsis exposed to ZnO NPs reveal a similar temporal pattern of differential gene expression where there is a rapid response at the initial time-points i.e. 3 and 6 hpa but expression patterns return back to basal levels relatively quickly at the later time-points analyzed. However, there was only 0.9% and 2.7% overlap of upregulated and downregulated genes respectively at 3 hpa suggesting differential recognition and subsequent responses in the monocot and dicot model species. One of the genes upregulated in both barley and Arabidopsis at 3 hpa is NRT1/ PTR FAMILY 3.1, which is induced by *Erysiphe necator* in susceptible *Vitis vinifera* grapevine and encodes a nitrate/nitrite transporter suggesting some limited overlap of responses.

The minor overlap of DEGs in both species suggests that plant perception of NPs differs between monocots and dicots. Soybean was found to be more tolerant to heavy metal stress than maize, and exhibited stronger defense responses suggesting similar differential responses in these monocot and dicot systems as well. However, common defense mechanisms have been observed in monocots and dicots against pathogens, and abiotic stresses. For example, subfamilies of Ethylene Responsive Factor (ERF) superfamilies of transcription factors are associated with abiotic stress and biotic stress responses in both monocots and dicots . The role of MLO/MLO2 protein and the syntaxin ROR2/PEN1 in defense responses against fungal pathogens have also been found to be conserved in both barley and Arabidopsis. These data suggest that it is not the divergence of these mechanisms but probably that they respond differentially due to divergent evolution in the receptors and responses to specific stimuli determining how or what they perceive

as the threat or advantage that the NP pose that results in the very different responses observed between the model species.

5.4.3. Salicylic Acid (SA)-Mediated Processes Dominate Over Jasmonic Acid (JA)-Mediated Processes in ZnO NP and Combined Application Treatments in Barley Line CI5791

GO term enrichment analysis identified the number of SA and JA-related DEGs in the treatments. Classification Superviewer yielded far more GO terms that were enriched for SA and JA-related processes as compared to TopGO. The application of ZnO NPs prior to pathogen inoculation in barley induced the expression of several SA-related genes as compared to ZnO NP or pathogen alone. Although TopGO and Classification Superviewer yielded slightly different results in terms of the number of significant DEGs enriched for SA and JA, the outcome was consistent where SA-related genes were higher than JA-related genes.

A close inspection of the Venn diagrams (Figure 5.10) identified common and unique genes to the treatments. It is interesting to note that 11 upregulated genes related to SA responses were unique to the combined application. An interesting gene involved in transcriptional regulation of SA defense response activation which was unique to combined application treatment was the barley homolog of the ATWRKY46 gene designated HvWRKY46. It had been previously shown that AtWRKY46 plays a role in abiotic stress responses, particularly in enhancing drought and osmotic stress tolerance, and in SA biosynthesis upon pathogen attack. Another SA-related gene unique to the combined application was the Wall Associated Kinase 2 (WAK2) gene, which spans both abiotic and biotic stress signaling processes. WAKs are pectin-binding plasma membrane receptors . The rice *OsWAK1* gene expression was significantly induced by infection by the rice blast fungus, *Magnaporthe oryzae*, mechanical wounding, SA and methyl jasmonate (MeJA),

indicating that it is involved in plant defense. Recently, OsWAK11 was implicated in mediating tolerance to copper toxicity in rice, as OsWAK11-silenced plants resulted in hypersensitivity to excess Cu, suggesting multiple roles of WAKs. It has been shown that the WAK genes play an important role in sensing the integrity of the plasma membrane cell wall continuum in plants. Thus, these cell surface receptors can sense a disruption of this continuum weather it is induced by shrinkage of cell membranes due to water shortage and drought conditions or cell wall degradation induced by pathogen cell wall degrading enzymes. In either case the WAK membrane receptors signal the plant of the biotic or abiotic stress conditions.

Several other genes were upregulated in both pathogen and combined application plants, but their expression was induced several folds higher in the combined application of ZnO NP+*Ptt* implicating the role of ZnO NPs in the amplification of defense responses when applied before the plant encounters the pathogen. The HvWRKY70 gene (Arabidopsis homolog AT3G56400) expression was amplified when the barley plants were previously exposed to ZnO NPs, which was also expressed in pathogen exposed plants at much lower levels. HvWRKY70 was upregulated in combined application plants 40.7 folds at 21 hpi, and 95 folds at 45 hpi, whereas in pathogen exposed plants, the fold change at 45 hpi was much lower at 42.7 folds. Interestingly, *WRKY70* overexpression in Arabidopsis was found to correlate with enhanced susceptibility to the fungal necrotroph *Alternaria brassicicola* . The authors indicated that WRKY70 was required for SA-induced suppression of JA-mediated defense responses against A. *brassicicola* that led to the susceptibility. Thus, it could be hypothesized that the upregulation of the HvWRKY70 gene could play a role in enhancing susceptibility to the necrotrophic pathogen *Ptt* in barley. The HvWRKY70 orthalog in rice, OsWRKY45 was also shown to be a marker of SA-mediated responses . Another WRKY transcription factor, AtWRKY30 was also shown to be a SA-dependent transcription

factor and was induced under pathogen attack and oxidative stress . In our dataset, WRKY30 was induced 6.3 folds and 5.4 folds at 3 and 45 hpi respectively in combined application plants and was only induced 4.6 folds at 3 hpi in the pathogen inoculated plants.

In ZnO NP-exposed Arabidopsis, a higher number of JA-related genes were upregulated as compared to SA-related genes. This observation is contradictory to barley responses, as well as other existing reports. SA was found to be stimulated, and jasmonic acid was suppressed in leaves and roots of Arabidopsis exposed to ZnO NPs. Thus, further experiments using Arabidopsis necrotrophic and biotrophic pathogens need to be conducted to determine how the model dicot defense mechanisms will respond to subsequent pathogens after exposure to the ZnO NPs.

5.4.4. Application of ZnO NPs Prior to Pathogen Inoculation Promotes Susceptibility to *Pyrenophora teres f. teres* in the Resistant Barley CI5791 and is Linked to the Induction of SA-Related Genes and Oxidation-Reduction Genes

Barley line CI5791 has effective and broad resistance to diverse isolates of *Pyrenophora teres* f. *teres*, the causal agent of NFNB and the resistance locus was mapped to the centromeric region of the barley 6H chromosome. The application of ZnO NPs prior to pathogen exposure resulted in increased PCD-induced necrotic lesions and enhanced disease on the leaves of CI5791 as compared to the plants inoculated with the pathogen alone. This compromised resistance against NFNB in the ZnO NP exposed plants is most likely a result of the upregulation of SA-related genes and oxidation-reduction processes in the combined application, and subsequent SA-mediated induction of HR responses and PCD after pathogen encounter. The mutual antagonism between the plant hormones, SA and JA played a key role in the downregulation of JA-related genes that otherwise participates in JA-mediated defense against necrotrophic pathogens (Figure 5.14). The

upregulation of SA-related genes in the combined application plants can be attributed to the presence of ZnO NPs in the soil as SA is found to alleviate symptoms of abiotic stress in plants. The role of SA in the alleviation of abiotic stress has been well documented as the exogenous application of SA improved Cu tolerance in *Phaseolus vulgaris* L. SA pretreatment also alleviated the symptoms of Cd-induced toxicity in flax .

Similar observations to those observed in this ZnO NP+*Ptt* interaction have been recorded in the case of plants exposed to combined stresses like abiotic stress and plant pathogens. In tomato, mild and moderate salt stress enhanced susceptibility to powdery mildew and was linked to the high expression of ethylene biosynthesis genes in the combined stressed plants. Arabidopsis subjected to combined drought and heat conditions had enhanced susceptibility to turnip mosaic virus, and the molecular mechanisms underlying susceptibility was linked to differential expression of a TIR-NBS-LRR genes, altered hexose signaling due to heat stress, and downregulation of PR-genes in the combined stressed plants.

In barley, wheat, and *Zea mays*, drought conditions enhanced susceptibility to the fungal phytopathogens *Ramularia collocygni*, *Ervsiphe arainins f. sp. hordei*, *Puccinia recondite*, and *Ustilago maydis*. On the contrary, drought promoted resistance in barley against *Blumeria graminis*, the causal agent of powdery mildew . In tomato, and potato, drought enhanced resistance to *Oidium neolycopersici*, and *Botrytis cinerea*, respectively. *Cucumis sativus* L (cucumber) cultivars, Sardes and Beith alpha were affected on exposure to salt stress and the pathogen, *Pseudoperospora cubensis* Berk. and Curt. Rostov.

Although a higher number of SA-related genes were upregulated in the combined application plants, the involvement of JA in the defense responses cannot be undermined. There was substantial upregulation of JA-inducible genes in the combined application. This indicates

that the presence of ZnO NP and pathogen together triggered a concerted defense response involving both SA and JA-mediated signaling, however SA-related signaling may have played a dominant role.

The increased necrosis in the combined application plants can be attributed to the induction of oxidation-reduction genes that causes oxidative bursts, H_2O_2 accumulation, and subsequent PCD responses. The induction of the oxidation-reduction genes is thought to be linked to the escalation of ZnO NP induced SA-mediated processes or due to unknown processes mediating from ZnO NP application. Some of the genes involved in oxidation-reduction processes are Cytochrome P450 family genes, Peroxidase superfamily genes, and Flavin-binding monooxygenase family genes. It was observed from the RNA Seq dataset that at 3 hpi, 21 hpi, and 45 hpi, 87.27%, 73.59%, and 85% of the oxidation-reduction genes had a higher fold change in the combined application treatments than the pathogen-inoculated treatments. Hence, the increased necrosis observed in the combined application plants can be attributed to the higher expression of oxidation-reduction genes in the combined application plants. qPCR analysis verified the expression of an important gene involved in oxidation-reduction processes, Cytochrome P450 gene. HvCYP450 (HORVU2Hr1G004550) had significantly higher expression at 45 hpi in combined application plants as compared to pathogen-inoculated plants.

5.5. Conclusion

The interaction of NPs with plants and other biotic components of the ecosystem is largely unknown at the molecular level. In this pioneering study, we have explored the dynamics of NP-plant interaction together with a biotic stress inducer, a necrotrophic phytopathogen. Barley line CI5791 which is resistant to the causal agent of NFNB, *Pyrenophora teres* f. *teres*, when exposed to ZnO NPs and subsequently to the pathogen, displayed enhanced susceptibility to the disease as

compared to the pathogen exposed plants alone. This compromised resistance was traced to the ZnO NP mediated upregulation of SA-related genes in the combined application plants, which antagonized JA-related gene expression. Upregulation of SA-related genes were also observed in ZnO NP exposed barley. In this study, we have proposed a model that explains the observed disease symptoms of barley CI5791 upon combined ZnO NP and pathogen exposure (Figure 5.14). The cell surface receptor proteins which are putatively involved in perception of both ZnO NP and pathogen leads to the signaling of the downstream genes in the network, which induce SA-mediated defense responses. Such SA-responsive genes include the PR genes, PR1 and PR4 that mediate defense responses leading to increased necrosis and subsequently may upregulate the oxidation-reduction genes and processes which lead to enhanced PCD and disease caused by the necrotrophic pathogen. These genes are speculated to function in defense responses spanning NP perception and biotic stress, and cross link JA and SA-mediated pathways. Genes that are not related to SA and JA-mediated signaling are also differentially regulated several folds in the combined application compared to the pathogen, and some are exclusively expressed in the combined application, indicating that they are induced by ZnO NPs in the presence of the pathogen. This suggests that the observed susceptibility to the pathogen in the combined application is not the absolute function of enhanced SA-mediated processes but may also be due to unknown processes mediated by unique gene expression and genes that were also upregulated by the ZnO NPs or had amplified upregulation by the ZnO NP and pathogen interaction.

The effects in ZnO NP exposed Arabidopsis was contradictory. JA-related gene expression was dominant in Arabidopsis. Although the responses were subtle, it provided a glimpse of the physiological reprogramming that occurred due to NP exposure in both the species. From the barley and Arabidopsis expression data, it could be concluded that both species react differently

to ZnO NPs, giving a glimpse of the differential responses that ZnO NPs may elicit in different plant species. Extensive and intricate research is required to understand the plethora of plant responses to NPs and their effect on host-pathogen interactions.

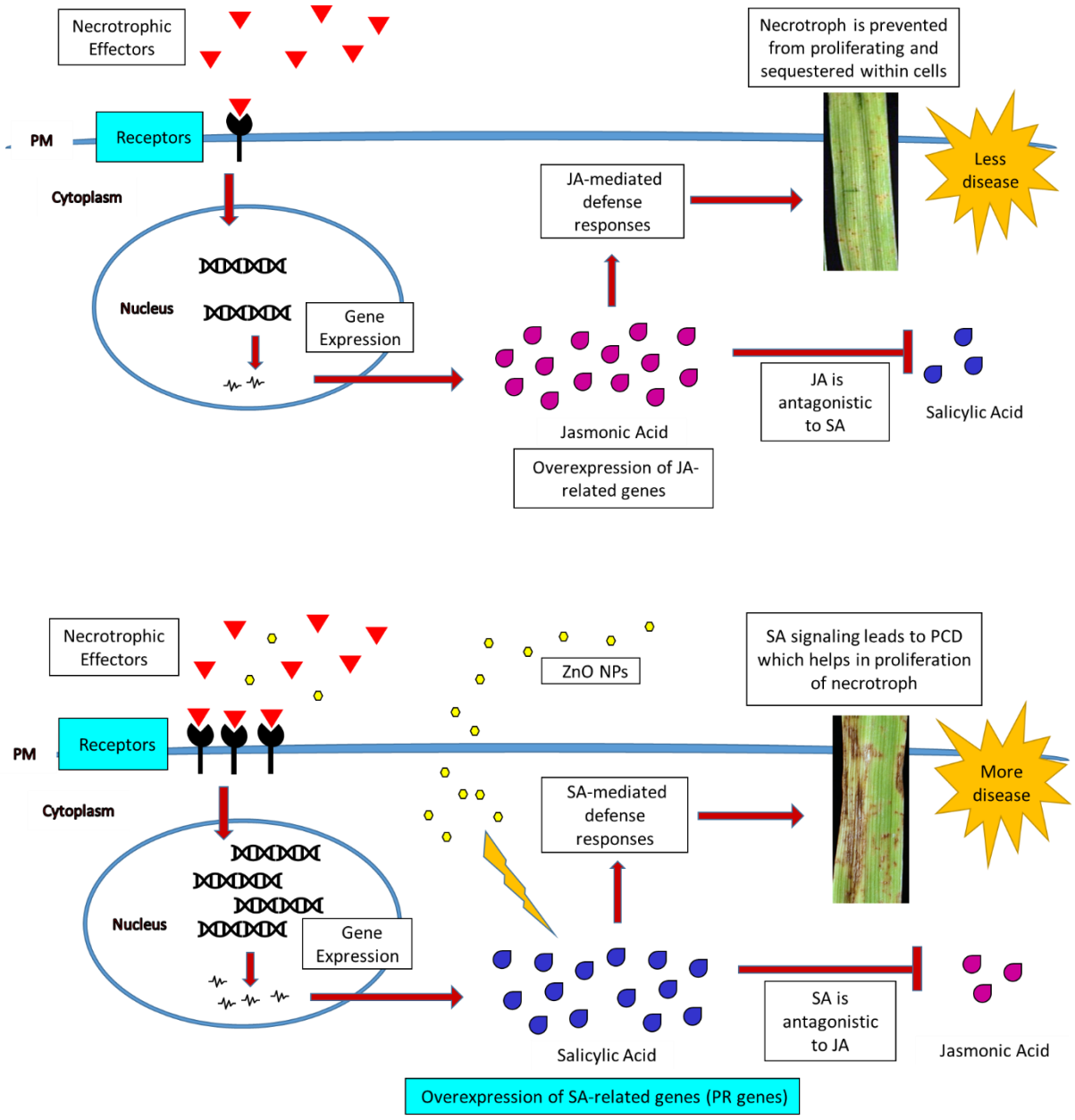

Figure 5.14. A model showing the hypothetical mechanism for induced susceptibility in Net Blotch-resistant barley line CI5791 upon exposure to ZnO NPs. (a) The proposed model when only necrotrophic effectors are present. Putative receptor kinases present in the cell membrane recognizes the effectors, leading to gene expression that elicits defense responses in the plant. Jasmonic acid-mediated signaling plays a key role in the defense responses that prevents the pathogen to proliferate. (b) The proposed model when ZnO NPs are present together with the necrotrophic pathogen. SA-related genes are induced in plants in response to the presence of ZnO NPs that antagonizes JA. The necrotrophic pathogens employ the SA-mediated signaling pathway to promote disease in the plants by eliciting PCD-induced necrosis in the leaves of the combined application plants (ZnO NP + Pathogen).

5.6. References

achuo, E. A.; Prinsen, E.; Höfte, M. Influence Of Drought, Salt Stress And Abscisic Acid On The Resistance Of Tomato To Botrytis Cinerea And Oidium Neolycopersici. **Plant Pathology,** V. 55, N. 2, P. 178-186, 2006. Issn 1365-3059.

Alexa, A.; Rahnenfuhrer, J. Topgo: Enrichment Analysis For Gene Ontology. **R Package Version,** V. 2, N. 0, 2010.

Alexa, A.; Rahnenführer, J.; Lengauer, T. Improved Scoring Of Functional Groups From Gene Expression Data By Decorrelating Go Graph Structure. **Bioinformatics,** V. 22, N. 13, P. 1600-1607, 2006. Issn 1460-2059.

Almutairi, Z. M. Expression Profiling Of Certain Mads-Box Genes In Arabidopsis Thaliana Plant Treated With Silver Nanoparticles. **Czech Journal Of Genetics And Plant Breeding,** V. 53, N. 1, P. 30-36, 2017. Issn 1212-1975.

Baker, S. Et Al. Nanoagroparticles Emerging Trends And Future Prospect In Modern Agriculture System. **Environmental Toxicology And Pharmacology,** V. 53, N. Supplement C, P. 10-17, 2017/07/01/ 2017. Issn 1382-6689. Disponível Em: < Http://Www.Sciencedirect.Com/Science/Article/Pii/S1382668917301114 >.

Belkadhi, A. Et Al. Positive Effects Of Salicylic Acid Pretreatment On The Composition Of Flax Plastidial Membrane Lipids Under Cadmium Stress. **Environmental Science And Pollution Research,** V. 22, N. 2, P. 1457-1467, 2015. Issn 0944-1344.

Bertini, L. Et Al. Pathogen-Responsive Wheat Pr4 Genes Are Induced By Activators Of Systemic Acquired Resistance And Wounding. **Plant Science,** V. 164, N. 6, P. 1067-1078, 2003/06/01/ 2003. Issn 0168-9452. Disponível Em: < Http://Www.Sciencedirect.Com/Science/Article/Pii/S0168945203001122 >.

Bethenod, O.; Huber, L.; Slimi, H. Photosynthetic Response Of Wheat To Stress Induced By Puccinia Recondita And Post-Infection Drought. **Photosynthetica,** V. 39, N. 4, P. 581-590, 2001. Issn 0300-3604.

Boland, G. J. Et Al. Climate Change And Plant Diseases In Ontario. **Canadian Journal Of Plant Pathology,** V. 26, N. 3, P. 335-350, 2004. Issn 0706-0661.

Brodersen, P. Et Al. The Role Of Salicylic Acid In The Induction Of Cell Death In Arabidopsis Acd11. **Plant Physiology,** V. 138, N. 2, P. 1037-1045, 2005. Issn 0032-0889.

Caillaud, M.-C. Et Al. A Downy Mildew Effector Attenuates Salicylic Acid–Triggered Immunity In Arabidopsis By Interacting With The Host Mediator Complex. **Plos Biology,** V. 11, N. 12, P. E1001732, 2013. Issn 1545-7885.

Davila Olivas Nelson, H. Et Al. Effect Of Prior Drought And Pathogen Stress On Arabidopsis Transcriptome Changes To Caterpillar Herbivory. **New Phytologist,** V. 210, N. 4, P. 1344-1356, 2016/06/01 2016. Issn 0028-646x. Disponível Em: < Https://Doi.Org/10.1111/Nph.13847 >. Acesso Em: 2018/06/03.

Dey, S.; Corina Vlot, A. Ethylene Responsive Factors In The Orchestration Of Stress Responses In Monocotyledonous Plants. **Frontiers In Plant Science,** V. 6, P. 640, 2015. Issn 1664-462x. Disponível Em: < Https://Www.Frontiersin.Org/Article/10.3389/Fpls.2015.00640 >.

Dimkpa, C. O. Et Al. Cuo And Zno Nanoparticles: Phytotoxicity, Metal Speciation, And Induction Of Oxidative Stress In Sand-Grown Wheat. **Journal Of Nanoparticle Research,** V. 14, N. 9, Sep 2012. Issn 1388-0764. Disponível Em: < <Go To Isi>://Wos:000308225800053 >.

Ding Zhong, J. Et Al. Transcription Factor Wrky46 Modulates The Development Of Arabidopsis Lateral Roots In Osmotic/Salt Stress Conditions Via Regulation Of Aba Signaling And Auxin Homeostasis. **The Plant Journal,** V. 84, N. 1, P. 56-69, 2015/10/01 2015. Issn 0960-7412. Disponível Em: < Https://Doi.Org/10.1111/Tpj.12958 >. Acesso Em: 2018/06/04.

El Oirdi, M. Et Al. Botrytis Cinerea Manipulates The Antagonistic Effects Between Immune Pathways To Promote Disease Development In Tomato. **The Plant Cell,** V. 23, N. 6, P. 2405-2421, 2011. Issn 1532-298x.

Flor, H. H. Current Status Of The Gene-For-Gene Concept. **Annual Review Of Phytopathology,** V. 9, N. 1, P. 275-296, 1971. Issn 0066-4286.

Franceschini, A. Et Al. String V9. 1: Protein-Protein Interaction Networks, With Increased Coverage And Integration. **Nucleic Acids Research,** V. 41, N. D1, P. D808-D815, 2012. Issn 0305-1048.

Friesen, T. L. Et Al. Identification And Chromosomal Location Of Major Genes For Resistance To Pyrenophora Teres In A Doubled-Haploid Barley Population. **Genome,** V. 49, N. 7, P. 855-859, Jul 2006. Issn 0831-2796. Disponível Em: < <Go To Isi>://Wos:000240079600015 >.

_____. Host-Specific Toxins: Effectors Of Necrotrophic Pathogenicity. **Cellular Microbiology,** V. 10, N. 7, P. 1421-1428, 2008. Issn 1462-5822.

Glazebrook, J. Contrasting Mechanisms Of Defense Against Biotrophic And Necrotrophic Pathogens. **Annu. Rev. Phytopathol.,** V. 43, P. 205-227, 2005. Issn 0066-4286.

Goyal, R. K. Et Al. Pathogenesis-Related Protein 1b1 (Pr1b1) Is A Major Tomato Fruit Protein Responsive To Chilling Temperature And Upregulated In High Polyamine Transgenic Genotypes. **Frontiers In Plant Science,** V. 7, P. 901, 2016. Issn 1664-462x. Disponível Em: < Https://Www.Frontiersin.Org/Article/10.3389/Fpls.2016.00901 >.

Hagberg, A.; Swart, P.; S Chult, D. **Exploring Network Structure, Dynamics, And Function Using Networkx**. Los Alamos National Lab.(Lanl), Los Alamos, Nm (United States). 2008

Hammond-Kosack, K. E.; Rudd, J. J. Plant Resistance Signalling Hijacked By A Necrotrophic Fungal Pathogen. **Plant Signal Behav,** V. 3, N. 11, P. 993-5, Nov 2008. Issn 1559-2316 (Print)

1559-2316.

Herrera-Vásquez, A.; Salinas, P.; Holuigue, L. Salicylic Acid And Reactive Oxygen Species Interplay In The Transcriptional Control Of Defense Genes Expression. **Frontiers In Plant Science,** V. 6, P. 171-171, 2015. Issn 1664-462x. Disponível Em: < Https://Www.Ncbi.Nlm.Nih.Gov/Pubmed/25852720 >.Disponível Em: < Https://Www.Ncbi.Nlm.Nih.Gov/Pmc/Pmc4365548/ >.

Hong, J. K.; Hwang, I. S.; Hwang, B. K. Functional Roles Of The Pepper Leucine-Rich Repeat Protein And Its Interactions With Pathogenesis-Related And Hypersensitive-Induced Proteins In Plant Cell Death And Immunity. **Planta,** V. 246, N. 3, P. 351-364, 2017/09/01 2017. Issn 1432-2048. Disponível Em: < Https://Doi.Org/10.1007/S00425-017-2709-5 >.

Humphry, M. Et Al. A Regulon Conserved In Monocot And Dicot Plants Defines A Functional Module In Antifungal Plant Immunity. **Proceedings Of The National Academy Of Sciences,** V. 107, N. 50, P. 21896, 2010. Disponível Em: < Http://Www.Pnas.Org/Content/107/50/21896.Abstract >.

Hwang, F. K.; Richards, D. S. Steiner Tree Problems. **Networks,** V. 22, N. 1, P. 55-89, 1992. Issn 1097-0037.

Hwang In, S. Et Al. Pathogenesis-Related Protein 4b Interacts With Leucine-Rich Repeat Protein 1 To Suppress Pr4b-Triggered Cell Death And Defense Response In Pepper. **The Plant Journal,** V. 77, N. 4, P. 521-533, 2014/02/01 2013. Issn 0960-7412. Disponível Em: < Https://Doi.Org/10.1111/Tpj.12400 >. Acesso Em: 2018/06/06.

Karuppanapandian, T. Et Al. Reactive Oxygen Species In Plants: Their Generation, Signal Transduction, And Scavenging Mechanisms. **Australian Journal Of Crop Science,** V. 5, N. 6, P. 709, 2011.

Kaveh, R. Et Al. Changes In Arabidopsis Thaliana Gene Expression In Response To Silver Nanoparticles And Silver Ions. **Environmental Science & Technology,** V. 47, N. 18, P. 10637-10644, Sep 17 2013. Issn 0013-936x. Disponível Em: < <Go To Isi>://Wos:000330096000070 >.

Kim, N. H.; Hwang, B. K. Pepper Pathogenesis-Related Protein 4c Is A Plasma Membrane-Localized Cysteine Protease Inhibitor That Is Required For Plant Cell Death And Defense Signaling. **The Plant Journal,** V. 81, N. 1, P. 81-94, 2015/01/01 2014. Issn 0960-7412. Disponível Em: < Https://Doi.Org/10.1111/Tpj.12709 >. Acesso Em: 2018/12/09.

Kim, S. Y. Et Al. Overexpression Of Bak1 Causes Salicylic Acid Accumulation And Deregulation Of Cell Death Control Genes. **Biochemical And Biophysical Research Communications,** V. 484, N. 4, P. 781-786, 2017/03/18/ 2017. Issn 0006-291x. Disponível Em: < Http://Www.Sciencedirect.Com/Science/Article/Pii/S0006291x1730236x >.

Kim, Y. J. Et Al. Cloning And Characterization Of Pathogenesis-Related Protein 4 Gene From Panax Ginseng. **Russian Journal Of Plant Physiology,** V. 61, N. 5, P. 664-671, 2014/09/01 2014. Issn 1608-3407. Disponível Em: < Https://Doi.Org/10.1134/S1021443714050100 >.

Kissoudis, C. Et Al. Responses To Combined Abiotic And Biotic Stress In Tomato Are Governed By Stress Intensity And Resistance Mechanism. **J Exp Bot,** V. 67, N. 17, P. 5119-32, Sep 2016. Issn 0022-0957.

Knogge, W. Fungal Infection Of Plants. **The Plant Cell,** V. 8, N. 10, P. 1711-1722, 1996. Issn 1040-4651

1532-298x. Disponível Em: < Http://Www.Ncbi.Nlm.Nih.Gov/Pmc/Articles/Pmc161309/ >.

Kohorn, B. D. Et Al. Rapid Oligo-Galacturonide Induced Changes In Protein Phosphorylation In Arabidopsis. **Molecular &Amp; Cellular Proteomics,** V. 15, N. 4, P. 1351, 2016. Disponível Em: < Http://Www.Mcponline.Org/Content/15/4/1351.Abstract >.

Koladia, V. M. Et Al. Genetic Analysis Of Net Form Net Blotch Resistance In Barley Lines Ciho 5791 And Tifang Against A Global Collection Of P. Teres F. Teres Isolates. **Theor Appl Genet,** V. 130, N. 1, P. 163-173, Jan 2017. Issn 0040-5752.

Kou, L. T.; Makki, K. An Even Faster Approximation Algorithm For The Steiner Tree Problem In Graphs. **Congressus Numerantium,** V. 59, P. 147-154, 1987.

Landa, P. Et Al. The Transcriptomic Response Of Arabidopsis Thaliana To Zinc Oxide: A Comparison Of The Impact Of Nanoparticle, Bulk, And Ionic Zinc. **Environmental Science & Technology,** V. 49, N. 24, P. 14537-14545, Dec 2015. Issn 0013-936x. Disponível Em: < <Go To Isi>://Wos:000366872300076 >.

_____. Nanoparticle-Specific Changes In Arabidopsis Thaliana Gene Expression After Exposure To Zno, Tio2, And Fullerene Soot. **Journal Of Hazardous Materials,** V. 241, P. 55-62, Nov 30 2012. Issn 0304-3894. Disponível Em: < <Go To Isi>://Wos:000313088300004 >.

Li, H. Et Al. A Novel Wall-Associated Receptor-Like Protein Kinase Gene, Oswak1, Plays Important Roles In Rice Blast Disease Resistance. **Plant Molecular Biology,** V. 69, N. 3, P. 337-346, 2009/02/01 2009. Issn 1573-5028. Disponível Em: < Https://Doi.Org/10.1007/S11103-008-9430-5 >.

Li, J. Et Al. Wrky70 Modulates The Selection Of Signaling Pathways In Plant Defense. **The Plant Journal,** V. 46, N. 3, P. 477-491, 2006/05/01 2006. Issn 0960-7412. Disponível Em: < Https://Doi.Org/10.1111/J.1365-313x.2006.02712.X >. Acesso Em: 2018/06/06.

Li, M. Et Al. A Topology Potential-Based Method For Identifying Essential Proteins From Ppi Networks. **Ieee/Acm Transactions On Computational Biology And Bioinformatics (Tcbb),** V. 12, N. 2, P. 372-383, 2015. Issn 1545-5963.

Li, Y. Et Al. Expression Analysis Of Three Serk-Like Genes In Barley Under Abiotic And Biotic Stresses. **Journal Of Plant Interactions,** V. 12, N. 1, P. 279-285, 2017/01/01 2017. Issn 1742-9145. Disponível Em: < Https://Doi.Org/10.1080/17429145.2017.1339836 >.

Liu, Z. Et Al. Necrotrophic Effector-Triggered Susceptibility (Nets) Underlies The Barley-Pyrenophora Teres F. Teres Interaction Specific To Chromosome 6h. **Molecular Plant Pathology,** V. 16, N. 2, P. 188-200, Feb 2015. Issn 1464-6722. Disponível Em: < <Go To Isi>://Wos:000348741600007 >.

Liu, Z. H. Et Al. Pyrenophora Teres: Profile Of An Increasingly Damaging Barley Pathogen. **Molecular Plant Pathology,** V. 12, N. 1, P. 1-19, Jan 2011. Issn 1464-6722. Disponível Em: < <Go To Isi>://Wos:000284854600001 >.

Ma, J. Et Al. Overexpression Of Tawrky146 Increases Drought Tolerance Through Inducing Stomatal Closure In Arabidopsis Thaliana. **Frontiers In Plant Science,** V. 8, P. 2036, 2017. Issn 1664-462x. Disponível Em: < Https://Www.Frontiersin.Org/Article/10.3389/Fpls.2017.02036 >.

Ma, X. Et Al. Serking Coreceptors For Receptors. **Trends In Plant Science,** V. 21, N. 12, P. 1017-1033, 2016/12/01/ 2016. Issn 1360-1385. Disponível Em: < Http://Www.Sciencedirect.Com/Science/Article/Pii/S136013851630125x >.

Makandar, R. Et Al. Salicylic Acid Regulates Basal Resistance To Fusarium Head Blight In Wheat. **Molecular Plant-Microbe Interactions,** V. 25, N. 3, P. 431-439, 2012. Issn 0894-0282.

Makepeace, J. C. Et Al. A Method Of Inoculating Barley Seedlings With Ramularia Collo-Cygni. **Plant Pathology,** V. 57, N. 6, P. 991-999, 2008. Issn 1365-3059.

Nostar, O. Et Al. Combined Effects Of Salt Stress And Cucurbit Downy Mildew (Pseudoperospora Cubensis Berk. And Curt. Rostov.) Infection On Growth, Physiological Traits And Antioxidant Activity In Cucumber (Cucumis Sativus L.) Seedlings. **Physiological And Molecular Plant Pathology,** V. 83, P. 84-92, 2013/07/01/ 2013. Issn 0885-5765. Disponível Em: < Http://Www.Sciencedirect.Com/Science/Article/Pii/S0885576513000337 >.

Okada, K.; Abe, H.; Arimura, G.-I. Jasmonates Induce Both Defense Responses And Communication In Monocotyledonous And Dicotyledonous Plants. **Plant And Cell Physiology,** V. 56, N. 1, P. 16-27, 2015. Issn 0032-0781. Disponível Em: < Http://Dx.Doi.Org/10.1093/Pcp/Pcu158 >.

Onaga, G.; Wydra, K. Advances In Plant Tolerance To Biotic Stresses. In: Abdurakhmonov, I. Y. (Ed.). **Plant Genomics**. Rijeka: Intech, 2016. P.Ch. 10.

Pagel, P. Et Al. The Mips Mammalian Protein–Protein Interaction Database. **Bioinformatics,** V. 21, N. 6, P. 832-834, 2004. Issn 1460-2059.

Pandey, D. Et Al. Plant Defense Signaling And Responses Against Necrotrophic Fungal Pathogens. **Journal Of Plant Growth Regulation,** V. 35, N. 4, P. 1159-1174, 2016. Issn 0721-7595.

Pandey, P. Et Al. Impact Of Combined Abiotic And Biotic Stresses On Plant Growth And Avenues For Crop Improvement By Exploiting Physio-Morphological Traits. **Frontiers In Plant Science,** V. 8, P. 537, 04/18

11/07/Received

03/27/Accepted 2017. Issn 1664-462x. Disponível Em: < Http://Www.Ncbi.Nlm.Nih.Gov/Pmc/Articles/Pmc5394115/ >.

Parisi, C.; Vigani, M.; Rodriguez-Cerezo, E. Agricultural Nanotechnologies: What Are The Current Possibilities? **Nano Today,** V. 10, N. 2, P. 124-127, Apr 2015. Issn 1748-0132. Disponível Em: < <Go To Isi>://Wos:000356985700005 >.

Pike, S. Et Al. Members Of The Npf3 Transporter Subfamily Encode Pathogen-Inducible Nitrate/Nitrite Transporters In Grapevine And Arabidopsis. **Plant And Cell Physiology,** V. 55, N. 1, P. 162-170, 2014. Issn 0032-0781. Disponível Em: < Http://Dx.Doi.Org/10.1093/Pcp/Pct167 >.

Pirselova, B. Et Al. Biochemical And Physiological Comparison Of Heavy Metal-Triggered Defense Responses In The Monocot Maize And Dicot Soybean Roots. **Molecular Biology Reports,** V. 38, N. 5, P. 3437-3446, Jun 2011. Issn 0301-4851. Disponível Em: < <Go To Isi>://Wos:000290102100075 >.

Pokhrel, L. R.; Dubey, B. Evaluation Of Developmental Responses Of Two Crop Plants Exposed To Silver And Zinc Oxide Nanoparticles. **Science Of The Total Environment,** V. 452, P. 321-332, May 2013. Issn 0048-9697. Disponível Em: < <Go To Isi>://Wos:000318530600035 >.

Prasch, C. M.; Sonnewald, U. Simultaneous Application Of Heat, Drought, And Virus To Arabidopsis Plants Reveals Significant Shifts In Signaling Networks. **Plant Physiol,** V. 162, N. 4, P. 1849-66, Aug 2013. Issn 0032-0889.

Provart, N.; Zhu, T. A Browser-Based Functional Classification Superviewer For Arabidopsis Genomics. **Currents In Computational Molecular Biology,** V. 2003, P. 271-272, 2003.

Raffaele, S.; Rivas, S.; Roby, D. An Essential Role For Salicylic Acid In Atmyb30-Mediated Control Of The Hypersensitive Cell Death Program In Arabidopsis. **Febs Letters,** V. 580, N. 14, P. 3498-3504, 2006/06/12/ 2006. Issn 0014-5793. Disponível Em: < Http://Www.Sciencedirect.Com/Science/Article/Pii/S0014579306006193 >.

Rahman, T. A. E. Et Al. Necrotrophic Pathogens Use The Salicylic Acid Signaling Pathway To Promote Disease Development In Tomato. **Molecular Plant-Microbe Interactions,** V. 25, N. 12, P. 1584-1593, 2012. Issn 0894-0282.

Raliya, R. Et Al. Mechanistic Evaluation Of Translocation And Physiological Impact Of Titanium Dioxide And Zinc Oxide Nanoparticles On The Tomato (Solanum Lycopersicum L.) Plant. **Metallomics,** V. 7, N. 12, P. 1584-1594, 2015. Issn 1756-5901. Disponível Em: < <Go To Isi>://Wos:000365906300005 >.

Ramegowda, V.; Senthil-Kumar, M. The Interactive Effects Of Simultaneous Biotic And Abiotic Stresses On Plants: Mechanistic Understanding From Drought And Pathogen Combination.

Journal Of Plant Physiology, V. 176, P. 47-54, 2015/03/15/ 2015. Issn 0176-1617. Disponível Em: < Http://Www.Sciencedirect.Com/Science/Article/Pii/S0176161714003447 >.

Rossi, L. Et Al. The Impact Of Cerium Oxide Nanoparticles On The Salt Stress Responses Of Brassica Napus L. **Environmental Pollution,** V. 219, P. 28-36, Dec 2016. Issn 0269-7491. Disponível Em: < <Go To Isi>://Wos:000390734100004 >.

Scarpeci, T. E. Et Al. Overexpression Of Atwrky30 Enhances Abiotic Stress Tolerance During Early Growth Stages In Arabidopsis Thaliana. **Plant Molecular Biology,** V. 83, N. 3, P. 265-277, 2013/10/01 2013. Issn 1573-5028. Disponível Em: < Https://Doi.Org/10.1007/S11103-013-0090-8 >.

Servin, A. D.; White, J. C. Nanotechnology In Agriculture: Next Steps For Understanding Engineered Nanoparticle Exposure And Risk. **Nanoimpact,** V. 1, P. 9-12, 2016. Issn 2452-0748. Disponível Em: < Http://Www.Sciencedirect.Com/Science/Article/Pii/S2452074815300185 >.

Shimono, M. Et Al. Rice Wrky45 Plays A Crucial Role In Benzothiadiazole-Inducible Blast Resistance. **The Plant Cell,** V. 19, N. 6, P. 2064-2076, 2007. Issn 1040-4651.

Szklarczyk, D. Et Al. String V10: Protein–Protein Interaction Networks, Integrated Over The Tree Of Life. **Nucleic Acids Research,** V. 43, N. D1, P. D447-D452, 2014. Issn 1362-4962.

Tang, X. Et Al. Predicting Essential Proteins Based On Weighted Degree Centrality. **Ieee/Acm Transactions On Computational Biology And Bioinformatics (Tcbb),** V. 11, N. 2, P. 407-418, 2014. Issn 1545-5963.

Tekauz, A. A Numerical Scale To Classify Reactions Of Barley To Pyrenophora Teres. **Canadian Journal Of Plant Pathology,** V. 7, N. 2, P. 181-183, 1985. Issn 0706-0661.

Thaler, J. S.; Owen, B.; Higgins, V. J. The Role Of The Jasmonate Response In Plant Susceptibility To Diverse Pathogens With A Range Of Lifestyles. **Plant Physiology,** V. 135, N. 1, P. 530-538, 2004. Issn 1532-2548.

Tumburu, L. Et Al. Molecular And Physiological Responses To Titanium Dioxide And Cerium Oxide Nanoparticles In Arabidopsis. **Environmental Toxicology And Chemistry,** V. 36, N. 1, P. 71-82, Jan 2017. Issn 0730-7268. Disponível Em: < <Go To Isi>://Wos:000391029800011 >.

Typas, A.; Sourjik, V. Bacterial Protein Networks: Properties And Functions. **Nature Reviews Microbiology,** V. 13, N. 9, P. 559, 2015. Issn 1740-1534.

Van Der Does, D. Et Al. Salicylic Acid Suppresses Jasmonic Acid Signaling Downstream Of Scfcoi1-Jaz By Targeting Gcc Promoter Motifs Via Transcription Factor Ora59. **The Plant Cell,** V. 25, N. 2, P. 744-761, 2013. Issn 1532-298x.

Van Verk, M. C.; Bol, J. F.; Linthorst, H. J. M. Wrky Transcription Factors Involved In Activation Of Sa Biosynthesis Genes. **Bmc Plant Biology,** V. 11, N. 1, P. 89, 2011/05/19 2011. Issn 1471-2229. Disponível Em: < Https://Doi.Org/10.1186/1471-2229-11-89 >.

Vankova, R. Et Al. Zno Nanoparticle Effects On Hormonal Pools In Arabidopsis Thaliana. **Sci Total Environ,** V. 593-594, P. 535-542, Sep 1 2017. Issn 0048-9697.

Vogiatzis, C.; Camur, M. C. Identification Of Essential Proteins Using Induced Stars In Protein-Protein Interaction Networks. **Arxiv Preprint Arxiv:1708.00574**, 2017.

Wang, J. Et Al. Identification Of Essential Proteins Based On Edge Clustering Coefficient. **Ieee/Acm Transactions On Computational Biology And Bioinformatics (Tcbb),** V. 9, N. 4, P. 1070-1080, 2012. Issn 1545-5963.

Wang, Z. Y. Et Al. Cuo Nanoparticle Interaction With Arabidopsis Thaliana: Toxicity, Parent-Progeny Transfer, And Gene Expression. **Environmental Science & Technology,** V. 50, N. 11, P. 6008-6016, Jun 2016. Issn 0013-936x. Disponível Em: < <Go To Isi>://Wos:000377629900070 >.

Wiese, J.; Kranz, T.; Schubert, S. Induction Of Pathogen Resistance In Barley By Abiotic Stress. **Plant Biology,** V. 6, N. 5, P. 529-536, 2004. Issn 1435-8603.

Wittek, F. Et Al. Folic Acid Induces Salicylic Acid-Dependent Immunity In Arabidopsis And Enhances Susceptibility To Alternaria Brassicicola. **Molecular Plant Pathology,** V. 16, N. 6, P. 616-622, 2015/08/01 2015. Issn 1464-6722. Disponível Em: < Https://Doi.Org/10.1111/Mpp.12216 >. Acesso Em: 2019/01/09.

Xenarios, I. Et Al. Dip, The Database Of Interacting Proteins: A Research Tool For Studying Cellular Networks Of Protein Interactions. **Nucleic Acids Research,** V. 30, N. 1, P. 303-305, 2002. Issn 1362-4962.

Xia, Y. Et Al. Oswak11, A Rice Wall-Associated Kinase, Regulates Cu Detoxification By Alteration The Immobilization Of Cu In Cell Walls. **Environmental And Experimental Botany,** V. 150, P. 99-105, 2018/06/01/ 2018. Issn 0098-8472. Disponível Em: < Http://Www.Sciencedirect.Com/Science/Article/Pii/S0098847218303435 >.

Yang, L. Et Al. Salicylic Acid Biosynthesis Is Enhanced And Contributes To Increased Biotrophic Pathogen Resistance In Arabidopsis Hybrids. **Nature Communications,** V. 6, P. 7309, 2015. Issn 2041-1723.

Yoon, S.-J. Et Al. Zinc Oxide Nanoparticles Delay Soybean Development: A Standard Soil Microcosm Study. **Ecotoxicology And Environmental Safety,** V. 100, P. 131-137, Feb 2014. Issn 0147-6513. Disponível Em: < <Go To Isi>://Wos:000330161000018 >.

Zengin, F. Exogenous Treatment With Salicylic Acid Alleviating Copper Toxicity In Bean Seedlings. **Proceedings Of The National Academy Of Sciences, India Section B: Biological Sciences,** V. 84, N. 3, P. 749-755, 2014. Issn 0369-8211.

Zhang, J. Et Al. Expression Of Pathogenesis Related Genes In Response To Salicylic Acid, Methyl Jasmonate And 1-Aminocyclopropane-1-Carboxylic Acid In Malus Hupehensis (Pamp.) Rehd. **Bmc Research Notes,** V. 3, P. 208-208, 2010. Issn 1756-0500. Disponível Em: < Https://Www.Ncbi.Nlm.Nih.Gov/Pubmed/20659347 >.Disponível Em: < Https://Www.Ncbi.Nlm.Nih.Gov/Pmc/Pmc3161363/ >.

CHAPTER 6

6.1. Conclusion

In this research, the interactions of ZnO NPs with plants were studied. The phenotypical effects of ZnO NPs and the bioaccumulation of zinc was studied in soybean plants (*Glycine max*). $ZnSO_4$ was used as the ion control. Three different dosages (0, 5, 50, and 500 mg of zinc kg^{-1} soil) of ZnO NP and $ZnSO_4$ were applied as treatments in the soil. No significant difference in plant growth parameters were found in all the treatments, indicating that ZnO NPs do not negatively affect the plants. ICP-OES analysis revealed bioaccumulation of zinc in the seeds, and other soybean products like soy concentrate and pulp of the ZnO NP exposed-plants. Zinc concentrations in the seeds increased with increasing dosage of ZnO NPs in the soil. There was no significant difference between the three forms of zinc in terms of bioaccumulation in seeds.

The second phase of this study was to understand the uptake of ZnO NPs and their speciation in plants. The detection of engineered nanomaterial (ENM) in plants is crucial for understanding the outcomes of plant-ENM interactions that occur both extracellularly (at the cell periphery) and intracellularly. Because different types of ENMs have different properties, each requires an individual approach for its detection in plants. In this study, the form of zinc oxide nanoparticles (ZnO NPs) was studied in spinach (*Spinacia oleracea*) roots using confocal laser scanning microscopy (CLSM) and transmission electron microscopy (TEM). It was found that ZnO NPs are taken up both as Zn^{2+} ions and in nanoparticle form by spinach roots grown in hydroponics. Ionic Zn^{2+} was detected using fluorescent Zn^{2+} sensor, Zinpyr-1 in CLSM, and validated with a Zn^{2+} chelator TPEN (N,N,N',N'-tetrakis(2-pyridylmethyl)ethane-1,2-diamine). Nano-sized zinc particles in the roots were detected using TEM with EDS. The particles were found to be localized inside the vacuoles and are hypothesized to be like zinc phytate.

The third part of the research focused on the physiological responses of plants to ZnO NPs in the environment. The model monocot, barley (*Hordeum vulgare*) was used as the experimental plant, and ZnO NPs were applied in the soil in environmentally relevant concentrations (~43 mg kg^{-1}). The transcriptome of barley following ZnO NP exposure was elucidated using a Next Generation sequencing (NGS) platform, RNA seq. In this study, $ZnSO_4$ was used as the Zn^{2+} ion control. A time-analysis course analysis revealed the differentially expressed genes (DEGs) in response to ZnO NPs and $ZnSO_4$. Comparisons between both the treatments revealed nearly identical DEG profiles at 6 hpa, however responses ebbed to basal levels at 48 hpa in ZnO NPs treatments. From GO term enrichment, stress response genes were found to be induced in $ZnSO_4$ treatments rather than ZnO NP treatments. However, genes for photosynthesis and other cellular processes like signal transduction, and electron transport were downregulated in both ZnO NP, and $ZnSO_4$ treatments at an early time-point (6 hpa). It was concluded that ZnO NPs do not elicit responses in plants typical of stress at environmentally relevant concentrations.

The final section of this dissertation investigated the effects of ZnO NPs on plants and on host-pathogen interactions, simulating actual environmental conditions. The study consisted of three treatments, ZnO NP application, inoculation with the necrotrophic pathogen, *Pyrenophora teres* f. *teres* (*Ptt*), and a combined application where both ZnO NPs and the pathogen were applied. The study was conducted with the barley line CI5791, which is resistant to the disease Net Form Net Blotch caused by *Ptt*. Time-course transcriptomic analyses identified DEGs in response to the treatments showing rapid responses to ZnO NPs (6 hpa) that quickly returned to basal levels (24 hpa). However, treatment with the pathogen alone and pathogen + ZnO NP, showed DEG profiles that persisted to 48 hpi. The number of DEGs in the combined application was the highest across all time-points compared to the pathogen and ZnO NPs alone. 7-day disease

evaluations for pathogen and combined application plants revealed a higher disease reaction score for the combined application plants, indicating susceptibility to NFNB in the otherwise resistant barley line CI5791. This compromised resistance to the necrotrophic pathogen was traced to salicylic acid (SA) signaling pathways that persisted at 48 hpi in the combined application plants. The antagonistic interactions between salicylic acid and jasmonic acid (JA) modulated the downregulation of JA-related genes at 48 hpi, leading to the suppression of JA-mediated necrotrophic pathogen resistance responses, thereby resulting in compromised immunity.

In conclusion, this research investigated plant uptake of ZnO NPs, and provided insight on the physiological responses of plants exposed to ZnO NPs, and their effects on host-pathogen interactions.

6.2. Future Directions

The research sheds light on the molecular-level effects of ZnO NPs on plants. The focus of this pioneering research was to determine the molecular events that led to compromised immunity in the plants when exposed to ZnO NPs + pathogen. The findings of this research are based on gene enrichment analysis. The future goal is to functionally validate the described gene model using virus induced gene silencing (VIGS). Comparable studies using a second pathosystems like the necrotrophic pathogen *Botrytis cinerea* and its host plant *Arabidopsis thaliana* can also be conducted that would provide a second level of verification of the current findings.

In this research, RNA seq analyses yielded the complete transcriptome of the plants that could be used to study other cellular pathways and molecular cross-talk in response to NP exposure. Studies using a similar approach can be conducted on other NPs and plants, that would provide valuable information on plant behaviors towards NPs. Such research will help us to

understand plant-NP interactions in a more holistic way, that is relevant in actual environmental conditions.

APPENDIX A

Table A1. Mineral content (in mg/kg) in the seeds of soybean plant exposed to different treatments as determined by ICP-OES

Treatment	Ca	Fe	K	Mg	Mn	Mo	P	Si
ZnO NP X	81.87±145.9	12.97±12.9	1272.58±1190.0	37.925±71.4	8.95±9.5	4.63±5.2	408.24±269.5	3.65±3.8
ZnO NP 10X	293.00±204.8	9.66±9.3	1261.17±1040.6	54.53±75.7	7.26±14.3	13.40±8.2	465.92±235.5	12.49±23.3
ZnO NP 100X	228.34±267.2	14.15±5.9	1429.26±314.1	149.06±82.0	1.50±1.7	7.52±6.5	285.97±203.5	9.07±4.0
$ZnSO_4$ X	300.30±269.4	8.41±9.5	1081.97±1297.2	62.72±69.9	11.89±15.6	18.20±15.3	314.15±485.5	2.92±5.2
$ZnSO_4$ 10X	287.14±274.2	10.40±10.1	1190.82±1394.1	109.17±132.6	3.91±2.7	12.25±8.9	755.40±661.8	2.52±2.8
$ZnSO_4$ 100X	112.26±193.8	5.77±9.0	1798.25±1499.9	23.49±42.5	4.04±5.1	6.64±6.5	241.54±259.1	4.23±5.4
Control	139.37±278.1	10.67±16.9	3249.49±5247.4	293.03±581.6	2.05±1.5	11.39±13.4	632.77±724.0	4.22±6.4

Table A2. Zinc content (mg/kg) in the soil of different treatments as determined by ICP-OES

Treatment	Zn content (mg/kg)
ZnO NP X	34.85±3.0
ZnO NP 10X	72.82±71.7
ZnO NP 100X	276.47±344.7
$ZnSO_4$ X	42.29±14.7
$ZnSO_4$ 10X	131.96±83.5
$ZnSO_4$ 100X	321.70±384.3
Control	29.51±2.1

APPENDIX B

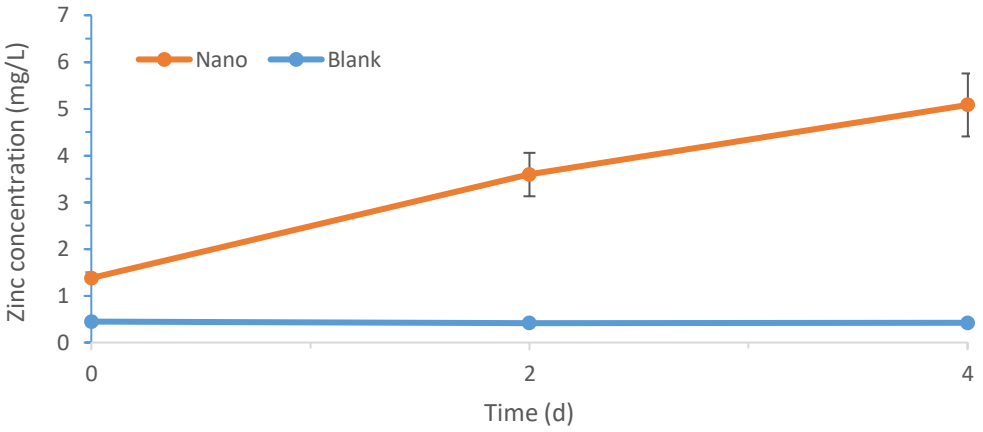

Figure B1. Dissolution of ZnO NP in DI water (40.69 mg of ZnO NPs L^{-1} added initially to water). The time reflects the day on which samples were collected. The experiment was conducted in triplicate.

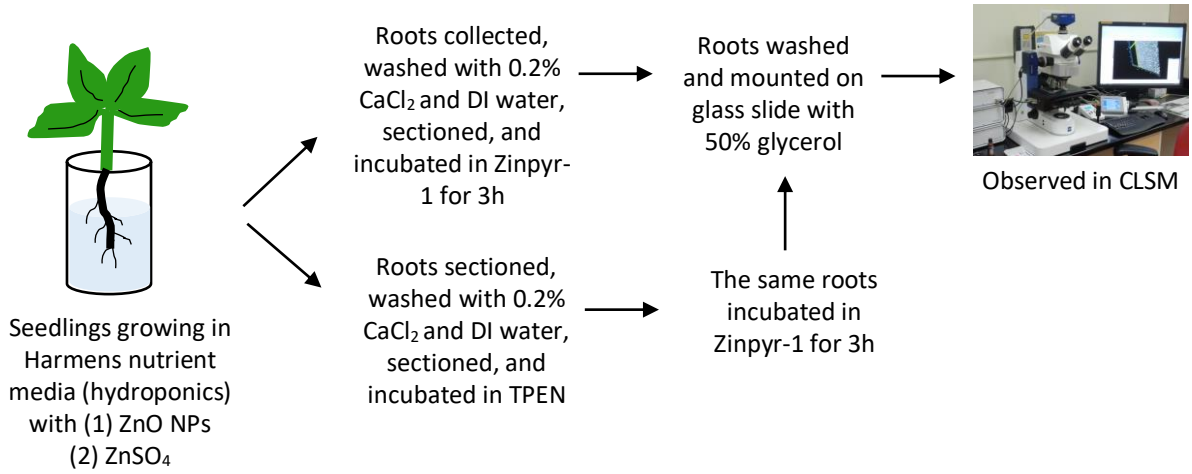

Figure B2. Schematic of the experimental design used for Zn^{2+} sensor Zinpyr-1 study

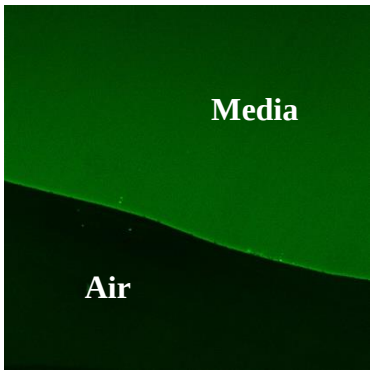

Figure B3. ZnO NP in hydroponic media (Harmen solution) stained with Zn^{2+} sensor Zinpyr-1 in a glass slide covered by a cover-slip. The fluorescence (green color) observed is due to the dissolution of the ZnO NPs to Zn^{2+} ions in the aqueous media.

Table B1. A list of detection techniques for ENMs (other than ZnO NPs) in plant matrix

NP	Plant	Method of detection			
		Light Microscopy	Electron Microscopy	Other Techniques (Spectroscopy-based, Synchrotron-based, Others)	Observation
CeO_2	*Zea mays* (Corn)			µ-XRF	Indirect
CeO_2	*Glycine max* (Soybean)			µXRF, µXANES	Indirect
CeO_2	*Cucumis sativus* (Cucumber)			µXRF, ICP-OES, ICP-MS	Indirect
CuO	*Fagopyrum esculentum* (Buckwheat)		TEM		Direct
CeO_2	*Zea mays* (Corn)	FITC, Confocal Microscopy		µXRF, µXANES	Direct
TiO_2	*Nicotiana tabacum* (Tobacco)			AFM	
TiO_2	*Phaseolus vulgaris* (Bean), *Triticum aestivum* (Wheat), *Elodea canadensis* Mich. X (Canadian waterweed), *Rumex crispus* L. (Curly dock)			ICP-OES	Indirect
Si	*Arabidopsis thaliana*		TEM		Direct
Fe	*Cucurbita pepo* (Pumpkin)	Differential contrast interference (DIC), bright field, dark field, autofluorescence	TEM	Magnetic field	Direct

Table B1. A list of detection techniques for ENMs (other than ZnO NPs) in plant matrix (Continued)

NP	Plant	Method of detection (Continued)			
		Light Microscopy	Electron Microscopy	Other Techniques (Spectroscopy-based, Synchrotron-based, Others)	Observation
Carbon-coated Fe	*Cucurbita pepo* (Pumpkin)	Phase contrast, bright field, dark field microscopy	TEM		Direct
Fe_3O_4	*Cucurbita pepo* (Pumpkin)			Vibrating Sample Magnetometer	Indirect
Anatase-TiO_2	*Arabidopsis thaliana*	Bright field, fluorescence microscopy			Direct
TiO_2	*Triticum* (Wheat), *Brassica napus* (rapeseed)			µ-XRF	Indirect
Fe	*Arabidopsis thaliana*		TEM		Direct
Ag, Ag_2S	Alfalfa (*Medicago sativa*)		TEM	XRF	Direct
Ag	*Phaseolus radiates* (Mung bean), *Sorghum Bicolor* (Millet)		TEM		Direct
O-SWCNT	BY-2 *Nicotiana tabacum* (Tobacco) suspension cells	FITC tagging, confocal microscopy			Direct
Fullerene C_{70}	*Oryza sativa* (Rice)	Bright field microscopy	TEM		Direct

Table B1. A list of detection techniques for ENMs (other than ZnO NPs) in plant matrix (Continued)

NP	Plant	Method of detection (Continued)			
		Light Microscopy	**Electron Microscopy**	**Other Techniques (Spectroscopy-based, Synchrotron-based, Others)**	**Observation**
MWCNT	*Basella alba* (Red Spinach)		TEM, SEM		Direct
MWCNT	*Nicotiana tabacum* (Tobacco)		TEM	Raman Spectroscopy	Direct

Table B2. Harmens hydroponic media composition

Element	Desired Concentration L^{-1}
KNO_3	0.015 mmol
$NH_4H_2PO_4$	0.005 mmol
$MgSO_4.7H_2O$	0.0025 mmol
KCl	0.05 µmol
H_3BO_3	0.025 µmol
$MnSO_4.5H_2O$	0.002 µmol
$CuSO_4.5H_2O$	0.0001 µmol
$(NH_4)6Mo_7O_{24}.4H_2O$	0.0005 µmol
Fe(Na)EDTA	0.02 µmol
$Ca(NO_3)_2$	0.01 mmol
Experimental treatments	
A. $ZnSO_4.7H_2O$	7.87 mmol
B. ZnO NPs	7.62 mmol

B1. References

Abbasi, Nazia, Youn-Il Park, and Sang-Bong Choi. "Pumilio Puf Domain Rna-Binding Proteins in Arabidopsis." *Plant signaling & behavior* 6, no. 3 (2011): 364-68.

Abdal Dayem, A., M. K. Hossain, S. B. Lee, K. Kim, S. K. Saha, G. M. Yang, H. Y. Choi, and S. G. Cho. "The Role of Reactive Oxygen Species (Ros) in the Biological Activities of Metallic Nanoparticles." [In eng]. *Int J Mol Sci* 18, no. 1 (Jan 10 2017).

Achuo, E. A., E. Prinsen, and Monica Höfte. "Influence of Drought, Salt Stress and Abscisic Acid on the Resistance of Tomato to Botrytis Cinerea and Oidium Neolycopersici." *Plant pathology* 55, no. 2 (2006): 178-86.

Adam, Nathalie, Claudia Schmitt, Josep Galceran, Encarna Companys, Alexander Vakurov, Rachel Wallace, Dries Knapen, and Ronny Blust. "The Chronic Toxicity of Zno Nanoparticles and Zncl2 to Daphnia Magna and the Use of Different Methods to Assess Nanoparticle Aggregation and Dissolution." *Nanotoxicology* 8, no. 7 (2014/11/01 2014): 709-17.

Albanese, A., and W. C. W. Chan. "Effect of Gold Nanoparticle Aggregation on Cell Uptake and Toxicity." *Acs Nano* 5, no. 7 (Jul 2011): 5478-89.

Alexa, Adrian, and Jorg Rahnenfuhrer. "Topgo: Enrichment Analysis for Gene Ontology." *R package version* 2, no. 0 (2010).

Alexa, Adrian, Jörg Rahnenführer, and Thomas Lengauer. "Improved Scoring of Functional Groups from Gene Expression Data by Decorrelating Go Graph Structure." *Bioinformatics* 22, no. 13 (2006): 1600-07.

"Alibabagroup.Com." 2018.

Alloway, B. J. "Soil Factors Associated with Zinc Deficiency in Crops and Humans." [In eng]. *Environ Geochem Health* 31, no. 5 (Oct 2009): 537-48.

Almutairi, Zainab Majed. "Expression Profiling of Certain Mads-Box Genes in Arabidopsis Thaliana Plant Treated with Silver Nanoparticles." *CZECH JOURNAL OF GENETICS AND PLANT BREEDING* 53, no. 1 (2017): 30-36.

Angelé-Martínez, Carlos, Khanh Van T. Nguyen, Fathima S. Ameer, Jeffrey N. Anker, and Julia L. Brumaghim. "Reactive Oxygen Species Generation by Copper(Ii) Oxide Nanoparticles Determined by Dna Damage Assays and Epr Spectroscopy." *Nanotoxicology* 11, no. 2 (2017/02/07 2017): 278-88.

Asano, T., A. Miwa, K. Maeda, M. Kimura, and T. Nishiuchi. "The Secreted Antifungal Protein Thionin 2.4 in Arabidopsis Thaliana Suppresses the Toxicity of a Fungal Fruit Body Lectin from Fusarium Graminearum." *Plos Pathogens* 9, no. 8 (Aug 2013).

Baker, Syed, Tatiana Volova, Svetlana V. Prudnikova, S. Satish, and Nagendra Prasad M.N. "Nanoagroparticles Emerging Trends and Future Prospect in Modern Agriculture System." *Environmental Toxicology and Pharmacology* 53, no. Supplement C (2017/07/01/ 2017): 10-17.

Balážová, Ľudmila, Petr Babula, Matej Baláž, Miriam Bačkorová, Zdenka Bujňáková, Jaroslav Briančin, Assylay Kurmanbayeva, and Moshe Sagi. "Zinc Oxide Nanoparticles Phytotoxicity on

Halophyte from Genus Salicornia." *Plant Physiology and Biochemistry* 130 (2018/09/01/ 2018): 30-42.

Bandyopadhyay, S., G. Plascencia-Villa, A. Mukherjee, C. M. Rico, M. Jose-Yacaman, J. R. Peralta-Videa, and J. L. Gardea-Torresdey. "Comparative Phytotoxicity of Zno Nps, Bulk Zno, and Ionic Zinc onto the Alfalfa Plants Symbiotically Associated with Sinorhizobium Meliloti in Soil." *Science of the Total Environment* 515 (May 2015): 60-69.

Begum, Parvin, and Bunshi Fugetsu. "Phytotoxicity of Multi-Walled Carbon Nanotubes on Red Spinach (Amaranthus Tricolor L) and the Role of Ascorbic Acid as an Antioxidant." *Journal of Hazardous Materials* 243 (Dec 2012): 212-22.

Belkadhi, Aïcha, Antonio De Haro, Sara Obregon, Wided Chaïbi, and Wahbi Djebali. "Positive Effects of Salicylic Acid Pretreatment on the Composition of Flax Plastidial Membrane Lipids under Cadmium Stress." *Environmental Science and Pollution Research* 22, no. 2 (2015): 1457-67.

Bertini, Laura, Luca Leonardi, Carlo Caporale, Marina Tucci, Nunzia Cascone, Iris Di Berardino, Vincenzo Buonocore, and Carla Caruso. "Pathogen-Responsive Wheat Pr4 Genes Are Induced by Activators of Systemic Acquired Resistance and Wounding." *Plant Science* 164, no. 6 (2003/06/01/ 2003): 1067-78.

Bethenod, O., L. Huber, and H. Slimi. "Photosynthetic Response of Wheat to Stress Induced by Puccinia Recondita and Post-Infection Drought." *Photosynthetica* 39, no. 4 (2001): 581-90.

Bezbaruah, A. N., and T. C. Zhang. "Performance of a Constructed Wetland with a Sulfur/Limestone Denitrification Section for Wastewater Nitrogen Removal." *Environmental Science & Technology* 37, no. 8 (Apr 2003): 1690-97.

Bhowmick, Sourav S., and Boon Siew Seah. "Clustering and Summarizing Protein-Protein Interaction Networks: A Survey." *IEEE Transactions on Knowledge and Data Engineering* 28, no. 3 (2016): 638-58.

Bilgin, Damla D., Jorge A. Zavala, J. I. N. Zhu, Steven J. Clough, Donald R. Ort, and Evan H. DeLucia. "Biotic Stress Globally Downregulates Photosynthesis Genes." *Plant, Cell & Environment* 33, no. 10 (2010/10/01 2010): 1597-613.

Boland, G. J., M. S. Melzer, A. Hopkin, V. Higgins, and A. Nassuth. "Climate Change and Plant Diseases in Ontario." *Canadian Journal of Plant Pathology* 26, no. 3 (2004): 335-50.

Boonyanitipong, Prapatsorn, Boonthida Kositsup, Prabhat Kumar, Sunandan Baruah, and Joydeep Dutta. "Toxicity of Zno and Tio2 Nanoparticles on Germinating Rice Seed Oryza Sativa L." *International Journal of Bioscience, Biochemistry and Bioinformatics* 1, no. 4 (2011): 282.

Borrill, Philippa, James M. Connorton, Janneke Balk, Anthony J. Miller, Dale Sanders, and Cristobal Uauy. "Biofortification of Wheat Grain with Iron and Zinc: Integrating Novel Genomic Resources and Knowledge from Model Crops." *Frontiers in Plant Science* 5 (Feb 21 2014).

Broadley, Martin R., Philip J. White, John P. Hammond, Ivan Zelko, and Alexander Lux. "Zinc in Plants." *New Phytologist* 173, no. 4 (2007): 677-702.

Brodersen, Peter, Frederikke Gro Malinovsky, Kian Hématy, Mari-Anne Newman, and John Mundy. "The Role of Salicylic Acid in the Induction of Cell Death in Arabidopsis Acd11." *Plant Physiology* 138, no. 2 (2005): 1037-45.

Burman, U., M. Saini, and Kumar Praveen. "Effect of Zinc Oxide Nanoparticles on Growth and Antioxidant System of Chickpea Seedlings." *Toxicological and Environmental Chemistry* 95, no. 4 (Apr 2013): 605-12.

Caillaud, Marie-Cécile, Shuta Asai, Ghanasyam Rallapalli, Sophie Piquerez, Georgina Fabro, and Jonathan D. G. Jones. "A Downy Mildew Effector Attenuates Salicylic Acid–Triggered Immunity in Arabidopsis by Interacting with the Host Mediator Complex." *PLoS biology* 11, no. 12 (2013): e1001732.

Carter, Kyle P., Alexandra M. Young, and Amy E. Palmer. "Fluorescent Sensors for Measuring Metal Ions in Living Systems." *Chemical Reviews* 114, no. 8 (Apr 23 2014): 4564-601.

Chaudhary, Asha, Naresh Kumar, Ravinder Kumar, and Raj Kumar Salar. "Antimicrobial Activity of Zinc Oxide Nanoparticles Synthesized from Aloe Vera Peel Extract." *SN Applied Sciences* 1, no. 1 (2018/12/31 2018): 136.

Chen, Jing, Runzhi Dou, Zhongzhou Yang, Tingting You, Xiang Gao, and Li Wang. "Phytotoxicity and Bioaccumulation of Zinc Oxide Nanoparticles in Rice (Oryza Sativa L.)." *Plant Physiology and Biochemistry* 130 (2018/09/01/ 2018): 604-12.

Chen, Lingyun, Shengnan Yang, Ying Liu, Min Mo, Xin Guan, Liu Huang, Chao Sun, Sheng-Tao Yang, and Xue-Ling Chang. "Toxicity of Graphene Oxide to Naked Oats (Avena Sativa L.) in Hydroponic and Soil Cultures." *RSC Advances* 8, no. 28 (2018): 15336-43.

Chen, Xiaolin, John O'Halloran, and Marcel A. K. Jansen. "Time Matters: The Toxicity of Zinc Oxide Nanoparticles to Lemna Minor L. Increases with Exposure Time." *Water, Air, & Soil Pollution* 229, no. 3 (2018/03/05 2018): 99.

Cvjetko, P., A. Milosic, A. M. Domijan, I. V. Vrcek, S. Tolic, P. P. Stefanic, I. Letofsky-Papst, M. Tkalec, and B. Balen. "Toxicity of Silver Ions and Differently Coated Silver Nanoparticles in Allium Cepa Roots." *Ecotoxicology and Environmental Safety* 137 (Mar 2017): 18-28.

Dai, Yanhui, Zhenyu Wang, Jian Zhao, Lili Xu, Lina Xu, Xiaoyu Yu, Yongpeng Wei, and Baoshan Xing. "Interaction of Cuo Nanoparticles with Plant Cells: Internalization, Oxidative Stress, Electron Transport Chain Disruption, and Toxicogenomic Responses." *Environmental Science: Nano* 5, no. 10 (2018): 2269-81.

Davila Olivas Nelson, H., Silvia Coolen, Pingping Huang, Edouard Severing, C. Verk Marcel, Richard Hickman, H. J. Wittenberg Alexander, *et al.* "Effect of Prior Drought and Pathogen Stress on Arabidopsis Transcriptome Changes to Caterpillar Herbivory." *New Phytologist* 210, no. 4 (2016/06/01 2016): 1344-56.

de Andrade, L. R., A. S. Brito, Amgd Melero, H. Zanin, H. J. Ceragioli, V. Baranauskas, K. S. Cunha, and S. P. Irazusta. "Absence of Mutagenic and Recombinagenic Activity of Multi-Walled Carbon Nanotubes in the Drosophila Wing-Spot Test and Allium Cepa Test." *Ecotoxicology and Environmental Safety* 99 (Jan 2014): 92-97.

Dey, Sanjukta, and A. Corina Vlot. "Ethylene Responsive Factors in the Orchestration of Stress Responses in Monocotyledonous Plants." *Frontiers in Plant Science* 6 (2015): 640.

Dhanemozhi, A. Clara, V. Rajeswari, and S. Sathyajothi. "Green Synthesis of Zinc Oxide Nanoparticle Using Green Tea Leaf Extract for Supercapacitor Application." *Materials Today: Proceedings* 4, no. 2, Part A (2017/01/01/ 2017): 660-67.

DiDonato, R. J., Jr., L. A. Roberts, T. Sanderson, R. B. Eisley, and E. L. Walker. "Arabidopsis Yellow Stripe-Like2 (Ysl2): A Metal-Regulated Gene Encoding a Plasma Membrane Transporter of Nicotianamine-Metal Complexes." [In eng]. *Plant J* 39, no. 3 (Aug 2004): 403-14.

Dimkpa, Christian O., Joan E. McLean, Drew E. Latta, Eliana Manangon, David W. Britt, William P. Johnson, Maxim I. Boyanov, and Anne J. Anderson. "Cuo and Zno Nanoparticles: Phytotoxicity, Metal Speciation, and Induction of Oxidative Stress in Sand-Grown Wheat." *Journal of Nanoparticle Research* 14, no. 9 (Sep 2012).

Ding Zhong, Jie, Ying Yan Jing, Xiao Li Chun, Xin Li Gui, Rong Wu Yun, and Jian Zheng Shao. "Transcription Factor Wrky46 Modulates the Development of Arabidopsis Lateral Roots in Osmotic/Salt Stress Conditions Via Regulation of Aba Signaling and Auxin Homeostasis." *The Plant Journal* 84, no. 1 (2015/10/01 2015): 56-69.

Dogaroglu, Z. G., and N. Koleli. "Tio2 and Zno Nanoparticles Toxicity in Barley (Hordeum Vulgare L.)." *Clean-Soil Air Water* 45, no. 11 (Nov 2017).

Du, Wenchao, Wenjuan Tan, Ying Yin, Rong Ji, Jose R. Peralta-Videa, Hongyan Guo, and Jorge L. Gardea-Torresdey. "Differential Effects of Copper Nanoparticles/Microparticles in Agronomic and Physiological Parameters of Oregano (Origanum Vulgare)." *Science of The Total Environment* 618 (2018/03/15/ 2018): 306-12.

Duhan, J. S., R. Kumar, N. Kumar, P. Kaur, K. Nehra, and S. Duhan. "Nanotechnology: The New Perspective in Precision Agriculture." [In eng]. *Biotechnol Rep (Amst)* 15 (Sep 2017): 11-23.

Egerton, R. F. "Electron Energy-Loss Spectroscopy in the Tem." *Reports on Progress in Physics* 72, no. 1 (Jan 2009).

El Oirdi, Mohamed, Taha Abd El Rahman, Luciano Rigano, Abdelbasset El Hadrami, María Cecilia Rodriguez, Fouad Daayf, Adrian Vojnov, and Kamal Bouarab. "Botrytis Cinerea Manipulates the Antagonistic Effects between Immune Pathways to Promote Disease Development in Tomato." *The Plant Cell* 23, no. 6 (2011): 2405-21.

Flor, Harold H. "Current Status of the Gene-for-Gene Concept." *Annual review of phytopathology* 9, no. 1 (1971): 275-96.

Franceschini, Andrea, Damian Szklarczyk, Sune Frankild, Michael Kuhn, Milan Simonovic, Alexander Roth, Jianyi Lin, *et al.* "String V9. 1: Protein-Protein Interaction Networks, with Increased Coverage and Integration." *Nucleic acids research* 41, no. D1 (2012): D808-D15.

Friesen, T. L., J. D. Faris, Z. Lai, and B. J. Steffenson. "Identification and Chromosomal Location of Major Genes for Resistance to Pyrenophora Teres in a Doubled-Haploid Barley Population." *Genome* 49, no. 7 (Jul 2006): 855-59.

Friesen, Timothy L., Justin D. Faris, Peter S. Solomon, and Richard P. Oliver. "Host-Specific Toxins: Effectors of Necrotrophic Pathogenicity." *Cellular microbiology* 10, no. 7 (2008): 1421-28.

Gao, Caiji, Qiong Zhao, and Liwen Jiang. "Vacuoles Protect Plants from High Magnesium Stress." *Proceedings of the National Academy of Sciences of the United States of America* 112, no. 10 (02/26 2015): 2931-32.

Ghosh, M., A. Jana, S. Sinha, M. Jothiramajayam, A. Nag, A. Chakraborty, and A. Mukherjee. "Effects of Zno Nanoparticles in Plants: Cytotoxicity, Genotoxicity, Deregulation of Antioxidant

Defenses, and Cell-Cycle Arrest." *Mutation Research-Genetic Toxicology and Environmental Mutagenesis* 807 (Sep 2016): 25-32.

Girilal, M., A. Mohammed Fayaz, L. K. Elumalai, A. Sathiyaseelan, J. Gandhiappan, and P. T. Kalaichelvan. "Comparative Stress Physiology Analysis of Biologically and Chemically Synthesized Silver Nanoparticles on Solanum Lycopersicum L." *Colloid and Interface Science Communications* 24 (2018/05/01/ 2018): 1-6.

Glazebrook, Jane. "Contrasting Mechanisms of Defense against Biotrophic and Necrotrophic Pathogens." *Annu. Rev. Phytopathol.* 43 (2005): 205-27.

Goldsmith, Christian R., and Stephen J. Lippard. "Analogues of Zinpyr-1 Provide Insight into the Mechanism of Zinc Sensing." *Inorganic Chemistry* 45, no. 16 (Aug 7 2006): 6474-78.

Goyal, Ravinder K., Tahira Fatima, Muhamet Topuz, Anne Bernadec, Richard Sicher, Avtar K. Handa, and Autar K. Mattoo. "Pathogenesis-Related Protein 1b1 (Pr1b1) Is a Major Tomato Fruit Protein Responsive to Chilling Temperature and Upregulated in High Polyamine Transgenic Genotypes." *Frontiers in Plant Science* 7 (2016): 901.

Gregory, Peter J., Ammar Wahbi, Joseph Adu-Gyamfi, Maria Heiling, Roman Gruber, Edward J. M. Joy, and Martin R. Broadley. "Approaches to Reduce Zinc and Iron Deficits in Food Systems." *Global Food Security* 15 (2017/12/01/ 2017): 1-10.

Guo, Dan, Guoxin Xie, and Jianbin Luo. "Mechanical Properties of Nanoparticles: Basics and Applications." *Journal of Physics D: Applied Physics* 47, no. 1 (2013): 013001.

Gupta, U. C., and S. C. Gupta. "Sources and Deficiency Diseases of Mineral Nutrients in Human Health and Nutrition: A Review." *Pedosphere* 24, no. 1 (2014/02/01/ 2014): 13-38.

Hackenberg, Stephan, Agmal Scherzed, Angela Zapp, Katrin Radeloff, Christian Ginzkey, Thomas Gehrke, Pascal Ickrath, and Norbert Kleinsasser. "Genotoxic Effects of Zinc Oxide Nanoparticles in Nasal Mucosa Cells Are Antagonized by Titanium Dioxide Nanoparticles." *Mutation Research/Genetic Toxicology and Environmental Mutagenesis* 816-817 (2017/04/01/ 2017): 32-37.

Hagberg, Aric, Pieter Swart, and Daniel S Chult. "Exploring Network Structure, Dynamics, and Function Using Networkx." Los Alamos National Lab.(LANL), Los Alamos, NM (United States), 2008.

Hall, J. L. "Cellular Mechanisms for Heavy Metal Detoxification and Tolerance." [In eng]. *J Exp Bot* 53, no. 366 (Jan 2002): 1-11.

Hammond-Kosack, K. E., and J. J. Rudd. "Plant Resistance Signalling Hijacked by a Necrotrophic Fungal Pathogen." [In eng]. *Plant Signal Behav* 3, no. 11 (Nov 2008): 993-5.

Harris, Andrew T., and Roza Bali. "On the Formation and Extent of Uptake of Silver Nanoparticles by Live Plants." *Journal of Nanoparticle Research* 10, no. 4 (Apr 2008): 691-95.

Hernandez-Viezcas, J. A., H. Castillo-Michel, A. D. Servin, J. R. Peralta-Videa, and J. L. Gardea-Torresdey. "Spectroscopic Verification of Zinc Absorption and Distribution in the Desert Plant Prosopis Juliflora-Velutina (Velvet Mesquite) Treated with Zno Nanoparticles." [In eng]. *Chem Eng J* 170, no. 1-3 (Jun 1 2011): 346-52.

Hernandez-Viezcas, Jose A., Hiram Castillo-Michel, Joy Cooke Andrews, Marine Cotte, Cyren Rico, Jose R. Peralta-Videa, Yuan Ge, *et al.* "In Situ Synchrotron X-Ray Fluorescence Mapping and Speciation of Ceo2 and Zno Nanoparticles in Soil Cultivated Soybean (Glycine Max)." *Acs Nano* 7, no. 2 (Feb 2013): 1415-23.

Herrera-Vásquez, Ariel, Paula Salinas, and Loreto Holuigue. "Salicylic Acid and Reactive Oxygen Species Interplay in the Transcriptional Control of Defense Genes Expression." *Frontiers in plant science* 6 (2015): 171-71.

Hershfinkel, Michal, Williaim F. Silverman, and Israel Sekler. "The Zinc Sensing Receptor, a Link between Zinc and Cell Signaling." *Molecular Medicine* 13, no. 7-8 (Jul-Aug 2007): 331-36.

Hofstetter, Silvia Schelbert, Alexey Dudnik, Heidi Widmer, and Robert Dudler. "Arabidopsis Yellow Stripe-Like7 (Ysl7) and Ysl8 Transporters Mediate Uptake of Pseudomonas Virulence Factor Syringolin a into Plant Cells." *Molecular Plant-Microbe Interactions* 26, no. 11 (2013): 1302-11.

Hong, Jeum Kyu, In Sun Hwang, and Byung Kook Hwang. "Functional Roles of the Pepper Leucine-Rich Repeat Protein and Its Interactions with Pathogenesis-Related and Hypersensitive-Induced Proteins in Plant Cell Death and Immunity." *Planta* 246, no. 3 (2017/09/01 2017): 351-64.

Humphry, Matt, Paweł Bednarek, Birgit Kemmerling, Serry Koh, Mónica Stein, Ulrike Göbel, Kurt Stüber, *et al.* "A Regulon Conserved in Monocot and Dicot Plants Defines a Functional Module in Antifungal Plant Immunity." *Proceedings of the National Academy of Sciences* 107, no. 50 (2010): 21896.

Hussain, Afzal, Shafaqat Ali, Muhammad Rizwan, Muhammad Zia ur Rehman, Muhammad Rizwan Javed, Muhammad Imran, Shahzad Ali Shahid Chatha, and Rashid Nazir. "Zinc Oxide Nanoparticles Alter the Wheat Physiological Response and Reduce the Cadmium Uptake by Plants." *Environmental Pollution* 242 (2018/11/01/ 2018): 1518-26.

Hwang, F. K., and Dana S. Richards. "Steiner Tree Problems." *Networks* 22, no. 1 (1992): 55-89.

Hwang In, Sun, Seok Choi Du, Hyun Kim Nak, Sung Kim Dae, and Kook Hwang Byung. "Pathogenesis-Related Protein 4b Interacts with Leucine-Rich Repeat Protein 1 to Suppress Pr4b-Triggered Cell Death and Defense Response in Pepper." *The Plant Journal* 77, no. 4 (2014/02/01 2013): 521-33.

Jacob, Donna L., Joshua D. Borchardt, Leelaruban Navaratnam, Marinus L. Otte, and Achintya N. Bezbaruah. "Uptake and Translocation of Ti from Nanoparticles in Crops and Wetland Plants." *International Journal of Phytoremediation* 15, no. 2 (2013 2013): 142-53.

Jain, Aditi, Shivendu Ranjan, Nandita Dasgupta, and Chidambaram Ramalingam. "Nanomaterials in Food and Agriculture: An Overview on Their Safety Concerns and Regulatory Issues." *Critical Reviews in Food Science and Nutrition* 58, no. 2 (2018/01/22 2018): 297-317.

Jamdagni, Pragati, Poonam Khatri, and J. S. Rana. "Green Synthesis of Zinc Oxide Nanoparticles Using Flower Extract of Nyctanthes Arbor-Tristis and Their Antifungal Activity." *Journal of King Saud University - Science* 30, no. 2 (2018/04/01/ 2018): 168-75.

Jiang, Jingkun, Gunter Oberdorster, and Pratim Biswas. "Characterization of Size, Surface Charge, and Agglomeration State of Nanoparticle Dispersions for Toxicological Studies." *Journal of Nanoparticle Research* 11, no. 1 (Jan 2009): 77-89.

Jo, Mi-Rae, Hae-Eun Chung, Hyun-Jin Kim, Song-Hwa Bae, Mi-Ran Go, Jin Yu, and Soo-Jin Choi. "Effects of Zinc Oxide Nanoparticle Dispersants on Cytotoxicity and Cellular Uptake." *Molecular & Cellular Toxicology* 12, no. 3 (2016/09/01 2016): 281-88.

Joy, Edward J. M., Waqar Ahmad, Munir H. Zia, Diriba B. Kumssa, Scott D. Young, E. Louise Ander, Michael J. Watts, Alexander J. Stein, and Martin R. Broadley. "Valuing Increased Zinc (Zn) Fertiliser-Use in Pakistan." *Plant and Soil* 411, no. 1 (2017/02/01 2017): 139-50.

Joy, Edward J. M., Alexander J. Stein, Scott D. Young, E. Louise Ander, Michael J. Watts, and Martin R. Broadley. "Zinc-Enriched Fertilisers as a Potential Public Health Intervention in Africa." *Plant and Soil* 389, no. 1 (2015/04/01 2015): 1-24.

Karuppanapandian, Thirupathi, Jun-Cheol Moon, Changsoo Kim, Kumariah Manoharan, and Wook Kim. "Reactive Oxygen Species in Plants: Their Generation, Signal Transduction, and Scavenging Mechanisms." *Australian Journal of Crop Science* 5, no. 6 (2011): 709.

Kaveh, Rashid, Yue-Sheng Li, Sibia Ranjbar, Rouzbeh Tehrani, Christopher L. Brueck, and Benoit Van Aken. "Changes in Arabidopsis Thaliana Gene Expression in Response to Silver Nanoparticles and Silver Ions." *Environmental Science & Technology* 47, no. 18 (Sep 17 2013): 10637-44.

Khodakovskaya, M. V., K. de Silva, D. A. Nedosekin, E. Dervishi, A. S. Biris, E. V. Shashkov, E. I. Galanzha, and V. P. Zharov. "Complex Genetic, Photothermal, and Photoacoustic Analysis of Nanoparticle-Plant Interactions." [In English]. *Proceedings of the National Academy of Sciences of the United States of America* 108, no. 3 (Jan 2011): 1028-33.

Kiekens, L. "Zinc." In *Heavy Metals in Soils*, edited by B.J. Alloway, Ed., 284-305. London: Blackie Academic and Professional, 1995.

Kim, Jae-Hwan, Yongjik Lee, Eun-Ju Kim, Sungmin Gu, Eun Ju Sohn, Young Sook Seo, Hyun Joo An, and Yoon-Seok Chang. "Exposure of Iron Nanoparticles to Arabidopsis Thaliana Enhances Root Elongation by Triggering Cell Wall Loosening." *Environmental Science & Technology* 48, no. 6 (Mar 18 2014): 3477-85.

Kim, Nak Hyun, and Byung Kook Hwang. "Pepper Pathogenesis-Related Protein 4c Is a Plasma Membrane-Localized Cysteine Protease Inhibitor That Is Required for Plant Cell Death and Defense Signaling." *The Plant Journal* 81, no. 1 (2015/01/01 2014): 81-94.

Kim, S., J. Kim, and I. Lee. "Effects of Zn and Zno Nanoparticles and Zn2+on Soil Enzyme Activity and Bioaccumulation of Zn in Cucumis Sativus." *Chemistry and Ecology* 27, no. 1 (2011): 49-55.

Kim, Sun Young, Yun Shang, Se-Hwan Joo, Seong-Ki Kim, and Kyoung Hee Nam. "Overexpression of Bak1 Causes Salicylic Acid Accumulation and Deregulation of Cell Death Control Genes." *Biochemical and Biophysical Research Communications* 484, no. 4 (2017/03/18/ 2017): 781-86.

Kim, Sunghyun, Sooyeon Lee, and Insook Lee. "Alteration of Phytotoxicity and Oxidant Stress Potential by Metal Oxide Nanoparticles in Cucumis Sativus." *Water, Air, & Soil Pollution* 223, no. 5 (2012): 2799-806.

Kim, Y. J., H. J. Lee, M. G. Jang, W. S. Kwon, S. Y. Kim, and D. C. Yang. "Cloning and Characterization of Pathogenesis-Related Protein 4 Gene from Panax Ginseng." *Russian Journal of Plant Physiology* 61, no. 5 (2014/09/01 2014): 664-71.

King, Janet C. "Zinc: An Essential but Elusive Nutrient." *American Journal of Clinical Nutrition* 94, no. 2 (Aug 2011): 679S-84S.

Kissoudis, C., S. Sunarti, C. van de Wiel, R. G. Visser, C. G. van der Linden, and Y. Bai. "Responses to Combined Abiotic and Biotic Stress in Tomato Are Governed by Stress Intensity and Resistance Mechanism." [In eng]. *J Exp Bot* 67, no. 17 (Sep 2016): 5119-32.

Kitajima, S., and F. Sato. "Plant Pathogenesis-Related Proteins: Molecular Mechanisms of Gene Expression and Protein Function." [In eng]. *J Biochem* 125, no. 1 (Jan 1999): 1-8.

Knogge, W. "Fungal Infection of Plants." *The Plant Cell* 8, no. 10 (1996): 1711-22.

Kohorn, Bruce D., Divya Hoon, Benjamin B. Minkoff, Michael R. Sussman, and Susan L. Kohorn. "Rapid Oligo-Galacturonide Induced Changes in Protein Phosphorylation in Arabidopsis." *Molecular & Cellular Proteomics* 15, no. 4 (2016): 1351.

Koladia, V. M., J. D. Faris, J. K. Richards, R. S. Brueggeman, S. Chao, and T. L. Friesen. "Genetic Analysis of Net Form Net Blotch Resistance in Barley Lines Ciho 5791 and Tifang against a Global Collection of P. Teres F. Teres Isolates." [In eng]. *Theor Appl Genet* 130, no. 1 (Jan 2017): 163-73.

Kou, L. T., and K. Makki. "An Even Faster Approximation Algorithm for the Steiner Tree Problem in Graphs." *Congressus Numerantium* 59 (1987): 147-54.

Kouhi, Seyed Mousa Mousavi, Mehrdad Lahouti, Ali Ganjeali, and Mohammad H. Entezari. "Long-Term Exposure of Rapeseed (Brassica Napus L.) to Zno Nanoparticles: Anatomical and Ultrastructural Responses." *Environmental Science and Pollution Research* 22, no. 14 (2015): 10733-43.

Kowalczyk, Tim, Ziliang Lin, and Troy Van Voorhis. "Fluorescence Quenching by Photoinduced Electron Transfer in the Zn2+ Sensor Zinpyr-1: A Computational Investigation." *Journal of Physical Chemistry A* 114, no. 38 (Sep 30 2010): 10427-34.

Kumari, M., S. S. Khan, S. Pakrashi, A. Mukherjee, and N. Chandrasekaran. "Cytogenetic and Genotoxic Effects of Zinc Oxide Nanoparticles on Root Cells of Allium Cepa." *Journal of Hazardous Materials* 190, no. 1-3 (Jun 2011): 613-21.

Landa, P., S. Prerostova, S. Petrova, V. Knirsch, R. Vankova, and T. Vanek. "The Transcriptomic Response of Arabidopsis Thaliana to Zinc Oxide: A Comparison of the Impact of Nanoparticle, Bulk, and Ionic Zinc." *Environmental Science & Technology* 49, no. 24 (Dec 2015): 14537-45.

Landa, Premysl, Radomira Vankova, Jana Andrlova, Jan Hodek, Petr Marsik, Helena Storchova, Jason C. White, and Tomas Vanek. "Nanoparticle-Specific Changes in Arabidopsis Thaliana Gene Expression after Exposure to Zno, Tio2, and Fullerene Soot." *Journal of Hazardous Materials* 241 (Nov 30 2012): 55-62.

Lee, Sooyeon, Hyein Chung, Saeyeon Kim, and Insook Lee. "The Genotoxic Effect of Zno and Cuo Nanoparticles on Early Growth of Buckwheat, Fagopyrum Esculentum." *Water Air and Soil Pollution* 224, no. 9 (Sep 2013).

Lee, W. M., Y. J. An, H. Yoon, and H. S. Kweon. "Toxicity and Bioavailability of Copper Nanoparticles to the Terrestrial Plants Mung Bean (Phaseolus Radiatus) and Wheat (Triticum Aestivum): Plant Agar Test for Water-Insoluble Nanoparticles." [In English]. *Environmental Toxicology and Chemistry* 27, no. 9 (Sep 2008): 1915-21.

Lee, Woo-Mi, Jin Il Kwak, and Youn-Joo An. "Effect of Silver Nanoparticles in Crop Plants Phaseolus Radiatus and Sorghum Bicolor: Media Effect on Phytotoxicity." *Chemosphere* 86, no. 5 (Feb 2012): 491-99.

Li, Cui, Peng Wang, Enzo Lombi, Miaomiao Cheng, Caixian Tang, Daryl L. Howard, Neal W. Menzies, and Peter M. Kopittke. "Absorption of Foliar-Applied Zn Fertilizers by Trichomes in Soybean and Tomato." *Journal of Experimental Botany* 69, no. 10 (2018): 2717-29.

Li, Hui, Shan-Yue Zhou, Wen-Sheng Zhao, Sheng-Chang Su, and You-Liang Peng. "A Novel Wall-Associated Receptor-Like Protein Kinase Gene, Oswak1, Plays Important Roles in Rice Blast Disease Resistance." *Plant Molecular Biology* 69, no. 3 (2009/02/01 2009): 337-46.

Li, Jing, Günter Brader, Tarja Kariola, and E. Tapio Palva. "Wrky70 Modulates the Selection of Signaling Pathways in Plant Defense." *The Plant Journal* 46, no. 3 (2006/05/01 2006): 477-91.

Li, Min, Yu Lu, Jianxin Wang, Fang-Xiang Wu, and Yi Pan. "A Topology Potential-Based Method for Identifying Essential Proteins from Ppi Networks." *IEEE/ACM Transactions on Computational Biology and Bioinformatics (TCBB)* 12, no. 2 (2015): 372-83.

Li, X., S. Hou, Q. Gao, P. Zhao, S. Chen, D. Qi, B. H. Lee, L. Cheng, and G. Liu. "Lcsain1, a Novel Salt-Induced Gene from Sheepgrass, Confers Salt Stress Tolerance in Transgenic Arabidopsis and Rice." [In eng]. *Plant Cell Physiol* 54, no. 7 (Jul 2013): 1172-85.

Li, Xingyi, Wenkai Li, Min Zeng, Ruiqing Zheng, and Min Li. "Network-Based Methods for Predicting Essential Genes or Proteins: A Survey." *Briefings in bioinformatics* (2019).

Li, Yingbo, Chenghong Liu, Guimei Guo, Ting He, Zhiwei Chen, Runhong Gao, Hongwei Xu, *et al.* "Expression Analysis of Three Serk-Like Genes in Barley under Abiotic and Biotic Stresses." *Journal of Plant Interactions* 12, no. 1 (2017/01/01 2017): 279-85.

Lim, H. Karen, J. Lynn Riddell, A. Caryl Nowson, O. Alison Booth, and A. Ewa Szymlek-Gay. "Iron and Zinc Nutrition in the Economically-Developed World: A Review." *Nutrients* 5, no. 8 (2013).

Linares, J., M. C. Matesanz, M. Vila, M. J. Feito, G. Goncalves, M. Vallet-Regi, Paap Marques, and M. T. Portoles. "Endocytic Mechanisms of Graphene Oxide Nanosheets in Osteoblasts, Hepatocytes and Macrophages." *Acs Applied Materials & Interfaces* 6, no. 16 (Aug 2014): 13697-706.

Liu, Jun-Jun, Rona Sturrock, and Abul K. M. Ekramoddoullah. "The Superfamily of Thaumatin-Like Proteins: Its Origin, Evolution, and Expression Towards Biological Function." *Plant Cell Reports* 29, no. 5 (2010/05/01 2010): 419-36.

Liu, Qiaoling, Bo Chen, Qinli Wang, Xiaoli Shi, Zeyu Xiao, Jinxin Lin, and Xiaohong Fang. "Carbon Nanotubes as Molecular Transporters for Walled Plant Cells." *Nano Letters* 9, no. 3 (Mar 2009): 1007-10.

Liu, Z. H., S. R. Ellwood, R. P. Oliver, and T. L. Friesen. "Pyrenophora Teres: Profile of an Increasingly Damaging Barley Pathogen." *Molecular Plant Pathology* 12, no. 1 (Jan 2011): 1-19.

Liu, Zhaohui, Danielle J. Holmes, Justin D. Faris, Shiaoman Chao, Robert S. Brueggeman, Michael C. Edwards, and Timothy L. Friesen. "Necrotrophic Effector-Triggered Susceptibility (Nets) Underlies the Barley-Pyrenophora Teres F. Teres Interaction Specific to Chromosome 6h." *Molecular Plant Pathology* 16, no. 2 (Feb 2015): 188-200.

Lopes, Sílvia, Fabianne Ribeiro, Jacek Wojnarowicz, Witold Łojkowski, Kerstin Jurkschat, Alison Crossley, M. V. M. Soares Amadeu, and Susana Loureiro. "Zinc Oxide Nanoparticles Toxicity to Daphnia Magna: Size-Dependent Effects and Dissolution." *Environmental Toxicology and Chemistry* 33, no. 1 (2014/01/01 2013): 190-98.

Lopez-Moreno, Martha L., Guadalupe de la Rosa, Jose A. Hernandez-Viezcas, Hiram Castillo-Michel, Cristian E. Botez, Jose R. Peralta-Videa, and Jorge L. Gardea-Torresdey. "Evidence of the Differential Biotransformation and Genotoxicity of Zno and Ceo2 Nanoparticles on Soybean (Glycine Max) Plants." *Environmental Science & Technology* 44, no. 19 (Oct 1 2010): 7315-20.

Lv, Jitao, Shuzhen Zhang, Lei Luo, Jing Zhang, Ke Yang, and Peter Christie. "Accumulation, Speciation and Uptake Pathway of Zno Nanoparticles in Maize." *Environmental Science-Nano* 2, no. 1 (Feb 2015): 68-77.

Ma, C. X., H. Liu, H. Y. Guo, C. Musante, S. H. Coskun, B. C. Nelson, J. C. White, B. S. Xing, and O. P. Dhankher. "Defense Mechanisms and Nutrient Displacement in Arabidopsis Thaliana Upon Exposure to Ceo2 and In2o3 Nanoparticles." *Environmental Science-Nano* 3, no. 6 (2016): 1369-79.

Ma, Jianhui, Xiaolong Gao, Qing Liu, Yun Shao, Daijing Zhang, Lina Jiang, and Chunxi Li. "Overexpression of Tawrky146 Increases Drought Tolerance through Inducing Stomatal Closure in Arabidopsis Thaliana." *Frontiers in Plant Science* 8 (2017): 2036.

Ma, Xiyu, Guangyuan Xu, Ping He, and Libo Shan. "Serking Coreceptors for Receptors." *Trends in Plant Science* 21, no. 12 (2016/12/01/ 2016): 1017-33.

Ma, Y. H., L. L. Kuang, X. He, W. Bai, Y. Y. Ding, Z. Y. Zhang, Y. L. Zhao, and Z. F. Chai. "Effects of Rare Earth Oxide Nanoparticles on Root Elongation of Plants." [In English]. *Chemosphere* 78, no. 3 (Jan 2010): 273-79.

Madden, Thomas. "The Blast Sequence Analysis Tool." (2013).

Makandar, Ragiba, Vamsi J. Nalam, Hyeonju Lee, Harold N. Trick, Yanhong Dong, and Jyoti Shah. "Salicylic Acid Regulates Basal Resistance to Fusarium Head Blight in Wheat." *Molecular plant-microbe interactions* 25, no. 3 (2012): 431-39.

Makepeace, J. C., N. D. Havis, J. I. Burke, S. J. P. Oxley, and J. K. M. Brown. "A Method of Inoculating Barley Seedlings with Ramularia Collo-Cygni." *Plant Pathology* 57, no. 6 (2008): 991-99.

Marslin, Gregory, Caroline J. Sheeba, and Gregory Franklin. "Nanoparticles Alter Secondary Metabolism in Plants Via Ros Burst." *Frontiers in Plant Science* 8 (2017): 832.

Martinoia, Enrico, Masayoshi Maeshima, and H. Ekkehard Neuhaus. "Vacuolar Transporters and Their Essential Role in Plant Metabolism." *Journal of Experimental Botany* 58, no. 1 (2007): 83-102.

Meeusen, Jeffrey W., Andrew Nowakowski, and David H. Petering. "Reaction of Metal-Binding Ligands with the Zinc Proteome: Zinc Sensors and N,N,N ',N '-Tetrakis(2-Pyridylmethyl)Ethylenediamine." *Inorganic Chemistry* 51, no. 6 (Mar 19 2012): 3625-32.

Milani, Narges. "Zinc Oxide Nanoparticles in the Soil Environment: Dissolution, Speciation, Retention, and Bioavailability." The University of Adelaide, 2011.

Miralles, P., T. L. Church, and A. T. Harris. "Toxicity, Uptake, and Translocation of Engineered Nanomaterials in Vascular Plants." *Environmental Science & Technology* 46, no. 17 (Sep 2012): 9224-39.

———. "Toxicity, Uptake, and Translocation of Engineered Nanomaterials in Vascular Plants." *Environmental Science & Technology* 46, no. 17 (Sep 2012): 9224-39.

Misra, Rajesh Chandra, Sandeep, Mohan Kamthan, Santosh Kumar, and Sumit Ghosh. "A Thaumatin-Like Protein of Ocimum Basilicum Confers Tolerance to Fungal Pathogen and Abiotic Stress in Transgenic Arabidopsis." *Scientific Reports* 6 (05/06

10/14/received

04/13/accepted 2016): 25340.

Mortari, S. R., C. R. Cocco, F. R. Bartz, V. L. Dresssler, and E. M. D. Flores. "Fast Digestion Procedure for Determination of Catalyst Residues in La- and Ni-Based Carbon Nanotubes." [In English]. *Analytical Chemistry* 82, no. 10 (May 2010): 4298-303.

Mousavi Kouhi, Seyed Mousa, Mehrdad Lahouti, Ali Ganjeali, and Mohammad H. Entezari. "Comparative Phytotoxicity of Zno Nanoparticles, Zno Microparticles, and Zn2+ on Rapeseed (Brassica Napus L.): Investigating a Wide Range of Concentrations." *Toxicological & Environmental Chemistry* 96, no. 6 (2014): 861-68.

Movafeghi, Ali, Alireza Khataee, Mahboubeh Abedi, Roshanak Tarrahi, Mohammadreza Dadpour, and Fatemeh Vafaei. "Effects of Tio2 Nanoparticles on the Aquatic Plant Spirodela Polyrrhiza: Evaluation of Growth Parameters, Pigment Contents and Antioxidant Enzyme Activities." *Journal of Environmental Sciences* 64 (2018/02/01/ 2018): 130-38.

Mukherjee, A., J. R. Peralta-Videa, S. Bandyopadhyay, C. M. Rico, L. J. Zhao, and J. L. Gardea-Torresdey. "Physiological Effects of Nanoparticulate Zno in Green Peas (Pisum Sativum L.) Cultivated in Soil." *Metallomics* 6, no. 1 (2014): 132-38.

Nair, P. M. G., and I. M. Chung. "Regulation of Morphological, Molecular and Nutrient Status in Arabidopsis Thaliana Seedlings in Response to Zno Nanoparticles and Zn Ion Exposure." *Science of the Total Environment* 575 (Jan 2017): 187-98.

Navarro, E., A. Baun, R. Behra, N. B. Hartmann, J. Filser, A. J. Miao, A. Quigg, P. H. Santschi, and L. Sigg. "Environmental Behavior and Ecotoxicity of Engineered Nanoparticles to Algae, Plants, and Fungi." [In English]. *Ecotoxicology* 17, no. 5 (Jul 2008): 372-86.

Nawrot, Robert, Jakub Barylski, Grzegorz Nowicki, Justyna Broniarczyk, Waldemar Buchwald, and Anna Goździcka-Józefiak. "Plant Antimicrobial Peptides." *Folia Microbiologica* 59, no. 3 (10/04 04/18/received 09/17/accepted 2014): 181-96.

Nostar, Ozge, Filiz Ozdemir, Melike Bor, Ismail Turkan, and Necip Tosun. "Combined Effects of Salt Stress and Cucurbit Downy Mildew (Pseudoperospora Cubensis Berk. And Curt. Rostov.) Infection on Growth, Physiological Traits and Antioxidant Activity in Cucumber (Cucumis Sativus L.) Seedlings." *Physiological and Molecular Plant Pathology* 83 (2013/07/01/ 2013): 84-92.

Odzak, Niksa, David Kistler, Renata Behra, and Laura Sigg. "Dissolution of Metal and Metal Oxide Nanoparticles in Aqueous Media." *Environmental Pollution* 191 (Aug 2014): 132-38.

Oh, N., and J. H. Park. "Endocytosis and Exocytosis of Nanoparticles in Mammalian Cells." *International Journal of Nanomedicine* 9 (2014): 51-63.

Okada, Kazunori, Hiroshi Abe, and Gen-ichiro Arimura. "Jasmonates Induce Both Defense Responses and Communication in Monocotyledonous and Dicotyledonous Plants." *Plant and Cell Physiology* 56, no. 1 (2015): 16-27.

Onaga, Geoffrey, and Kerstin Wydra. "Advances in Plant Tolerance to Biotic Stresses." In *Plant Genomics*, edited by Ibrokhim Y. Abdurakhmonov. Ch. 10. Rijeka: InTech, 2016.

Pagel, Philipp, Stefan Kovac, Matthias Oesterheld, Barbara Brauner, Irmtraud Dunger-Kaltenbach, Goar Frishman, Corinna Montrone, *et al.* "The Mips Mammalian Protein–Protein Interaction Database." *Bioinformatics* 21, no. 6 (2004): 832-34.

Pakrashi, S., N. Jain, S. Dalai, J. Jayakumar, P. T. Chandrasekaran, A. M. Raichur, N. Chandrasekaran, and A. Mukherjee. "In Vivo Genotoxicity Assessment of Titanium Dioxide Nanoparticles by Allium Cepa Root Tip Assay at High Exposure Concentrations." *Plos One* 9, no. 2 (Feb 2014).

Panda, K. K., D. Golari, A. Venugopal, V. M. M. Achary, G. Phaomei, N. L. Parinandi, H. K. Sahu, and B. B. Panda. "Green Synthesized Zinc Oxide (Zno) Nanoparticles Induce Oxidative Stress and Dna Damage in Lathyrus Sativus L. Root Bioassay System." [In eng]. *Antioxidants (Basel)* 6, no. 2 (May 18 2017).

Pandey, Dinesh, Subin Raj Cheri Kunnumal Rajendran, Manu Gaur, P. K. Sajeesh, and Anil Kumar. "Plant Defense Signaling and Responses against Necrotrophic Fungal Pathogens." *Journal of Plant Growth Regulation* 35, no. 4 (2016): 1159-74.

Pandey, Prachi, Vadivelmurugan Irulappan, Muthukumar V. Bagavathiannan, and Muthappa Senthil-Kumar. "Impact of Combined Abiotic and Biotic Stresses on Plant Growth and Avenues for Crop Improvement by Exploiting Physio-Morphological Traits." *Frontiers in Plant Science* 8 (04/1811/07/received03/27/accepted 2017): 537.

Parisi, C., M. Vigani, and E. Rodriguez-Cerezo. "Agricultural Nanotechnologies: What Are the Current Possibilities?". *Nano Today* 10, no. 2 (Apr 2015): 124-27.

Peralta-Videa, Jose R., Jose A. Hernandez-Viezcas, Lijuan Zhao, Baltazar Corral Diaz, Yuan Ge, John H. Priester, Patricia Ann Holden, and Jorge L. Gardea-Torresdey. "Cerium Dioxide and Zinc Oxide Nanoparticles Alter the Nutritional Value of Soil Cultivated Soybean Plants." *Plant Physiology and Biochemistry* 80 (Jul 2014): 128-35.

Pike, Sharon, Fei Gao, Min Jung Kim, Sang Hee Kim, Daniel P. Schachtman, and Walter Gassmann. "Members of the Npf3 Transporter Subfamily Encode Pathogen-Inducible Nitrate/Nitrite Transporters in Grapevine and Arabidopsis." *Plant and Cell Physiology* 55, no. 1 (2014): 162-70.

Pirselova, B., R. Kuna, J. Libantova, J. Moravcikova, and I. Matusikova. "Biochemical and Physiological Comparison of Heavy Metal-Triggered Defense Responses in the Monocot Maize and Dicot Soybean Roots." *Molecular Biology Reports* 38, no. 5 (Jun 2011): 3437-46.

Pogodin, S., and V. A. Baulin. "Can a Carbon Nanotube Pierce through a Phospholipid Bilayer?" [In English]. *Acs Nano* 4, no. 9 (Sep 2010): 5293-300.

Pokhrel, L. R., and B. Dubey. "Evaluation of Developmental Responses of Two Crop Plants Exposed to Silver and Zinc Oxide Nanoparticles." *Science of the Total Environment* 452 (May 2013): 321-32.

Poliseli-Scopel, F. H., M. Hernandez-Herrero, B. Guamis, and V. Ferragut. "Comparison of Ultra High Pressure Homogenization and Conventional Thermal Treatments on the Microbiological, Physical and Chemical Quality of Soymilk." *Lwt-Food Science and Technology* 46, no. 1 (Apr 2012): 42-48.

Powers, Kevin W., Scott C. Brown, Vijay B. Krishna, Scott C. Wasdo, Brij M. Moudgil, and Stephen M. Roberts. "Research Strategies for Safety Evaluation of Nanomaterials. Part Vi. Characterization of Nanoscale Particles for Toxicological Evaluation." *Toxicological Sciences* 90, no. 2 (2006): 296-303.

Prasad, T. N. V. K. V., P. Sudhakar, Y. Sreenivasulu, P. Latha, V. Munaswamy, K. Raja Reddy, T. S. Sreeprasad, P. R. Sajanlal, and T. Pradeep. "Effect of Nanoscale Zinc Oxide Particles on the Germination, Growth and Yield of Peanut." *Journal of Plant Nutrition* 35, no. 6 (2012/04/01 2012): 905-27.

Prasch, C. M., and U. Sonnewald. "Simultaneous Application of Heat, Drought, and Virus to Arabidopsis Plants Reveals Significant Shifts in Signaling Networks." [In eng]. *Plant Physiol* 162, no. 4 (Aug 2013): 1849-66.

Priester, J. H., S. C. Moritz, K. Espinosa, Y. Ge, Y. Wang, R. M. Nisbet, J. P. Schimel, *et al.* "Damage Assessment for Soybean Cultivated in Soil with Either Ceo2 or Zno Manufactured Nanomaterials." *Science of the Total Environment* 579 (Feb 2017): 1756-68.

Priester, John H., Yuan Ge, Randall E. Mielke, Allison M. Horst, Shelly Cole Moritz, Katherine Espinosa, Jeff Gelb, *et al.* "Soybean Susceptibility to Manufactured Nanomaterials with Evidence for Food Quality and Soil Fertility Interruption." *Proceedings of the National Academy of Sciences of the United States of America* 109, no. 37 (Sep 11 2012): E2451-E56.

Provart, Nicholas, and Tong Zhu. "A Browser-Based Functional Classification Superviewer for Arabidopsis Genomics." *Currents in Computational Molecular Biology* 2003 (2003): 271-72.

Pérez-de-Luque, Alejandro. "Interaction of Nanomaterials with Plants: What Do We Need for Real Applications in Agriculture?". *Frontiers in Environmental Science* 5 (2017): 12.

Raffaele, Sylvain, Susana Rivas, and Dominique Roby. "An Essential Role for Salicylic Acid in Atmyb30-Mediated Control of the Hypersensitive Cell Death Program in Arabidopsis." *FEBS Letters* 580, no. 14 (2006/06/12/ 2006): 3498-504.

Rahman, Taha Abd El, Mohamed El Oirdi, Rocio Gonzalez-Lamothe, and Kamal Bouarab. "Necrotrophic Pathogens Use the Salicylic Acid Signaling Pathway to Promote Disease Development in Tomato." *Molecular Plant-Microbe Interactions* 25, no. 12 (2012): 1584-93.

Rahmani, Fatemeh, Arghavan Peymani, Elhameh Daneshvand, and Poorya Biparva. "Impact of Zinc Oxide and Copper Oxide Nano-Particles on Physiological and Molecular Processes in Brassica Napus." *Indian journal of plant physiology* 21, no. 2 (2016): 122-28.

Rajakumar, Govindasamy, Muthu Thiruvengadam, Govindarasu Mydhili, Thandapani Gomathi, and Ill-Min Chung. "Green Approach for Synthesis of Zinc Oxide Nanoparticles from Andrographis Paniculata Leaf Extract and Evaluation of Their Antioxidant, Anti-Diabetic, and Anti-Inflammatory Activities." *Bioprocess and Biosystems Engineering* 41, no. 1 (2018/01/01 2018): 21-30.

Rajeshwari, A., S. Kavitha, Sruthi Ann Alex, Deepak Kumar, Anita Mukherjee, Natarajan Chandrasekaran, and Amitava Mukherjee. "Cytotoxicity of Aluminum Oxide Nanoparticles on Allium Cepa Root Tip—Effects of Oxidative Stress Generation and Biouptake." *Environmental Science and Pollution Research* 22, no. 14 (2015/07/01 2015): 11057-66.

Rajput, Vishnu D., Tatiana M. Minkina, Arvind Behal, Svetlana N. Sushkova, Saglara Mandzhieva, Ritu Singh, Andrey Gorovtsov, *et al.* "Effects of Zinc-Oxide Nanoparticles on Soil, Plants, Animals and Soil Organisms: A Review." *Environmental Nanotechnology, Monitoring & Management* 9 (2018/05/01/ 2018): 76-84.

Raliya, R., R. Nair, S. Chavalmane, W. N. Wang, and P. Biswas. "Mechanistic Evaluation of Translocation and Physiological Impact of Titanium Dioxide and Zinc Oxide Nanoparticles on the Tomato (Solanum Lycopersicum L.) Plant." *Metallomics* 7, no. 12 (2015): 1584-94.

Ramegowda, Venkategowda, and Muthappa Senthil-Kumar. "The Interactive Effects of Simultaneous Biotic and Abiotic Stresses on Plants: Mechanistic Understanding from Drought and Pathogen Combination." *Journal of Plant Physiology* 176 (2015/03/15/ 2015): 47-54.

Rangan, Anna M., and Samir Samman. "Zinc Intake and Its Dietary Sources: Results of the 2007 Australian National Children's Nutrition and Physical Activity Survey." *Nutrients* 4, no. 7 (2012).

Rao, S., and G. S. Shekhawat. "Toxicity of Zno Engineered Nanoparticles and Evaluation of Their Effect on Growth, Metabolism and Tissue Specific Accumulation in Brassica Juncea." *Journal of Environmental Chemical Engineering* 2, no. 1 (2014/03/01/ 2014): 105-14.

Raskar, S. V., and S. L. Laware. "Effect of Zinc Oxide Nanoparticles on Cytology and Seed Germination in Onion." *Int J Curr Microbiol App Sci* 3, no. 2 (2014): 467-73.

Reed, Robert B., David A. Ladner, Christopher P. Higgins, Paul Westerhoff, and James F. Ranville. "Solubility of Nano-Zinc Oxide in Environmentally and Biologically Important Matrices." *Environmental toxicology and chemistry* 31, no. 1 (2012): 93-99.

Rico, C. M., J. Hong, M. I. Morales, L. J. Zhao, A. C. Barrios, J. Y. Zhang, J. R. Peralta-Videa, and J. L. Gardea-Torresdey. "Effect of Cerium Oxide Nanoparticles on Rice: A Study Involving the Antioxidant Defense System and in Vivo Fluorescence Imaging." *Environmental Science & Technology* 47, no. 11 (Jun 2013): 5635-42.

Roco, M. C. "Nanotechnology: Convergence with Modern Biology and Medicine." [In English]. *Current Opinion in Biotechnology* 14, no. 3 (Jun 2003): 337-46.

Rossi, L., W. L. Zhang, L. Lombardini, and X. M. Ma. "The Impact of Cerium Oxide Nanoparticles on the Salt Stress Responses of Brassica Napus L." *Environmental Pollution* 219 (Dec 2016): 28-36.

Sabir, Sidra, Muhammad Arshad, and Sunbal Khalil Chaudhari. "Zinc Oxide Nanoparticles for Revolutionizing Agriculture: Synthesis and Applications." *The Scientific World Journal* 2014 (2014).

Santhoshkumar, J., S. Venkat Kumar, and S. Rajeshkumar. "Synthesis of Zinc Oxide Nanoparticles Using Plant Leaf Extract against Urinary Tract Infection Pathogen." *Resource-Efficient Technologies* 3, no. 4 (2017/12/01/ 2017): 459-65.

Scarpeci, Telma E., María I. Zanor, Bernd Mueller-Roeber, and Estela M. Valle. "Overexpression of Atwrky30 Enhances Abiotic Stress Tolerance During Early Growth Stages in Arabidopsis Thaliana." *Plant Molecular Biology* 83, no. 3 (2013/10/01 2013): 265-77.

Schwegmann, H., A. J. Feitz, and F. H. Frimmel. "Influence of the Zeta Potential on the Sorption and Toxicity of Iron Oxide Nanoparticles on S. Cerevisiae and E. Coli." [In English]. *Journal of Colloid and Interface Science* 347, no. 1 (Jul 2010): 43-48.

Sels, Jan, Janick Mathys, Barbara M. A. De Coninck, Bruno P. A. Cammue, and Miguel F. C. De Bolle. "Plant Pathogenesis-Related (Pr) Proteins: A Focus on Pr Peptides." *Plant Physiology and Biochemistry* 46, no. 11 (2008/11/01/ 2008): 941-50.

Serag, M. F., N. Kaji, C. Gaillard, Y. Okamoto, K. Terasaka, M. Jabasini, M. Tokeshi, *et al.* "Trafficking and Subcellular Localization of Multiwalled Carbon Nanotubes in Plant Cells." [In English]. *Acs Nano* 5, no. 1 (Jan 2011): 493-99.

Servin, Alia D., and Jason C. White. "Nanotechnology in Agriculture: Next Steps for Understanding Engineered Nanoparticle Exposure and Risk." *NanoImpact* 1 (2016): 9-12.

Shah, Shaily Umang. "Importance of Genotoxicity & S2a Guidelines for Genotoxicity Testing for Pharmaceuticals." *IOSR Journal of Pharmacy and Biological Sciences* 1, no. 2 (2012): 43-54.

Shimono, Masaki, Shoji Sugano, Akira Nakayama, Chang-Jie Jiang, Kazuko Ono, Seiichi Toki, and Hiroshi Takatsuji. "Rice Wrky45 Plays a Crucial Role in Benzothiadiazole-Inducible Blast Resistance." *The Plant Cell* 19, no. 6 (2007): 2064-76.

Shin, Yu-Jin, Woo-Mi Lee, Jin Il Kwak, and Youn-Joo An. "Dissolution of Zinc Oxide Nanoparticles in Exposure Media of Algae, Daphnia, and Fish Embryos for Nanotoxicological Testing." *Chemistry and Ecology* 34, no. 3 (2018/03/16 2018): 229-40.

Siemianowski, Oskar, Anna Barabasz, Aleksandra Weremczuk, Anna Ruszczynska, Ewa Bulska, Lorraine Elizabeth Williams, and Danuta Maria Antosiewicz. "Development of Zn-Related Necrosis in Tobacco Is Enhanced by Expressing Athma4 and Depends on the Apoplastic Zn Levels." *Plant Cell and Environment* 36, no. 6 (Jun 2013): 1093-104.

Sinclair, S. A., and U. Kramer. "The Zinc Homeostasis Network of Land Plants." *Biochimica Et Biophysica Acta-Molecular Cell Research* 1823, no. 9 (Sep 2012): 1553-67.

Sinclair, Scott A., Sarah M. Sherson, Renee Jarvis, James Camakaris, and Christopher S. Cobbett. "The Use of the Zinc-Fluorophore, Zinpyr-1, in the Study of Zinc Homeostasis in Arabidopsis Roots." *New Phytologist* 174, no. 1 (2007 2007): 39-45.

Slomberg, Danielle L., and Mark H. Schoenfisch. "Silica Nanoparticle Phytotoxicity to Arabidopsis Thaliana." *Environmental Science & Technology* 46, no. 18 (Sep 18 2012): 10247-54.

Song, W. Y., G. L. Wang, L. L. Chen, H. S. Kim, L. Y. Pi, T. Holsten, J. Gardner, *et al.* "A Receptor Kinase-Like Protein Encoded by the Rice Disease Resistance Gene, Xa21." *Science* 270, no. 5243 (Dec 15 1995): 1804-06.

Stintzi, A., T. Heitz, V. Prasad, S. Wiedemann-Merdinoglu, S. Kauffmann, P. Geoffroy, M. Legrand, and B. Fritig. "Plant 'Pathogenesis-Related' Proteins and Their Role in Defense against Pathogens." [In eng]. *Biochimie* 75, no. 8 (1993): 687-706.

Su, MY, C Liu, CX Qu, L Zheng, L Chen, H Huang, XQ Liu, X Wu, and FS Hong. "Nano-Anatase Relieves the Inhibition of Electron Transport Caused by Linolenic Acid in Chloroplasts of Spinach." [In English]. *Biological Trace Element Research* (APR 2008 2008): 73-81.

Su, MY, J Liu, ST Yin, LL Ma, and FS Hong. "Effects of Nanoanatase on the Photosynthetic Improvement of Chloroplast Damaged by Linolenic Acid." [In English]. *Biological Trace Element Research* (AUG 2008 2008): 173-83.

Sutradhar, Apurba K., Daniel E. Kaiser, Carl J. Rosen, and J ohn A. Lamb. "Zinc for Crop Production." University of Minnesota Extension, https://www.extension.umn.edu/agriculture/nutrient-management/micronutrients/zinc-for-crop-production/.

Szklarczyk, Damian, Andrea Franceschini, Stefan Wyder, Kristoffer Forslund, Davide Heller, Jaime Huerta-Cepas, Milan Simonovic, *et al.* "String V10: Protein–Protein Interaction Networks, Integrated over the Tree of Life." *Nucleic acids research* 43, no. D1 (2014): D447-D52.

Taccola, Liuba, Vittoria Raffa, Cristina Riggio, Orazio Vittorio, Maria Carla Iorio, Renato Vanacore, Andrea Pietrabissa, and Alfred Cuschieri. "Zinc Oxide Nanoparticles as Selective Killers of Proliferating Cells." *International Journal of Nanomedicine* 6 (05/30

05/28/received 2011): 1129-40.

Takahashi, Ryuichi, Khurram Bashir, Yasuhiro Ishimaru, Naoko K. Nishizawa, and Hiromi Nakanishi. "The Role of Heavy-Metal Atpases, Hmas, in Zinc and Cadmium Transport in Rice." *Plant signaling & behavior* 7, no. 12 (2012): 1605-07.

Tang, Xiwei, Jianxin Wang, Jiancheng Zhong, and Yi Pan. "Predicting Essential Proteins Based on Weighted Degree Centrality." *IEEE/ACM Transactions on Computational Biology and Bioinformatics (TCBB)* 11, no. 2 (2014): 407-18.

Tekauz, A. "A Numerical Scale to Classify Reactions of Barley to Pyrenophora Teres." *Canadian Journal of Plant Pathology* 7, no. 2 (1985): 181-83.

Thakur, Sveta, Lakhveer Singh, Zularisam Ab Wahid, Muhammad Faisal Siddiqui, Samson Mekbib Atnaw, and Mohd Fadhil Md Din. "Plant-Driven Removal of Heavy Metals from Soil: Uptake, Translocation, Tolerance Mechanism, Challenges, and Future Perspectives." *Environmental Monitoring and Assessment* 188, no. 4 (2016/03/03 2016): 206.

Thaler, Jennifer S., Blythe Owen, and Verna J. Higgins. "The Role of the Jasmonate Response in Plant Susceptibility to Diverse Pathogens with a Range of Lifestyles." *Plant Physiology* 135, no. 1 (2004): 530-38.

Trail, Frances. "For Blighted Waves of Grain: <Em>Fusarium Graminearum</Em> in the Postgenomics Era." *Plant Physiology* 149, no. 1 (2009): 103.

Trumbo, P., A. A. Yates, S. Schlicker, and M. Poos. "Dietary Reference Intakes: Vitamin a, Vitamin K, Arsenic, Boron, Chromium, Copper, Iodine, Iron, Manganese, Molybdenum, Nickel, Silicon, Vanadium, and Zinc." *Journal of the American Dietetic Association* 101, no. 3 (Mar 2001): 294-301.

Tumburu, L., C. P. Andersen, P. T. Rygiewicz, and J. R. Reichman. "Molecular and Physiological Responses to Titanium Dioxide and Cerium Oxide Nanoparticles in Arabidopsis." *Environmental Toxicology and Chemistry* 36, no. 1 (Jan 2017): 71-82.

Typas, Athanasios, and Victor Sourjik. "Bacterial Protein Networks: Properties and Functions." *Nature Reviews Microbiology* 13, no. 9 (2015): 559.

Umar, Huzaifa, Doga Kavaz, and Nahit Rizaner. "Biosynthesis of Zinc Oxide Nanoparticles Using Albizia Lebbeck Stem Bark, and Evaluation of Its Antimicrobial, Antioxidant, and Cytotoxic Activities on Human Breast Cancer Cell Lines." *International journal of nanomedicine* 14 (2018): 87-100.

Van der Does, Dieuwertje, Antonio Leon-Reyes, Annemart Koornneef, Marcel C. Van Verk, Nicole Rodenburg, Laurens Pauwels, Alain Goossens, *et al.* "Salicylic Acid Suppresses Jasmonic Acid Signaling Downstream of Scfcoi1-Jaz by Targeting Gcc Promoter Motifs Via Transcription Factor Ora59." *The Plant Cell* 25, no. 2 (2013): 744-61.

Van Steveninck, R. F. M., A. Babare, D. R. Fernando, and M. E. Van Steveninck. "The Binding of Zinc in Root Cells of Crop Plants by Phytic Acid." *Plant and Soil* 155, no. 1 (1993/10/01 1993): 525-28.

van Steveninck, R. F. M., A. Babare, D. R. Fernando, and M. E. van Steveninck. "The Binding of Zinc, but Not Cadmium, by Phytic Acid in Roots of Crop Plants." *Plant and Soil* 167, no. 1 (1994/11/01 1994): 157-64.

van Verk, Marcel C., John F. Bol, and Huub J. M. Linthorst. "Wrky Transcription Factors Involved in Activation of Sa Biosynthesis Genes." *BMC Plant Biology* 11, no. 1 (2011/05/19 2011): 89.

Vankova, R., P. Landa, R. Podlipna, P. I. Dobrev, S. Prerostova, L. Langhansova, A. Gaudinova, *et al.* "Zno Nanoparticle Effects on Hormonal Pools in Arabidopsis Thaliana." [In eng]. *Sci Total Environ* 593-594 (Sep 1 2017): 535-42.

Vogiatzis, Chrysafis, and Mustafa Can Camur. "Identification of Essential Proteins Using Induced Stars in Protein-Protein Interaction Networks." *arXiv preprint arXiv:1708.00574* (2017).

Wang, Jianxin, Min Li, Huan Wang, and Yi Pan. "Identification of Essential Proteins Based on Edge Clustering Coefficient." *IEEE/ACM Transactions on Computational Biology and Bioinformatics (TCBB)* 9, no. 4 (2012): 1070-80.

Wang, X. Q., and D. L. Kaplan. "Functionalization of Silk Fibroin with Neutravidin and Biotin." *Macromolecular Bioscience* 11, no. 1 (Jan 2011): 100-10.

Wang, Yue-Hong, Chun-Qin Zou, Zakaria Mirza, Hong Li, Zhen-Zhen Zhang, Dan-Ping Li, Chun-Li Xu, *et al.* "Cost of Agronomic Biofortification of Wheat with Zinc in China." *Agronomy for Sustainable Development* 36, no. 3 (2016/07/25 2016): 44.

Wang, Z., M. Gerstein, and M. Snyder. "Rna-Seq: A Revolutionary Tool for Transcriptomics." *Nature Reviews Genetics* 10, no. 1 (Jan 2009): 57-63.

Wang, Z. Y., X. Y. Xie, J. Zhao, X. Y. Liu, W. Q. Feng, J. C. White, and B. S. Xing. "Xylem- and Phloem-Based Transport of Cuo Nanoparticles in Maize (Zea Mays L.)." *Environmental Science & Technology* 46, no. 8 (Apr 2012): 4434-41.

"Xylem- and Phloem-Based Transport of Cuo Nanoparticles in Maize (Zea Mays L.)." *Environmental Science & Technology* 46, no. 8 (Apr 2012): 4434-41.

Wang, Z. Y., L. N. Xu, J. Zhao, X. K. Wang, J. C. White, and B. S. Xing. "Cuo Nanoparticle Interaction with Arabidopsis Thaliana: Toxicity, Parent-Progeny Transfer, and Gene Expression." *Environmental Science & Technology* 50, no. 11 (Jun 2016): 6008-16.

Waters, Brian M., Heng-Hsuan Chu, Raymond J. DiDonato, Louis A. Roberts, Robynn B. Eisley, Brett Lahner, David E. Salt, and Elsbeth L. Walker. "Mutations in Arabidopsis Yellow Stripe-Like1 and Yellow Stripe-Like3 Reveal Their Roles in Metal Ion Homeostasis and Loading of Metal Ions in Seeds." *Plant physiology* 141, no. 4 (2006): 1446-58.

White, Philip J., and Duncan J. Greenwood. "Properties and Management of Cationic Elements for Crop Growth." *Soil Conditions and Plant Growth* (2013): 160-94.

Wiese, J., T. Kranz, and S. Schubert. "Induction of Pathogen Resistance in Barley by Abiotic Stress." *Plant Biology* 6, no. 5 (2004): 529-36.

Wittek, Finni, Basem Kanawati, Marion Wenig, Thomas Hoffmann, Katrin Franz-Oberdorf, Wilfried Schwab, Philippe Schmitt-Kopplin, and A. Corina Vlot. "Folic Acid Induces Salicylic Acid-Dependent Immunity in Arabidopsis and Enhances Susceptibility to Alternaria Brassicicola." *Molecular Plant Pathology* 16, no. 6 (2015/08/01 2015): 616-22.

"World Health Statistics." 2013.

Xenarios, Ioannis, Lukasz Salwinski, Xiaoqun Joyce Duan, Patrick Higney, Sul-Min Kim, and David Eisenberg. "Dip, the Database of Interacting Proteins: A Research Tool for Studying Cellular Networks of Protein Interactions." *Nucleic acids research* 30, no. 1 (2002): 303-05.

Xia, Yan, Shengjie Yin, Kaili Zhang, Xiaoting Shi, Chunlan Lian, Hongsheng Zhang, Zhubing Hu, and Zhenguo Shen. "Oswak11, a Rice Wall-Associated Kinase, Regulates Cu Detoxification by Alteration the Immobilization of Cu in Cell Walls." *Environmental and Experimental Botany* 150 (2018/06/01/ 2018): 99-105.

Yang, Li, Bosheng Li, Xiao-yu Zheng, Jigang Li, Mei Yang, Xinnian Dong, Guangming He, Chengcai An, and Xing Wang Deng. "Salicylic Acid Biosynthesis Is Enhanced and Contributes to Increased Biotrophic Pathogen Resistance in Arabidopsis Hybrids." *Nature communications* 6 (2015): 7309.

Yoon, Sung-Ji, Jin Il Kwak, Woo-Mi Lee, Patricia A. Holden, and Youn-Joo An. "Zinc Oxide Nanoparticles Delay Soybean Development: A Standard Soil Microcosm Study." *Ecotoxicology and Environmental Safety* 100 (Feb 2014): 131-37.

Yuan, J., A. F. He, S. D. Huang, J. Hua, and G. D. Sheng. "Internalization and Phytotoxic Effects of Cuo Nanoparticles in Arabidopsis Thaliana as Revealed by Fatty Acid Profiles." *Environmental Science & Technology* 50, no. 19 (Oct 2016): 10437-47.

"Internalization and Phytotoxic Effects of Cuo Nanoparticles in Arabidopsis Thaliana as Revealed by Fatty Acid Profiles." *Environmental Science & Technology* 50, no. 19 (Oct 2016): 10437-47.

Yue, Le, Chuanxin Ma, Xinhua Zhan, Jason C. White, and Baoshan Xing. "Molecular Mechanisms of Maize Seedling Response to La 2 O 3 Np Exposure: Water Uptake, Aquaporin Gene Expression and Signal Transduction." *Environmental Science: Nano* 4, no. 4 (2017): 843-55.

Zafar, Hira, Attarad Ali, Joham S. Ali, Ihsan U. Haq, and Muhammad Zia. "Effect of Zno Nanoparticles on Brassica Nigra Seedlings and Stem Explants: Growth Dynamics and Antioxidative Response." *Frontiers in plant science* 7 (2016): 535.

Zengin, Fikriye. "Exogenous Treatment with Salicylic Acid Alleviating Copper Toxicity in Bean Seedlings." *Proceedings of the National Academy of Sciences, India Section B: Biological Sciences* 84, no. 3 (2014): 749-55.

Zhai, Guangshu, Katherine S. Walters, David W. Peate, Pedro J. J. Alvarez, and Jerald L. Schnoor. "Transport of Gold Nanoparticles through Plasmodesmata and Precipitation of Gold Ions in Woody Poplar." *Environmental Science & Technology Letters* 1, no. 2 (Feb 2014): 146-51.

"Transport of Gold Nanoparticles through Plasmodesmata and Precipitation of Gold Ions in Woody Poplar." *Environmental Science & Technology Letters* 1, no. 2 (Feb 2014): 146-51.

Zhang, Jiyu, Xiaoli Du, Qingju Wang, Xiukong Chen, Dong Lv, Kuanyong Xu, Shenchun Qu, and Zhen Zhang. "Expression of Pathogenesis Related Genes in Response to Salicylic Acid, Methyl Jasmonate and 1-Aminocyclopropane-1-Carboxylic Acid in Malus Hupehensis (Pamp.) Rehd." *BMC research notes* 3 (2010): 208-08.

Zhang, L. W., and N. A. Monteiro-Riviere. "Mechanisms of Quantum Dot Nanoparticle Cellular Uptake." *Toxicological Sciences* 110, no. 1 (Jul 2009): 138-55.

Zhang, R., H. Zhang, C. Tu, X. Hu, L. Li, Y. Luo, and P. Christie. "Phytotoxicity of Zno Nanoparticles and the Released Zn(Ii) Ion to Corn (Zea Mays L.) and Cucumber (Cucumis Sativus L.) During Germination." [In eng]. *Environ Sci Pollut Res Int* 22, no. 14 (Jul 2015): 11109-17.

Zhao, L. J., Y. P. Sun, J. A. Hernandez-Viezcas, A. D. Servin, J. Hong, G. H. Niu, J. R. Peralta-Videa, M. Duarte-Gardea, and J. L. Gardea-Torresdey. "Influence of Ceo2 and Zno Nanoparticles on Cucumber Physiological Markers and Bioaccumulation of Ce and Zn: A Life Cycle Study." *Journal of Agricultural and Food Chemistry* 61, no. 49 (Dec 2013): 11945-51.

Zhao, Lijuan, Jose R. Peralta-Videa, Minghua Ren, Armando Varela-Ramirez, Chunqiang Li, Jose A. Hernandez-Viezcas, Renato J. Aguilera, and Jorge L. Gardea-Torresdey. "Transport of Zn in a Sandy Loam Soil Treated with Zno Nps and Uptake by Corn Plants: Electron Microprobe and Confocal Microscopy Studies." *Chemical Engineering Journal* 184 (2012/03/01/ 2012): 1-8.

Zhu, Zheng-Jiang, Huanhua Wang, Bo Yan, Hao Zheng, Ying Jiang, Oscar R. Miranda, Vincent M. Rotello, Baoshan Xing, and Richard W. Vachet. "Effect of Surface Charge on the Uptake and Distribution of Gold Nanoparticles in Four Plant Species." *Environmental Science & Technology* 46, no. 22 (Nov 20 2012): 12391-98.

"Zinc." National Institutes of Health, Office of Dietary Supplements.

APPENDIX C

Table C1. GO terms enriched in biological processes in (a) 6 hpa ZnO NP treatment, and (b) 48 hpa ZnO NP, (c) 6 hpa $ZnSO_4$, and (d) 48 hpa $ZnSO_4$ expression data using TopGO.

(a) 6 hpa ZnO NP

	GO.ID	Term	p-value
Upregulated	GO:0006412	translation	2.10E-14
	GO:0042254	ribosome biogenesis	4.70E-09
	GO:0000028	ribosomal small subunit assembly	0.00029
	GO:0006334	nucleosome assembly	0.00194
	GO:0051290	protein heterotetramerization	0.00233
	GO:0070544	histone H3-K36 demethylation	0.00233
	GO:1901671	positive regulation of superoxide dismut...	0.00233
	GO:0042752	regulation of circadian rhythm	0.00039
	GO:0000447	endonucleolytic cleavage in ITS1 to sepa...	0.00465
	GO:0000461	endonucleolytic cleavage to generate mat...	0.00465
Downregulated	GO:0010100	negative regulation of photomorphogenesis	1.20E-05
	GO:0009768	photosynthesis, light harvesting in phot...	9.30E-05
	GO:0015995	chlorophyll biosynthetic process	9.80E-05
	GO:0009611	response to wounding	0.0002
	GO:0010017	red or far-red light signaling pathway	2.30E-05
	GO:0007623	circadian rhythm	2.00E-05
	GO:0009769	photosynthesis, light harvesting in phot...	0.00065
	GO:0018298	protein-chromophore linkage	0.00066
	GO:0009723	response to ethylene	0.00022
	GO:0009266	response to temperature stimulus	0.00039

Table C1. GO terms enriched in biological processes in (a) 6 hpa ZnO NP treatment, and (b) 48 hpa ZnO NP, (c) 6 hpa $ZnSO_4$, and (d) 48 hpa $ZnSO_4$ expression data using TopGO (continued)

(b) 48 hpa ZnO NP

	GO.ID	Term	p-value
Downregulated	GO:0009611	response to wounding	8.80E-05
	GO:0080167	response to karrikin	0.0013
	GO:0050691	regulation of defense response to virus ...	0.0034
	GO:0032544	plastid translation	0.005
	GO:0045727	positive regulation of translation	0.0059
	GO:1903507	negative regulation of nucleic acid-temp...	0.0042
	GO:0018119	peptidyl-cysteine S-nitrosylation	0.0067
	GO:0042742	defense response to bacterium	0.0102
	GO:2000022	regulation of jasmonic acid mediated sig...	0.0104
	GO:0002237	response to molecule of bacterial origin	0.0109

(c) 6 hpa $ZnSO_4$

	GO.ID	Term	p-value
Upregulated	GO:0006412	translation	4.80E-13
	GO:0042254	ribosome biogenesis	3.90E-10
	GO:0000028	ribosomal small subunit assembly	0.00031
	GO:0070544	histone H3-K36 demethylation	0.0024
	GO:1990592	protein K69-linked ufmylation	0.0024
	GO:0042752	regulation of circadian rhythm	0.00043
	GO:0000447	endonucleolytic cleavage in ITS1 to sepa...	0.0048
	GO:0000461	endonucleolytic cleavage to generate mat...	0.0048
	GO:0006407	rRNA export from nucleus	0.0048
	GO:0010265	SCF complex assembly	0.0048
Downregulated	GO:0009768	photosynthesis, light harvesting in photosystem	1.40E-10
	GO:0018298	protein-chromophore linkage	9.40E-09
	GO:0071483	cellular response to blue light	8.80E-05
	GO:0071472	cellular response to salt stress	0.0002
	GO:0009723	response to ethylene	0.0048
	GO:0009769	photosynthesis, light harvesting in photosystem	0.00053
	GO:0010100	negative regulation of photomorphogenesis	0.00077
	GO:0009409	response to cold	7.10E-05
	GO:0010218	response to far red light	0.00126

Table C1. GO terms enriched in biological processes in (a) 6 hpa ZnO NP treatment, and (b) 48 hpa ZnO NP, (c) 6 hpa $ZnSO_4$, and (d) 48 hpa $ZnSO_4$ expression data using TopGO (continued)

(d) 48 hpa $ZnSO_4$

48 h ZnSO4	GO.ID	Term	p-value
Upregulated	GO:0000463	maturation of LSU-rRNA from tricistronic...	0.00023
	GO:2000232	regulation of rRNA processing	0.00023
	GO:1900864	mitochondrial RNA modification	0.0029
	GO:0009414	response to water deprivation	0.02661
	GO:0009409	response to cold	0.02992
	GO:0009651	response to salt stress	0.04355
	GO:0000470	maturation of LSU-rRNA	0.00084
	GO:0000959	mitochondrial RNA metabolic process	0.00381
	GO:0001101	response to acid chemical	0.09312
	GO:0006139	nucleobase-containing compound metabolic...	0.02431
Downregulated	GO:0009611	response to wounding	8.50E-06
	GO:0080167	response to karrikin	0.00019
	GO:0009768	photosynthesis, light harvesting in phot...	0.00118
	GO:0009715	chalcone biosynthetic process	0.00221
	GO:0019373	epoxygenase P450 pathway	0.00221
	GO:0018298	protein-chromophore linkage	0.00429
	GO:0019305	dTDP-rhamnose biosynthetic process	0.00442
	GO:0015709	thiosulfate transport	0.00662
	GO:0071422	succinate transmembrane transport	0.00662
	GO:0006696	ergosterol biosynthetic process	0.00882

Table C2. Common and exclusive DEGs (a) 6 hpa ZnO NP Upregulated Exclusive Genes, (b) 6 hpa $ZnSO_4$ Upregulated Exclusive Genes, (c) 6 hpa ZnO NP and $ZnSO_4$ Upregulated Common Genes, (d) 6 hpa ZnO NP and $ZnSO_4$ Downregulated Common Genes, (e) 6 hpa ZnO NPs Downregulated Exclusive Genes, and (f) 6 hpa $ZnSO_4$ Downregulated Exclusive Genes

(a) 6 hpa ZnO NPs Upregulated Exclusive Genes

16 elements included exclusively in "6 hpa ZnO NP up":	Annotation	Fold Change
HORVU6Hr1G000720	Thionin 2.2	24.5438
HORVU3Hr1G069590	Heat stress transcription factor C-1b	8.3844
HORVU6Hr1G072650	50S ribosomal protein L7Ae	7.9092
HORVU2Hr1G109370	Adenosylhomocysteinase	5.5763
HORVU1Hr1G021120	4-hydroxy-tetrahydrodipicolinate reductase	5.0074
HORVU5Hr1G097940	undescribed protein	4.8896
HORVU4Hr1G014910	Ankyrin repeat protein SKIP35	4.4890
HORVU3Hr1G084310	60S ribosomal protein L1-A	4.2564
HORVU1Hr1G093980	unknown function	4.1944
HORVU6Hr1G051930	nucleosome assembly protein 1;2	4.0058
HORVU7Hr1G067060	60S ribosomal protein L13-1	3.7053
HORVU7Hr1G110660	60S ribosomal protein L30	3.6290
HORVU7Hr1G033900	10 kDa chaperonin	3.5912
HORVU6Hr1G041750	60S ribosomal protein L6	3.5690
HORVU6Hr1G059420	YELLOW STRIPE like 7	3.2849
HORVU5Hr1G075500	60S ribosomal protein L32-1	3.0757

Table C2. Common and exclusive DEGs (a) 6 hpa ZnO NP Upregulated Exclusive Genes, (b) 6 hpa $ZnSO_4$ Upregulated Exclusive Genes, (c) 6 hpa ZnO NP and $ZnSO_4$ Upregulated Common Genes, (d) 6 hpa ZnO NP and $ZnSO_4$ Downregulated Common Genes, (e) 6 hpa ZnO NPs Downregulated Exclusive Genes, and (f) 6 hpa $ZnSO_4$ Downregulated Exclusive Genes (continued)

(b) 6 hpa $ZnSO_4$ Upregulated Exclusive Genes

24 elements included exclusively in "6 hpa $ZnSO_4$ up":	Annotation	Fold Change
HORVU5Hr1G051970	osmotin 34	586.7111
HORVU5Hr1G067760	Kiwellin	374.7201
HORVU5Hr1G005230	N/A	270.2074
HORVU3Hr1G113120	Wound-induced protein	200.8414
HORVU1Hr1G012000	undescribed protein	100.5369
HORVU3Hr1G113620	Wound-induced protein	96.6482
HORVU1Hr1G065150	undescribed protein	56.7405
HORVU0Hr1G000760	undescribed protein	34.3333
HORVU1Hr1G065660	undescribed protein	24.2476
HORVU7Hr1G114660	Indole-3-glycerol phosphate synthase	19.1301
HORVU0Hr1G003480	Organic cation/carnitine transporter 3	10.3073
HORVU4Hr1G086110	F-box protein PP2-B1	7.3182
HORVU7Hr1G042080	Zinc finger protein CONSTANS-LIKE 16	4.3565
HORVU2Hr1G075460	undescribed protein	4.3056
HORVU7Hr1G057640	50S ribosomal protein L23	3.8974
HORVU4Hr1G081100	Glutathione S-transferase family protein	3.8494
HORVU5Hr1G109910	30S ribosomal protein S5	3.5836
HORVU5Hr1G104380	evolutionarily conserved C-terminal region 3	3.5393
HORVU5Hr1G021140	Mitochondrial import inner membrane translocase subunit Tim9	3.5141
HORVU4Hr1G014130	40S ribosomal protein S27	3.4072
HORVU4Hr1G023570	30S ribosomal protein S9	3.3563
HORVU3Hr1G111740	Ubiquitin-fold modifier 1	3.3078
HORVU4Hr1G046530	undescribed protein	3.2931
HORVU2Hr1G019160	60S ribosomal protein L22-2	3.0881

Table C2. Common and exclusive DEGs (a) 6 hpa ZnO NP Upregulated Exclusive Genes, (b) 6 hpa $ZnSO_4$ Upregulated Exclusive Genes, (c) 6 hpa ZnO NP and $ZnSO_4$ Upregulated Common Genes, (d) 6 hpa ZnO NP and $ZnSO_4$ Downregulated Common Genes, (e) 6 hpa ZnO NPs Downregulated Exclusive Genes, and (f) 6 hpa $ZnSO_4$ Downregulated Exclusive Genes (continued)

(c) 6 hpa ZnO NP and $ZnSO_4$ Upregulated Common Genes

55 common elements in "6 hpa ZnO NP up" and "6 hpa $ZnSO_4$ up":	Annotation	Fold Change in 6 hpa ZnO NP	Fold Change in 6 hpa $ZnSO_4$
HORVU3Hr1G114970	Two-component response regulator ARR1	128.5331	152.6109
HORVU4Hr1G089560	Chromosome 3B, genomic scaffold, cultivar Chinese Spring	124.4096	124.6629
HORVU6Hr1G064000	undescribed protein	24.35693	25.74906
HORVU4Hr1G085250	Aquaporin-like superfamily protein	13.74826	13.75149
HORVU2Hr1G113180	N/A	8.92573	38.69721
HORVU7Hr1G046980	Mitochondrial glycoprotein family protein	7.942737	10.44052
HORVU1Hr1G073460	Tetratricopeptide repeat (TPR)-like superfamily protein	5.38723	7.663767
HORVU3Hr1G011460	Mitochondrial glycoprotein family protein	5.34543	5.932529
HORVU2Hr1G028510	Ribosomal protein S4	5.286618	6.524318
HORVU1Hr1G072060	30S ribosomal protein S8	5.283058	5.780174
HORVU2Hr1G127090	tubulin folding cofactor B	5.226579	5.320255
HORVU7Hr1G054380	glutamate-1-semialdehyde-2,1-aminomutase	4.81252	5.381587
HORVU5Hr1G106550	histone H1-3	4.46992	5.982512
HORVU3Hr1G001140	Ribosomal protein L6 family	4.403558	4.637297
HORVU5Hr1G045620	30S ribosomal protein S9	4.038597	4.791403
HORVU4Hr1G064020	50S ribosomal protein L7Ae	4.01018	4.286949
HORVU7Hr1G050170	60S ribosomal protein L31	3.932598	4.232041
HORVU2Hr1G053290	40S ribosomal protein S12	3.878453	3.880759
HORVU5Hr1G076700	60S ribosomal protein L7a	3.726825	3.751224
HORVU6Hr1G090070	60S ribosomal protein L37-2	3.674378	3.860978
HORVU4Hr1G074270	40S ribosomal protein S27	3.657053	3.83592
HORVU4Hr1G052610	NIFU-like protein 2	3.569676	3.789591
HORVU2Hr1G043220	60S ribosomal protein L38	3.536442	4.002387
HORVU7Hr1G002060	Ribosomal protein L6 family	3.500836	3.96498
HORVU2Hr1G075470	Protein kinase superfamily protein	3.403196	3.520264
HORVU4Hr1G075710	60S ribosomal protein L4-1	3.383402	3.751546

Table C2. Common and exclusive DEGs (a) 6 hpa ZnO NP Upregulated Exclusive Genes, (b) 6 hpa $ZnSO_4$ Upregulated Exclusive Genes, (c) 6 hpa ZnO NP and $ZnSO_4$ Upregulated Common Genes, (d) 6 hpa ZnO NP and $ZnSO_4$ Downregulated Common Genes, (e) 6 hpa ZnO NPs Downregulated Exclusive Genes, and (f) 6 hpa $ZnSO_4$ Downregulated Exclusive Genes (continued)

(c) 6 hpa ZnO NP and $ZnSO_4$ Upregulated Common Genes

55 common elements in "6 hpa ZnO NP up" and "6 hpa $ZnSO_4$ up":	Annotation	Fold Change in 6 hpa ZnO NP	Fold Change in 6 hpa $ZnSO_4$
HORVU7Hr1G052960	60S ribosomal protein L32-1	3.369184	3.478859
HORVU7Hr1G069460	HSP20-like chaperones superfamily protein isoform 1	3.345963	3.659661
HORVU4Hr1G077240	40s ribosomal protein SA	3.260914	3.869959
HORVU7Hr1G014140	40S ribosomal protein S20	3.249566	3.405812
HORVU2Hr1G102610	60S ribosomal protein L12	3.126354	3.173446
HORVU5Hr1G119700	prohibitin 1	3.059127	3.794261
HORVU7Hr1G017190	Hypersensitive-induced response protein 4	3.043186	3.144584
HORVU2Hr1G104580	At5g37260-like protein	118.7541	80.37911
HORVU5Hr1G038840	pumilio 7	100.2857	76.47004
HORVU7Hr1G050460	undescribed protein	95.06121	76.91564
HORVU4Hr1G077480	Cold regulated gene 27, putative isoform 2	45.39086	38.9258
HORVU5Hr1G073330	Lysine-specific demethylase 8	45.13739	40.20142
HORVU7Hr1G044250	undescribed protein	39.33851	37.69312
HORVU6Hr1G057630	Two-component response regulator-like PRR1	26.76508	24.79318
HORVU0Hr1G021850	Protein of unknown function (DUF581)	17.11619	17.07578
HORVU6Hr1G071950	Zinc finger protein CONSTANS-LIKE 10	17.00185	15.33294
HORVU0Hr1G018830	Cell division protein FtsZ	11.54671	10.14083
HORVU2Hr1G020690	Nucleolar protein 58	11.13607	10.90223
HORVU6Hr1G065240	undescribed protein	8.886774	8.653398
HORVU3Hr1G063700	Chromosome 3B, genomic scaffold, cultivar Chinese Spring	8.767938	7.080809
HORVU3Hr1G093400	RNA-binding protein 1	7.55641	7.203371
HORVU7Hr1G115780	30S ribosomal protein S5	6.877291	6.574795
HORVU3Hr1G055870	Neutral ceramidase	5.908216	5.534095
HORVU5Hr1G105870	60S ribosomal protein L4-1	4.561585	4.503041
HORVU1Hr1G079370	60S ribosomal protein L28-1	3.95187	3.862714
HORVU1Hr1G072270	60S ribosomal protein L36-2	3.481822	3.400313

HORVU2Hr1G089070	60S ribosomal protein L14-1	3.441095	3.304486
HORVU4Hr1G012770	mitochondrial import receptor subunit TOM5 homolog	3.328753	3.241333
HORVU2Hr1G104940	unknown function	3.030617	3.023442

Table C2. Common and exclusive DEGs (a) 6 hpa ZnO NP Upregulated Exclusive Genes, (b) 6 hpa $ZnSO_4$ Upregulated Exclusive Genes, (c) 6 hpa ZnO NP and $ZnSO_4$ Upregulated Common Genes, (d) 6 hpa ZnO NP and $ZnSO_4$ Downregulated Common Genes, (e) 6 hpa ZnO NPs Downregulated Exclusive Genes, and (f) 6 hpa $ZnSO_4$ Downregulated Exclusive Genes (continued)

(d) 6 hpa ZnO NP and $ZnSO_4$ Downregulated Common Genes

76 common elements in "6 hpa ZnO NP down" and "6 hpa $ZnSO_4$ down":	Annotation	Fold Change in 6 hpa ZnO NP	Fold Change in 6 hpa $ZnSO_4$
HORVU6Hr1G025110	Elongation factor 4	-3.02391	-3.65907
HORVU4Hr1G028910	beta glucosidase 42	-3.35932	-4.09581
HORVU3Hr1G087850	Internal alternative NAD(P)H-ubiquinone oxidoreductase A1, mitochondrial	-3.60745	-4.04972
HORVU3Hr1G065960	Farnesyl pyrophosphate synthase	-3.88019	-5.06252
HORVU3Hr1G089390	Protein of unknown function (DUF1685)	-4.36349	-4.68578
HORVU6Hr1G033290	MLO-like protein 1	-4.42798	-9.25418
HORVU3Hr1G042680	dentin sialophosphoprotein-related.	-4.44373	-5.45674
HORVU2Hr1G077640	undescribed protein	-4.55082	-6.76
HORVU6Hr1G050440	senescence-associated family protein	-4.80449	-5.91427
HORVU5Hr1G081620	Two-component response regulator-like PRR95	-5.35168	-6.9043
HORVU4Hr1G087610	Transcription factor bHLH35	-5.35877	-8.87085
HORVU2Hr1G023560	Magnesium-chelatase subunit H	-6.05897	-7.33019
HORVU1Hr1G018720	unknown protein; BEST Arabidopsis thaliana protein match is: unknown protein .	-6.2289	-7.05083
HORVU2Hr1G078840	Mitochondrial uncoupling protein 3	-6.37066	-9.66671
HORVU1Hr1G070190	Nodulin-like / Major Facilitator Superfamily protein	-6.56708	-7.64275
HORVU2Hr1G077650	ferric reduction oxidase 7	-6.76023	-9.21114
HORVU6Hr1G073180	methyltransferase type 11	-6.85867	-7.09935
HORVU7Hr1G120660	PHYTOENE SYNTHASE	-6.9888	-8.66541
HORVU3Hr1G069290	Chaperone protein DnaJ	-7.5389	-9.04355
HORVU1Hr1G088870	Chlorophyll a-b binding protein, chloroplastic	-8.20865	-13.9817

Table C2. Common and exclusive DEGs (a) 6 hpa ZnO NP Upregulated Exclusive Genes, (b) 6 hpa $ZnSO_4$ Upregulated Exclusive Genes, (c) 6 hpa ZnO NP and $ZnSO_4$ Upregulated Common Genes, (d) 6 hpa ZnO NP and $ZnSO_4$ Downregulated Common Genes, (e) 6 hpa ZnO NPs Downregulated Exclusive Genes, and (f) 6 hpa $ZnSO_4$ Downregulated Exclusive Genes (continued)

(d) 6 hpa ZnO NP and $ZnSO_4$ Downregulated Common Genes (continued)

76 common elements in "6 hpa ZnO NP down" and "6 hpa $ZnSO_4$ down":	Annotation	Fold Change in 6 hpa ZnO NP	Fold Change in 6 hpa $ZnSO_4$
HORVU1Hr1G093180	RNA polymerase sigma-B factor	-8.34533	-15.6956
HORVU2Hr1G106410	Glycogen synthase 1	-8.36047	-34.9218
HORVU2Hr1G040780	Chlorophyll a-b binding protein 13, chloroplastic	-8.92441	-9.57575
HORVU6Hr1G066000	myb-like transcription factor family protein	-9.12164	-10.1779
HORVU2Hr1G062910	unknown function	-9.12527	-23.5385
HORVU3Hr1G006270	Chromosome 3B, genomic scaffold, cultivar Chinese Spring	-10.2741	-21.8718
HORVU2Hr1G123750	glutathione peroxidase 6	-10.4168	-13.9522
HORVU2Hr1G085000	B-box zinc finger family protein	-10.7947	-27.1238
HORVU5Hr1G087250	Chlorophyll a-b binding protein 2, chloroplastic	-10.9932	-11.5213
HORVU6Hr1G030910	B-box type zinc finger family protein	-11.4396	-13.0957
HORVU5Hr1G081190	B-box zinc finger family protein	-12.5653	-14.4255
HORVU4Hr1G040290	unknown function	-14.3712	-17.2062
HORVU1Hr1G057860	N/A	-14.3893	-16.2961
HORVU3Hr1G040870	unknown function	-14.4439	-16.0691
HORVU1Hr1G089180	Chlorophyll a-b binding protein, chloroplastic	-15.911	-26.0211
HORVU4Hr1G075730	unknown function	-16.8116	-20.2193
HORVU4Hr1G073090	Protochlorophyllide reductase A, chloroplastic	-21.0847	-42.79
HORVU2Hr1G119050	Protochlorophyllide reductase A, chloroplastic	-23.8397	-34.6164
HORVU7Hr1G070900	undescribed protein	-25.7262	-34.8113
HORVU5Hr1G086670	Flavin-binding monooxygenase family protein	-27.0941	-31.586
HORVU2Hr1G119080	undescribed protein	-27.1188	-30.2598
HORVU2Hr1G119090	Protochlorophyllide reductase A, chloroplastic	-27.286	-36.8352

Table C2. Common and exclusive DEGs (a) 6 hpa ZnO NP Upregulated Exclusive Genes, (b) 6 hpa $ZnSO_4$ Upregulated Exclusive Genes, (c) 6 hpa ZnO NP and $ZnSO_4$ Upregulated Common Genes, (d) 6 hpa ZnO NP and $ZnSO_4$ Downregulated Common Genes, (e) 6 hpa ZnO NPs Downregulated Exclusive Genes, and (f) 6 hpa $ZnSO_4$ Downregulated Exclusive Genes (continued)

(d) 6 hpa ZnO NP and $ZnSO_4$ Downregulated Common Genes (continued)

76 common elements in "6 hpa ZnO NP down" and "6 hpa $ZnSO_4$ down":	Annotation	Fold Change in 6 hpa ZnO NP	Fold Change in 6 hpa $ZnSO_4$
HORVU5Hr1G109260	Chlorophyll a-b binding protein, chloroplastic	-28.3994	-31.5064
HORVU6Hr1G091650	Chlorophyll a-b binding protein, chloroplastic	-29.7545	-50.2561
HORVU7Hr1G040370	Chlorophyll a-b binding protein, chloroplastic	-30.0545	-60.0369
HORVU1Hr1G078380	Chlorophyll a-b binding protein, chloroplastic	-30.3985	-53.307
HORVU1Hr1G088900	Chlorophyll a-b binding protein, chloroplastic	-35.8982	-53.538
HORVU5Hr1G109250	Chlorophyll a-b binding protein, chloroplastic	-46.2751	-61.1892
HORVU7Hr1G070870	circadian clock associated 1	-51.2525	-68.0335
HORVU0Hr1G016540	Ethylene-responsive transcription factor 4	-51.8682	-69.8952
HORVU6Hr1G016850	Chlorophyll a-b binding protein, chloroplastic	-73.2567	-89.6972
HORVU6Hr1G016940	Chlorophyll a-b binding protein, chloroplastic	-75.4525	-177.262
HORVU7Hr1G040380	Chlorophyll a-b binding protein, chloroplastic	-78.4138	-166.714
HORVU6Hr1G016890	Chlorophyll a-b binding protein, chloroplastic	-90.7612	-172.156
HORVU6Hr1G016880	Chlorophyll a-b binding protein, chloroplastic	-94.7919	-210.598
HORVU1Hr1G088920	Chlorophyll a-b binding protein, chloroplastic	-99.3718	-177.317
HORVU7Hr1G095810	mitogen-activated protein kinase 16	-3.42466	-3.14552
HORVU4Hr1G010410	4-hydroxy-3-methylbut-2-enyl diphosphate reductase	-4.0677	-3.57515
HORVU2Hr1G023450	Carboxypeptidase Y homolog A	-4.30449	-3.97978
HORVU3Hr1G089370	Protein of unknown function (DUF1685)	-4.64267	-4.46598
HORVU7Hr1G037180	Ethylene-responsive transcription factor 1A	-5.38586	-5.10204

Table C2. Common and exclusive DEGs (a) 6 hpa ZnO NP Upregulated Exclusive Genes, (b) 6 hpa $ZnSO_4$ Upregulated Exclusive Genes, (c) 6 hpa ZnO NP and $ZnSO_4$ Upregulated Common Genes, (d) 6 hpa ZnO NP and $ZnSO_4$ Downregulated Common Genes, (e) 6 hpa ZnO NPs Downregulated Exclusive Genes, and (f) 6 hpa $ZnSO_4$ Downregulated Exclusive Genes (continued)

(d) 6 hpa ZnO NP and $ZnSO_4$ Downregulated Common Genes (continued)

76 common elements in "6 hpa ZnO NP down" and "6 hpa $ZnSO_4$ down":	Annotation	Fold Change in 6 hpa ZnO NP	Fold Change in 6 hpa $ZnSO_4$
HORVU4Hr1G014270	Protein of unknown function (DUF1685)	-5.54346	-4.89618
HORVU7Hr1G098660	Fe/S biogenesis protein NfuA	-5.84627	-5.30958
HORVU4Hr1G025010	undescribed protein	-6.08631	-4.47484
HORVU1Hr1G072890	unknown function	-6.6405	-4.05459
HORVU7Hr1G116890	Chaperone protein DnaJ 1	-6.68537	-5.75591
HORVU2Hr1G029900	Protein kinase superfamily protein	-7.09181	-5.30733
HORVU0Hr1G016780	Cytochrome P450 superfamily protein	-7.13655	-5.1112
HORVU1Hr1G086930	Chromosome 3B, genomic scaffold, cultivar Chinese Spring	-7.30878	-6.31925
HORVU0Hr1G031850	myb-like transcription factor family protein	-8.68017	-8.22914
HORVU3Hr1G089380	Protein of unknown function (DUF1685)	-8.81608	-6.64184
HORVU1Hr1G088880	Chlorophyll a-b binding protein, chloroplastic	-13.5147	-11.1179
HORVU5Hr1G014170	Basic-leucine zipper (bZIP) transcription factor family protein	-15.6461	-12.7134
HORVU5Hr1G036150	undescribed protein	-19.0669	-12.8724
HORVU3Hr1G114250	unknown function	-19.9246	-9.04397
HORVU7Hr1G121210	At5g37260-like protein	-22.2182	-18.0583

Table C2. Common and exclusive DEGs (a) 6 hpa ZnO NP Upregulated Exclusive Genes, (b) 6 hpa $ZnSO_4$ Upregulated Exclusive Genes, (c) 6 hpa ZnO NP and $ZnSO_4$ Upregulated Common Genes, (d) 6 hpa ZnO NP and $ZnSO_4$ Downregulated Common Genes, (e) 6 hpa ZnO NPs Downregulated Exclusive Genes, and (f) 6 hpa $ZnSO_4$ Downregulated Exclusive Genes (continued)

(e) 6 hpa ZnO NPs Downregulated Exclusive Genes

58 elements included exclusively in "6 hpa ZnO NP down":	Annotation	Fold Change
HORVU5Hr1G005980	cysteine synthase D1	-3.0750
HORVU2Hr1G066430	Retrotransposon protein, putative, unclassified	-3.0765
HORVU6Hr1G014480	adenylate kinase family protein	-3.2563
HORVU4Hr1G071360	Cytochrome b561 and DOMON domain-containing protein	-3.2909
HORVU4Hr1G057550	pseudo-response regulator 7	-3.3053
HORVU4Hr1G013170	Subtilisin-like protease	-3.3387
HORVU1Hr1G036920	Heavy metal transport/detoxification superfamily protein	-3.5397
HORVU2Hr1G039070	calcium-dependent protein kinase 19	-3.6027
HORVU6Hr1G084190	trehalose phosphate synthase	-3.6041
HORVU5Hr1G093310	basic helix-loop-helix (bHLH) DNA-binding superfamily protein	-3.6105
HORVU7Hr1G024670	GDSL esterase/lipase	-3.6106
HORVU6Hr1G071190	Eukaryotic aspartyl protease family protein	-3.6212
HORVU6Hr1G014700	calcium-dependent protein kinase 28	-3.7427
HORVU3Hr1G013840	Metallothioneine type2	-3.9034
HORVU0Hr1G005210	Protein of unknown function, DUF584	-4.0676
HORVU2Hr1G098110	nudix hydrolase homolog 8	-4.0916
HORVU7Hr1G085350	F-box/kelch-repeat protein	-4.1414
HORVU3Hr1G025430	undescribed protein	-4.2157
HORVU2Hr1G013400	pseudo-response regulator 7	-4.2390
HORVU5Hr1G111590	NAC domain protein,	-4.3854
HORVU5Hr1G070290	Peroxidase superfamily protein	-4.4614
HORVU4Hr1G017390	Eukaryotic aspartyl protease family protein	-4.5945
HORVU3Hr1G034980	alpha/beta-Hydrolases superfamily protein	-4.6555
HORVU4Hr1G006100	Haloacid dehalogenase-like hydrolase (HAD) superfamily protein	-4.7451
HORVU3Hr1G064640	AP2/B3 transcription factor family protein	-4.8234
HORVU1Hr1G060880	undescribed protein	-4.8366
HORVU3Hr1G042650	Reverse transcriptase	-5.0305
HORVU3Hr1G088200	WRKY DNA-binding protein 33	-5.1608

Table C2. Common and exclusive DEGs (a) 6 hpa ZnO NP Upregulated Exclusive Genes, (b) 6 hpa $ZnSO_4$ Upregulated Exclusive Genes, (c) 6 hpa ZnO NP and $ZnSO_4$ Upregulated Common Genes, (d) 6 hpa ZnO NP and $ZnSO_4$ Downregulated Common Genes, (e) 6 hpa ZnO NPs Downregulated Exclusive Genes, and (f) 6 hpa $ZnSO_4$ Downregulated Exclusive Genes (continued)

(e) 6 hpa ZnO NPs Downregulated Exclusive Genes (continued)

58 elements included exclusively in "6 hpa ZnO NP down":	Annotation	Fold Change
HORVU1Hr1G020410	1-aminocyclopropane-1-carboxylate oxidase	-5.2076
HORVU6Hr1G058820	phenylalanine ammonia-lyase 2	-5.3261
HORVU1Hr1G071910	Plant protein 1589 of unknown function	-5.6315
HORVU1Hr1G047570	undescribed protein	-5.9020
HORVU1Hr1G047390	SAUR-like auxin-responsive protein family	-6.0589
HORVU3Hr1G084830	Nematode resistance protein-like HSPRO2	-6.2051
HORVU3Hr1G059220	WRKY family transcription factor	-6.2720
HORVU7Hr1G057330	Chaperone protein DnaJ	-7.3305
HORVU5Hr1G080830	undescribed protein	-7.3452
HORVU6Hr1G077610	RING/U-box superfamily protein	-7.6037
HORVU6Hr1G077770	EXORDIUM like 2	-7.6148
HORVU2Hr1G117500	undescribed protein	-7.8296
HORVU2Hr1G035550	undescribed protein	-7.8401
HORVU7Hr1G086340	undescribed protein	-8.2669
HORVU7Hr1G086250	undescribed protein	-8.5511
HORVU7Hr1G040030	unknown function	-8.6258
HORVU1Hr1G048700	F-box protein PP2-A13	-8.7351
HORVU5Hr1G010950	Glutaredoxin family protein	-8.8271
HORVU5Hr1G083200	unknown function	-9.1105
HORVU7Hr1G086260	undescribed protein	-9.1134
HORVU7Hr1G101740	Calcium-binding EF-hand family protein	-9.3418
HORVU3Hr1G108550	undescribed protein	-9.7621
HORVU7Hr1G027270	MATE efflux family protein	-10.0863
HORVU1Hr1G088680	Receptor-like protein kinase	-11.6737
HORVU2Hr1G103930	NAC domain containing protein 1	-13.1652
HORVU6Hr1G016860	undescribed protein	-14.3335
HORVU2Hr1G090730	GRAM domain-containing protein / ABA-responsive protein-related	-18.7766
HORVU2Hr1G066100	basic helix-loop-helix (bHLH) DNA-binding superfamily protein	-19.5659
HORVU3Hr1G085860	Regulator of chromosome condensation (RCC1) family protein	-26.5704

Table C2. Common and exclusive DEGs (a) 6 hpa ZnO NP Upregulated Exclusive Genes, (b) 6 hpa $ZnSO_4$ Upregulated Exclusive Genes, (c) 6 hpa ZnO NP and $ZnSO_4$ Upregulated Common Genes, (d) 6 hpa ZnO NP and $ZnSO_4$ Downregulated Common Genes, (e) 6 hpa ZnO NPs Downregulated Exclusive Genes, and (f) 6 hpa $ZnSO_4$ Downregulated Exclusive Genes (continued)

(f) 6 hpa $ZnSO_4$ Downregulated Exclusive Genes

46 elements included exclusively in "6 hpa $ZnSO_4$ down":	Annotation	Fold Change
HORVU4Hr1G013310	unknown protein	-3.0948
HORVU4Hr1G070720	Auxilin-related protein 2	-3.3341
HORVU5Hr1G098980	HAD-superfamily hydrolase, subfamily IG, 5'-nucleotidase	-3.6872
HORVU4Hr1G000510	haloacid dehalogenase-like hydrolase family protein	-3.7259
HORVU7Hr1G025390	Glycogen synthase	-3.7280
HORVU5Hr1G054000	Chlorophyll a-b binding protein C, chloroplastic	-3.8012
HORVU5Hr1G118120	unknown function	-3.8307
HORVU5Hr1G089230	Fatty acyl-CoA reductase 1	-3.8922
HORVU4Hr1G076180	unknown function	-3.9000
HORVU7Hr1G037600	sodium/calcium exchanger family protein / calcium-binding EF hand family protein	-4.2763
HORVU5Hr1G073950	dihydroflavonol 4-reductase-like1	-4.2920
HORVU0Hr1G016860	DNA-binding protein SMUBP-2	-4.4030
HORVU3Hr1G025820	Mitochondrial substrate carrier family protein	-4.8006
HORVU2Hr1G071860	NAD(P)-binding Rossmann-fold superfamily protein	-4.9793
HORVU6Hr1G025730	Quinone oxidoreductase-like protein 2 homolog	-5.2239
HORVU2Hr1G013870	fatty acid desaturase 8	-5.3091
HORVU5Hr1G070230	Dicarboxylate transporter 2.1, chloroplastic	-5.5289
HORVU2Hr1G094190	Nuclear transport factor 2 (NTF2) family protein	-5.6800
HORVU3Hr1G001940	undescribed protein	-5.7972
HORVU7Hr1G083360	NAD-dependent epimerase/dehydratase	-5.8901
HORVU0Hr1G012860	Alcohol dehydrogenase	-6.0990
HORVU2Hr1G021700	4-alpha-glucanotransferase	-6.1930
HORVU2Hr1G075110	PLC-like phosphodiesterases superfamily protein	-6.2089
HORVU3Hr1G094820	thylakoid rhodanese-like	-6.3854
HORVU5Hr1G044410	Hydroxymethylglutaryl-CoA lyase	-6.4067
HORVU7Hr1G046320	Chlorophyll a-b binding protein 1B-21, chloroplastic	-6.6622
HORVU3Hr1G089650	Rhodanese/Cell cycle control phosphatase superfamily protein	-7.0604
HORVU1Hr1G071180	Chaperone protein DnaJ	-7.7796
HORVU3Hr1G090760	Alpha/beta hydrolase domain-containing protein 11	-7.9779

Table C2. Common and exclusive DEGs (a) 6 hpa ZnO NP Upregulated Exclusive Genes, (b) 6 hpa $ZnSO_4$ Upregulated Exclusive Genes, (c) 6 hpa ZnO NP and $ZnSO_4$ Upregulated Common Genes, (d) 6 hpa ZnO NP and $ZnSO_4$ Downregulated Common Genes, (e) 6 hpa ZnO NPs Downregulated Exclusive Genes, and (f) 6 hpa $ZnSO_4$ Downregulated Exclusive Genes (continued)

(f) 6 hpa $ZnSO_4$ Downregulated Exclusive Genes (continued)

46 elements included exclusively in "6 hpa $ZnSO_4$ down":	Annotation	Fold Change
HORVU5Hr1G124160	Chlorophyll a-b binding protein 2, chloroplastic	-8.3891
HORVU2Hr1G001320	Protein NRT1/ PTR FAMILY 8.5	-9.2522
HORVU7Hr1G046050	Carboxyl-terminal-processing protease	-9.4317
HORVU7Hr1G076030	Beta-carotene isomerase D27, chloroplastic	-10.0639
HORVU6Hr1G073100	Protein CURVATURE THYLAKOID 1A, chloroplastic	-10.0797
HORVU2Hr1G079920	Chlorophyll a-b binding protein, chloroplastic	-10.2592
HORVU1Hr1G022840	Peroxisomal membrane protein 2	-10.5313
HORVU2Hr1G023540	Magnesium-chelatase subunit ChlH, chloroplastic	-11.7408
HORVU4Hr1G065560	Erythronate-4-phosphate dehydrogenase family protein	-12.0121
HORVU1Hr1G093660	ribonuclease 3	-13.1664
HORVU3Hr1G086190	Photosystem II reaction center Psb28 protein	-14.3926
HORVU0Hr1G039090	Harpin binding protein 1, putative, expressed	-15.7917
HORVU1Hr1G093780	Ribonuclease T2 family protein	-16.2294
HORVU5Hr1G004700	terpene synthase 21	-20.3926
HORVU7Hr1G090410	polyamine oxidase 1	-26.1139
HORVU1Hr1G093570	Ribonuclease T2 family protein	-49.9977
HORVU4Hr1G039870	unknown protein; BEST Arabidopsis thaliana protein match is: unknown protein	-52.8506

APPENDIX D

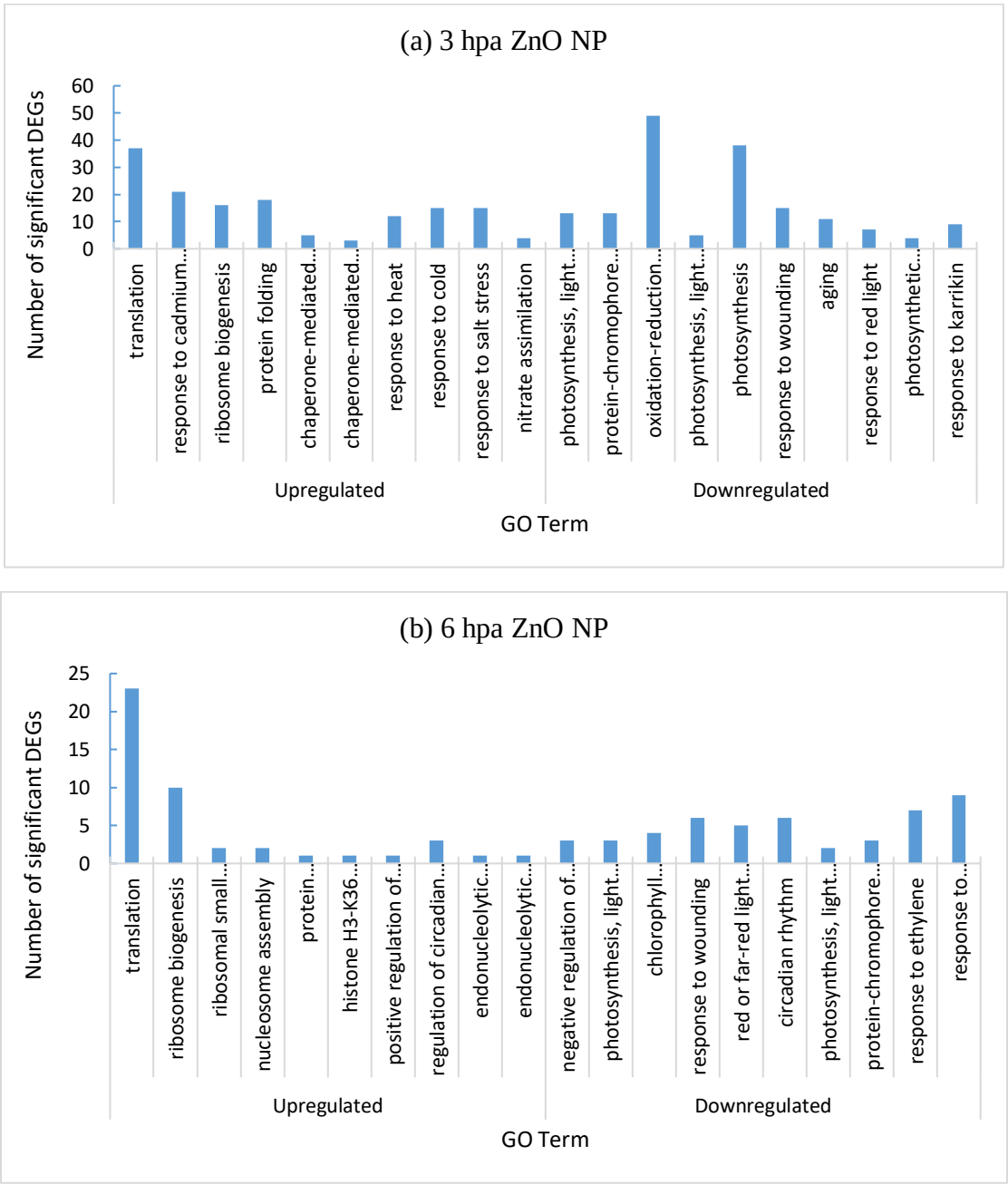

Figure D1. Bar charts showing gene enrichment for biological process using TopGO in (a) 3 hpa ZnO NP, (b) 6 hpa ZnO NP, (c) 3 hpi Pathogen, (d) 21 hpi Pathogen, (e) 45 hpi Pathogen, (f) 3 hpi NP+Pathogen, (g) 21 hpi NP+Pathogen, and (h) 45 hpi NP+Pathogen

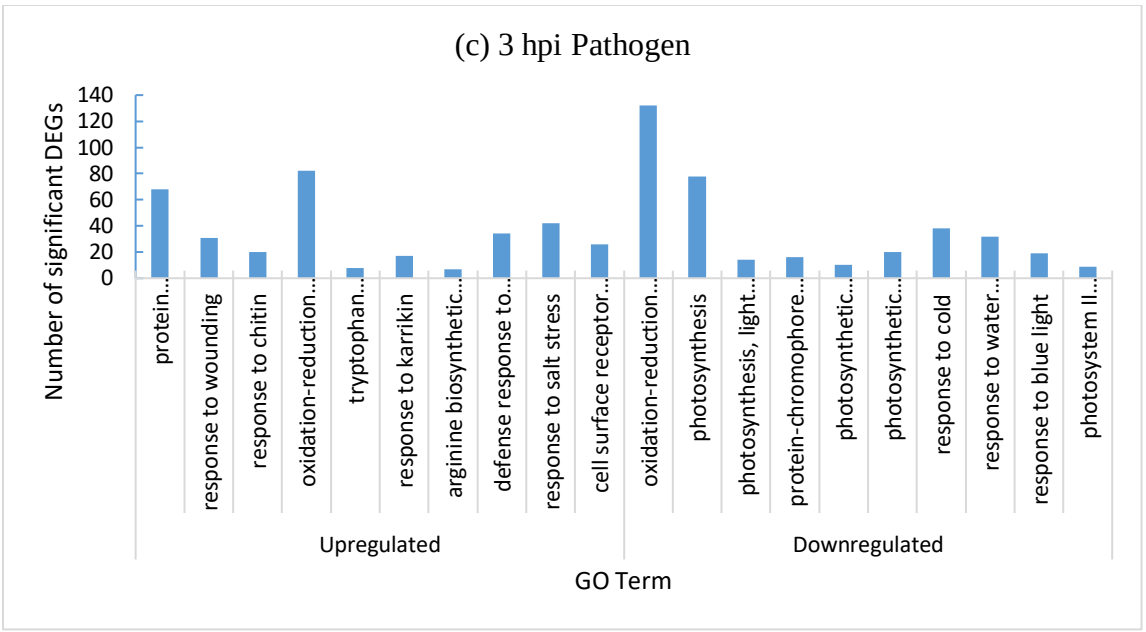

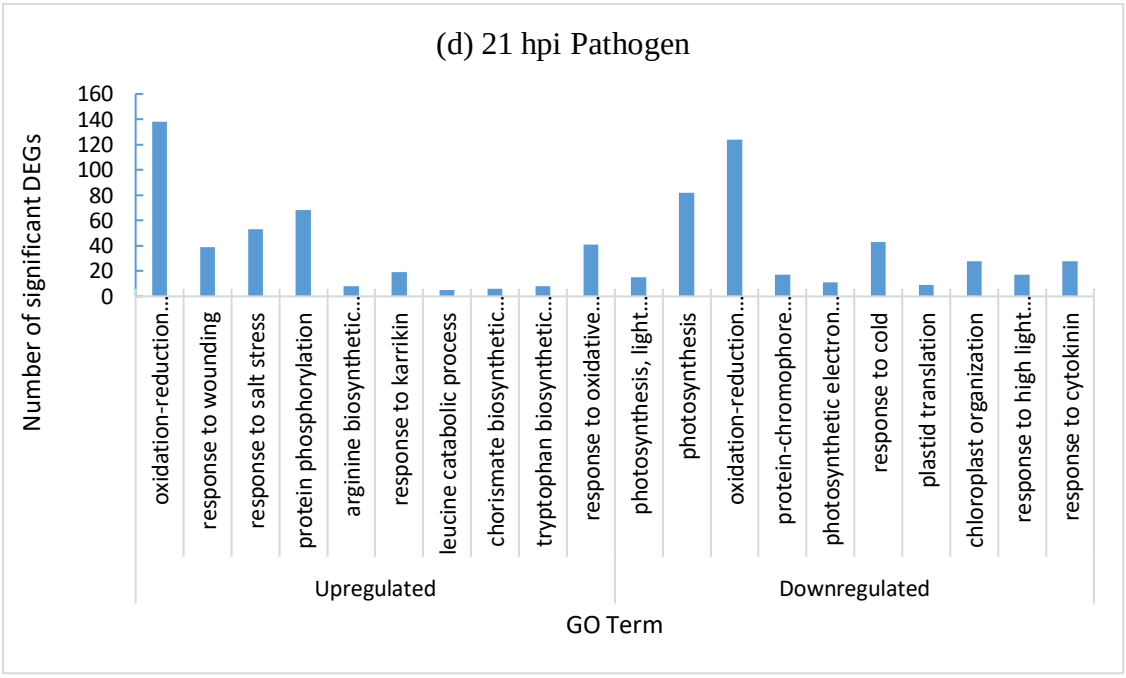

Figure D1. Bar charts showing gene enrichment for biological process using TopGO in (a) 3 hpa ZnO NP, (b) 6 hpa ZnO NP, (c) 3 hpi Pathogen, (d) 21 hpi Pathogen, (e) 45 hpi Pathogen, (f) 3 hpi NP+Pathogen, (g) 21 hpi NP+Pathogen, and (h) 45 hpi NP+Pathogen (continued)

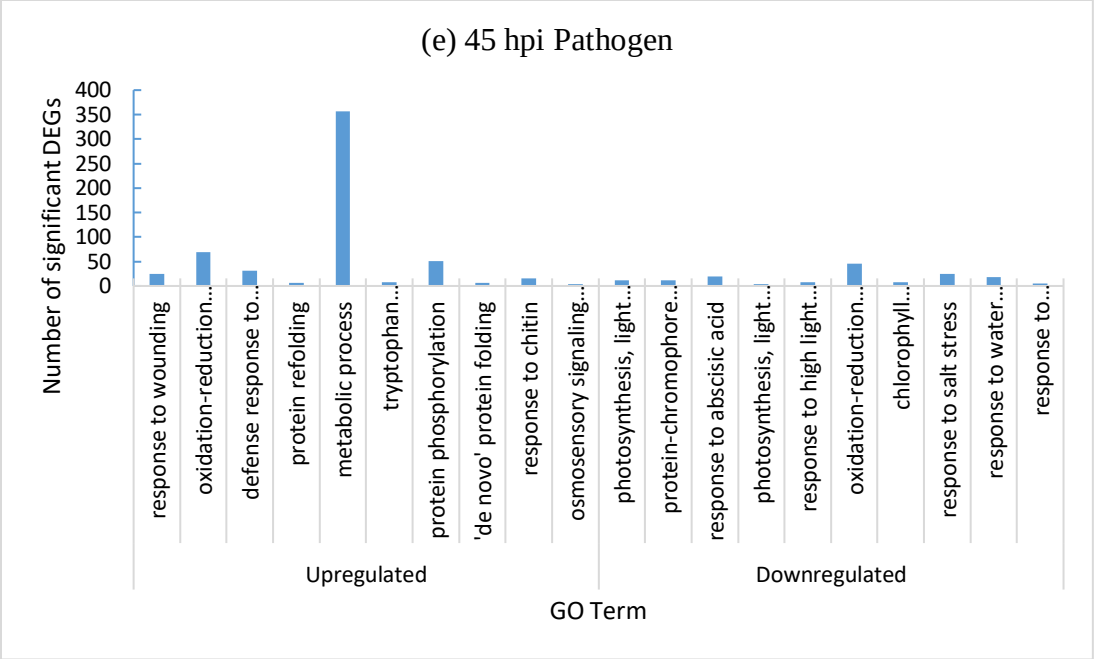

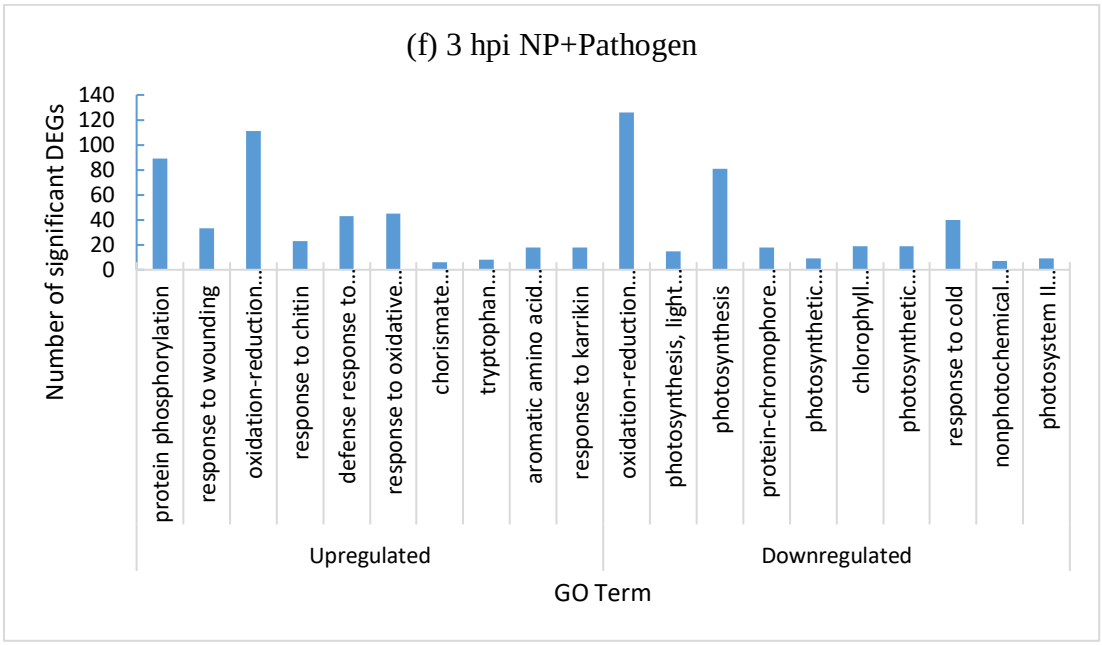

Figure D1. Bar charts showing gene enrichment for biological process using TopGO in (a) 3 hpa ZnO NP, (b) 6 hpa ZnO NP, (c) 3 hpi Pathogen, (d) 21 hpi Pathogen, (e) 45 hpi Pathogen, (f) 3 hpi NP+Pathogen, (g) 21 hpi NP+Pathogen, and (h) 45 hpi NP+Pathogen (continued)

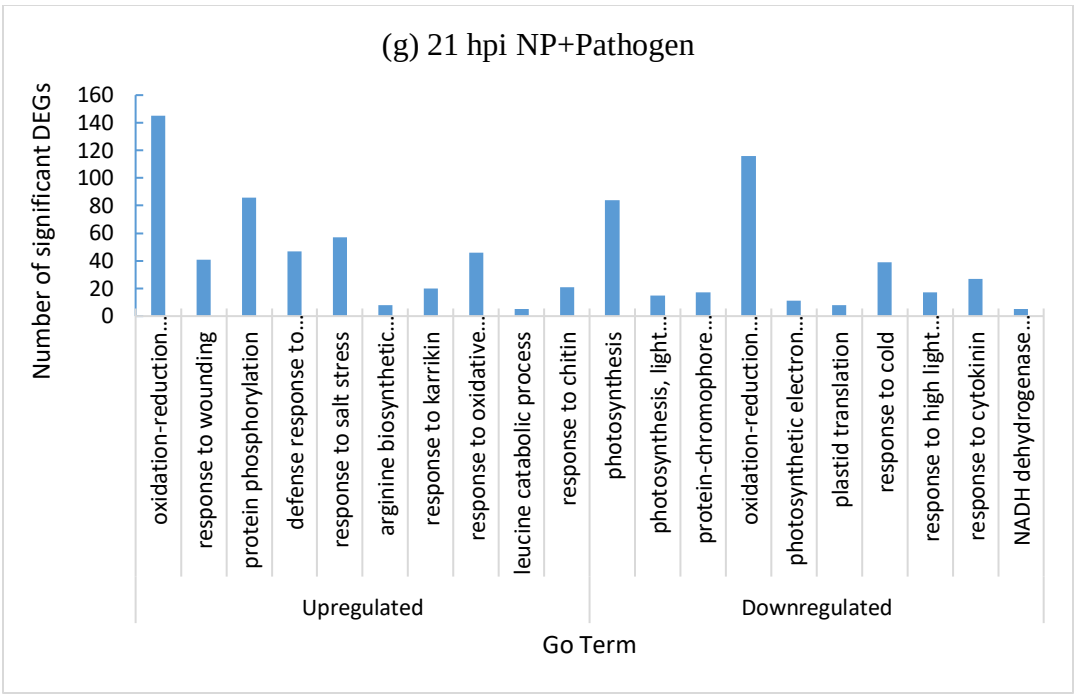

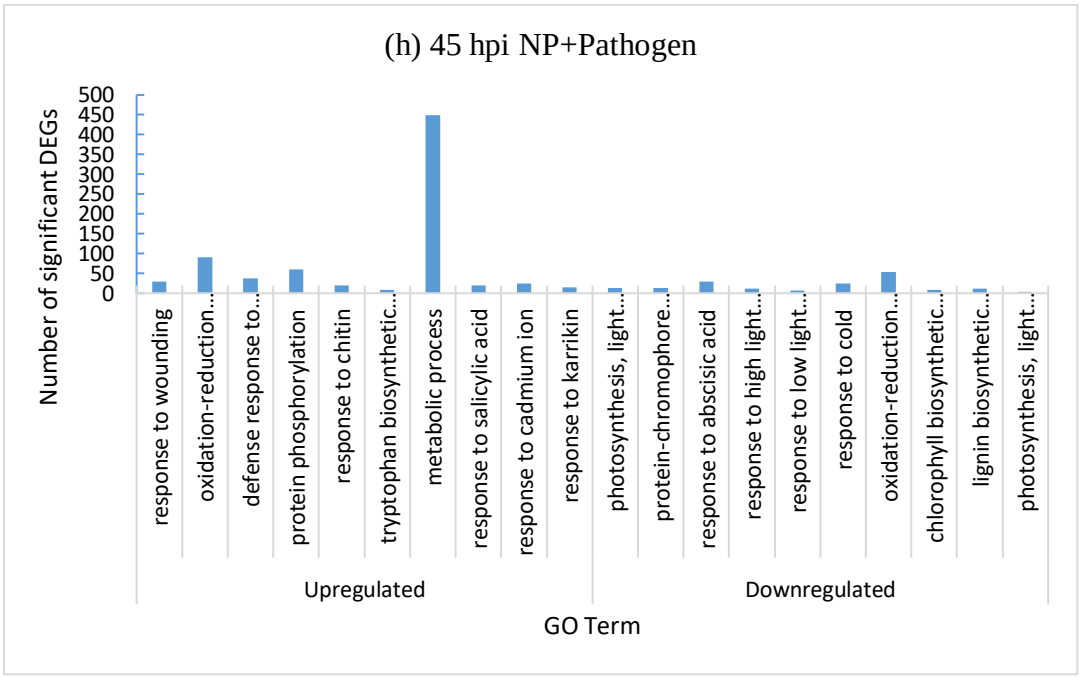

Figure D1. Bar charts showing gene enrichment for biological process using TopGO in (a) 3 hpa ZnO NP, (b) 6 hpa ZnO NP, (c) 3 hpi Pathogen, (d) 21 hpi Pathogen, (e) 45 hpi Pathogen, (f) 3 hpi NP+Pathogen, (g) 21 hpi NP+Pathogen, and (h) 45 hpi NP+Pathogen (continued)

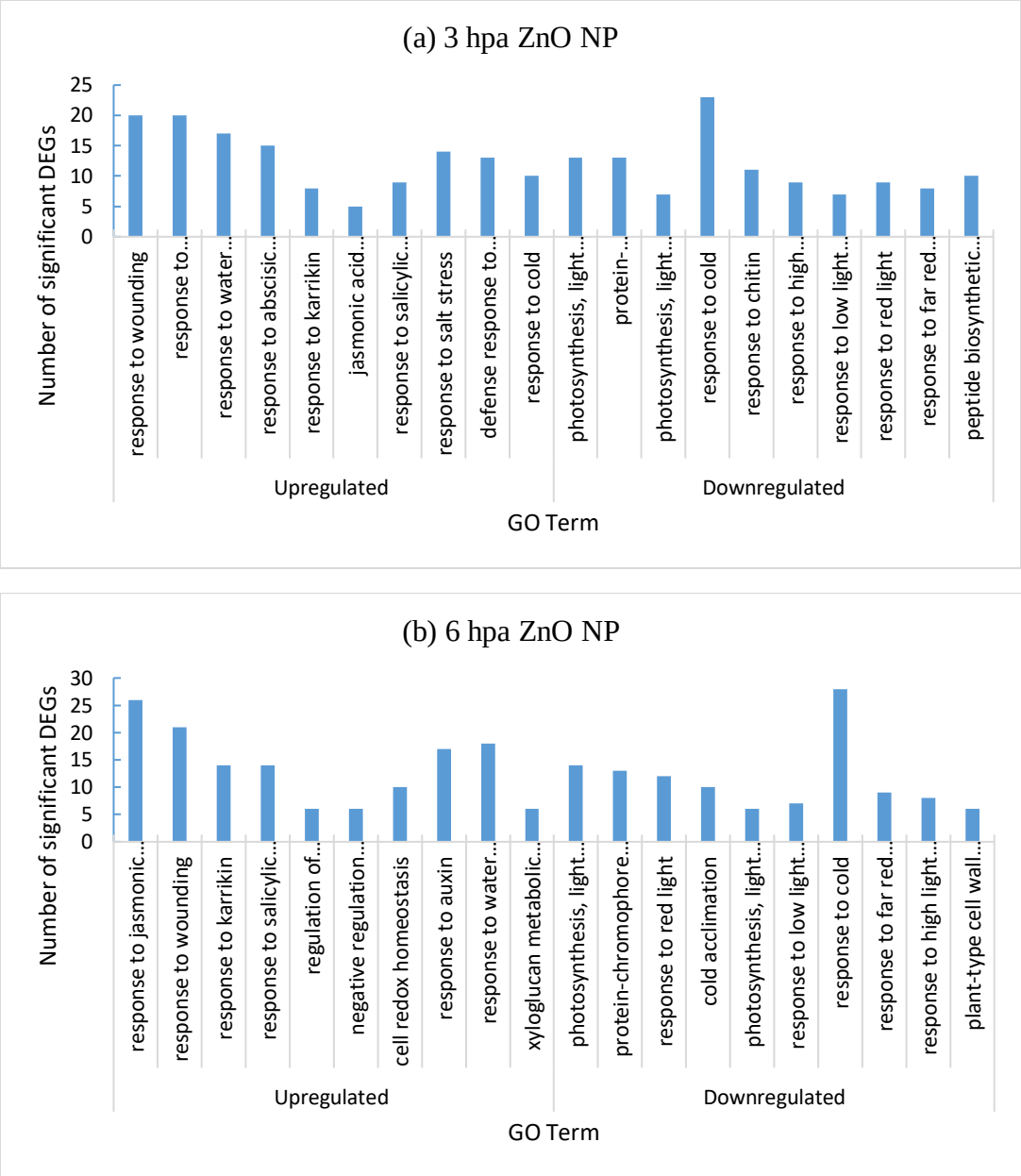

Figure D2. Bar charts showing gene enrichment for biological process using TopGO in Arabidopsis at (a) 3 hpa, (b) 6 hpa, (c) 24 hpa, and (d) 48 hpa

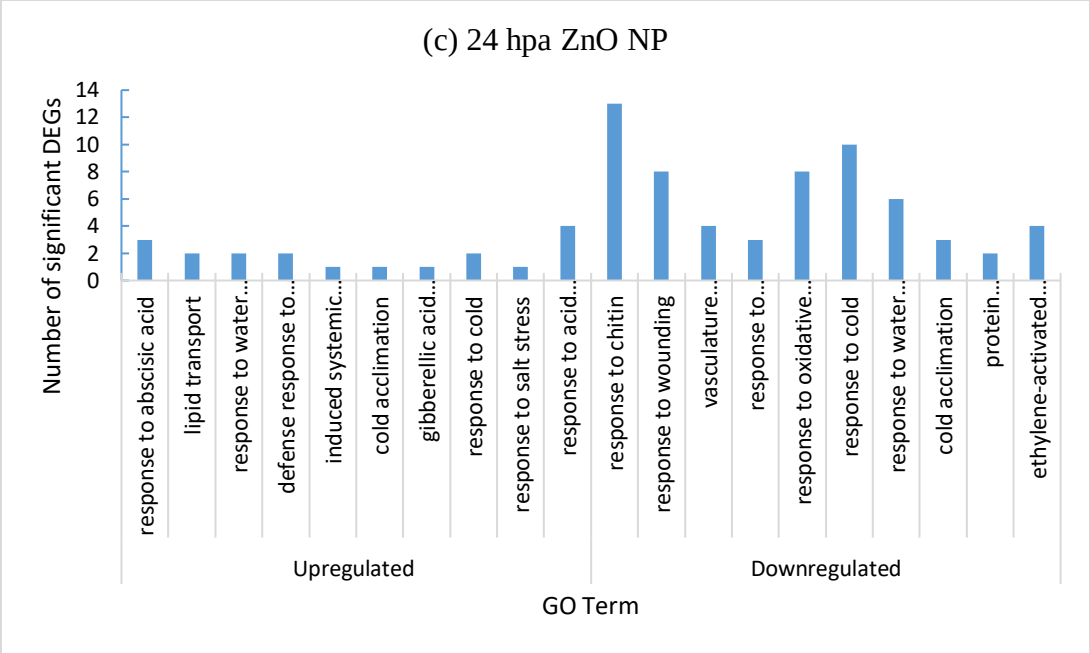

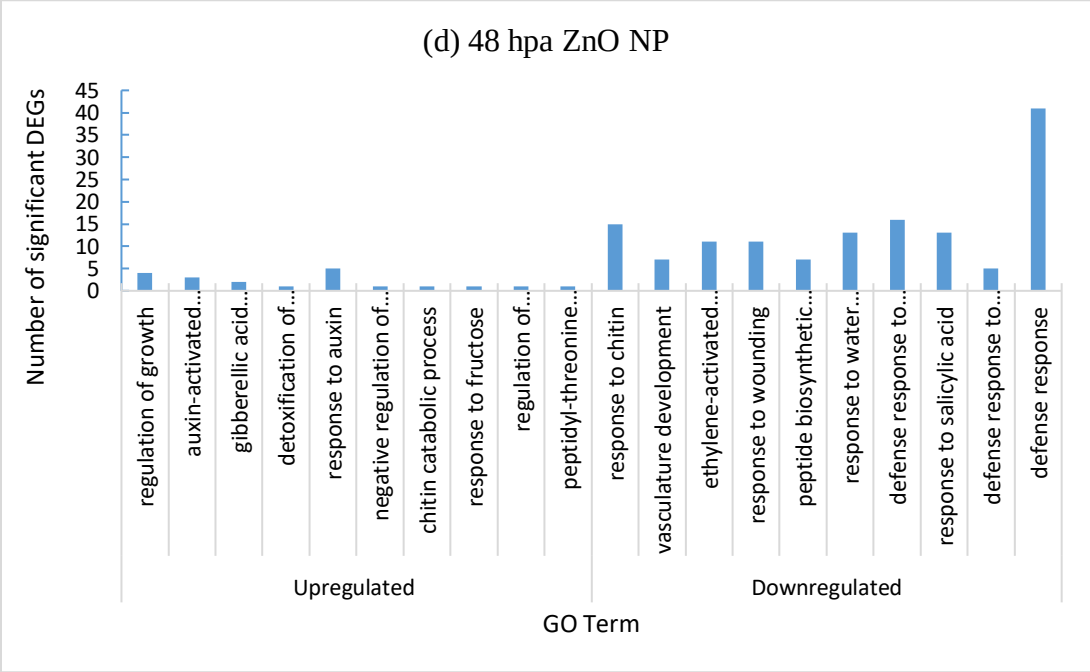

Figure D2. Bar charts showing gene enrichment for biological process using TopGO in Arabidopsis at (a) 3 hpa, (b) 6 hpa, (c) 24 hpa, and (d) 48 hpa (continued)

Table D1. Gene enrichment for biological process in TopGO in barley exposed to ZnO NP at (a) 3 hpa, (b) 6 hpa, (c) 24 hpa, and (d) 48 hpa, pathogen at (e) 3 hpi, (f) 21 hpi, and (g) 45 hpi, and combined application (ZnO NP+ pathogen) at (h) 3 hpi, (i) 21 hpi, and (j) 45 hpi

(a) 3 hpa ZnO NP

	GO.ID	Term	p-value
Upregulated	GO:0006412	translation	1.60E-12
	GO:0046686	response to cadmium ion	4.10E-14
	GO:0042254	ribosome biogenesis	1.80E-09
	GO:0006457	protein folding	1.90E-13
	GO:0061077	chaperone-mediated protein folding	1.60E-06
	GO:0051131	chaperone-mediated protein complex assem...	3.30E-06
	GO:0009408	response to heat	1.70E-08
	GO:0009409	response to cold	1.30E-07
	GO:0009651	response to salt stress	1.40E-05
	GO:0042128	nitrate assimilation	0.00023
Downregulated	GO:0009768	photosynthesis, light harvesting in phot...	4.70E-19
	GO:0018298	protein-chromophore linkage	1.60E-14
	GO:0055114	oxidation-reduction process	1.10E-08
	GO:0009769	photosynthesis, light harvesting in phot...	1.10E-07
	GO:0015979	photosynthesis	3.50E-28
	GO:0009611	response to wounding	3.50E-07
	GO:0007568	aging	4.00E-05
	GO:0010114	response to red light	5.30E-05
	GO:0009773	photosynthetic electron transport in pho...	5.50E-05
	GO:0080167	response to karrikin	6.90E-05

Table D1. Gene enrichment for biological process in TopGO in barley exposed to ZnO NP at (a) 3 hpa, (b) 6 hpa, (c) 24 hpa, and (d) 48 hpa, pathogen at (e) 3 hpi, (f) 21 hpi, and (g) 45 hpi, and combined application (ZnO NP+ pathogen) at (h) 3 hpi, (i) 21 hpi, and (j) 45 hpi (continued)

(b) 6 hpa ZnO NP

	GO.ID	Term	p-value
Upregulated	GO:0006412	translation	2.10E-14
	GO:0042254	ribosome biogenesis	4.70E-09
	GO:0000028	ribosomal small subunit assembly	0.00029
	GO:0006334	nucleosome assembly	0.00194
	GO:0051290	protein heterotetramerization	0.00233
	GO:0070544	histone H3-K36 demethylation	0.00233
	GO:1901671	positive regulation of superoxide dismut...	0.00233
	GO:0042752	regulation of circadian rhythm	0.00039
	GO:0000447	endonucleolytic cleavage in ITS1 to sepa...	0.00465
	GO:0000461	endonucleolytic cleavage to generate mat...	0.00465
Downregulated	GO:0010100	negative regulation of photomorphogenesi...	1.20E-05
	GO:0009768	photosynthesis, light harvesting in phot...	9.30E-05
	GO:0015995	chlorophyll biosynthetic process	9.80E-05
	GO:0009611	response to wounding	0.0002
	GO:0010017	red or far-red light signaling pathway	2.30E-05
	GO:0007623	circadian rhythm	2.00E-05
	GO:0009769	photosynthesis, light harvesting in phot...	0.00065
	GO:0018298	protein-chromophore linkage	0.00066
	GO:0009723	response to ethylene	0.00022
	GO:0009266	response to temperature stimulus	0.00039

Table D1. Gene enrichment for biological process in TopGO in barley exposed to ZnO NP at (a) 3 hpa, (b) 6 hpa, (c) 24 hpa, and (d) 48 hpa, pathogen at (e) 3 hpi, (f) 21 hpi, and (g) 45 hpi, and combined application (ZnO NP+ pathogen) at (h) 3 hpi, (i) 21 hpi, and (j) 45 hpi (continued)

(c) 24 hpa ZnO NP

	GO.ID	Term	p-value
Downregulated	GO:0009611	response to wounding	1.10E-06
	GO:0080167	response to karrikin	4.80E-05
	GO:0032544	plastid translation	0.00016
	GO:0045727	positive regulation of translation	0.00021
	GO:1903507	negative regulation of nucleic acid-temp...	0.00597
	GO:0018119	peptidyl-cysteine S-nitrosylation	0.00028
	GO:0019253	reductive pentose-phosphate cycle	0.0004
	GO:0009768	photosynthesis, light harvesting in phot...	0.00059
	GO:2000022	regulation of jasmonic acid mediated sig...	0.0007
	GO:0046323	glucose import	0.00101

(d) 48 hpa ZnO NP

	GO.ID	Term	p-value
Downregulated	GO:0009611	response to wounding	8.80E-05
	GO:0080167	response to karrikin	0.0013
	GO:0050691	regulation of defense response to virus ...	0.0034
	GO:0032544	plastid translation	0.005
	GO:0045727	positive regulation of translation	0.0059
	GO:1903507	negative regulation of nucleic acid-temp...	0.0042
	GO:0018119	peptidyl-cysteine S-nitrosylation	0.0067
	GO:0042742	defense response to bacterium	0.0102
	GO:2000022	regulation of jasmonic acid mediated sig...	0.0104
	GO:0002237	response to molecule of bacterial origin	0.0109

Table D1. Gene enrichment for biological process in TopGO in barley exposed to ZnO NP at (a) 3 hpa, (b) 6 hpa, (c) 24 hpa, and (d) 48 hpa, pathogen at (e) 3 hpi, (f) 21 hpi, and (g) 45 hpi, and combined application (ZnO NP+ pathogen) at (h) 3 hpi, (i) 21 hpi, and (j) 45 hpi (continued)

(e) 3 hpi P

	GO.ID	Term	p-value
Upregulated	GO:0006468	protein phosphorylation	3.70E-14
	GO:0009611	response to wounding	3.80E-14
	GO:0010200	response to chitin	5.20E-10
	GO:0055114	oxidation-reduction process	7.10E-10
	GO:0000162	tryptophan biosynthetic process	6.20E-08
	GO:0080167	response to karrikin	6.80E-08
	GO:0006526	arginine biosynthetic process	1.50E-08
	GO:0042742	defense response to bacterium	7.30E-10
	GO:0009651	response to salt stress	7.60E-09
	GO:0007166	cell surface receptor signaling pathway	1.10E-09
Downregulated	GO:0055114	oxidation-reduction process	< 1e-30
	GO:0015979	photosynthesis	< 1e-30
	GO:0009768	photosynthesis, light harvesting in phot...	1.20E-16
	GO:0018298	protein-chromophore linkage	3.00E-14
	GO:0009773	photosynthetic electron transport in pho...	2.20E-12
	GO:0009767	photosynthetic electron transport chain	8.70E-17
	GO:0009409	response to cold	6.40E-11
	GO:0009414	response to water deprivation	7.80E-09
	GO:0009637	response to blue light	1.20E-12
	GO:0010207	photosystem II assembly	6.50E-09

Table D1. Gene enrichment for biological process in TopGO in barley exposed to ZnO NP at (a) 3 hpa, (b) 6 hpa, (c) 24 hpa, and (d) 48 hpa, pathogen at (e) 3 hpi, (f) 21 hpi, and (g) 45 hpi, and combined application (ZnO NP+ pathogen) at (h) 3 hpi, (i) 21 hpi, and (j) 45 hpi (continued)

(f) 21 hpi P

	GO.ID	Term	p-value
Upregulated	GO:0055114	oxidation-reduction process	1.20E-26
	GO:0009611	response to wounding	2.30E-17
	GO:0009651	response to salt stress	1.30E-10
	GO:0006468	protein phosphorylation	2.40E-09
	GO:0006526	arginine biosynthetic process	2.20E-09
	GO:0080167	response to karrikin	9.10E-08
	GO:0006552	leucine catabolic process	2.90E-07
	GO:0009423	chorismate biosynthetic process	3.20E-07
	GO:0000162	tryptophan biosynthetic process	4.10E-07
	GO:0006979	response to oxidative stress	4.50E-08
Downregulated	GO:0009768	photosynthesis, light harvesting in phot...	5.90E-18
	GO:0015979	photosynthesis	< 1e-30
	GO:0055114	oxidation-reduction process	6.20E-25
	GO:0018298	protein-chromophore linkage	4.30E-15
	GO:0009773	photosynthetic electron transport in pho...	7.20E-14
	GO:0009409	response to cold	5.30E-13
	GO:0032544	plastid translation	4.30E-12
	GO:0009658	chloroplast organization	1.40E-13
	GO:0009644	response to high light intensity	2.80E-10
	GO:0009735	response to cytokinin	3.30E-09

Table D1. Gene enrichment for biological process in TopGO in barley exposed to ZnO NP at (a) 3 hpa, (b) 6 hpa, (c) 24 hpa, and (d) 48 hpa, pathogen at (e) 3 hpi, (f) 21 hpi, and (g) 45 hpi, and combined application (ZnO NP+ pathogen) at (h) 3 hpi, (i) 21 hpi, and (j) 45 hpi (continued)

(g) 45 hpi P

	GO.ID	Term	p-value
Upregulated	GO:0009611	response to wounding	5.60E-12
	GO:0055114	oxidation-reduction process	4.90E-10
	GO:0042742	defense response to bacterium	8.10E-11
	GO:0042026	protein refolding	6.50E-09
	GO:0008152	metabolic process	1.40E-19
	GO:0000162	tryptophan biosynthetic process	8.60E-09
	GO:0006468	protein phosphorylation	2.00E-10
	GO:0006458	'de novo' protein folding	2.10E-07
	GO:0010200	response to chitin	2.00E-08
	GO:0007231	osmosensory signaling pathway	9.30E-07
Downregulated	GO:0009768	photosynthesis, light harvesting in phot...	8.40E-15
	GO:0018298	protein-chromophore linkage	3.60E-11
	GO:0009737	response to abscisic acid	0.00055
	GO:0009769	photosynthesis, light harvesting in phot...	9.60E-06
	GO:0009644	response to high light intensity	2.90E-05
	GO:0055114	oxidation-reduction process	6.20E-06
	GO:0015995	chlorophyll biosynthetic process	3.80E-05
	GO:0009651	response to salt stress	7.60E-06
	GO:0009414	response to water deprivation	6.70E-06
	GO:0010583	response to cyclopentenone	0.00014

Table D1. Gene enrichment for biological process in TopGO in barley exposed to ZnO NP at (a) 3 hpa, (b) 6 hpa, (c) 24 hpa, and (d) 48 hpa, pathogen at (e) 3 hpi, (f) 21 hpi, and (g) 45 hpi, and combined application (ZnO NP+ pathogen) at (h) 3 hpi, (i) 21 hpi, and (j) 45 hpi (continued)

(h) 3 hpi NP+P

	GO.ID	Term	p-value
Upregulated	GO:0006468	protein phosphorylation	6.10E-18
	GO:0009611	response to wounding	2.20E-12
	GO:0055114	oxidation-reduction process	1.30E-13
	GO:0010200	response to chitin	3.50E-10
	GO:0042742	defense response to bacterium	1.40E-11
	GO:0006979	response to oxidative stress	1.50E-09
	GO:0009423	chorismate biosynthetic process	3.80E-07
	GO:0000162	tryptophan biosynthetic process	5.30E-07
	GO:0009073	aromatic amino acid family biosynthetic ...	3.10E-14
	GO:0080167	response to karrikin	7.10E-07
Downregulated	GO:0055114	oxidation-reduction process	2.60E-25
	GO:0009768	photosynthesis, light harvesting in phot...	7.60E-18
	GO:0015979	photosynthesis	< 1e-30
	GO:0018298	protein-chromophore linkage	2.60E-16
	GO:0009773	photosynthetic electron transport in pho...	2.30E-10
	GO:0015995	chlorophyll biosynthetic process	2.00E-14
	GO:0009767	photosynthetic electron transport chain	7.10E-15
	GO:0009409	response to cold	5.40E-11
	GO:0010196	nonphotochemical quenching	7.70E-09
	GO:0010207	photosystem II assembly	1.30E-08

Table D1. Gene enrichment for biological process in TopGO in barley exposed to ZnO NP at (a) 3 hpa, (b) 6 hpa, (c) 24 hpa, and (d) 48 hpa, pathogen at (e) 3 hpi, (f) 21 hpi, and (g) 45 hpi, and combined application (ZnO NP+ pathogen) at (h) 3 hpi, (i) 21 hpi, and (j) 45 hpi (continued)

(i) 21 hpi NP+P

	GO.ID	Term	p-value
Upregulated	GO:0055114	oxidation-reduction process	3.30E-24
	GO:0009611	response to wounding	6.00E-17
	GO:0006468	protein phosphorylation	6.80E-14
	GO:0042742	defense response to bacterium	2.40E-12
	GO:0009651	response to salt stress	2.50E-10
	GO:0006526	arginine biosynthetic process	6.30E-09
	GO:0080167	response to karrikin	1.50E-07
	GO:0006979	response to oxidative stress	1.20E-08
	GO:0006552	leucine catabolic process	5.60E-07
	GO:0010200	response to chitin	6.30E-08
Downregulated	GO:0015979	photosynthesis	< 1e-30
	GO:0009768	photosynthesis, light harvesting in phot...	2.60E-18
	GO:0018298	protein-chromophore linkage	1.80E-15
	GO:0055114	oxidation-reduction process	6.50E-23
	GO:0009773	photosynthetic electron transport in pho...	4.00E-14
	GO:0032544	plastid translation	2.00E-10
	GO:0009409	response to cold	2.50E-11
	GO:0009644	response to high light intensity	1.20E-10
	GO:0009735	response to cytokinin	4.40E-09
	GO:0010258	NADH dehydrogenase complex (plastoquinon...	1.90E-08

Table D1. Gene enrichment for biological process in TopGO in barley exposed to ZnO NP at (a) 3 hpa, (b) 6 hpa, (c) 24 hpa, and (d) 48 hpa, pathogen at (e) 3 hpi, (f) 21 hpi, and (g) 45 hpi, and combined application (ZnO NP+ pathogen) at (h) 3 hpi, (i) 21 hpi, and (j) 45 hpi (continued)

(j) 45 hpi NP+P

	GO.ID	Term	p-value
Upregulated	GO:0009611	response to wounding	3.40E-13
	GO:0055114	oxidation-reduction process	1.40E-12
	GO:0042742	defense response to bacterium	3.90E-12
	GO:0006468	protein phosphorylation	3.60E-10
	GO:0010200	response to chitin	6.60E-10
	GO:0000162	tryptophan biosynthetic process	6.90E-08
	GO:0008152	metabolic process	3.30E-19
	GO:0009751	response to salicylic acid	8.20E-06
	GO:0046686	response to cadmium ion	9.80E-06
	GO:0080167	response to karrikin	1.20E-05
Downregulated	GO:0009768	photosynthesis, light harvesting in phot...	1.90E-17
	GO:0018298	protein-chromophore linkage	6.00E-13
	GO:0009737	response to abscisic acid	1.10E-06
	GO:0009644	response to high light intensity	2.50E-08
	GO:0009645	response to low light intensity stimulus	1.10E-06
	GO:0009409	response to cold	3.00E-07
	GO:0055114	oxidation-reduction process	2.30E-06
	GO:0015995	chlorophyll biosynthetic process	1.70E-06
	GO:0009809	lignin biosynthetic process	5.90E-08
	GO:0009769	photosynthesis, light harvesting in phot...	2.10E-05

Table D2. Gene enrichment for biological process in TopGO in Arabidopsis at (a) 3 hpa, (b) 6 hpa, (c) 24 hpa, and (d) 48 hpa

(a) 3 hpa ZnO NP

	GO Term		p-value
Upregulated	GO:0009611	response to wounding	3.80E-21
	GO:0009753	response to jasmonic acid	1.30E-20
	GO:0009414	response to water deprivation	1.90E-13
	GO:0009737	response to abscisic acid	3.30E-08
	GO:0080167	response to karrikin	8.60E-08
	GO:0009695	jasmonic acid biosynthetic process	1.00E-07
	GO:0009751	response to salicylic acid	4.10E-07
	GO:0009651	response to salt stress	2.00E-07
	GO:0050832	defense response to fungus	6.40E-07
	GO:0009409	response to cold	8.40E-06
Downregulated	GO:0009768	photosynthesis, light harvesting in phot...	3.60E-23
	GO:0018298	protein-chromophore linkage	1.40E-18
	GO:0009769	photosynthesis, light harvesting in phot...	6.20E-14
	GO:0009409	response to cold	2.70E-15
	GO:0010200	response to chitin	1.60E-09
	GO:0009644	response to high light intensity	3.70E-09
	GO:0009645	response to low light intensity stimulus	3.80E-11
	GO:0010114	response to red light	1.10E-09
	GO:0010218	response to far red light	7.30E-09
	GO:0043043	peptide biosynthetic process	0.47

Table D2. Gene enrichment for biological process in TopGO in Arabidopsis at (a) 3 hpa, (b) 6 hpa, (c) 24 hpa, and (d) 48 hpa (continued)

(b) 6 hpa ZnO NP

	GO Term		p-value
Upregulated	GO:0009753	response to jasmonic acid	2.40E-19
	GO:0009611	response to wounding	1.60E-14
	GO:0080167	response to karrikin	8.00E-11
	GO:0009751	response to salicylic acid	6.90E-08
	GO:2000022	regulation of jasmonic acid mediated sig...	1.90E-07
	GO:1903507	negative regulation of nucleic acid-temp...	0.038
	GO:0045454	cell redox homeostasis	2.20E-06
	GO:0009733	response to auxin	2.70E-06
	GO:0009414	response to water deprivation	3.70E-08
	GO:0010411	xyloglucan metabolic process	2.90E-05
Downregulated	GO:0009768	photosynthesis, light harvesting in phot...	3.90E-25
	GO:0018298	protein-chromophore linkage	3.20E-18
	GO:0010114	response to red light	1.00E-13
	GO:0009631	cold acclimation	1.60E-12
	GO:0009769	photosynthesis, light harvesting in phot...	2.40E-11
	GO:0009645	response to low light intensity stimulus	5.80E-11
	GO:0009409	response to cold	5.80E-20
	GO:0010218	response to far red light	4.70E-10
	GO:0009644	response to high light intensity	1.10E-07
	GO:0009828	plant-type cell wall loosening	1.90E-07

Table D2. Gene enrichment for biological process in TopGO in Arabidopsis at (a) 3 hpa, (b) 6 hpa, (c) 24 hpa, and (d) 48 hpa (continued)

(c) 24 hpa ZnO NP

	GO Term		p-value
Upregulated	GO:0009737	response to abscisic acid	4.30E-05
	GO:0006869	lipid transport	0.00026
	GO:0009414	response to water deprivation	0.00105
	GO:0050832	defense response to fungus	0.00249
	GO:0009682	induced systemic resistance	0.00503
	GO:0009631	cold acclimation	0.00746
	GO:0009740	gibberellic acid mediated signaling path...	0.01261
	GO:0009409	response to cold	0.00133
	GO:0009651	response to salt stress	0.0852
	GO:0001101	response to acid chemical	5.20E-06
Downregulated	GO:0010200	response to chitin	5.70E-19
	GO:0009611	response to wounding	1.20E-08
	GO:0001944	vasculature development	2.20E-07
	GO:0009612	response to mechanical stimulus	7.40E-06
	GO:0006979	response to oxidative stress	3.90E-06
	GO:0009409	response to cold	5.90E-09
	GO:0009414	response to water deprivation	7.50E-05
	GO:0009631	cold acclimation	0.00013
	GO:0051865	protein autoubiquitination	0.00031
	GO:0009873	ethylene-activated signaling pathway	0.00057

Table D2. Gene enrichment for biological process in TopGO in Arabidopsis at (a) 3 hpa, (b) 6 hpa, (c) 24 hpa, and (d) 48 hpa (continued)

(d) 48 hpa ZnO NP

	GO Term		p-value
Upregulated	GO:0040008	regulation of growth	3.80E-05
	GO:0009734	auxin-activated signaling pathway	0.00034
	GO:0009740	gibberellic acid mediated signaling path...	0.00164
	GO:0071585	detoxification of cadmium ion	0.00434
	GO:0009733	response to auxin	1.00E-05
	GO:0010100	negative regulation of photomorphogenesi...	0.00867
	GO:0006032	chitin catabolic process	0.00939
	GO:0009750	response to fructose	0.01154
	GO:0031540	regulation of anthocyanin biosynthetic p...	0.01226
	GO:0018107	peptidyl-threonine phosphorylation	0.01369
Downregulated	GO:0010200	response to chitin	4.70E-18
	GO:0001944	vasculature development	7.30E-12
	GO:0009873	ethylene-activated signaling pathway	2.20E-10
	GO:0009611	response to wounding	1.00E-09
	GO:0043043	peptide biosynthetic process	0.32
	GO:0009414	response to water deprivation	1.30E-09
	GO:0050832	defense response to fungus	3.80E-10
	GO:0009751	response to salicylic acid	3.00E-12
	GO:0009816	defense response to bacterium, incompati...	1.90E-06
	GO:0006952	defense response	4.70E-23